2010, VOLUME 1

PROGRESS IN PHYSICS

The Journal on Advanced Studies in Theoretical and Experimental Physics, including Related Themes from Mathematics

PROGRESS IN PHYSICS

A quarterly issue scientific journal, registered with the Library of Congress (DC, USA). This journal is peer reviewed and included in the abstracting and indexing coverage of: Mathematical Reviews and MathSciNet (AMS, USA), DOAJ of Lund University (Sweden), Zentralblatt MATH (Germany), Scientific Commons of the University of St. Gallen (Switzerland), Open-J-Gate (India), Referativnyi Zhurnal VINITI (Russia), etc.

This journal is powered by LaTeX

A variety of books can be downloaded free from the Digital Library of Science:
http://www.gallup.unm.edu/~smarandache

JANUARY 2010   VOLUME 1

CONTENTS

Information for Authors and Subscribers

Progress in Physics has been created for publications on advanced studies in theoretical and experimental physics, including related themes from mathematics and astronomy. All submitted papers should be professional, in good English, containing a brief review of a problem and obtained results.

All submissions should be designed in LaTeX format using *Progress in Physics* template. This template can be downloaded from *Progress in Physics* home page http://www.ptep-online.com. Abstract and the necessary information about author(s) should be included into the papers. To submit a paper, mail the file(s) to the Editor-in-Chief.

All submitted papers should be as brief as possible. We accept brief papers, no larger than 8 typeset journal pages. Short articles are preferable. Large papers can be considered in exceptional cases to the section *Special Reports* intended for such publications in the journal. Letters related to the publications in the journal or to the events among the science community can be applied to the section *Letters to Progress in Physics*.

All that has been accepted for the online issue of *Progress in Physics* is printed in the paper version of the journal. To order printed issues, contact the Editors.

This journal is non-commercial, academic edition. It is printed from private donations. (Look for the current author fee in the online version of the journal.)

————————————

The Kruskal-Szekeres "Extension": Counter-Examples

Stephen J. Crothers

Queensland, Australia
thenarmis@gmail.com

The Kruskal-Szekeres "coordinates" are said to "extend" the so-called "Schwarzschild solution", to remove an alleged "coordinate singularity" at the event horizon of a black hole at $r = 2m$, leaving an infinitely dense point-mass singularity at "the origin" $r = 0$. However, the assumption that the point at the centre of spherical symmetry of the "Schwarzschild solution" is at "the origin" $r = 0$ is erroneous, and so the Kruskal-Szekeres "extension" is invalid; demonstrated herein by simple counter-examples.

1 Introduction

According to the astrophysical scientists the solution for Einstein's static vacuum gravitational field must satisfy the following conditions [1–11]:

(a) It must be static; i.e. all the components of the metric tensor must be independent of time and the geometry must be unchanged under time reversal;

(b) It must be spherically symmetric;

(c) It must satisfy the equations $R_{\mu\nu} = 0$; no matter present;

(d) It must be asymptotically Minkowski spacetime.

The so-called "Schwarzschild solution" (which is not in fact Schwarzschild's solution at all) is (using $c = 1$ and $G = 1$),

$$ds^2 = \left(1 - \frac{2m}{r}\right)dt^2 - \left(1 - \frac{2m}{r}\right)^{-1} dr^2 - \tag{1}$$
$$- r^2 \left(d\theta^2 + \sin^2\theta\, d\varphi^2\right).$$

The astrophysical scientists merely inspect this line-element and thereby assert that there are singularities at $r = 2m$ and at $r = 0$ [3, 4, 7, 9]; the former they claim to be a "coordinate" or "removable" singularity which denotes the "radius" of an event horizon of a black hole of mass m located at the "real" or "physical" singularity at $r = 0$. They call $r = 2m$ the "Schwarzschild radius" and $r = 0$ "the origin".

It is plainly evident that metric (1) changes its signature from $(+, -, -, -)$ to $(-, +, -, -)$ when $0 < r < 2m$, despite the fact that metric (1) is supposed to be a generalisation of Minkowski spacetime, described by (using $c = 1$),

$$ds^2 = dt^2 - dr^2 - r^2 \left(d\theta^2 + \sin^2\theta\, d\varphi^2\right) \tag{2}$$

$$0 \leqslant r < \infty,$$

which has *fixed* signature $(+, -, -, -)$; and so there is in fact no possibility for Minkowski spacetime to change signature from $(+, -, -, -)$ to $(-, +, -, -)$ [5]. Consequently, $0 \leqslant r < 2m$ on Eq. (1) has no counterpart in Minkowski spacetime. Nonetheless, although the astrophysical scientists *deliberately* fix the signature to $(+, -, -, -)$ at the very outset of their derivation of Eq. (1) [1–9, 11, 12], in order to maintain the signature of Minkowski spacetime, they nonetheless allow a change of signature to occur in Eq. (1) to $(-, +, -, -)$ [3, 4, 7, 9, 10, 13, 14] according to their assumption that $0 \leqslant r < \infty$ applies to Eq. (1); in direct violation of their initial construction. They then invoke a complicated "change of coordinates" to make the singularity at $r = 2m$ disappear; the Kruskal-Szekeres coordinates [3, 4, 9, 13, 14]. The astrophysical scientists merely assume that the point at the centre of spherical symmetry of the manifold described by Eq. (1) is located at "the origin", $r = 0$. To justify their assumptions on the variable r, which they evidently conceive of as radial distance in "Schwarzschild" spacetime (e.g. "Schwarzschild radius"), they also claim that because the Riemann tensor scalar curvature invariant (the "Kretschmann scalar"), given by $f = R_{\alpha\beta\gamma\delta}R^{\alpha\beta\gamma\delta}$, is finite at $r = 2m$ and unbounded at $r = 0$, there must be a "real" singularity only at $r = 0$. This argument they apply *post hoc*, without any proof that General Relativity requires such a condition on the Kretschmann scalar.

The assumption that "the origin" $r = 0$ marks the point at the centre of spherical symmetry of the manifold described by (1) is demonstrably false. Furthermore, a geometry is fully determined by its line-element [5, 15], not by arbitrary values assigned to any curvature invariant which is calculated from the line-element itself in the first place. Given a line-element of the form of Eq. (1) the admissible values of its associated curvature invariants and the location of its centre of spherical symmetry are fully fixed by it, and so they cannot be arbitrarily determined by simple inspection and *ad hoc* assumptions.

To illustrate the inadmissibility of the methods applied by the astrophysical scientists in their analysis of Eq. (1), I shall adduce counter-examples that satisfy all the required conditions (a)–(d) and their additional assumptions concerning r and the Kretschmann scalar, but nevertheless clearly contradict the claims made by the astrophysical scientists in relation to Eq. (1). By these counter-examples I will demonstrate, by application of the very same methods the astrophysical scientists apply to Eq. (1), that there are "spacetimes" in which the

singularity of a "black hole" is encountered before the event horizon, and that this event horizon can be "removed" by application of the Kruskal-Szekeres method. I will also give an example that not only inverts the locations of the event horizon and the singularity, relative to Eq. (1), but also locates them both at places other than the "origin" $r = 0$ at which the metric is well-defined. It is in fact rather easy to generate an infinite number of such counter-examples (but just one is sufficient to invalidate the Kruskal-Szekeres "extension").

These counter-examples amplify the fact that the usual assumption on Eq. (1) that "the origin" $r = 0$, simply by inspection, marks the point at the centre of spherical symmetry of the manifold it describes, is entirely false, and that the additional assumption that the Kretschmann scalar must be unbounded at a "real" or "physical" singularity is also false. This should not really be all that surprising, bearing in mind that the usual assumptions are just that, for which no proofs have ever been produced. It follows that there is no black hole associated with Eq. (1), and that the Kruskal-Szekeres "extension" is fallacious.

It is easily proven that r in Eq. (1) is the inverse square root of the Gaussian curvature of the spherically symmetric geodesic surface in the spatial section [16, 17, 19]. Being directly related to a curvature invariant, its values are fixed by the intrinsic geometry, fixed by the form of the line-element itself, as are all other related curvature invariants.

It must also be remarked that the transition from Minkowski spacetime to Schwarzschild spacetime involves no matter whatsoever. Therefore Schwarzschild spacetime is not in fact a generalisation of the laws of Special Relativity; only a generalisation of the geometry of Minkowski spacetime. The speed of light in vacuum, c, which appears in the Minkowski line-element is not a photon; it is a speed, the maximum speed with which a point is permitted to move in Minkowski spacetime. Similarly, the appearance of the constant c in Schwarzschild spacetime does not imply the presence of a photon there either. A photon must be present *a priori* to assign the speed c to the photon. Neither photons nor masses are present, by construction, in the generalisation of Minkowski spacetime to Schwarzschild spacetime, owing to the equations $R_{\mu\nu} = 0$ according to condition (c). Minkowski spacetime is not Special Relativity — the latter requires the *a priori* presence of matter, the former does not. Schwarzschild spacetime is a spacetime that by construction contains no matter, and hence no sources.

2 Counter-examples

Consider the metric

$$ds^2 = \left(1 - \frac{2m}{2m - r}\right)dt^2 - \left(1 - \frac{2m}{2m - r}\right)^{-1} dr^2 - \tag{3}$$
$$- (r - 2m)^2 \left(d\theta^2 + \sin^2\theta\, d\varphi^2\right).$$

First, it is clear that Eq. (3) satisfies all the conditions (a)–

(d), and so metric (3) is as good as metric (1). I now apply to Eq. (3) the very same methods that the astrophysical scientists apply to Eq. (1) and so assume that $0 \leqslant r < \infty$ on Eq. (3), and that "the origin" $r = 0$ marks the point at the centre of spherical symmetry of the manifold. By inspection there are two "singularities"; at $r = 2m$ and at $r = 0$, just as in the case of Eq. (1). When $r > 2m$ the signature of (3) is $(+, -, -, -)$, just as in Eq. (1). When $0 < r < 2m$ the signature is $(-, +, -, -)$, again just as in Eq. (1). Now when $r = 2m$, the coefficient of dt^2 in Eq. (1) is zero, but in Eq. (3) it is undefined. Similarly, when $r = 0$, the coefficient of dt^2 in Eq. (1) is undefined but in Eq. (3) it is zero. Furthermore, when $r = 2m$, the Kretschmann scalar is $f = 3/4m^4$ in Eq. (1) but is undefined in Eq. (3), and when $r = 0$, the Kretschmann scalar is $f = 3/4m^4$ in Eq. (3) but is undefined in Eq. (1). Therefore, according to the methods of the astrophysical scientists there is an infinitely dense point-mass singularity at $r = 2m$ and an event horizon at $r = 0$ in Eq. (3) (or alternatively a singularity of finite density and radius $r = 2m$ so that the event horizon is within the singularity). Thus the singularity is encountered before the event horizon, and the "Schwarzschild radius" of the black hole in Eq. (3) is $r = 0$. Again, following the very same methods that the astrophysical scientists apply to Eq. (1), apply the Kruskal-Szekeres method to remove the "coordinate singularity" at $r = 0$ in Eq. (3) by setting

$$u = \left(1 - \frac{2m - r}{2m}\right)^{\frac{1}{2}} e^{\frac{2m-r}{4m}} \sinh\frac{t}{4m},$$

$$v = \left(1 - \frac{2m - r}{2m}\right)^{\frac{1}{2}} e^{\frac{2m-r}{4m}} \cosh\frac{t}{4m}.$$

Then metric (3) becomes,

$$ds^2 = \frac{32m^3}{r - 2m} e^{\frac{r-2m}{2m}} \left(du^2 - dv^2\right) + \tag{4}$$
$$+ (r - 2m)^2 \left(d\theta^2 + \sin^2\theta\, d\varphi^2\right),$$

where r is a function of u and v, by means of

$$\left(\frac{r}{2m}\right) e^{\frac{2m-r}{2m}} = v^2 - u^2.$$

It is now apparent that Eq. (4) is not singular at $r = 0$. The singularity at the event horizon with its "Schwarzschild radius" $r = 0$ has been removed. The metric is singular only at $r = 2m$ where according to the astrophysical scientists there must be an infinitely dense point-mass singularity (or alternatively a singularity of finite density and radius $r = 2m$ so that the event horizon is within the singularity).

In obtaining Eq. (4) I have done nothing more than that which the astrophysical scientists do to Eq. (1), and since (1) and (3) satisfy conditions (a)–(d), the one is as good as the other, and so Eq. (3) is as valid as Eq. (1) insofar as the methods of the astrophysical scientists apply. Thus, the methods

employed by the astrophysical scientists are flawed. To amplify this even further, consider the metric,

$$ds^2 = \left(1 - \frac{2m}{4m-r}\right)dt^2 - \left(1 - \frac{2m}{4m-r}\right)^{-1}dr^2 - \tag{5}$$
$$ -(r-4m)^2\left(d\theta^2 + \sin^2\theta\, d\varphi^2\right).$$

It is clear that this metric also satisfies conditions (a)–(d), and so Eq. (5) is as good as eqs. (1) and (3). Once again, applying the very same methods of the astrophysical scientists, assume that $0 \leqslant r < \infty$ and that $r = 0$ is the "origin". Then by inspection there are singularities at $r = 4m$ and at $r = 2m$. For $r > 4m$ the signature of (5) is $(+, -, -, -)$; for $2m < r < 4m$ it is $(-, +, -, -)$ and for $0 \leqslant r < 2m$ it is $(+, -, -, -)$. Now at $r = 4m$ the coefficient of dt^2 is unbounded and at $r = 2m$ it is zero. But at $r = 0$ it is neither zero nor unbounded — the metric is well-defined there. Furthermore, at $r = 4m$ the Kretschmann scalar is unbounded and at $r = 2m$ it is $f = 3/4m^4$, but at $r = 0$ it is $f = 3/256m^4$. Thus, according to the methods of the astrophysical scientists there is an event horizon at $r = 2m$ with "Schwarzschild radius" $r = 2m$, and an infinitely dense point-mass singularity at $r = 4m$ (or alternatively a singularity of finite density and radius $r = 4m$ so that the event horizon is within the singularity). So the singularity is encountered before the event horizon. The "coordinate" event horizon singularity at "Schwarzschild radius" $r = 2m$ can be removed by again applying the Kruskal-Szekeres method, by setting

$$u = \left(\frac{4m-r}{2m} - 1\right)^{\frac{1}{2}} e^{\frac{4m-r}{4m}} \cosh \frac{t}{4m}$$

$$v = \left(\frac{4m-r}{2m} - 1\right)^{\frac{1}{2}} e^{\frac{4m-r}{4m}} \sinh \frac{t}{4m}$$

for $r < 2m$, and

$$u = \left(1 - \frac{4m-r}{2m}\right)^{\frac{1}{2}} e^{\frac{4m-r}{4m}} \sinh \frac{t}{4m}$$

$$v = \left(1 - \frac{4m-r}{2m}\right)^{\frac{1}{2}} e^{\frac{4m-r}{4m}} \cosh \frac{t}{4m}$$

for $r > 2m$.

Metric (5) then becomes

$$ds^2 = \frac{32m^3}{r-4m} e^{\frac{r-4m}{2m}}\left(du^2 - dv^2\right) + \tag{6}$$
$$(r-4m)^2\left(d\theta^2 + \sin^2\theta\, d\varphi^2\right),$$

where r is a function of u and v, by means of

$$\left(\frac{2m-r}{2m}\right)e^{\frac{4m-r}{2m}} = u^2 - v^2.$$

It is apparent that Eq. (6) is singular only at $r = 4m$, where, according to the astrophysical scientists, there is an infinitely

dense point-mass singularity (or alternatively a singularity of finite density and radius $r = 4m$ so that the event horizon is within the singularity). At the event horizon with "Schwarzschild radius" $r = 2m$, the metric is not singular. At the "origin", $r = 0$ the metric is well-defined, and since Eq.'s (1), (3) and (5) satisfy conditions (a)–(d), any one is as good as any other, and so Eq. (5) is as valid as Eq. (1) insofar as the methods of the astrophysical scientists apply. Since metrics (1), (3) and (5) all satisfy conditions (a)-(d) there is no *a priori* reason to favour one over the other. Moreover, all the faults associated with metrics (3) and (5) are shared by metric (1), insofar as the methods of the astrophysical scientists are concerned, despite them all satisfying the required conditions (a)–(d). Those faults lie in the assumptions of the astrophysical scientists, as applied to all the Schwarzschild spacetime metrics above.

It is of utmost importance to note that Eq. (1) is not in fact Schwarzschild's solution. Here is Schwarzschild's actual solution.

$$ds^2 = \left(1 - \frac{\alpha}{R}\right)dt^2 - \left(1 - \frac{\alpha}{R}\right)^{-1}dR^2 - R^2\left(d\theta^2 + \sin^2\theta\, d\varphi^2\right),$$

$$R = \left(r^3 + \alpha^3\right)^{\frac{1}{3}}, \quad 0 < r < \infty, \quad \alpha = const.$$

Here r is not a distance of any kind in the manifold; and it is not the inverse square root of the Gaussian curvature of the spherically symmetric geodesic surface in the spatial section of Schwarzschild's solution — it is a parameter (and so it is also in Eq. (1)). Schwarzschild's solution contains only one singularity, when $r = 0$, and so it precludes the black hole. The so-called "Schwarzschild solution" is a corruption, due to David Hilbert [22, 23], of Schwarzschild's solution, and the solution obtained independently by Johannes Droste [24].

The correct generalised treatment of Schwarzschild geometry is given in [16–21].

3 The usual derivation of the "Schwarzschild solution"

The astrophysical scientists begin with Eq. (2) and propose a generalisation of the form (or equivalent thereof),

$$ds^2 = e^{2\lambda}dt^2 - e^{2\beta}dr^2 - r^2\left(d\theta^2 + \sin^2\theta\, d\varphi^2\right), \tag{7}$$

the exponential functions being introduced to maintain the signature of Minkowski spacetime, $(+, -, -, -)$, thereby ensuring that the coordinates r, θ, φ remain space-like quantities and t remains a time-like quantity [1–9, 11, 12]. Both λ and β are real-valued analytic functions of only the real variable r. Eq. (1) is then obtained in accordance with conditions (a)–(d). Despite the fixed signature of Eq. (7), the astrophysical scientists permit a change of signature in their resultant Eq. (1), in violation of their construction of Eq. (7), by which they produce a black hole by the Kruskal-Szekeres method. Note that the change of signature in Eq. (1) to $(-, +, -, -)$, in violation of the construction of Eq. (7), causes the rôles

of the quantities t and r to be exchanged, i.e. t becomes a space-like quantity and r becomes a time-like quantity. This means that all the components of the metric tensor of Eq. (1) become functions of the time-like quantity r: but this is then a non-static metric, in violation of condition (a).

There is no matter present in the derivation of Eq. (1) from Eq. (7), since all matter, including sources, is eliminated by construction, according to condition (c), i.e. $R_{\mu\nu} = 0$, and since there is no matter present in Eq. (2) either. It is however claimed by the astrophysical scientists that matter is nonetheless present as a source of the alleged gravitational field "outside a body", and that the field caused by this source, permeating the spacetime "outside" it, in the spacetime of $R_{\mu\nu} = 0$, is Schwarzschild spacetime, obtained from Eq. (7). The constant appearing in the line-element for the "Schwarzschild solution" the astrophysical scientists arbitrarily assign as mass, *post hoc*, by simply inserting Newton's expression for escape velocity: a two-body relation into an alleged one-body problem (their "outside a body"). But it is obviously impossible for Schwarzschild spacetime, which is alleged by the astrophysical scientists by construction to contain one mass in an otherwise totally empty Universe, to reduce to or otherwise contain a relation that is defined in terms of the *a priori* interaction of two masses. Their invalid resort to Newtonian theory is amplified by writing Eq. (1) in terms of c and G explicitly,

$$ds^2 = \left(c^2 - \frac{2Gm}{r}\right)dt^2 - c^2\left(c^2 - \frac{2Gm}{r}\right)^{-1}dr^2 -$$
$$- r^2\left(d\theta^2 + \sin^2\theta d\varphi^2\right).$$

The term $2Gm/r$ is now immediately recognised as the square of the Newtonian escape velocity from a mass m at radius r. And so the astrophysical scientists assert that for a black hole the "escape velocity" is that of light in vacuum at an event horizon ("Schwarzschild radius") $r_s = 2Gm/c^2$. But escape velocity is a concept that involves *two bodies* - one body escapes from another body. Even though one mass appears in the expression for Newton's escape velocity, it cannot be determined without recourse to a fundamental two-body gravitational interaction by means of Newton's theory of gravitation. The *post hoc* introduction of mass into the "Schwarzschild solution" is thus, inadmissible. Furthermore, the quantity r appearing in Newton's expression for escape velocity is a radial distance, but it is not radial distance in Schwarzschild spacetime because it is not even a distance in Schwarzschild spacetime.

4 Conclusions

The foregoing counter-examples show that the methods used by the astrophysical scientists in analysing Eq. (1), by which they construct the black hole, are invalid. Instead of using the line-element to determine all the intrinsic geometric properties of the manifold, as they should, they instead make false

assumptions, by mere inspection, as to the "origin", the geometric identity of the quantity r, the values of the Riemann tensor scalar curvature invariant (the Kretschmann scalar), and the presence of matter. The fact is that the quantity r appearing in all the line-elements discussed herein is not even a distance, let alone a radial one, in any of the line-elements. Moreover, in Eq. (1), $r = 0$ certainly does not mark the "origin" or point at the centre of spherical symmetry of the "Schwarzschild" solution, contrary to the arbitrary assertions of the astrophysical scientists. The identity of the point at the centre of spherical symmetry is also determined from the line-element, by calculation. The astrophysical scientists have never correctly identified the geometric identity of r in Eq. (1). Without knowing the true identity of r, and by making their concomitant additional false assumptions, they have violated the intrinsic geometry of the line-element. It is from these violations that the black hole has been constructed by the astrophysical scientists. There is in truth no solution to Einstein's field equations that predicts the black hole.

Minkowski spacetime is not Special Relativity: there is no matter involved in the transition from Minkowski spacetime to Schwarzschild spacetime, and so Schwarzschild spacetime does not generalise the laws of Special Relativity, and so does not describe Einstein's gravitational field.

References

1. Einstein A. The meaning of relativity. Science Paperbacks and Methuen & Co. Ltd., 1967, 56–57.

2. Schwarzschild K. On the gravitational field of a mass point according to Einstein's theory. *Sitzungsber. Preuss. Akad. Wiss., Phys. Math. Kl.*, 189, 1916.

3. Schutz B. F. A first course in general relativity. Cambridge University Press, UK, 1990.

4. Misner, C. W., Thorne K. S., Wheeler, J. A. Gravitation. W. H. Freeman and Company, New York, 1970.

5. Tolman R. C. Relativity, thermodynamics, and cosmology. Dover Publications Inc., New York, 1987.

6. Pauli W. The theory of relativity. Dover Publications, Inc., New York, 1981.

7. Dirac P. A. M. General theory of relativity. Princeton Landmarks in Physics Series, Princeton University Press, Princeton, New Jersey, 1996.

8. Landau L., Lifshitz E. The classical theory of fields. Addison-Wesley Publishing Company, Inc., Reading, Massachusetts, 1951.

9. Foster J., Nightingale J. D. A short course in General Relativity. Springer-Verlag, New York, Inc., 1995.

10. Finkelstein D. Past-future asymmetry of the gravitational field of a point particle. *Phys. Rev.*, 1958, v. 110, no. 4, 965–967.

11. Eddington A. S. The mathematical theory of relativity. Cambridge University Press, Cambridge, 2nd edition, 1960.

12. Weyl H. Space, time, matter. Dover Publications Inc., New York, 1952.

13. Kruskal M. Maximal extension of Schwarzschild manifold. *Phys. Rev.*, 1960, v. 119, no. 5, 1743–1745.

14. Szekeres G. On the singularities of a Riemannian manifold. *Math. Debrecea*, 1960, v. 7, 285–301.

15. Efimov N. V. Higher geometry. Mir Publishers, Moscow, 1980.

16. Crothers S. J. Gravitation on a spherically symmetric metric manifold. *Progress in Physics*, 2007, v. 2, 68–74.

17. Crothers S. J. The Schwarzschild solution and its implications for gravitational waves. *Mathematics, Physics and Philosophy in the Interpretations of Relativity Theory*, Proceedings of the Conerence, Budapest, 4–6 September, 2009.

18. Crothers S. J. On the geometry of the general solution for the vacuum field of the point-mass. *Progress in Physics*, 2005, v. 2, 3–14.

19. Crothers S. J. Certain conceptual anomalies in Einstein's theory of relativity. *Progress in Physics*, 2008, v. 1, 52–57.

20. Crothers S. J. On isotropic coordinates and Einstein's gravitational field. *Progress in Physics*, 2006, v. 3, 7–12.

21. Crothers S. J. On the ramifications of the Schwarzschild space-time metric. *Progress in Physics*, 2005, v. 1, 74–80.

22. Abrams L. S. Black holes: the legacy of Hilbert's error. *Can. J. Phys.*, 1989, v. 67, 919.

23. Antoci S. David Hilbert and the origin of the "Schwarzschild" solution. 2001, www.sjcrothers.plasmaresources.com/hilbert.pdf

24. Droste J. The field of a single centre in Einstein's theory of gravitation, and the motion of a particle in that field. *Ned. Acad. Wet., S. A.*, 1917, v. 19, 197.

25. Brillouin M. The singular points of Einstein's Universe. *Journ Phys. Radium*, 1923, v. 23, 43.

————————————

Is Fundamental Particle Mass 4π Quantized?

Robert A. Stone Jr.

1313 Connecticut Ave, Bridgeport, CT 06484, USA
E-mail: robert.a.stone.jr@gmail.com

The Standard Model lacks an explanation for the specific mass values of the fundamental particles. This is to report that a single spin quantized mass formula can produce the masses of the proton, the W, and the three electron generations. The 4π mass quantization pattern limits the electron generations to three, while the particle's generational property is one of the components of the proposed intra-particle quantization process. Although the developed relationships are presently phenomenological, so was Bohr's atomic quantization proposal that lead to quantum mechanics.

1 Introduction

In an attempt to understand the reason for particle mass values, several authors have looked for mass relationships among the known particles.

Nambu [1] suggested that quark composite particle mass may be quantized, showing a 70 MeV quantization pattern.

Palazzi [2] (2007) revisits this hypothesis for mesons showing that this quantization pattern is statistically real.

Ne'eman and Sijacki [3] use the SL(4,R) group and spin (1/2,3/2,5/2, etc.) to produce the Regge trajectory like behavior of quark particle masses suggesting the possibility that mass may be spin quantized.

What has not been seen is that given the experimental and theoretical uncertainty, the measured $W^{\pm}$ mass of 80398 ± 25 MeV [4] is exactly $2m_p/m_e$ (3672.30534) times the mass value symmetrically between the electron and the proton ($\sqrt{m_p\,m_e} = 21.89648319$ MeV), i.e. 80410.57 MeV.

2 Fundamental particle mass, a spin quantized process?

Taking a mass symmetric approach to fundamental particle mass leads to an eloquently simple spin quantized mass relationship between the stable spin 1/2 electron and proton mass and the unstable spin 1 $W^{\pm}$ particle mass given by

$$m_x = M_{\text{sp}}\,(2S\,m_p/m_e)^{(SCM)}, \qquad (1)$$

where x is {p,e,W}, the mass symmetry point M_{sp} is 21.89648319 MeV, S is the spin quantum number $\{\frac{1}{2},1\}$, C is the charge quantum number $\{\pm 1\}$, and M is the matter type quantum number {matter = +, anti-matter = −}.

Thus equation (1) is both mass and charge up/down symmetric, spin quantized and indicates Nature may be fundamentally mass symmetric.

As indicated in §9, this mass up/down symmetry is in keeping with the measured cosmological constant.

3 Nature's constants, as functions of 4π

Proposing natures coupling constants are a function of 4π and the fine structure coupling constant and the weak (angle) coupling constant are connected to mass, yields the following 4π definitions.

The fine structure constant $\alpha_{\text{cs}} = \pi\varsigma(4\pi\varrho)^{-2}/(2\sqrt{2})$, the charged weak angle $\alpha_{\text{sg}} = 2\sqrt{2}(4\pi\varrho)^{-1}$ ($\sim$.2344 vs .2312 [5]), where "g" is the other force that couples to produce the weak coupling constant. The relationship to mass is $\pi m_e/m_p = \alpha_{\text{cs}}\alpha_{\text{sg}} = \alpha_{\text{cg}} = \pi\varsigma(4\pi\varrho)^{-3}$ and thus $m_p/m_e = (4\pi\varrho)^3/\varsigma$. The uncharged (neutrino) weak angle $\alpha_{\text{sg}(1)} = 2\sqrt{2}(4\pi 1)^{-1}$ ($\sim$.2251 vs .2277 [6]). The new constant $\varrho = \alpha_{cs}\,\alpha_{sg(1)}\,m_p/(m_e\,\pi) = 0.959973785$ and $\varsigma = (4\pi\varrho)^3\,m_e/m_p = 0.956090324$.

4 Fundamental particle mass, a 4π quantized process?

Equation (1) rewritten with the 4π definition of m_p/m_e results in

$$m_x = M_{\text{sp}}\,(2S\,(4\pi\varrho)^3/\varsigma)^{(SCM)}. \qquad (2)$$

In addition to being spin quantized, equation (2) indicates that the fundamental particle mass quantization process is a function of $(4\pi)^x$. For example, the pure theory $m_{p(1,1)}/m_{e(1,1)}$ ratio ($\varrho = 1, \varsigma = 1$) is exactly $(4\pi)^3$ where the deviation from the pure theory 4π quantization process is given by ϱ.

5 Three electron generations, a 4π quantized process?

The electron generational mass ratios also appear to be a function of $(4\pi\varrho_x)^x$ or more precisely $(4\pi\varrho_x)^{(3-x)}$.

The first ($x = 1$) mass ratio μ to e (i.e m_{e_1}/m_{e_0}) is $\sqrt{2}(4\pi\varrho_1)^{(3-1)}$ where $\varrho_1 = .962220482$ while the second ($x = 2$) mass ratio m_{e_2}/m_{e_1} is $\sqrt{2}(4\pi\varrho_2)^{(3-2)}$ with $\varrho_2 = .946279794$.

Note that ϱ and ϱ_x are believed to be the deviation from pure theory for two separate frequency components of the quantization processes.

Thus the form of the first and second (x=1,2) generation mass ratios ($m_{e(x)}/m_{e(x-1)}$) is $\sqrt{2}(4\pi\varrho_x)^{3-x}$. The deviation from the generational pure theory 4π quantization process increases (smaller ϱ_x) with higher generations.

This $\sqrt{2}(4\pi)^{3-x}$ pattern also results in the $x = 3$ mass ratio (m_{e_3}/m_{e_2}) of $(4\pi)^{(3-3)}$, i.e. no higher $(4\pi)^x$ quantized mass states and thus no higher generations.

The similarity of 4π quantization allows the fundamental particle equation (1) to be combined with the generational re-

8

Robert A. Stone Jr. Is Fundamental Particle Mass 4π Quantized?

lationship into a single phenomenological equation given by,

$$m_x = M_{\text{sp}(n)} \left(2S \left(4\pi\varrho\right)^3 / \varsigma\right)^{(SCM)}, \qquad (3)$$

where $M_{\text{sp}(n)} = M_{\text{sp}} \, S^{-n/2} (4\pi\varrho_n)^{(6Sn-Sn(n+1))}$ and $\varrho_n = 1 - \log(1 + 64.75639 \, n/S)/(112S)$ are used and generation n is {0,1,2}.

From (3), the m_{e_1} (μ) mass is 105.6583668 MeV (μ = 105.6583668 ± .0000038 MeV [4]) and the m_{e_2} (τ) mass is 1776.83 MeV (τ = 1776.84 ± .17 MeV [4]).

Remember that even though both ϱ_n, and ϱ represent deviations from the pure theory $(4\pi)^x$ quantization nature of these particles' masses, their cause is understood to be related to two separate quantization process components.

6 The Standard Model and quantization

First, the quantization proposition is not in conflict with the existence of quarks. Rather quantization is an additional constraint. The quantization proposition is that if there is a (pseudo-) stable frequency quantized state, then there is an observed (persistent) massed particle resulting in;

    1) a specific stable quantization state energy/mass or

    2) a pseudo-stable quantized decay mass value.

Thus the quantization process constrains the stable particle base mass or unstable particle decay point mass while the types and symmetries of quarks construct the particle variations seen in the "particle zoo".

That quark composite particle masses are quantized was first suggested by Nambu [1] and recently statistically validated by Palazzi [2]. The quantization increments cited are 70 (n=integer) and 35 MeV (n=odd or n=even) which are approximately $M_{\text{sp}} \pi$ and $M_{\text{sp}} \pi/2$. Thus for example η (547) has n=16 [2] and using $M_{\text{sp}} \, n\pi/2$ gives $m_\eta = M_{\text{sp}} \, 8\pi \simeq 550$.

A Regge trajectory like spin quantum number based quantization pattern is given by Ne'eman and Sijacki [3] where the particle's measured mass vary about the predicted points. For the (3/2,1) group the points are approximately $(20, 22, 24) \, \pi \, M_{\text{sp}}$, for the (5/2,2) group they are approximately $(24, 26, 28, 30, 32) \, \pi \, M_{\text{sp}}$, and for the (7/2,3) group they are approximately $(28, 30, 32, 34, 36, 38, 40) \, \pi \, M_{\text{sp}}$.

Second, a quantizing mechanism as fundamental to the nature of massed particles is a natural explanation given QM's quantized nature.

Third, an intra-particle quantization process minimally needs two intra-particle frequency components. Equation (3) suggests one component is related to the particle's "invariant" mass/energy and a second component is related to the generational mass symmetry point. A generational component could be the source for and thus explain the generational exchange seen in the muon neutrino nucleon interaction $\nu_\mu + N \rightarrow P^+ + \mu^-$. The generational component's effect on the charged particle mass symmetry point is $M_{\text{sp}(n)}$.

Is the massed particle a "quantized photon"?

Is the first photonic component of the quantization process the underlying reason for the universality of Maxwell's equations for both photons and charged particles?

Is the second quantizing component responsible for the intra-particle mass and charge quantization, for the generational property, as well as the (inter-particle?) quantization of QM?

7 Equation 1 and new particles

If quantization is the source of (1) then, quark structure permitting, there may be a second generation proton. From the phenomenological equation (3), $m_{p_2} \simeq 194$ GeV. This second generation proton is within LHC's capabilities.

Note that equation (3) is phenomenological and another option exists for merging the electron generations.

Equation (1) also indicates the possibility of a new "lepton like" (mass down charge down) spin 1 light $W^\pm$ particle with a mass of ~ 5.96 KeV (m_{lW}). If such low frequency/energy quantization is possible, the $lW^\pm$'s decay, like the $W^\pm$'s decay, would be instantaneous. At KeV energy, attempted quantization may only result in enhanced photon production. At MeV energies, $lW^\pm$ pair production with instantaneous decay would look like an electron positron pair production but would actually be $lW^- \rightarrow e^- + \bar{\nu}$ and $lW^+ \rightarrow e^+ + \nu$ decays.

Finally, the super-symmetric (charge and mass symmetric) view that results from equation (1) can make some fundamental Standard Model problems go away.

8 The matter only universe problem

The present SM has only a matter anti-matter mass creation process, yet we appear to have a matter only universe. This aspect is presently unaccounted for.

The super-symmetric view indicated by the charge and mass up/down symmetry of (1) and (2) enables the possibility of an alternate mechanism for fundamental particle creation.

This alternate process symmetrically breaks the electron and proton of the same mass (for eq. (2), at $\varrho = (4\pi)^{-1}, \varsigma = 1$, $m_e = m_p$) into a proton of higher mass (up) and an electron of lower mass (down), yielding a matter only universe.

9 The cosmological constant problem

Given the symmetric mass up/down symmetry breaking of (2) that produces a matter only universe, the symmetry breaking contribution to the cosmological constant can be zero and thus consistent with the observed cosmological constant value. Based on the Standard Model's view, QCD's contribution to the cosmological constant produces a value that is off by 10^{46}, i.e 46 orders of magnitude wrong [7], with no substantive resolution. Using the Standard Model view for the electroweak contribution results in an even greater error.

The preciseness of the predicted $W^\pm$ particle mass of equation (1) and the pattern of quantization shown via (2)

and (3) call into question many of the Standard Model views and assumptions about the causality of the observed "invariant mass" values.

However, it is precisely the Standard Model view and the Standard Model symmetry breaking approach that results in these fundamental Standard Model problems. Maybe we should listen to these fundamental problems with more care.

10 Summary

The Standard Model is highly successful in many areas, especially QM and QED. One of the open questions for the Standard Model is the cause of the specific invariant mass values of fundamental particles.

The accepted Standard Model view hides the fact that the measured $W^\pm$ mass of 80398 ± 25 MeV [4] is exactly $2m_p/m_e$ (3672.30534) times the mass value symmetrically between the electron and the proton ($M_{sp} = (m_p \, m_e)^{1/2}$) and the Standard Model gives no reason for the electron generations nor their masses.

A mass and charge symmetric, 4π quantized and spin quantized mass formula is given that produces the exact $W^\pm$ particle mass. The electron generation mass ratios can be produced using a 4π related magnitude, i.e $m_{e(x)}/m_{e(x-1)} = \sqrt{2}(4\pi\varrho_x)^{3-x}$ for x=(1,2).

The common 4π formulation allows the single mass formula (3) to produce the masses of the proton, the W, and the three electron generations.

Equations (1), (2) and (3) strongly suggest several new aspects.

First, in addition to the atomic orbital quantization of QM, there is an intra-particle quantization mechanism which gives the fundamental particles and generations their invariant mass values.

Second, the fundamental particle quantization process is spin $\{\frac{1}{2},1\}$ and 4π quantized.

Third, equation (1) indicates that nature is actually highly symmetric, being charge and mass up/down symmetric.

This symmetry allows for the possibility of an alternate matter creation process for the early universe which results in creating only matter.

In addition the mass and charge super-symmetric view of equation (1) should yield a near zero cosmological constant in keeping with the observed value.

A quantization proposition is not in conflict with the existence of quarks.

A dual approach is required to explain the 4π and spin mass pattern of equation (1), the 4π electron generation mass pattern, and Palazzi's [2] results.

This dual approach involves a quantizing mechanism as the source of the stability and mass value of the spin 1/2 particles, the mass values of the fundamental $W^\pm$ particles, and the decay point mass of quark composites, while the types and symmetries of quarks construct the variations seen in the "particle zoo".

The quantized view of equation (3) indicates that one of the intra-particle quantization components can be the source for the generational identity and a foundation for the generational exchange seen in the muon neutrino interaction $\nu_\mu + N \rightarrow P^+ + \mu^-$.

Is "A quantized form of energy." the answer to the question "What is mass?".

If relationship (1) and the quantization interpretation of (1), (2) and (3) are fundamental, then the recognition of an intra-particle quantization process is required to move the Standard Model to a massed particle model.

References

1. Nambu Y. An empirical mass spectrum of elementary particles. *Prog. Theor. Phys.*, 1952, v. 7, 595.

2. Palazzi P. The meson mass system. *Int. J. of Mod. Phys.*, 2007, v. A22 (2/3), 546–549.

3. Ne'eman Y., Sijacki Dj. SL(4,R) Classification for hadrons. *Phys. Lett.*, 1985, v. B157 (4), 267–274.

4. Amsler C. et al. *Phys. Lett.*, 2008, v. B667, 1; Updated Particle Data Group, Particle Listings 2009 http://pdg.lbl.gov/2009/listings/rpp2009-list-electron.pdf, rpp2009-list-muon.pdf, rpp2009-list-tau.pdf, rpp2009-list-p.pdf, rpp2009-list-w-boson.pdf.

5. Particle Data Group, Physical Constants 2009: http://pdg.lbl.gov/2009/constants/rpp2009-phys-constants.pdf

6. Zeller G.P. et al. (NuTeV collaboration) Precise determination of electroweak parameters in neutrino-nucleon scattering. *Phys. Rev. Lett.*, 2002, v. 88, 091802.

7. Carroll S.M. The cosmological constant. *Living Rev. Relativity*, 2001, v. 4, 1; arXiv: astro-ph/0004075.

From Inspired Guess to Physical Theory: Finding a Theory of Gravitation

Pieter Wagener

Department of Physics, NMMU South Campus, Port Elizabeth, South Africa
E-mail: Pieter.Wagener@nmmu.ac.za

A theory of gravitation satisfying all experimental results was previously proposed in this journal. The dynamics was determined by a proposed Lagrangian. In this paper it is shown how this Lagrangian can be derived heuristically. A Newtonian approach is used, as well as other methods.

1 Introduction

A theory proposed in previous articles in this journal [1–4] relied on two postulates, one of which is that the dynamics of a system is determined by a Lagrangian,

$$L = - m_0 \left(c^2 + v^2\right) \exp \frac{R}{r}, \qquad (1)$$

where m_0 is the *gravitational rest mass* of a test body moving at velocity **v** in the vicinity of a massive, central body of mass M, $\gamma = 1/\sqrt{1 - v^2/c^2}$ and $R = 2GM/c^2$ is the Schwarzschild radius of the central body.

This Lagrangian leads to equations of motion that satisfy all experimental observation of gravitational effects. It also leads to expressions for electromagnetic and nuclear interactions. In this regard it gives the fine spectrum of the hydrogen atom and the Yukawa potential for the nuclear force.

No explanation was given of how this Lagrangian had been determined, but only that its validity is confirmed by the consistency of its resultant equations of motion and agreement with experiment.

It is informative to show how such a Lagrangian can be derived. The procedure leads to an understanding of the creation and development of physical theories.

When a Lagrangian embodies the fundamentals of a physical model it cannot be derived from first principles. What is needed is an inspired guess to start with. The equations of motion derived from the initial Lagrangian are compared with observation. If they do not fit satisfactorily with the first try, then one adjusts the Lagrangian to conform closer to experimental results. This modelling cycle is repeated until a satisfactory agreement is found with observation.

In the case of the above Lagrangian various approaches are possible. We consider some of them.

2 Newton's approach

We follow a *Gedanken* speculation of how Isaac Newton would have derived a law of gravitation if he had been aware of the modern classical tests for a theory of gravitation.

The development of theories of gravitation at the beginning of the previous century is well documented [5, 6]. The essential test for a theory of gravitation at that time was whether it explained the anomalous perihelion precession of the orbit of Mercury, first calculated by Leverrier in 1859. This was satisfactorily explained by Einstein's theory of general relativity. Further predictions of this theory, i.e. the bending of light by a massive body and of gravitational redshift, have subsequently become part of the three benchmark tests for a model of gravitation.

2.1 Modern Newton

It is not generally known that Newton first derived his inverse square law of gravitation by first considering circular orbits [7, 8]. He applied Huygens's law for the acceleration in a circular orbit,

$$a = \frac{v^2}{r}, \qquad (2)$$

and Kepler's third law to arrive at the inverse-square relation. He then proceeded to show in his *Philosophiae Naturalis Principia Mathematica* (there is some doubt about this [9]) that elliptical motion follows in general from this relation.

We follow a similar procedure by assuming a scenario along which Newton could have reasoned today to arrive at a refinement of his law of gravitation.

He would have been aware of the three classical tests for a theory of gravitation and that particles traveling near the speed of light obey relativistic mechanics. Following an iterative procedure he would have started with the simple model of circular orbits, derived the appropriate law of gravity, but modified to accommodate relativistic effects and then generalised it to include the other conical sections. It would finally be compared with other experimental results.

2.2 Finding a Lagrangian

For motion in a circular orbit under the gravitational attraction of a mass M one must have:

$$\frac{v^2}{r} = \frac{GM}{r^2}. \qquad (3)$$

Because of relativistic considerations, the ratio v^2/c^2 must be compared relative to unity, i.e.

$$1 - \frac{v^2}{c^2} = 1 - \frac{GM}{r\,c^2}. \qquad (4)$$

Note that (4) is not an approximation of (2) for $v \ll c$. If we surmise that the inverse square law is only valid for $r \gg R$, one could incorporate higher order gravitational effects by generalising the right-hand side of (4) to a polynomial. Furthermore, to allow other motion besides circles, we multiply the right-hand side by an arbitrary constant K:

$$1 - \frac{v^2}{c^2} = \left(1 + \frac{a'R}{r} + \frac{b'R^2}{r^2} + \dots\right) K \, ,$$

$$= KP'(r) \, , \tag{5}$$

or

$$\left(1 - \frac{v^2}{c^2}\right) P(r) = K \, , \tag{6}$$

where

$$P(r) = 1 + \frac{aR}{r} + \frac{bR^2}{r^2} \dots \, , \tag{7}$$

is the inverse of $P'(r)$.

In order to compare (6) with experiment, we have to convert it to some standard form in physics. To do this we first rewrite (6) as:

$$(1 - K)\frac{c^2}{2} = \frac{v^2}{2} - \frac{GMa}{r} - \frac{av^2R}{2r} + \dots \tag{8}$$

If we multiply this equation by a constant, m_0, with the dimension of mass, we obtain a conservation equation with the dimensions of energy:

$$(1 - K)\frac{m_0 c^2}{2} = \frac{m_0 v^2}{2} - \frac{GMm_0 a}{r} - \frac{m_0 av^2R}{2r} + \dots \tag{9}$$

For $r \gg R$, this equation must approach the Newtonian limit:

$$\frac{m_0 v^2}{2} - \frac{m_0 MGa}{r} = E_N \, , \tag{10}$$

where E_N is the total Newtonian energy. Comparison of (10) with the Newtonian expression gives $a = 1$.

To simplify the notation, we define a constant E with dimensions of energy, such that

$$K = \frac{E}{m_0 c^2} \, . \tag{11}$$

From (6),

$$E = m_0 c^2 \left(1 - \frac{v^2}{c^2}\right) P(r) \, . \tag{12}$$

If we consider (12) as the total energy of the system, we can find a corresponding Lagrangian by separating the potential and kinetic energies:

$$T = -m_0 v^2 P(r) \, ,$$
$$V = m_0 c^2 P(r) \, .$$

The corresponding Lagrangian is therefore:

$$L = T - V = -m_0 \left(c^2 + v^2\right) P(r) \, . \tag{13}$$

Applying the Euler-Lagrange equations to this Lagrangian one can find the equations of motion of the system. The conservation of energy (12) follows again, while for the conservation of angular momentum we find

$$P(r) r^2 \dot{\theta} = \text{constant} = h \, . \tag{14}$$

The equations of motion for the system can then be derived from (12) and (14) as a generalised Kepler problem. From these equations one finds a differential equation of motion of the form

$$\frac{d\theta}{du} = Au^2 + Bu + C \, , \tag{15}$$

where

$$u = \frac{1}{r} \, ,$$

$$A = bR^2 \frac{4 - E}{2h} - 1 \, , \tag{16}$$

$$B = \frac{R(2 - E)}{h^2} \, , \tag{17}$$

$$C = \frac{1 - E}{h^2} \, . \tag{18}$$

The convention $m_0 = c = 1$ was used, and terms higher than R^2/r^2 were ignored.

2.3 Perihelion precession

In the case of an ellipse, the presence of the coefficient A gives rise to a precession of the perihelion. For one revolution this can be calculated as:

$$\frac{6b\pi cR}{\bar{a}(1 - e^2)} \, , \tag{19}$$

where $\bar{a}$ is the semi-major axis and e is the eccentricity of the ellipse. Comparison with the observed value for Mercury gives $b = 1/2$. With this result the polynomial of (7) becomes:

$$P(r) = 1 + \frac{R}{r} + \frac{R^2}{2r^2} + \dots \tag{20}$$

Equation (20) could be regarded as simply a fit to experimental data. The theoretical physicist, however, will look for a pattern or a generalisation of some underlying physical law. The form of the equation leads one to propose that the above terms are the first three terms in the Taylor expansion of

$$P(r) = \exp \frac{R}{r} \, . \tag{21}$$

Confirmation of this form, which is aesthetically more acceptable, must come from other experimental results, such as the bending of light by a massive object. This is shown in the first article referred to above [1].

The Lagrangian of (13) can now be rewritten in the form of (1):

$$L = -m_0 \left(c^2 + v^2\right) \exp \frac{R}{r} \, , \tag{22}$$

or in terms of the potential Φ as

$$L = -m_0 \left(c^2 + v^2\right) \exp \frac{2\Phi}{c^2}. \tag{23}$$

The conservation of energy equation (12) can be written as

$$E = m_0 c^2 \frac{e^{R/r}}{\gamma^2}. \tag{24}$$

We define a variable *gravitational mass* as

$$m = \frac{m_0}{\gamma^2}, \tag{25}$$

so that (24) can also be written as

$$E = mc^2 e^{R/r}. \tag{26}$$

3 A gravitational redshift approach

We continue with the hypothetical Newton, but starting from another experimental observation. In the presence of a body of mass M a photon undergoes a frequency shift relative to its frequency ν_0 in the absence of the body:

$$\nu = \nu_0 \left(1 - \frac{R}{2r}\right),$$

where ν_0 is an invariant.

In line with our inspired guess approach, we surmise that the right-hand side of this equation is a first order approximation to

$$\nu = \nu_0 e^{-R/2r}, \tag{27}$$

or

$$\nu_0 = \nu e^{R/2r}. \tag{28}$$

Substituting time for the frequency, $\nu = 1/t$ and rearranging:

$$dt = B e^{R/2r} d\tau, \tag{29}$$

where $d\tau$ is an invariant time interval, or proper time, and B is a proportionality constant. Substituting the special relativity relation $dt = \gamma d\tau$ in (29),

$$\frac{1}{B} = \frac{e^{R/2r}}{\gamma}. \tag{30}$$

This is a conservation equation involving the variables r, v and M. In order to relate this equation to the classical conservation of energy equation and its Newtonian limit, the equation must be squared and multiplied by $m_0 c^2$:

$$\frac{m_0 c^2}{B^2} = m_0 c^2 \frac{e^{R/r}}{\gamma^2}. \tag{31}$$

This is the same equation as (24) for $E = m_0 c^2 / B^2$.

From (11) we note that $B^2 = 1/K$. Separating the kinetic and potential energy terms we again find the Lagrangian of (1).

4 An Einstein approach

It is understandable that the large corpus of publications on general relativity (GR) over the past few decades tend to underrate the heuristic approach, or inspired guesses, which are used to derive the field equations of GR. The classic texts do not. On page 152 of Weinberg's *Gravitation and Cosmology* [10] the author emphasises the guesswork that leads to the field equations. Eddington [11, p.82] mentions that "This preliminary argument need not be rigorous; the final test is whether the formulae suggested by it satisfy the equations to be solved". This is a classical heuristic argument.

One can therefore wonder why the heuristic derivation was not continued to generalise the metric of GR,

$$ds^2 = \left(1 - \frac{R}{r}\right) dt^2 - \\ - \frac{1}{1 - \frac{R}{r}} dr^2 - r^2 d\theta^2 - r^2 \sin^2\theta \, d\phi^2, \tag{32}$$

to an exponential form:

$$ds^2 = e^{-R/r} dt^2 - e^{R/r}(dr^2 + r^2 d\theta^2 + r^2 \sin^2\theta \, d\phi^2). \tag{33}$$

The equations of motion derived from this metric are the same as those derived from the Lagrangian of (1), but are conceptually and mathematically simpler [1]. From the resulting conservation equations one can, similarly to the procedures above, derive our Lagrangian.

5 Nordström's first theory

Although not an example of a heuristic derivation, Gunnar Nordström's first theory [12, 13] is an intriguing example of how theories of gravitation could have taken a different direction in 1912.

Nordström's theory, a noncovariant one, is based on a Lagrangian,

$$L = \exp \frac{R}{2r}. \tag{34}$$

In the case of a static, spherically symmetrical field the Lagrangian gives a conservation equation,

$$\gamma \exp\left(-\frac{R}{2r}\right) = A_N. \tag{35}$$

Comparison with (30) shows that $A_N = B$. Nordström's first theory therefore gives the same conservation of energy equation as our theory.

The absence of the $\left(c^2 + v^2\right)$ term in Nordström's Lagrangian accounts for its difference from our theory and Nordström's wrong predictions. This shows up in his conservation of angular momentum,

$$r^2 \frac{d\theta}{dt} = h, \tag{36}$$

where h = constant.

Nordström's theory [14] also gives a variation of mass,

$$m = m_0\, e^{-R/2r}. \tag{37}$$

From (11) and (26) our theory gives

$$m = Km_0\, e^{-R/r}. \tag{38}$$

The close correlation between our theory and that of Nordström raises the possibility of Nordström, or anyone else reading his paper of 1912, deriving the Lagrangian of (1). If this had happened, and the resultant agreement with Mercury's perihelion precession were found, then the study of gravitation could have followed a different direction.

References

1. Wagener P. C. A classical model of gravitation. *Progress in Physics*, 2008 v.3, 21–23.

2. Wagener P. C. A unified theory of interaction: Gravitation and electrodynamics. *Progress in Physics*, 2008, v.4, 3–9.

3. Wagener P. C. A unified theory of interaction: Gravitation, electrodynamics and the strong force. *Progress in Physics*, 2009, v.1, 33–35.

4. Wagener P. C. Experimental verification of a classical model of gravitation. *Progress in Physics*, 2009, v.3, 24–26.

5. Whitrow G.J. and Morduch G.E. In: Beer A., editor. *Vistas in Astronomy*. Pergamon, London,1965, v.6, 1–67.

6. Pais A. Subtle is the Lord: the science and the life of Albert Einstein. Oxford Univ. Press, Oxford, 1982.

7. Westfall R.S. Never at rest. Cambridge Univ. Press, Cambridge, 1986.

8. Guth E. In: Carmeli M., Fickler S.I. and Witten L., editors. *Relativity*. Plenum Press, New York, 1970, 161.

9. Weinstock R. Dismantling a centuries-old myth: Newton's principia and inverse-square orbits. *Am. J. Phys.*, 1982, v.50, 610.

10. Weinberg S. Gravitation and cosmology. John Wiley, New York, 1972.

11. Eddington A.S. The mathematical theory of relativity. 2 ed. Cambridge Univ. Press, Cambridge, 1960.

12. Nordström G. *Phys. Z.*, 1912, v.13, 1126.

13. Nordström G. *Ann. Phys. (Leipzig)*, 1913, v.40, 856.

14. Behacker M. *Physik. Zeitschr.*, 1913, v.14, 989.

Resolving Inconsistencies in de Broglie's Relation

Pieter Wagener

Department of Physics, NMMU South Campus, Port Elizabeth, South Africa
E-mail: Pieter.Wagener@nmmu.ac.za

Modern quantum theory is based on de Broglie's relation between momentum and wave-length. In this article we investigate certain inconsistencies in its formulation and propose a reformulation to resolve them.

1 Inconsistencies in de Broglie's relation

Edward MacKinnon made a critical analysis [1–3] of Louis de Broglie's doctoral thesis of 1924 [4]. With this thesis de Broglie is credited with deriving the first relationship between the momentum of a particle and its associated quantum wavelength. MacKinnon's discussion draws some remarkable conclusions. He points out that the most paradoxical feature of de Broglie's thesis is the fact that, although his fundamental argument is essentially relativistic, the only successful applications of his ideas were essentially nonrelativistic. It is well known that his relationship $\lambda = h/mv$ was applied to the Bohr atom and later to the derivation of Schrödinger's equation, both of which are strictly nonrelativistic models. What is not so well known is that the arguments leading to $\lambda = h/mv$ are very much relativistic. De Broglie's problem was to find the relativistic transformation of

$$h\nu_0 = \widetilde{m}_0 c^2, \tag{1}$$

where the relativistic rest mass $\widetilde{m}_0$ and the frequency ν_0 are invariant.

His considerations led him to assign three different frequencies to the same particle:

$$\nu_0 = \frac{\widetilde{m}_0 c^2}{h},$$

the internal frequency in the rest system;

$$\nu_1 = \nu_0 \sqrt{1 - v^2/c^2},$$

the internal frequency as measured by an external observer who sees the system moving with velocity v;

$$\nu = \frac{\nu_0}{\sqrt{1 - v^2/c^2}},$$

the frequency this observer would associate with the particle's total energy.

MacKinnon further points out that de Broglie emphasized the frequency associated with an electron, rather than the wavelength. His wavelength-momentum relationship occurs only once in the thesis, and then only as an approximate expression for the length of the stationary phase waves characterizing a gas in equilibrium. Most of MacKinnon's article is devoted to analyzing the reasons why de Broglie's

formula proved successful, despite the underlying conceptual confusion. He finally expresses amazement that this confusion could apparently have gone unnoticed for fifty years.

In addition to MacKinnon's criticism, one can also have doubts about some of the applications of de Broglie's formula in quantum mechanics, particularly to electron diffraction. In standard physics texts [5, p. 567], in order to apply the de Broglie relation, the following assumption is made

$$\widetilde{E}^2 = |\mathbf{p}|^2 c^2 + \widetilde{m}_0^2 c^4 \simeq |\mathbf{p}|^2 c^2. \tag{2}$$

The notation is in accordance with previous articles by the author in this journal [6, 8].

From this equation the momentum of the electron is calculated as $|\mathbf{p}| = \widetilde{E}/c$, and from the de Broglie relation it follows that $\lambda = hc/\widetilde{E}$.

Various explanations are given to support the approximation of (2). The most common is to assume that it is allowed for $\widetilde{E} \gg \widetilde{m}_0 c^2$. Although this assumption satisfies experiment, it is not mathematically or conceptually acceptable. Electron diffraction becomes measurable at high energies and velocities, where relativistic equations are applicable. For these equations to be mathematically consistent all terms must be retained, particularly those in the conservation of energy equation. Another approach is to ignore (2) and to apply a semi-nonrelativistic result, $\widetilde{E} = p^2/2\widetilde{m}$ or $T = \mathbf{p}^2/2\widetilde{m}$ [5, p.147], where $\widetilde{m} = \gamma \widetilde{m}_0$ is the relativistic mass of a particle and T is its kinetic energy. This is clearly untenable because of the high velocities.

Another justification for the approximation is that it works for "experimental purposes" [9]. These assumptions might not be serious to verify predictions expeerimentally, but in the spirit of present attempts to formulate a quantum theory of gravity, these assumptions warrants closer scrutiny.

The use of the above approximation is sometimes subtle and not so apparent. In a popular textbook [10, Problem 12.10] the following equation is given for the conservation of energy in Compton scattering:

$$\frac{hc}{\lambda} + m_0 c^2 = \frac{hc}{\lambda'} + m c^2, \tag{3}$$

where m_0 and m are respectively the rest and final mass of the electron.

The equation is inconsistent since wave and corpuscular expressions are combined in one equation. The expression hc/λ is simply a shortcut for $\sqrt{p^2 c^2 + m_{\nu_0}^2 c^4}$, where the rest mass of the photon $m_{\nu 0}$ is set to zero and de Broglie's relation is then applied to p. In general, the assumption of $\widetilde{m}_0 = 0$ for a photon has had an uneasy niche in theoretical physics [1].

In a previous paper [6] we presented a unified theory of gravitation and electromagnetism. We show below that the model of that theory resolves the inconsistencies discussed above.

2 A scalar momentum

In the aforementioned paper the following conservation of energy equation, derived in an earlier paper [7], was given for the gravitational model:

$$E = m_0 c^2 \, \frac{e^{2\Phi/c^2}}{\gamma^2} = \text{total energy}, \tag{4}$$

where

$$\left.\begin{array}{l} \Phi = \text{ gravitational potential}, \\[4pt] m_0 = \text{gravitational rest mass of a test body} \\ \qquad \text{moving about a central mass } M. \end{array}\right\} \tag{5}$$

We have generalized the exponential term in this paper to a general potential $\Phi = Rc^2/2r$, where $R = 2GM/c^2$ is the Schwarzschild radius of the central body.

We now define a scalar momentum appropriate to our model.

A constant P_0 with dimensions of linear momentum can be defined in terms of the energy E as

$$P_0^2 = m_0 E. \tag{6}$$

Eq. (4) can then be written as

$$P_0 = \frac{m_0 c}{\gamma} \exp \frac{\Phi}{c^2}, \tag{7}$$

or, if the mass constant m_0 is not required in the energy equation, as

$$E = \frac{P_0 c}{\gamma} \exp \frac{\Phi}{c^2}, \tag{8}$$

$$= Pc \exp \frac{\Phi}{c^2}, \tag{9}$$

where

$$P = \frac{P_0}{\gamma}. \tag{10}$$

In reference [6] we found the following relationship between the gravitational and electromagnetic energies:

$$E = \widetilde{E}\, e^{\Phi/c^2}, \tag{11}$$

where $\widetilde{E} = \widetilde{m}c^2$ is the energy function of Special Relativity.

Comparing (9) and (11) we get

$$\widetilde{E} = Pc. \tag{12}$$

3 Derivation of de Broglie's relation

3.1 Preliminaries

Using the relationship between frequency ν and wavelength λ,

$$c = \lambda\nu = \sigma\omega, \tag{13}$$

where

$$\sigma = \frac{\lambda}{2\pi} = \frac{c}{2\pi\nu} = \frac{c}{\omega}, \tag{14}$$

we rewrite (12) as

$$\widetilde{E} = P\sigma\omega. \tag{15}$$

Since time does not appear explicitly in the above equation for $\widetilde{E}$, we can write down an equivalent Hamiltonian as

$$\widetilde{H} = P\sigma\omega. \tag{16}$$

This form of the Hamiltonian resembles that of the simple harmonic oscillator, after a canonical transformation with generating function $F = (\widetilde{m}_0/2)\, q^2 \cot Q$, where q and Q are the appropriate canonical variables. The significance of this transformation was first pointed out by Max Born [11, §7].

Briefly, it states that the Hamiltonian of a simple harmonic oscillator, given by

$$\widetilde{H} = \frac{p^2}{2\widetilde{m}_0} + \frac{\widetilde{m}_0 \,\omega^2 q^2}{2}, \tag{17}$$

can, by a canonical transformation with the above generating function, be expressed as

$$\widetilde{H} = \Lambda\omega, \tag{18}$$

where $\Lambda = \text{constant}$.

If our system behaves as an oscillator it follows from (16) and (18) that

$$P\sigma = \text{constant}. \tag{19}$$

This result prompts us to provisionally write the constant in (19) as $\hbar$, Planck's constant divided by 2π. This step is taken *a priori*, and its validity will depend on the overall consistency of the subsequent results. Keeping this supposition in mind, we rewrite (19) as

$$P\sigma = \hbar, \tag{20}$$

and (15) as

$$\widetilde{E} = \hbar\omega = h\nu. \tag{21}$$

3.2 The photo-electric effect

Eq. (21), combined with $\widetilde{E} = \widetilde{m}c^2$, gives the photo-electric effect, $\widetilde{m}c^2 = \hbar\omega = h\nu$. Eq. (21) also confirms the use of the constant h in the expression for gravitational redshift,

$$E = \widetilde{E} \exp \frac{R}{2r} = h\nu \exp \frac{R}{2r}. \tag{22}$$

Eq. (22) is significant in that it contains both h and G in one relation.

The results of (21) and (22) further confirm the consistency of the derivation of (20).

We emphasize that the ω_0, or ω, used above is an internal property of the test particle; it is not its angular velocity about a central body. We cannot say with certainty what the internal physical structure of the test particle should be; only that if some periodic mechanism exists with respect to the test particle the frequency of that mechanism is controlled by the above equations. This, for example, determines the gravitational redshift. As a model for such a type of test particle we shall simply refer to it as a virtual oscillator.

3.3 Derivation

From (14) and (20),

$$P = \frac{h}{\lambda}. \tag{23}$$

Although (23) is similar to the de Broglie relationship between momentum and wavelength, the momentum P is not equal to the classical momentum,

$$\mathbf{p} = \widetilde{m}\mathbf{v}. \tag{24}$$

Nevertheless, we shall see that (23) is consistent with the application of the de Broglie relation, and actually resolves some ambiguities in quantum mechanics [1].

3.4 The relationship between p and P

From (12) and $\widetilde{E} = \widetilde{m}c^2$ we obtain

$$P = \widetilde{m}c. \tag{25}$$

From this we can see that $P = \widetilde{E}/c$ can be regarded as the fourth component of the relativistic four-vector, p_i:

$$p_i = \left(\mathbf{p}, \frac{\widetilde{E}}{c} \right), \quad i = 1, 2, 3, 4, \tag{26}$$

or

$$p_i = (\mathbf{p}, P), \quad i = 1, 2, 3, 4. \tag{27}$$

To find a direct relation between $\mathbf{p}$ and P we note from (24) and (25) that

$$\mathbf{p} = \frac{P\mathbf{v}}{c} \quad \text{or} \quad \mathbf{p}c = P\mathbf{v}. \tag{28}$$

The well-known expression of Special Relativity,

$$\widetilde{E}^2 = \mathbf{p}^2 c^2 + \widetilde{m}_0^2 c^4, \tag{29}$$

can be rewritten, using (28), as

$$\widetilde{E}^2 = P^2 v^2 + \widetilde{m}_0^2 c^4. \tag{30}$$
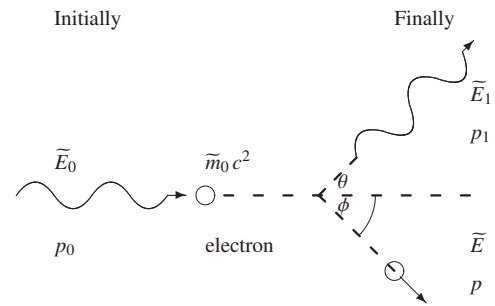
Fig. 1: Compton scattering

4 Applications of de Broglie's relation

The relation of (23), $P = h/\lambda$, is clearly different from the conventional de Broglie relationship. This form is, however, not in conflict with either theory or experiment, but actually simplifies the various formulations.

4.1 Compton scattering

For a photon, $v = c$, and it follows from (23) and (28) that

$$P = |\mathbf{p}| = \frac{h}{\lambda}. \tag{31}$$

An advantage of (31) is that, when applied to Compton scattering, it is not necessary to make the assumption $\widetilde{m}_0 = 0$ in (29). It must also be noted that the assumption $\widetilde{m}_0 = 0$ for a photon is not required in our theory; only $v = c$. The paradox of the photon rest mass is resolved in reference [6].

The Compton effect is described schematically in Fig. 1. The equations below follow from this diagram.

Conservation of momentum:

$$p_0 = p_1 \cos\theta + p \cos\phi, \tag{32}$$
$$p_1 \sin\theta = p \sin\phi. \tag{33}$$

From (32) and (33),

$$p^2 = p_0^2 + p_1^2 - 2p_0 p_1 \cos\theta, \tag{34}$$

and applying (31) gives

$$p^2 = \frac{h^2}{\lambda_0^2} + \frac{h^2}{\lambda_1^2} - \frac{2h^2 \cos\theta}{\lambda_0 \lambda_1}. \tag{35}$$

Since

$$\widetilde{E}^2 = p^2 c^2 + \widetilde{m}_0^2 c^4,$$

it follows that

$$\frac{\widetilde{E}^2}{c^2} - \widetilde{m}_0^2 c^2 = \frac{h^2}{\lambda_0^2} + \frac{h^2}{\lambda_1^2} - \frac{2h^2 \cos\theta}{\lambda_0 \lambda_1}. \tag{36}$$

Conservation of energy:

$$\widetilde{E}_0 + \widetilde{m}_0 c^2 = \widetilde{E}_1 + \widetilde{E}, \tag{37}$$

therefore

$$(\widetilde{E} - \widetilde{m}_0 c^2)^2 = \widetilde{E}_0^2 + \widetilde{E}_1^2 - 2\widetilde{E}_0 \widetilde{E}_1 \,.$$

From (31) and rearranging,

$$\frac{\widetilde{E}^2}{c^2} + \widetilde{m}_0^2 c^2 - 2\widetilde{E}\widetilde{m}_0 = \frac{h^2}{\lambda_0^2} + \frac{h^2}{\lambda_1^2} - \frac{2h^2}{\lambda_0 \lambda_1} \,. \qquad (38)$$

Eq. (38) minus (36), and rearranging:

$$\widetilde{m}_0 c^2 - \widetilde{E} = -\frac{h^2(1 - \cos\theta)}{\widetilde{m}_0 \lambda_0 \lambda_1} \,. \qquad (39)$$

Subsituting (12) and (31) in (39) gives

$$\lambda_1 - \lambda_0 = \frac{h(1 - \cos\theta)}{\widetilde{m}_0 c} \,, \qquad (40)$$

the standard formulation for Compton scattering.

4.2 Electron diffraction

Another advantage of our formulation applies to electron diffraction. From the results $P = h/\lambda$ and $\widetilde{E} = \hbar\omega$ it follows directly that $\widetilde{E} = Pc$. This obviates the approximation used in standard texts on electron diffraction, i.e. $\widetilde{E}^2 \cong \mathbf{p}^2 c^2$.

5 Conclusion

The above derivation and formulation of de Broglie's relation resolves the inconsistencies in de Broglie's original derivation. It also obviates the questionable approximations made in Compton scattering and electron diffraction.

References

1. MacKinnon E. De Broglie's thesis: A critical retrospective. *Am. J. Phys*, 1976, v.44, 1047–1055.

2. MacKinnon E. *Am. J. Phys*, 1977, v.45, 872.

3. Schlegel R. *Am. J. Phys.*, 1977, v.45, 871.

4. De Broglie L. *Ann. Phys. (Paris)*, 1925, v.3, 22.

5. Eisberg R.M. *Fundamentals of modern physics*. John Wiley, New York, 1961.

6. Wagener P.C. A unified theory of interaction: gravitation and electrodynamics. *Progress in Physics*, 2008, v.4, 3–9.

7. Wagener P.C. A classical model of gravitation. *Progress in Physics*, 2008, v.3, 21–23.

8. Wagener P.C. A unified theory of interaction: gravitation, electrodynamics and the strong force. *Progress in Physics*, 2009, v.1, 33–35.

9. Wagner M. Elemente der Theoretischen Physik 1. Friedr. Vieweg, Braunschweig, 1980.

10. Gautreau R. and Savin W. Modern physics: Schaum outline series. McGraw-Hill, 1978.

11. Born M. The mechanics of the atom. Frederick Ungar Publ. Co., New York, 1960.

Solving Many Point Particle Interactions Using the Kepler Route

Riadh H. Al Rabeh

College of Engineering, University of Basra, Iraq
Present address: Lydgate Close, Manningtree, Essex, UK. E-mail: alrabeh_rh@yahoo.com

Events in nature can be described using fields and their associated partial differential equations, or equivalently, the mechanics of interaction of point particles described by ordinary differential equations. The field approach can be looked at as the statistical average of the particle approach and in this sense is more economical for computing. The particle approach, on the other hand, is more fundamental but requires enormous computing power as the model has to follow the movements of every individual particle in the interaction. The present work aims at reducing such computing task by solving the problem of many particle interactions (under a central force environment) in an analytical form for one pair of particles using a Kepler type formula- giving the position of the particle as a function of time only. The resulting (analytical) formula is then used to write the result of the many-particle interaction using simple vector superposition. This approach takes less computing time and can give greater numerical stability when the distances between the particles become small and the force grows as the inverse square of the separation distance.

1 Introduction

The problems of physics can be equally described using interacting particles or fields. The flow of fluids, for example, is the result of basic interactions of an enormous number of small particles moving under an inverse square force system. Such processes can be described correctly using force fields that lead to PDE's like those for fluid mechanics and electrodynamics of material media. It is also possible to achieve a description of the same phenomena using interacting particles following what truly happens in the real world. In the present approach, all particles are assumed identical point masses that may carry charges too. The particles interact under a central force environment in which only the separation distance is of any significance. The coupling constants of such interactions can correspond to any of the known forces of nature — gravitation, electrostatic, or any other similarly behaving force. The resultant coupling constant is simply the arithmetic sum of such constants for all the component forces, with a negative sign to distinguish attractive forces from repulsive forces. The numerical values of the individual constants determine the relative strength of each force. In the most basic interaction involving say a doublet of two oppositely charged point masses, the Coulomb force is the most dominant. When very large groups of particles are considered, magnetic, and gravitational forces start becoming more significant.

By using the particle approach, it is possible to do away with the need for closure models (constitutive equations) that describe the properties of matter - such as the elasticity constants in dynamics and the permittivity and permeability of electrodynamics. In fact, one can use the particle interaction model to derive or check the validity of such closure models. The real difficulty with the particle approach is the computing burden which involves solving one ODE corresponding to every single particle in the interaction. We try to address this problem here by performing an initial integration of the ODE, then using vector superposition find the answer of the original many particle interaction problems. In addition to the obvious gain in computing time, the stability of the solution can be enhanced as the singularity is shifted from Inverse Square to simple Inverse of the separation distance. The accumulation error also reduces as a result in long time predictions.

Predicting the behavior of a single particle is well known- as in calculating the position of the landing of a projectile before it is fired for example. The same can be said, at least in principle, for predicting the behavior of multi-point interactions. The equation of motion tells us that once we fix the initial states of position and velocity of every participating point particle, the outcome is determined. The normal way to solve such problems is to find the velocity of each particle from the acceleration by integration (after superposition of all forces) then do a second integration to find the new position and this is to be performed over a large set of simultaneous Ode's since every particle effects every other. In the present work we instead calculate (analytically) the velocity and position in terms of time only for every particle then use vector superposition to find the final picture.

As we are dealing with point particles only, moments of forces and angular momentum and spin are not considered. The gain is an enhanced stability and reduced computing time coming from the fact that we integrate analytically first then use superposition (simple algebraic operation) for displacement as opposed to affecting the superposition of forces first then integrating for the displacement for every point particle. The method can be described as a multi-particle generalization of the Kepler method originally put (and still in use) for the motion of planets.

2 Theory

In an inverse square interaction (electrostatic/gravitational) of point masses, the expression for the force (acceleration since mass is unity) of a pair of such point masses is given by

$$a = \frac{d^2 r}{dt^2} = \frac{k}{r^2}, \qquad (1)$$

where $a = a(t)$, $r = r(t)$ are the acceleration and separation distances between an isolated pair of particles as a function of time t, and k is the coupling constant (negative for attractive and positive for repulsive forces). The magnitude of k is dependent on the type of interaction and equals the sum of the k's of all the forces at play. For example, in the case of repulsive Coulomb forces $k = \frac{1}{4}\pi\epsilon_0$ and for gravitational forces $k = -G$, where ϵ_0 is the permittivity of empty space and G is the universal gravitational constant. For a small number of interacting particles, the Coulomb forces by far dominate all other forces. All charges and masses of all particles are assumed unity as given above. The actual values can be incorporated in the coupling constant. As the interacting masses are points, there is no need to consider angular velocity, spin, angular momentum or any form of moments of forces on the particle. Mass can simply be taken as the number of particles in any setup.

For a group of interacting particles, the net acceleration of particle j is given by

$$\left.\begin{array}{c} a_j = \dfrac{dv_j}{dt} = \sum\limits_i \dfrac{k_{ij}\, r_{ij}}{r_{ij}^3} \\[2mm] r_{ij} = |r_{ij}|, \qquad i,j = 1,2,\ldots N \end{array}\right\}, \qquad (2)$$

where a_j is the resultant acceleration, v is velocity, k_{ij} is the total coupling constant between particles i and j, and $r_{ij} = r_j - r_i$ is the vector from i to j positions and N is the total number of particles. Equation (2) is a set of simultaneous Ode's that must be integrated once in order to find $v_j(t)$ and twice to find the position $r_j(t)$. For a large number of particles, the task becomes formidable. One way to reduce this burden is by going back to (1) and performing the integration for a pair of particles first, then use the resulting closed form formula to perform superposition of displacements and find the result of the interaction. Since the function $r(t)$ is not known before hand, we follow the Kepler route [2].

Assume a solution in the form $r = t^n$, where t is time and n is an exponent. Substituting in (1) we find that for the equality to hold for any r, the value of n should be $\frac{2}{3}$, and hence,

$$r = \frac{9}{4}\, k t^{2/3}. \qquad (3)$$

This result can be directly checked by differentiating twice and substituting back to recover the original inverse square law. We are using scalar quantities because the force, acceleration and displacement are all along the separation line. The form of (3) is similar to Kepler's third law for orbital motion. In the original Kepler form the distance r refers to the average radius of the orbit and t refers to the mean time of one revolution. Formula (3) however, is more general and refers to motion along the line joining any two interacting particles under an inverse square relation. It is seen that the same formula is suitable for both types of motions. In fact direct substitution in the centrifugal force formula v^2/r using (3), with $v = dr/dt$ gives the same relation between r and t as that derived form (3). A similar result is obtained if we substitute for the Coriolis and the magnetic (Ampere) forces. In fact, such a substitution in the general acceleration definition d^2r/dt^2 reduces it to an inverse square relation. Kepler formula is also shown to be a direct consequence of mechanical similarity [1], and the form $1/r^n$ satisfy similarity for any n, but only $n = (2, -2)$ produces bounded motion, which corresponds to the inverse square force and to the space oscillator type (spring oscillators) interaction forces. The spring type force is also shown to be a special case of the inverse square law for small displacements around an equilibrium point. When (3) is differentiated with respect to time we get

$$v(t) = \frac{dr}{dt} = \frac{2}{3}\, k t^{-1/3} = k r^{-1/2} \qquad (4)$$

further differentiation gives

$$a(t) = \frac{d^2 r}{dt^2} = \left(-\frac{2}{9}\right) k t^{-4/3} = \left(-\frac{2}{9}\right) k r^{-2} \qquad (5)$$

thus we have recovered the inverse square law. Substituting from (4) for the centrifugal force gives

$$\frac{v^2}{r} = \frac{4}{9}\, k^2 t^{-4/3} = k^2 r^{-2} \qquad (6)$$

which is, apart from a constant, has the same form of dependency of t on r. The velocity is given by

$$v_j = v_{j_0} - \frac{2}{3}\, t^{1/3} \sum_i \frac{r_j - r_i}{|r_j - r_i|}, \quad j, i = 1; n, \quad i \ne j \qquad (7)$$

and the position r_j is given by the vector relation

$$r_j = r_{j_0} + v_{j_0} t + \frac{9}{4}\, t^{2/3} \sum_i \frac{r_j - r_i}{|r_j - r_i|}, \qquad (8)$$

where r is the net position vector of all particles and is given, for each, as the vector sum of $n - 1$ vector displacements in addition to the initial position of the particles r_0 and the initial velocity v_0 multiplied by the time t.

The form in (8) is similar to the usual form of the equation of motion for n interacting particles which can be written as

$$r_j = r_{j0} + (dt)v_{j0} + (dt)^2 \sum_i \frac{r_j - r_i}{|r_j - r_i|^3} \qquad (9)$$

with the obvious difference that (9) involves dt rather than t and therefore must be advanced in very small steps to reach the final solution.
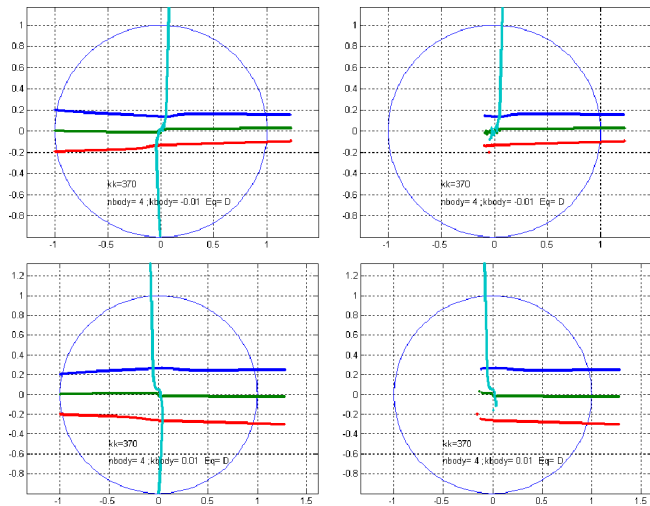
Fig. 1: Four point particles interacting under attractive (top) and re-
pulsive inverse square forces (bottom). Prediction using (8) starts
from time step $kk = 1$ (left) and $kk = 150$ (right), showing the capa-
bility of writing the correct solution for many particles at any time
without going through time evolution.
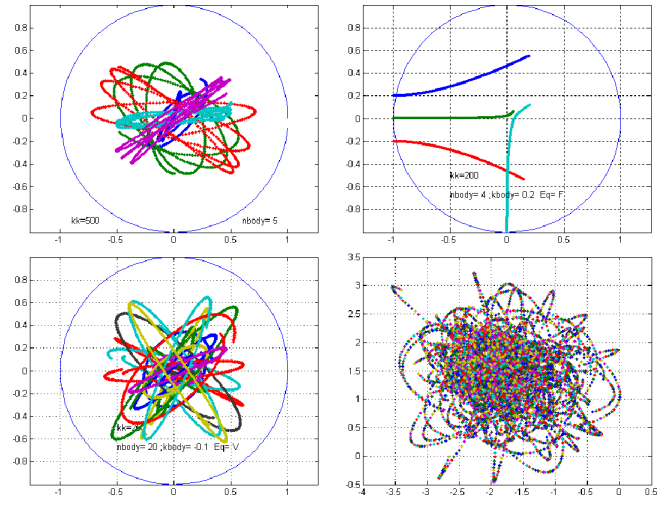
Fig. 3: T: interaction using force (9) for five bodies (confined) and
three bodies (not confined). B: interaction using velocity formula
(7) for 20 & 200 particles under attractive forces with and without a
restraining circular boundary.
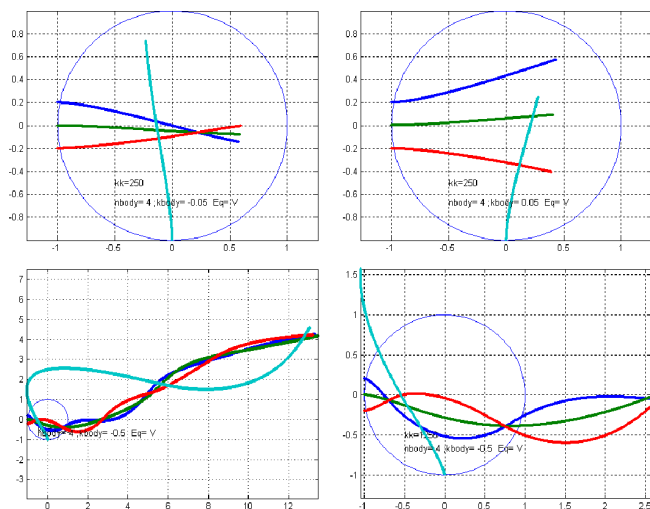
Fig. 2: Predictions using (7) keeping the circular boundary neutral.
T: four point particles interacting under attractive and repulsive in-
verse square forces. B: four point particles interacting under attrac-
tion forces for longer time showing the stability of the velocity solu-
tion at close encounters. Particle paths interweave as a result of the
attraction forces and the (inertia) forces.
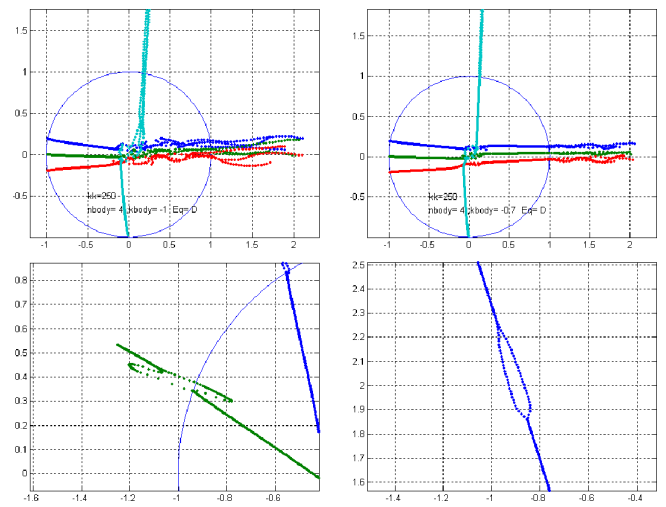
Fig. 4: Instability in the distance formula (8) at small interaction
distances. Each particle path branches into three but recovers back
to a single path as the particles further separate (top figures). The
path disintegrates to only two branches at the encounter of a particle
and a wall of particles. The minimum separation distance needed
for such behaviour increasing with the increase in the value of the
separation constant.
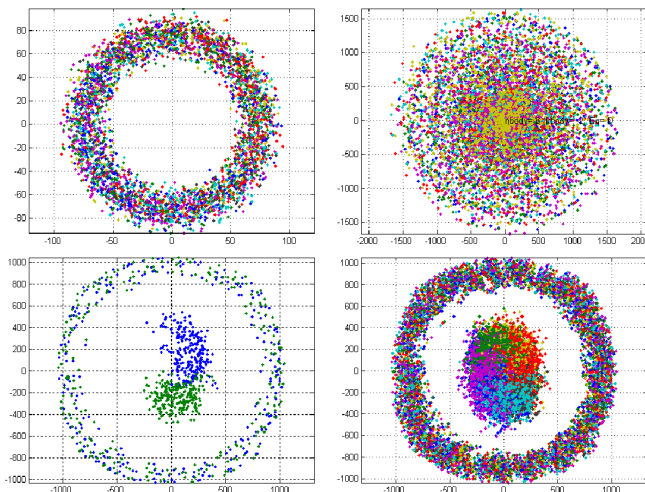
Fig. 5: Rotation, stratification and condensation for large numbers using (8). T: 150 particles under attractive forces only but at different coupling constants. B: one time step and many time steps results of the interaction of 500 particles of equal mix of charges.

3 Results

In this section we concentrate on showing that (7) and (8) give the expected behavior in the case of interacting particles under attraction or repulsion for the case of free particles and for the case of particles trapped inside a constraining circular wall. Comparison is then given with predictions using the usual integration of the inverse square law (9). The distances and coupling constants in these tests are arbitrary- chosen to produce magnified effects of the forces involved. The actual values used are marked on each figure.

Figure 1 shows four particles moving to the right with initial velocities mainly in the horizontal direction. The relative values of initial kinetic energy and the coupling constant determine the behavior of the interacting particles. When the initial velocity is large, as expected, the particles do not change direction appreciably, and when it is small, the repulsion and attraction forces have bigger effect — creating appreciable changes in the particle path. The trajectories are calculated using the displacement expression (8). When using this method it is possible to write the solution at any required time instant as shown in the right hand side frames, wherein the solution is now started at an advanced time location (at the 150th time step kk) and still agreeing with the results of the previous solutions starting at the first time step ($t = 0$) — using the same original set of initial conditions.

Figure 2 shows the results using the velocity expression (7) for the case of attractive and repulsive forces. The stability of the solution is clearly demonstrated by the last frame showing an interweaving paths forced by the equally effective inertial and attractive forces. The velocity formula gives more stable solutions at closer encounters because of the absence of the inverse square term from (7), being replaced by a quantity dependent on t. We should note here also that we

still have the direction cosines to consider for the vector superposition. This, however, has a more favorable behavior at very small separation distances since the quantities x_{ij}/r_{ij}, go to unity as r goes to zero.

In Figure 3, the top two frames show the results of using the force formula (9) for the case of four free particles and five particles respectively confined in a circular boundary. The bottom two frames show the result for large number of particles, when using the velocity formula (7), in which 20 particles are confined in a circular boundary and 200 particles under attraction without a restraining boundary.

Problems have been experienced when using the distance formula (8) when the separation distance is small. As shown in Figure 4, the particle path divides into 3 branches but recovers afterwards as the two bodies separate and the separation distance increases depending also on the strength of the coupling constant. Note the effects on the path even before the target is reached. At the interaction with a wall of charges, the path divides instead, into two parts and recovers back again. This phenomenon requires further investigation as it is found to occur only at larger separation distances if the coupling constant is increased. It is numerical in origin, which is somehow different to what one would expect of this formula.

Figure 5 shows the results of using (9) for a large number of particle interactions. Results for 150 and 500 particles under attractive forces are shown. The results show signs of rotation and pulsation behavior as well as coagulation to form separated groups.

4 Conclusion

It has been shown that it is possible to reduce the computation time and enhance the solution stability for multi-point particle interactions. As a result it has been possible to follow the interaction of very large number of particles using modest computer memory and time. In the author opinion the method shown here is worthy of further development and use to numerically investigate the fascinating world of particle interactions. Evidence of grouping appears when the number of interacting particles is large and without the need of retaining external boundaries or forces.

A consistent phenomenon of path splitting into three and two branches has been observed. It is a direct result of evaluating distances using the square root, as it is treatable by adding a very small constant value to the inverse of the rooted quantities. Clearly this phenomenon needs to be corrected first before the present method acquires its full potential.

References

1. Landau L.D., Lifshitz, E.M. Mechanics. Pergamon press, 1960.
2. Murray C.D. and Dermott S.F. Solar system synamics. Cambridge University Press, 2000.

On a Formalization of Cantor Set Theory for Natural Models of the Physical Phenomena

Alexander S. Nudel'man

Sobolev Institute of Mathematics, Siberian Branch of Russian Academy of Science, Novosibirsk, Russia
E-mail: anudelman@yandex.ru

This article presents a set theory which is an extension of ZFC. In contrast to ZFC, a new theory admits absolutely non-denumerable sets. It is feasible that a symbiosis of the proposed theory and Vdovin set theory will permit to formulate a (presumably) non-contradictory axiomatic set theory which will represent the core of Cantor set theory in a maximally full manner as to the essence and the contents of the latter. This is possible due to the fact that the generalized principle of choice and the generalized continuum hypothesis are proved in Vdovin theory. The theory, being more complete than ZF and more natural according to Cantor, will allow to construct and study (in its framework) only natural models of the real physical phenomena.

This paper is dedicated to the memory of
Alexander M. Vdovin (1949–2007)

I. It is generally accepted that the (presumably) non-contradictory Zermelo-Fraenkel set theory ZF with the axiom of choice is the most accurate and complete axiomatic representation of the core of Cantor set theory. However, it is acknowledged [3, p. 109], that "Cantor's set theory is so copious as to admit absolutely non-denumerable sets while axiomatic set theory [in particular, ZFC] is so limited [Skolem's paradox] that every non-denumerable set becomes denumerable in a higher system or in an absolute sense". An axiomatic set theory defined here and abbreviated as ZFK admits absolutely non-denumerable sets, as it does Cantor theory.

It is feasible that a symbiosis of the proposed theory and Vdovin set theory [1, 2] will permit to formulate a (presumably) non-contradictory axiomatic set theory which will represent the core of Cantor set theory in a maximally full manner as to the essence and the contents. This is possible due to the fact that the generalized principle of choice and the generalized continuum hypothesis are proved in Vdovin theory.

II. Our definition of ZFK will be based on the traditional (classical) concept of formalized theory explained in [4]. But ZFK is a theory which is axiomatic not completely in the traditional sense, so the syntactic aspects of this theory will be described with references to the principal interpretation of ZFK.

Formulae of ZFK are formulae of the signature $\langle \in, S \rangle$, where $\in$ — is a two-place predicate symbol for denoting the (standard) membership relation on the collection S_k of all Cantor's (intuitive) sets, and S — is a null-place functional symbol (a constant) denoting the family of all axiomatized sets, and in the ZFK formulae containing the symbol "S", the latter symbol is always placed to the right of the symbol "$\in$".

In what follows, we use the conventional notation and abbreviations of ZF. In particular, the relativization of a formula φ to the family S is denoted by $[\varphi]^S$. Besides, depending on the context, records "$\in$" and "S" denote either the signature symbols or denoted by them the relation and the family, respectively. Cantor's (intuitive) sets of S_k will be called k-sets, and the axiomatized sets of S will be simply called as sets.

The axioms of ZFK are divided into two groups: G and G_k. The axioms of group G describe the axiomatized sets, and the axioms of group G_k characterize the relationship between Cantor's (intuitive) sets and the axiomatized sets.

The axioms of group G are the axioms of ZFC (formulae of the signature $\langle \in \rangle$), with exception of the axiom of empty set, which are relativized to the family S.

The axioms of group G_k:

1) Axiom of embedding S into S_k

$$\forall x \in S \, \exists y \, (y = x).$$

2) Axiom of (absolutely) empty set

$$\exists x \in S \, \forall y \, (y \notin x).$$

3) Axiom of transitivity of S in S_k

$$\forall x \in S \, \forall y \, (y \in x \rightarrow y \in S).$$

4) Axiom (schema) of generalization

$$[\varphi]^S \rightarrow \varphi,$$

where φ — is a formula of ZFK.

5) Axiom (schema) of mappings to S_k

$$\forall t \, (\forall v, w_1, w_2 (\varphi(v, w_1, t) \, \& \, \varphi(v, w_2, t) \rightarrow w_1 = w_2) \rightarrow$$
$$\rightarrow \forall x \exists y \forall z (z \in y \leftrightarrow \exists v \in x \, \exists w (z = \langle v, w \rangle \, \& \, \varphi(v, w, t)))),$$

where φ — is a formula of ZFK and the variable y does not occur free in φ.

6) Axiom of general replacement

$$\forall x \, (\mathrm{map}(x) \,\&\, \mathrm{dom}(x) \in S \,\&\, \mathrm{rang}(x) \subseteq S \;\to$$
$$\to\; \mathrm{rang}(x) \in S \,\&\, x \in S),$$

where $\mathrm{map}(x)$ is the formula

$$\forall z \, (z \in x \to \exists v, w \, (z = \langle v, w \rangle)) \,\&\, \forall v, w_1, w_2 \, (\langle v, w_1 \rangle \in$$
$$x \,\&\, \langle v, w_2 \rangle \in x \to w_1 = w_2),$$

and k-sets $\mathrm{dom}(x)$ and $\mathrm{rang}(x)$ satisfy

$$\forall v \, (v \in \mathrm{dom}(x) \leftrightarrow \exists w \, (\langle v, w \rangle \in x))$$

and

$$\forall w \, (w \in \mathrm{rang}(x) \leftrightarrow \exists v \, (\langle v, w \rangle \in x)).$$

The logic underlying ZFK is the calculus of predicates in the language of ZFK.

III. It is well known [3, p. 27] that "An axiomatic system is in general constructed in order to axiomatize a certain scientific discipline previously given in a pre-systematic, "naive", or 'genetic' form". ZFK formulated here has been constructed, like ZFC, to axiomatize the "naive" set theory of G. Cantor, or more precisely, to axiomatize its non-contradictory core. But ZFK has a more explicit and tight connection to Cantor set theory than it does ZFC, since ZFK in its principal interpretation defines the collection of all k-sets of S_k (more precisely, $\langle S_k; \in \rangle$) as Cantor pre-axiomatic "world" of sets, and the family S (more precisely, $\langle S; \in \cap (S \times S) \rangle$, where $S \subseteq S_k$) as the axiomatic fragment of Cantor "world" of sets.

It seems natural that ZFK is non-contradictory if ZFC is non-contradictory. Let us show that it is true.

Suppose that ZFC is a non-contradictory theory. Then, ZFC has a model and, in particular, a standard transitive model $\mathfrak{M} = \langle M; \in \cap (M \times M) \rangle$ such that for any set $m \in M$ absolutely all its subsets belong to the family M. It is clear that the model $\mathfrak{M}$ (the family M) includes absolutely denumerable sets. We consider the family M as the interpretation of the signature symbol "S" and will show that any axiom of ZFK is either true in the model $\mathfrak{M}$ or it does not deny the existence of such a model.

It is natural that all axioms of group G are true in the model $\mathfrak{M}$.

Axioms G_k–1 and G_k–2 affirm an obvious fact: any ZFC-set (a set of the family M) is also a set of Cantor "world" of sets S_k.

Axiom G_k–3 affirms natural transitivity of the family M.

Axiom G_k–4 affirms an obvious fact: any statement concerning sets of the family M is also true for sets of Cantor "world" of sets S_k due to the fact that ZFC is a formalization of the (presumably) non-contradictory core of Cantor set theory.

Axiom G_k–5) is a natural generalization of ZFC axiom of replacement which is true in the model $\mathfrak{M}$.

Axiom G_k–6), in fact, affirms that the model $\mathfrak{M}$ is naturally $\subseteq$-complete in the sense that any subset of the family M belongs to that M if its power is equal to the power of a certain set of M.

IV. Let $x \in S$. Then, a k-set $\{y \mid y \subseteq x \,\&\, y \in S\}$ is denoted by $P(x)$. It is clear that $P(x) \in S$ ($P(x)$ is a set) by axioms of group G and G_k–1).

THEOREM (ZFK).

$$\forall x \in S \, \forall y \, (y \subseteq x \to y \in P(x)).$$

Proof. Let us suppose that the contrary is fulfilled and let k-sets x_0 and y_0 be such that $x_0 \in S$, $y_0 \subseteq x_0$ and $y_0 \notin P(x)$. If $y_0 \in S$, than $y_0 \in P(x)$ by an axiom of group G. Therefore, $y_0 \notin S$. Since $\varnothing \in S$, then $y_0 \neq \varnothing$. Since $y_0 \subseteq x_0 \in S$ and S is transitive in S_k (the axiom G_k–3)) then $y_0 \subseteq S$.

Denote by z_0 some element of a k-set y_0. The axiom G_k–5) says that there is a k-set (k-function) f such that

$$f = \{\langle v, w \rangle \mid v \in x_0, (v \in y_0 \to w = v), (v \notin y_0 \to w = z_0)\}.$$

Since $\mathrm{map}(f)$, $\mathrm{dom}(f) = x_0 \in S$ and $\mathrm{rang}(f) = y_0 \subseteq S$, then $y_0 \in S$ by the axiom G_k–6). A contradiction.

V. Let x be a k-set ($x \in S$ or $x \notin S$). Then $P_k(x)$ denotes k-set $\{y \mid y \subseteq x\}$. Since $x \in S_k$, then $P_k(x) \in S_k$ (by the axiom of generalization), i. e. $P_k(x)$ is an element of Cantor pre-axiomatic "world" of sets, whose power by the theorem of G. Cantor is **absolutely** greater than the power of the k-set x.

Let ω be a denumerably infinite set in S. Since $\omega \in S$ then $\omega \in S_k$ (the axiom G_k–1)). It is clear that the k-set $P_k(\omega)$ is absolutely non-denumerable. **THEOREM** says that any k-set y of S_k is such that $y \subseteq \omega$ (i. e. $y \in P_k(\omega)$) is an element of the set $P(\omega)$ of S. Therefore, the equality $P(\omega) = P_k(\omega)$ is always fulfilled. Thus the set $P(\omega)$ is **absolutely non-denumerable** in any axiomatized model of ZFK, i. e. in any model of the type $\langle S; \in \cap (S \times S) \rangle$.

Thus the concept "The set of all subsets of a set X" which is formalized by the axioms of ZFK is absolute (in view of the **THEOREM**) in the sense that it coincides with Cantor concept "The set of all (absolutely all existing in the Cantor 'world' of sets) subsets of a set X".

VI. Finally it should be noted that a symbiosis of the set theory of Vdovin A. M. and the proposed theory may permit to formulate an axiomatic non-contradictory (presumably) set theory, the only standard model of which will be the most important fragment of Cantor "world" of sets. This is ensured by the fact that Vdovin set theory proves the axioms of ZF, the generalized principle of choice, and the generalized continuum-hypothesis which are natural for Cantor "world" of sets, and the theory presented above proves the absolute

character of the concept "The set of all subsets of a set X" which is natural for Cantor "world" of sets, as well.

Since ZF is a generally acknowledged theory and it is applied as a framework for mathematical disciplines used to describe (study) the real physical world, the natural (Cantor-like) character of the future set theory will permit to develop and investigate only natural models of real physical phenomena.

References

1. Vdovin A. M. Foundations of a new axiomatic set theory. *Izv. Akad. Nauk SSSR Ser. Mat.*, 1990, v. 54, 1113–1118; English transl. in *Math. USSR Izv.*, 1991, v. 37.

2. Vdovin A. M. Extension of a new axiomatic set theory. *Izv. Akad. Nauk SSSR Ser. Mat.*, 1993, v. 57, 208–212; English transl. in *Math. USSR Izv.*, 1994, v. 42.

3. Fraenkel A. A. and Bar-Hillel Y. Foundations of set theory. North-Holland, Amsterdam, 1958.

4. Ershov Yu. L., Palyutin E. A. Mathematical logic. Mir Publishers, Moscow, 1984.

"The Arrow of Time" in the Experiments in which Alpha-Activity was Measured Using Collimators Directed at East and West

Simon E. Shnoll*, Ilya A. Rubinstein†, and Nikolai N. Vedenkin†

*Department of Physics, Moscow State University, Moscow 119992, Russia
*Inst. of Theor. and Experim. Biophysics, Russian Acad. of Sci., Pushchino, Moscow Region, 142290, Russia
*Puschino State University, Prospect Nauki 3, Pushchino, Moscow Region, 142290, Russia
†Skobeltsin's Institute of Nuclear Physics, Moscow State University, Moscow 119991, Russia
E-mail: shnoll@mail.ru

In our previous paper (Shnoll and Rubinstein, Progress in Physics, 2009, v. 2, 83–95), we briefly reported about a phenomenon, which can be called the "arrow of time": when we compared histograms constructed from the results of 239-Pu alpha-activity measurements that were obtained using West- and East-directed collimators, daytime series of the "eastern" histograms were similar to the inverted series of the following night, whereas daytime series of the "western" histograms resembled the inverted series of the preceding night. Here we consider this phenomenon in more detail.

1 Introduction

As follows from all our past results, the fine structure of the spectrum of amplitude fluctuations (the shape of the corresponding histograms) is determined by the motion (orientation) of the object studied (the laboratory) in relation to spatial inhomogeneities [2]. The spatial pattern (arrangement in space) of these inhomogeneities is stable: as the Earth rotates about its axis and moves along the circumsolar orbit, similar histogram shapes are realized repeatedly with the corresponding periods (daily, near-monthly, yearly) [3, 4]. The inhomogeneities themselves are analogous to the "numerals on the dial of the celestial sphere", which determine one or another shape of histograms. In the experiments with rotating collimators, beams of α-particles periodically go in the direction of the same inhomogeneities, and similar histograms appear with the corresponding periods [5]. Earlier, when the collimator-equipped devices were immobile (with one collimator directed West and another East), we showed that histograms from either of the collimators would have their analogs (similar shapes) from the other collimator lagging behind by half a day [6] (i.e., by the time needed for the collimators, rotating with the Earth, to face the same spatial inhomogeneities). In the experiments with "daily palindromes", however, this periodicity turned out to be asymmetrical. Asymmetry manifested itself in the daytime series of the "eastern" histograms being similar to the inverted series of the *following* night and the daytime series of the "western" histograms being similar to the inverted series of the *preceding* night [1]. Below we describe this phenomenon in more detail and discuss its possible nature.

2 Materials and methods

The material for this study was series of histograms constructed from the results of long-term measurements of α-activity registered from two ^{239}Pu preparations using two indepen-
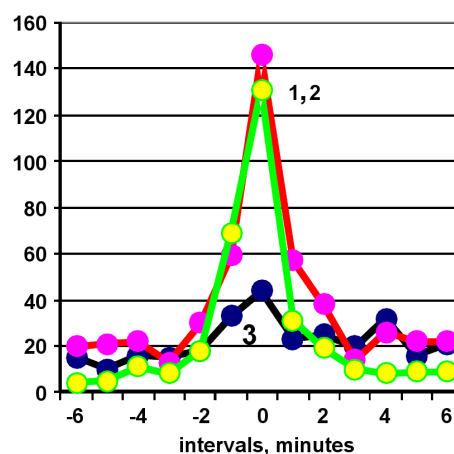
Fig. 1: Illustration of the "palindrome phenomenon". A high probability of histograms of the same order numbers to be similar in the direct daytime/inverse nighttime sequences (line 1) and the direct nighttime/inverse daytime ones (line 2). A low probability of histograms to be similar at comparing the direct daytime and nighttime sequences (line 3). The counter did not contain a collimator. Date of measurements, September 23, 2005. Every line sums up the results of approximately 10000 pairwise comparisons. X axis, interval between the histograms compared (min); Y axis, the number of similar pairs.

dent collimator-equipped devices. The collimators were used to isolate beams of α-particles flying at certain directions. In this study, one collimator was directed East and another was directed West. The technical information on the devices, which were constructed by I. A. Rubinstein and N. N. Vedenkin, can be found in [2]. The analysis of histogram series consists in the estimation of histogram similarity depending on the interval between them. A detailed description of the methodology for constructing and comparing histograms, as well as for obtaining distributions of the number of similar pairs over the length of the interval between the histograms compared, is given in [2]. To characterize correlations in

Fig. 2: Palindrome effects in the simultaneous measurements of ^{239}Pu α-activity with two independent collimator-equipped devices directed East (A) and West (B). Date of measurements, September 22–23, 2003. The axes as in Fig. 1. (A) "East": (1) "day" versus the *following* inverse "night"; (2) "day" versus the *preceding* inverse "night". (B) "West": (1) "day" versus the *preceding* inverse "night"; (2) "day" versus the *following* inverse "night".

Fig. 3: In the measurements of ^{239}Pu α-activity with the West-directed collimator, a direct sequence of daytime histograms is similar to the reverse histogram sequence of the *preceding* night; in the measurements of ^{239}Pu α-activity with the East-directed collimator, a direct sequence of daytime histograms is similar to the reverse histogram sequence of the *following* night. A sum of four experiments.

the change of the histogram shape over time, we used the "palindrome phenomenon" [7] — the high probability of a sequence of histograms con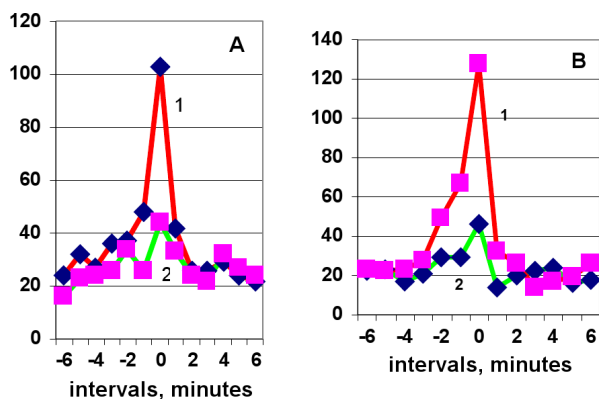structed from the results of daytime measurements (from 6:00 to 18:00, by local longitude time) to be similar to the *inverse* sequence of histograms constructed from the results of nighttime measurements (from 18:00 to 6:00 of the next day). Fig. 1 demonstrates this phenomenon. The source material is series of ^{239}Pu α-activity measurements registered with a counter without collimator (frequency of measurement, 1 point per second). From these data, 1-min histogram sequences were constructed (60 points per histogram), with the histograms smoothed 7-fold by the moving summation method (for visual convenience). Two histogram sequences were compared: (1) from 6:00 to 18:00 by accurate local time ("daytime" sequence) and (2) from 18:00 to 6:00 of the next day ("nighttime" series), each sequence consisting of 720 histograms. The sequences could be direct (from no. 1 to 720) or inverse (from no. 720 to 1).

As seen in Fig. 1, if compared are the direct daytime and nighttime sequences, the similarity (the probability to be similar) of histograms of the same order numbers is low (line 3). In contrast, the direct daytime/inverse nighttime (line 1) or inverse daytime/direct nighttime (line 2) comparisons reveal a high similarity of the same histogram numbers — the "effect of palindrome" [7].

3 Results

The phenomenon of palindrome was easily reproduced in the analysis of measurements performed in different seasons without a collimator. However, the analysis of data obtained in the experiments with collimators (western and eastern) showed varying results; the phenomenon became irregular. In the experiments with the western collimator, palindromes were reproduced regularly when a direct daytime sequence
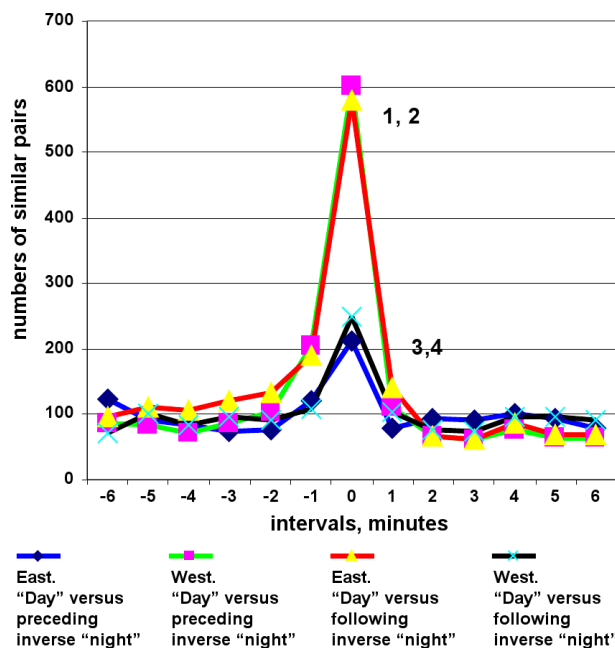
was compared with the inverse sequence of the preceding night; with the eastern collimator, it must have been a direct daytime sequence versus the inverse sequence of the following night. This phenomenon is illustrated in Fig. 2.

Fig. 2 shows that in the measurements with the eastern collimator, a clear palindrome can be seen when the direct sequence of histograms obtained from 6:00 to 18:00 on September 22 ("day") is compared with the inverse sequence of histograms obtained from 18:00 on September 22 to 6:00 on September 23 ("night"). At the same time, comparing the direct sequence of nighttime histograms (measurements from 18:00 on September 22 to 6:00 on September 23) with the inverse sequence of the following daytime histograms (measurements from 6:00 to 18:00 on September 23) shows no palindromes.

In the experiments with the "western" collimator, the situation is opposite. A clear palindrome is seen when the direct sequence of histograms obtained from 6:00 to 18:00 on September 22 ("day") is compared with the inverse sequence of histograms obtained from 18:00 on September 21 to 6:00 on September 22 ("night"). No palindromes is revealed when the direct sequence of histograms obtained from 6:00 to 18:00 on September 22 ("day") is compared with the inverse sequence of histograms obtained from 18:00 on September 22 to 6:00 on September 23 ("night"). To put it briefly: the eastern collimator will give palindromes upon the direct-day-to-*following*-inverse-night comparing; the western collima-
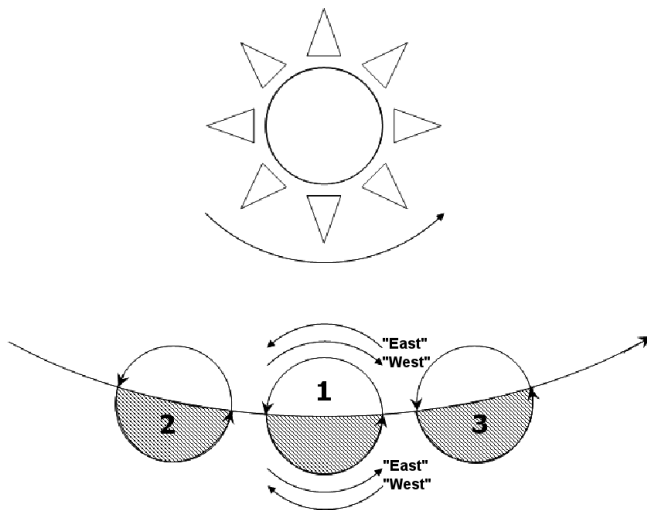
Fig. 4: The relation between the directions of motion during the daily rotation of the Earth, its translation along the circumsolar orbit, the rotation of the Sun about its axis and the directions of α-particles flying through the "western" and "eastern" collimators.

tor will show palindromes upon the direct-day-to-*preceding*-inverse-night comparing. Since the regularities found were of principle importance, we conducted more than 25 analogous experiments. The regularities were reproduced well and did not depend on the season. This can be seen in Fig. 3, which represents a summary result of four independent experiments.

4   Discusion

The phenomenon under discussion concerns regularities revealed in the experiments, in which ^{239}Pu α-activity was measured with collimator-equipped devices. The collimator were directed either West or East, and the sequence of histograms obtained with the western collimator from 6:00 to 18:00 by local time ("day") turned out to be similar to the inverse sequence of the preceding night (from 18:00 to 6:00), whereas the sequence of daytime histograms obtained with the eastern collimator were similar to the inverse sequence of the following night.

    Here we would remind the reader that the matter does not concern any "effects on α-decay"; it concerns changes of the fine structure of amplitude fluctuation spectra (the shape of the corresponding histograms). The intensity of α-decay, a mean number of decay acts per time unit, does not depend on the direction of the collimator; it will fluctuate according to the Poisson statistics — proportionally to $\pm \sqrt{N}$, where N is the decay intensity.

    Earlier we established that the changes of the histogram shape would depend on the orientation of collimators in space [8]. It seems that certain histogram shapes correspond to certain directions, possibly, to the spatial locations of gravitational inhomogeneities. Changes of the histogram shape are determined by the motion of our objects in relation to these quite long-living (for more than a year) stable inhomo-

geneities. Now we see that apart from the dependence on the spatial vector, there is also a dependence on the vector of time.

    Fig. 4 schematically illustrates spatial relations in the experiments described above. There are two devices in the laboratory (on the Earth), which differ only by the orientation of the collimators: one isolates a beam of α-particles flying West (i.e., against the direction that the Earth rotates in) and the other is directed East (i.e., along the Earth rotation). The Earth rotates about its axis and moves along the circumsolar orbit. Both these motions, as well as rotation of the Sun, have the same direction: they are directed counterclockwise. However, combining the first two motions results in the rotation of the Earth to be counter-directed to its translocation along the orbit in the daytime and co-directed in the nighttime [9]. Accordingly, α-particles from the "eastern" collimator would fly *against* the orbital Earth motion in the daytime and *along* this motion in the nighttime, this being the opposite for the "western" collimator. Hence, the collimators alternatively (one during the day- and the other during the nighttime) take the same orientation — either "along" or "against" the orbital motion of the Earth. Therefore, the phenomenon discussed cannot be explained by the change of the collimator orientation towards the Earth motion along the circumsolar orbit.

> Thus, the "arrow of time" in our experiments is determined only by the difference in the orientation of the collimators in relation to the direction of the Earth rotation about its axis.

References

1. Shnoll S. E. and Rubinstein I. A. Regular changes in the fine structure of histograms revealed in the experiments with collimators which isolate beams of alpha-particles flying at certain directions. *Progress in Physics*, 2009, v. 2, 83–95.

2. Shnoll S. E. Cosmic physical factors in random processes. Svenska fysikarkivet, Stockholm, 2009, 388 pages.

3. Shnoll S. E., Zenchenko K. I. and Udaltsova N. V. Cosmophysical effects in the structure of daily and yearly periods of changes in the shape of histograms constructed from the measurements of ^{239}Pu alpha-activity. *Biophysics*, 2004, v. 49(1), 155–164.

4. Shnoll S. E. The "scattering of the results of measurements" of processes of diverse nature is determined by the Earth's motion in the inhomogeneous space-time continuum. The effect of "half-year palindromes". *Progress in Physics*, 2009, v. 1, 3–7.

5. Shnoll S. E., Rubinshtein I. A., Zenchenko K. I., Shlekhtarev V. A., Kaminsky A. V., Konradov A. A., Udaltsova N. V. Experiments with rotating collimators cutting out pencil of alpha-particles at radioactive decay of Pu-239 evidence sharp anisotropy of space. *Progress in Physics*, 2005, v. 1, 81–84.

6. Shnoll S. E. Changes in fine structure of stochastic distributions as a consequence of space-time fluctuations. *Progress in Physics*, 2006, v. 2, 39–45.

7. Shnoll S. E., Panchelyuga V. A. and Shnoll A. E. The palindrome effect. *Progress in Physics*, 2008, v. 2, 151–153.

8. Shnoll S. E., Zenchenko K. I., Berulis I. I., Udaltsova N. V. and Rubinstein I. A. Fine structure of histograms of alpha-activity measurements depends on direction of alpha particles flow and the Earth rotation: experiments with collimators. arXiv: physics/0412007.

9. Perelman Ya. I. Physics for entertainment. Book 1. Nauka Press, 22nd Edition, 1986, p. 16–21.

———————————

SPECIAL REPORT

Two-World Background of Special Relativity. Part I

Akindele O. J. Adekugbe

P. O. Box 2575, Akure, Ondo State 340001, Nigeria
E-mail: adekugbe@alum.mit.edu

A new sheet of spacetime is isolated and added to the existing sheet, thereby yielding a pair of co-existing sheets of spacetimes, which are four-dimensional inversions of each other. The separation of the spacetimes by the special-relativistic event horizon compels an interpretation of the existence of a pair of symmetrical worlds (or universes) in nature. Further more, a flat two-dimensional intrinsic spacetime that underlies the flat four-dimensional spacetime in each universe is introduced. The four-dimensional spacetime is outward manifestation of the two-dimensional intrinsic spacetime, just as the Special Theory of Relativity (SR) on four-dimensional spacetime is mere outward manifestation of the intrinsic Special Theory of Relativity (ϕSR) on two-dimensional intrinsic spacetime. A new set of diagrams in the two-world picture that involves relative rotation of the coordinates of the two-dimensional intrinsic spacetime is drawn and intrinsic Lorentz transformation derived from it. The Lorentz transformation in SR is then written directly from intrinsic Lorentz transformation in ϕSR without any need to draw diagrams involving relative rotation of the coordinates of four-dimensional spacetime, as usually done until now. Indeed every result of SR can be written directly from the corresponding result of ϕSR. The non-existence of the light cone concept in the two-world picture is shown and good prospect for making the Lorentz group SO(3,1) compact in the two-world picture is highlighted.

1 Introduction

The concept of other universe(s) or world(s) is not new in physics. In 1898, Schuster contemplated a universe containing negative mass [1]. The discovery in particle physics of the existence of an anti-particle to every particle afterwards, led some physicists to suggest the existence of an anti-atom (composed of anti-particles) to every atom (composed of particles); an anti-molecule to every molecule and an anti-macroscopic-object to every macroscopic object. Then in order to explain the preponderance of particles and matter over anti-particles and anti-matter respectively in this our universe, the existence of an anti-universe containing a preponderance of anti-matter over matter was suggested, as discussed in [2, see p. 695], for instance. However it has remained unknown until now whether the speculated universe containing negative mass of Schuster and an anti-universe containing a preponderance of anti-matter exist or not.

The purpose of this article is to show formally that the Special Theory of Relativity rests on a background of a two-world picture, in which an identical partner universe in a different spacetime to this universe of ours in our spacetime co-exist, and to commence the development of the two-world picture thus introduced. The placement of the other universe relative to our universe, as well as the configuration of matter in it shall be derived. The symmetry of state and symmetry of laws between the two universes shall be established. The definite interaction between the two universes in relativistic phenomena shall also be shown.

This article may be alternatively entitled as *Isolating a Symmetry-Partner Universe to Our Universe in the Context of the Special Theory of Relativity*. Apart from the derivation of the Lorentz transformation (LT) and its inverse with the aid of a new set of spacetime/intrinsic spacetime diagrams on the combined spacetimes/intrinsic spacetimes of the two co-existing identical "anti-parallel" universes, there are no further implications on the other results of SR usually derived from the LT and its inverse in the existing one-world picture. However SR must be deemed to be tremendously expanded or made more complete by exposing its two-world background and by the addition of a parallel two-dimensional intrinsic Special Theory of Relativity (ϕSR) on a flat two-dimensional intrinsic spacetime that underlies the flat four-dimensional spacetime of SR in each of the two universes.

There are several new implications of the two-world picture for SR as well, which include the non-existence of the light cone concept, good prospect for making SO(3,1) compact, a feat that has proved impossible in the existing one-world picture and inter-universe transitions of symmetry-partner particles between the two universes (at super-high energy regimes), on which the prospect for experimental test ultimately of the two-world picture rests. This initial articles goes as far as a single article can on the vast subject of two-world symmetry that lies at the foundation of the Special Theory of Relativity and possibly the whole of physics.

2 Two schemes towards the Lorentz boost

As can be easily demonstrated, the two schemes summarized in Table 1 both lead to the Lorentz boost, (which shall also

Scheme I	Scheme II
$x = x' \cosh\alpha + ct' \sinh\alpha$	$x = x' \sec\psi + ct' \tan\psi$
$ct = ct' \cosh\alpha + x' \sinh\alpha$	$ct = ct' \sec\psi + x' \tan\psi$
$y = y'\ ;\ z = z'$	$y = y'\ ;\ z = z'$
$\cosh\alpha = \dfrac{1}{\sqrt{1 - v^2/c^2}} = \gamma$	$\sec\psi = \dfrac{1}{\sqrt{1 - v^2/c^2}} = \gamma$
$\sinh\alpha = \dfrac{v/c}{\sqrt{1 - v^2/c^2}} = \beta\gamma$	$\tan\psi = \dfrac{v/c}{\sqrt{1 - v^2/c^2}} = \beta\gamma = \beta\gamma$
$\tanh\alpha = v/c = \beta$	$\sin\psi = v/c = \beta$

Table 1: Two schemes towards the derivation of the Lorentz boost graphically.

be referred to as the Lorentz transformation (LT)) and the Lorentz invariance (LI). Although the $\gamma = \cosh\alpha$ parametrization of the LT in Scheme I is more familiar, the $\gamma = \sec\psi$ parametrization in Scheme II is also known.

Now by letting $v/c = 0$ in Table 1 we obtain the following:

$$\cosh\alpha = 1;\ \sinh\alpha = \tanh\alpha = 0\ \Rightarrow\ \alpha = 0,$$
$$\sec\psi = 1;\ \tan\psi = \sin\psi = 0\ \Rightarrow\ \psi = 0.$$

By letting $v/c = 1$ we have

$$\cosh\alpha = \sinh\alpha = \infty;\ \tanh\alpha = 1\ \Rightarrow\ \alpha = \infty,$$
$$\sec\psi = \tan\psi = \infty;\ \sin\psi = 1\ \Rightarrow\ \psi = \tfrac{\pi}{2}, \tfrac{5\pi}{2}, \tfrac{9\pi}{2}, \dots$$

And by letting $v/c = -1$ we have

$$\cosh\alpha = \infty;\ \sinh\alpha = -\infty;\ \tanh\alpha = -1\ \Rightarrow\ \alpha = -\infty,$$
$$\sec\psi = \infty;\ \tan\psi = -\infty;\ \sin\psi = -1\ \Rightarrow\ \psi = -\tfrac{\pi}{2}, \tfrac{3\pi}{2}, \tfrac{7\pi}{2}, \dots$$

Thus there are the following equivalent ranges of values of the parameter α and the angle ψ between the two schemes:

$$0 \leqslant \alpha \leqslant \infty \text{ (Scheme I)} \ \equiv\ 0 \leqslant \psi \leqslant \tfrac{\pi}{2} \text{ (Scheme II)}$$
$$-\infty \leqslant \alpha \leqslant \infty \text{ (Scheme I)} \ \equiv\ -\tfrac{\pi}{2} \leqslant \psi \leqslant \tfrac{\pi}{2} \text{ (Scheme II)}$$

The second range, which is $-\infty \leqslant \alpha \leqslant \infty$ (Scheme I) or $-\tfrac{\pi}{2} \leqslant \psi \leqslant \tfrac{\pi}{2}$ (Scheme II), generates the positive half-plane shown shaded in Figs. 1a and 1b.

If we consider Scheme I, then clearly there is only the positive half-plane as illustrated in Fig. 1a. This is so since the range $-\infty \leqslant \alpha \leqslant \infty$ generates the positive half-plane only, and there are no other values of α outside this range. Thus going to the negative half-plane is impossible in the context of SR in Scheme I.

If we consider Scheme II, on the other hand, then the range $-\tfrac{\pi}{2} \leqslant \psi \leqslant \tfrac{\pi}{2}$, which generates the positive half-plane in Fig. 1b is not exhaustive of the values of angle ψ in the first cycle. There is also the range $\tfrac{\pi}{2} \leqslant \psi \leqslant \tfrac{3\pi}{2}$, which generates the negative half-plane. Thus going into the negative half-plane is possible in SR in the context of Scheme II. There
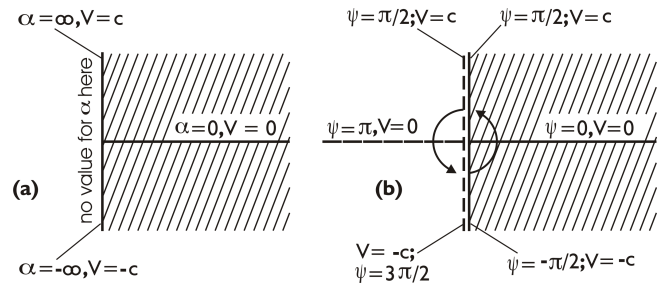

Fig. 1: a) All values of the number α generate the positive half-plane in Scheme I and b) all values of the angle ψ in the first cycle generate the positive and negative half-planes in Scheme II.

is actually no gap between the solid line and the broken line along the vertical as appears in Fig. 1b.

It must quickly be pointed out that there has not seemed to be any need to consider the second range $\tfrac{\pi}{2} \leqslant \psi \leqslant \tfrac{3\pi}{2}$ (or the negative half-plane) in Fig. 1b in physics until now because the parity inversion and time reversal associated with it can be achieved by reflection of coordinates of 3-space in the first range $-\tfrac{\pi}{2} \leqslant \psi \leqslant \tfrac{\pi}{2}$ (or in the positive half-plane) that also includes time reversal. However we consider it worthy of investigation whether the range $\tfrac{\pi}{2} \leqslant \psi \leqslant \tfrac{3\pi}{2}$ and the parity inversion it implies exist naturally apart from the possibility of parity inversion by coordinate reflection in the positive half-plane. Reasoning that parity inversion and time reversal will not be the only physical significance of the second range $\tfrac{\pi}{2} \leqslant \psi \leqslant \tfrac{3\pi}{2}$ (or the negative half-plane) in Fig. 1b, should it exist in nature, we deem it judicious to carry both ranges $-\tfrac{\pi}{2} \leqslant \psi \leqslant \tfrac{\pi}{2}$ and $\tfrac{\pi}{2} \leqslant \psi \leqslant \tfrac{3\pi}{2}$ along in the present development with the hope that the theory shall ultimately justify the existence of the second range or otherwise.

In translating Figs. 1a and 1b into spacetime diagrams, the positive horizontal lines along which, $v = 0$, $\alpha = 0$ and $\psi = 0$, in the figure, correspond to the 3-dimensional Euclidean space Σ with mutually orthogonal dimensions x, y and z in the Cartesian system of coordinates; the positive vertical lines along which, $v = c$, $\alpha = \infty$ and $\psi = \tfrac{\pi}{2}$, correspond to the positive time dimension ct, while the negative vertical lines along which $v = -c$, $\alpha = -\infty$ and $\psi = -\tfrac{\pi}{2}$, correspond to the negative time dimension (or the time reversal dimension) $-ct^*$. In addition, the horizontal line in the negative half-plane in Fig. 1b corresponds to a negative 3-dimensional Euclidean space (not known in physics until now) to be denoted by $-\Sigma^*$ with mutually orthogonal dimensions $-x^*, -y^*$ and $-z^*$ in the rectangular system. Thus Figs. 1a and 1b translate into the space-time diagrams of Figs. 2a and 2b respectively. Representation of the Euclidean 3-spaces by lines along the horizontal and the time dimensions by vertical normal lines to the "space axes", as done in Figs. 2a and 2b, is a well known practice in the graphical representation of four-dimensional spacetime, exemplified by the modern Minkowski diagrams [3].

Figure 2a pertains to Scheme I in Table 1. The four-dimensional spacetime with dimensions x, y, z and ct is the
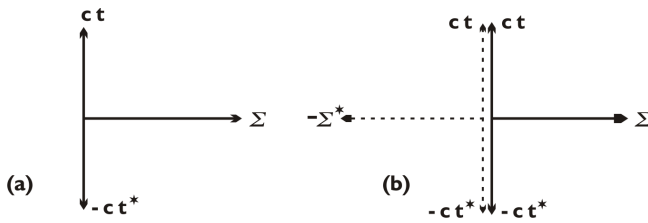
Fig. 2: The spacetime domains generated by a) all values of the number α in Scheme I and b) all values of the angle ψ in the first cycle in Scheme II.

Minkowski space as known. In addition, there is the negative time dimension $-ct^*$ that serves the role of time reversal dimension, (which is different from the *past time* axis in the past light cone). There are no second and third quadrants in Fig. 2a, since the negative half-plane is inaccessible in Scheme I.

Figure 2b pertains to Scheme II in Table 1. There are two "anti-parallel" Minkowski spaces in Fig. 2b namely, the one with positive dimensions, $(\Sigma, ct) \equiv (x, y, z, ct)$, generated by the range of angles $0 \leqslant \psi \leqslant \frac{\pi}{2}$ in the first quadrant in Fig. 1b, to be referred to as the positive Minkowski space, and the other with all negative dimensions, $(-\Sigma^*, -ct^*) \equiv (-x^*, -x^*, -y^*, -ct^*)$, generated by the range of angles $\pi \leqslant \psi \leqslant \frac{3\pi}{2}$ in the third quadrant, to be referred to as the negative Minkowski space. There are in addition the negative time dimension $-ct^*$ that serves the role of the time reversal dimension to the positive Minkowski space, while the positive time dimension ct serves the role of time reversal dimension to the negative Minkowski space.

It shall again be quickly added that the spacetime dimensions of the negative Minkowski space constitute parity inversion and time reversal with respect to the spacetime dimensions of the positive Minkowski space and conversely. Figure 2b says that this situation exists naturally, quite apart from the fact that parity inversion (by coordinate reflection), $x \to -x$; $y \to y$; $z \to z$ or $x \to -x$; $y \to -y$; $z \to -z$ and time reversal $t \to -t$ are achievable within the positive half-plane, that is within the positive Minkowski space (fist quadrant) plus the fourth quadrant in Figs. 2a and 2b. Schemes I and II have been known to imply the existence of the positive half plane only in physics until now. The investigation of the implications of the existence naturally of the negative half-plane in parallel with the positive half-plane in Figs. 1b and 2b shall be started in this paper.

3 Minkowski's diagrams as graphical representation of Lorentz transformation in Scheme I

There is essentially nothing new in this section. Its inclusion is necessary so that the derivation newly of the LT and its inverse graphically in the context of Scheme II from the next section can be compared with the known derivation of the LT and its inverse graphically in the context of Scheme I, which

shall be re-presented in this section.

For the relative motion of two frames, (which involves positive time dimension), the time reversal dimension $-ct^*$ is irrelevant, leaving only the first quadrant in Fig. 2a, (in the context of Scheme I). Thus relative rotations of the spacetime coordinates of the particle's (or primed) frame and the observer's (or unprimed) frame, for every pair of frames in relative motion, are limited to the interior of the first quadrant in Scheme I, which corresponds to the first quadrant in Figs. 1a and 2a. As is clear from Fig. 2a, Scheme I pertains to a one-world picture, including the time reversal dimension.

Now the Lorentz transformation (LT) is usually derived analytically in the Special Theory of Relativity (SR), following Albert Einstein's 1905 paper [4]. In his paper, Einstein inferred from two principles of relativity, the LT and its inverse for motion along the x'-direction of the coordinate system (ct', x', y', z') attached to a particle moving at speed v relative to an observer's frame (ct, x, y, z), where the coordinates x' and x are taken to be collinear, respectively as follows:

$$ t' = \gamma\left(t - \frac{v}{c^2}x\right); \quad x' = \gamma\,(x - vt); \quad y' = y; \quad z' = z \quad (1) $$

and

$$ t = \gamma\left(t' + \frac{v}{c^2}x'\right); \quad x = \gamma\,(x' + vt'); \quad y = y'; \quad z = z', \quad (2) $$

where $\gamma = (1 - v^2/c^2)^{-1/2}$. As demonstrated in Einstein's paper, each of systems (1) and (2) satisfies the Lorentz invariance,

$$ c^2t'^2 - x'^2 - y'^2 - z'^2 = c^2t^2 - x^2 - y^2 - z^2. \quad (3) $$

Somewhat later, Minkowski explored the graphical (or coordinate- geometrical) implication of the LT and its inverse [5]. In the graphical approach, the first two equations of the inverse LT, system (2), is interpreted as representing rotations of the coordinates x' and ct' of the particle's (or primed) frame relative to the coordinates x and ct respectively of the observer's (or unprimed) frame, while the last two equations are interpreted as representing no special-relativistic rotations of coordinates y' and z' relative to y and z respectively (since relative motion of SR does not occur along these coordinates).

The Minkowski spacetime diagrams from which the LT and its inverse have sometimes been derived for two frames in relative motion along their collinear x'- and x-axes, are shown as Figs. 3a and 3b, where the surface of the future light cone is shown by the broken lines.

The coordinates y' and z' of the particle's frame, as well as the coordinates y and z of the observer's frame remain not rotated from the horizontal, and have not been shown in Figs. 3a and 3b. The net coordinate projection along the horizontal in Fig. 3a, which in ordinary Euclidean geometry would be $x' \cos\phi + ct' \sin\phi$, is given in the Minkowski geometry as $x' \cosh\alpha + ct' \sinh\alpha$. This is the net coordinate projection to be denoted by x, along the X-axis of the observer's frame.

Similarly the net coordinate projection along the vertical in Fig. 3a is $ct' \cosh \alpha + x' \sinh \alpha$ in the Minkowski geometry. This is the net coordinate projection, to be denoted by ct, along the cT-axis of the observer's frame. Thus the following familiar transformation of coordinates has been derived from Fig. 3a:

$$\left. \begin{array}{l} ct = ct' \cosh \alpha + x' \sinh \alpha; \\ x = x' \cosh \alpha + ct' \sinh \alpha; \quad y = y'; \quad z = z' \end{array} \right\}, \quad (4)$$

where the trivial transformations, $y = y'$ and $z = z'$ of the coordinates along which relative motion of SR does not occur have been added.

The inverse of system (4) that can be similarly derived from Fig. 3b is the following:

$$\left. \begin{array}{l} ct' = ct \cosh \alpha - x \sinh \alpha; \\ x' = x \cosh \alpha - ct \sinh \alpha; \quad y' = y; \quad z' = z \end{array} \right\}, \quad (5)$$

System (5) can be presented in a matrix form as follows:

$$\begin{pmatrix} ct' \\ x' \\ y' \\ z' \end{pmatrix} = \begin{pmatrix} \cosh \alpha & -\sinh \alpha & 0 & 0 \\ -\sinh \alpha & \cosh \alpha & 0 & 0 \\ 0 & 0 & 1 & 0 \\ 0 & 0 & 0 & 1 \end{pmatrix} \begin{pmatrix} ct \\ x \\ y \\ z \end{pmatrix} \quad (6)$$

which of the form $\mathbf{x}' = L \, \mathbf{x}$.

By considering the spatial origin, $x' = y' = z' = 0$, of the primed frame, system (4) reduces as follows:

$$x = ct' \sinh \alpha \quad \text{and} \quad ct = ct' \cosh \alpha. \quad (7)$$

Division of the first into the second equation of system (7) gives

$$\frac{x}{ct} = \frac{v}{c} = \tanh \alpha, \quad (8)$$

where, $x/t = v$, is the speed of the primed frame relative to the unprimed frame.

Using (8) along with $\cosh^2 \alpha - \sinh^2 \alpha = 1$ gives the following:

$$\cosh \alpha = \frac{1}{\sqrt{1 - v^2/c^2}} \equiv \gamma, \quad (9a)$$

$$\sinh \alpha = \frac{v/c}{\sqrt{1 - v^2/c^2}} \equiv \beta \gamma. \quad (9b)$$

Substitution of equations (9a) and (9b) into systems (4) and (5) gives the LT and its inverse in the usual forms of systems (1) and (2).

The transformation from the usual trigonometric ratios, cosine and sine, of the angle ϕ in Figs. 3a and 3b, where $\tan \phi = v/c$; $-\frac{\pi}{4} < \phi < \frac{\pi}{4}$ (the light-cone), to hyperbolic functions, cosh and sinh of a number α in expressing coordinate projections on spacetime, in order to reproduce the Lorentz transformation in the Minkowski graphical approach, is compelled by the need for the parameter α to take on values in
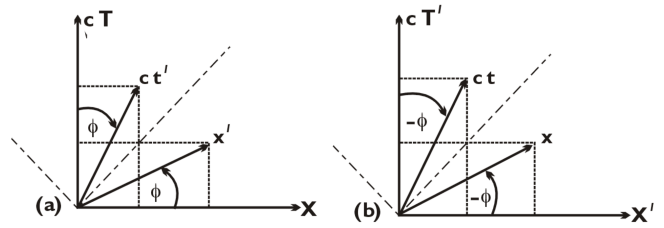
Fig. 3: The Minkowski diagrams sometimes used to derive the Lorentz transformation and its inverse in the existing one-world picture.

the unbounded range $(-\infty, \infty)$ (in Fig. 1a) of Scheme I, as the speed v of the particle relative to the observer takes on values in the unbounded range $(-c, c)$. In other words, the need to transform from the trigonometric ratios, cosine and sine, of the angle ϕ in Figs. 3a and 3b to hyperbolic functions, cosh and sinh, of a number α is compelled by the need to restrict to the positive half-plane of Fig. 1a or to the one-world picture in Special Relativity until now.

There is also a known mathematical significance to the LT system (5) or (6) and its inverse system (4) derived from the Minkowski diagrams of Figs. 3a and 3b. This is the fact that the 4×4 matrix L that generates the Lorentz boost (6), which contains the parameter α in the unbounded range $(-\infty, \infty)$, is a member of the pseudo-orthogonal Lorentz group SO(3,1), which is a non-compact Lie group with an unbounded parameter space [6]. Moreover the matrix L is non-singular for any finite value of α as required for all group SO(3,1) matrices. This implies that non-physical discontinuities do not appear in the Minkowski space generated. Singularities appear in systems (4) and (5) for the extreme values of α namely, $\alpha = \infty$ and $\alpha = -\infty$ only, which are not included in the range of α. These extreme values of α correspond to speeds $v = c$ and $v = -c$ respectively, which material particles cannot attain in relative motion.

The Lorentz boost is just a special Lorentz transformation. The general Lorentz transformation Λ is written in the factorized form [6] as follows:

$$\Lambda = R(\gamma, \beta, 0) \, L_3(\alpha) \, R(\phi, \theta, \varphi)^{-1}, \quad (10)$$

where $L_3(\alpha)$ is the Lorentz boost along the z-axis with speed $v = c \tanh \alpha$; $0 \leqslant \alpha < \infty$, and the Euler angles for rotation in the Euclidean 3-space have their usual finite ranges.

Since the group SO(3) matrices are closed and bounded, and are hence compact, the compactness or otherwise of Λ is determined by the Lorentz boost. Thus since the Lorentz boost is non-compact, the Lorentz group SO(3,1) is non-compact as known. There is no way of making SO(3,1) compact within the Minkowski one-world picture since the parameter α naturally lies within the unbounded range $-\infty < \alpha < \infty$ in this picture. Thus the Minkowski diagrams of Figs. 3a and 3b and the LT and its inverse of systems (5) and (4) or the implied transformation matrix L in Eq. (6) derived from them, have been seen as physical significance of

the Lorentz group in mathematics, or perhaps the other way round.

From the point of view of physics, on the other hand, one observes that the coordinates x' and ct' of the primed frame are non-orthogonal (or are skewed) in Fig. 3a, and the coordinates x and ct of the unprimed frame are skewed in Fig. 3b. These coordinates are orthogonal in the absence of relative motion of the frames. Even in relative motion, an observer at rest relative to the primed frame could not detect the uniform motion of his frame. Hence the primed frame is stationary relative to an observer at rest relative to it with or without the motion of the primed frame relative to the unprimed frame. Yet Fig. 3a shows that the coordinates of the primed frame are skewed with respect to an observer at rest relative to it while it is in uniform motion relative to the unprimed frame. This skewness of the spacetime coordinates of a frame is then an effect of the uniform motion of the frame, which an observer at rest relative to it could detect. This contradicts the fact that an observer cannot detect any effect of the uniform motion of his frame. Skewness of rotated coordinates cannot be avoided in Minkowski's diagrams because relative rotation of coordinates must be restricted to the first quadrant in Scheme I (or in the one-world picture), as deduced earlier.

Skewness of spacetime coordinates of frames of reference is not peculiar to the Minkowski diagrams. It is a general feature of all the existing spacetime diagrams (in the one-world picture) in Special Relativity. There are at least two other spacetime diagrams in Special Relativity, apart from the Minkowski diagrams namely, the Loedel diagram [7] and the Brehme diagram [8]. The spacetime coordinates of two frames in relative motion are skewed in the Loedel and Brehme diagrams shown as Figs. 4a and 4b respectively, for two frames in relative motion along their collinear x'- and x-axes.

Skewness of the coordinates of a frame of reference in uniform relative motion is undesirable because it is an effect of uniform motion of a frame which an observer at rest relative to the frame could detect, which negates the fundamental principle that no effect of uniform motion is detectable, as mentioned earlier. Moreover it gives apparent preference for one of two frames of reference in uniform relative motion, which, again, is a contradiction of a tenet of Special Relativity.

4 Geometric representation of Lorentz transformation in Scheme II

Having discussed the existing geometric representation of the Lorentz transformation and its inverse in Special Relativity in the context of Scheme I in Table 1 (or in the one-world picture) in the preceding section, we shall develop a new set of spacetime diagrams that are compatible with the Lorentz transformation and its inverse in the context of Scheme II in Table 1 in the rest of this paper. We shall, in particular, watch out for the possibility of making the Lorentz group SO(3,1)
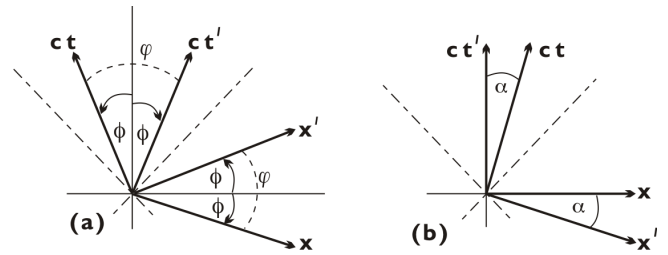
Fig. 4: a) The Loedel diagram and b) the Brehme diagram for two frames in uniform relative motion.

compact and for removing the skewness of rotated spacetime coordinates of frames of reference in the existing spacetime diagrams of Special Relativity (in the one-world picture or in the context of Scheme I).

4.1 Co-existence of two identical universes in the context of Scheme II

As shall be sufficiently justified with progress in this article, the co-existence of two anti-parallel Minkowski spaces in Fig. 2b implies the co-existence of two "anti-parallel" worlds (or universes) in nature. The dimensions x, y, z and ct of the positive Minkowski space, which are accessible to us by direct experience, are the dimensions of our universe (or world). The dimensions $-x^*, -y^*, -z^*$ and $-ct^*$ of the negative Minkowski space, which are inaccessible to us by direct experience, and hence, which have remained unknown until now, are the dimensions of another universe. Dummy star label has been put on the dimensions of the other universe, which are non-observable to us in our universe, in order to distinguish them from the dimensions of our universe.

The negative spacetime dimensions $-x^*, -y^*, -z^*$ and $-ct^*$ are inversions in the origin (or four-dimensional inversion) of the positive spacetime dimensions x, y, z and ct. Thus the spacetime dimensions of the universe with negative dimensions, to be referred to as the negative universe for brevity, and the spacetime dimensions of our universe, (to sometimes be referred to as the positive universe), have an inversion-in-the-origin symmetry. There is a one-to-one mapping of points in spacetimes between the positive (or our) universe and the negative universe. In other words, to every point in spacetime in our universe, there corresponds a unique symmetry-partner point in spacetime in the negative universe.

In addition to the inversion in the origin relationship between the spacetime dimensions of the positive and negative universes, we shall prescribe a reflection symmetry of spacetime geometry between the two universes. In other words, if we denote the spacetime manifold of the positive universe by $\mathbf{M}$ and that of the negative universe by $-\mathbf{M}^*$, then spacetime geometry at a point in spacetime in the positive universe shall be prescribed by $\mathbf{M}$ and the metric tensor $g_{\mu\nu}$ at that point, that is, by $(\mathbf{M}, g_{\mu\nu})$, while spacetime geometry shall be prescribed at the symmetry-partner point in the negative universe by $(-\mathbf{M}^*, g_{\mu\nu})$, where it must be remembered that the metric

tensor is invariant with reflections of coordinates. Symmetry of spacetime geometry between the two universes can only be prescribed at this point of development of the two-world picture.

Now Mach's principle is very fundamental. We shall make recourse to the principle here for the purpose of advancing our argument for the symmetry of state between the positive and negative universes, while knowing that the principle in itself has noting to do with Special Relativity. Essentially the Mach's principle states that the geometry of a space is determined by the distribution of mass - energy in that space [9, see p. 400]. It follows from the foregoing paragraph and Mach's principle that there is a reflection symmetry of the distribution of mass-energy in spacetimes between the two universes. Actually this is also a prescription at this point since the symmetry of spacetime geometry is a prescription.

Reflection symmetry of geometry of spacetime and of the distribution of mass-energy in spacetime also imply reflection symmetry of motions of particles and objects, natural or caused by animate object, between the two universes. In other words, corresponding to an event, natural or man-made, taking place within a local region of spacetime in our universe, there is an identical event within the symmetry-partner local region of spacetime in the negative universe. (This is the symmetry of state between the two universes). The two universes are perfectly identical in state at all times. The perfect symmetry of natural and man-made events (or perfect symmetry of state) between the two universes is a prescription at this point.

There is also a perfect symmetry of laws between the two universes, which implies that natural laws take on perfectly identical forms in the two universes. Symmetry of laws between the two universes is simply the extension of the invariance of laws found in our universe to the negative universe, which follows partly from the validity of local Lorentz invariance in the negative universe to be demonstrated shortly. The two universes could not possess symmetry of state if the laws that guide events and phenomena in them are different. The perfect symmetry of laws between the two universes shall be demonstrated with the advancement of the two-world picture.

The negative spacetime dimensions of the negative universe implies that distance in space, which is a positive scalar quantity in our (positive) universe, is a negative scalar quantity in the negative universe, and that interval of time, which is a positive quantity in the positive universe is a negative quantity in the negative universe; (it does not connote going to the past in our time dimension). This can be easily ascertained from the definition of distance, which is given in 3-space in the negative universe as, $d = \sqrt{(-x^*)^2 + (-y^*)^2 + (-z^*)^2}$. If we consider motion along the dimension $-x^*$ solely, then we must let $-y^* = -z^* = 0$, to have $d = \sqrt{(-x^*)^2} = -x^*$. Likewise the distance element of Special Relativity in the negative universe is, $ds^* = \sqrt{(-ct^*)^2 - (-x^*)^2 - (-y^*)^2 - (-z^*)^2}$. If we
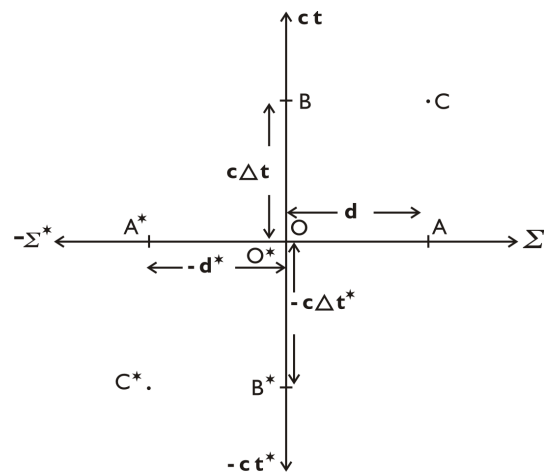
Fig. 5: Combined positive and negative Minkowski's spaces of the positive and negative universes.

let $-x^* = -y^* = -z^* = 0$, for propagation in time only, then $ds^* = \sqrt{(-ct^*)^2} = -ct^*$. Interestingly the negative worldline element ($ds^* < 0$) in the negative universe is the negative root ($-ds$) of the quadratic line element ds^2, which is usually discarded since it conveys nothing to us from the point of view of experience in the positive universe.

4.2 Non-separation of symmetry-partner points in spacetimes in the positive and negative universes

It shall be shown here that a point in spacetime in our (or positive) universe is effectively not separated in space or in time dimension from its symmetry-partner point in spacetime in the negative universe, for every pair of symmetry-partner points in spacetimes in the two universes. Now let us consider the larger spacetime of combined positive and negative universes, Fig. 2b, which is re-illustrated as Fig. 5.

Point A* in the negative Euclidean 3-space $-\Sigma^*$ of the negative universe is the symmetry-partner to point A in the positive Euclidean 3-space Σ of the positive universe. Point B* in the negative time dimension $-ct^*$ of the negative universe is the symmetry-partner to point B in the positive time dimension ct of the positive universe. Hence points C* and C are symmetry-partner points on four-dimensional spacetimes in the two universes.

Now let points A and O in the positive 3-space Σ of the positive universe be separated by a positive distance d, say, since distances in space are positive scalar quantities in the positive universe. Then the symmetry-partner points A* and O* in the negative 3-space $-\Sigma^*$ of the negative universe are separated by negative distance $-d^*$, since distances in space are negative scalar quantities in the negative universe. Hence the distance in 3-space between point A in the positive universe and its symmetry-partner point A* in the negative universe is, $d - d^* = 0$, since d and $-d^*$ are equal in magnitude. This implies that the symmetry-partner points A and A* are effectively separated by zero distance in space with respect to

observers (or people) in the positive and negative universes.

Likewise, if the interval of positive time dimension ct between point O and point B is the positive quantity $c\Delta t$, then the interval of the negative time dimension $-ct^*$ between point O* and point B* is the negative quantity $-c\Delta t^*$, since intervals of time are negative quantities in the negative universe. Hence the interval of time dimension between point B in ct in the positive universe and its symmetry-partner point B* in $-ct^*$ in the negative universe is, $c\Delta t - c\Delta t^* = 0$. This implies that the symmetry-partner points B and B* in the time dimensions are effectively separated by zero interval of time dimension with respect to observers (or people) in the positive and negative universes. It then follows that the time t of an event in the positive universe is effectively separated by zero time interval from the time $-t^*$ of the symmetry-partner event in the negative universe. Thus an event in the positive universe and its symmetry-partner in the negative universe occur simultaneously.

It follows from the foregoing two paragraphs that symmetry-partner points C and C* in spacetimes in the positive and negative universes are not separated in space or time, and this is true for every pair of symmetry-partner points in spacetimes in the two universes. Although symmetry-partner points in spacetimes in the positive and negative universes coincide at the same point, or are not separated, they do not touch because they exist in different spacetimes.

One consequence of the foregoing is that local spacetime coordinates, $(\Sigma, ct) \equiv (x, y, z, ct)$, originating from a point O in the positive universe and the symmetry-partner local spacetime coordinates, $(-\Sigma^*, -ct^*) \equiv (-x^*, -y^*, -z^*, -ct^*)$, originating from the symmetry-partner point O* in spacetime in the negative universe can be drawn from the same point on paper, as done in Fig. 5, and geometrical construction whose predictions will conform with observation or experiment in each of the two universes can be based on this in the two-world picture, as shall be done in the rest of this section.

4.3 Introducing a flat two-dimensional intrinsic spacetime underlying the flat four-dimensional spacetime

Since it is logically required for this article to propagate beyond this point and since space limitation in this paper does not permit the presentation of its derivation, which shall be presented elsewhere, we shall present (as *ansatz*) at this point certain flat two-dimensional intrinsic spacetime with dimensions to be denoted by $\phi\rho$ and $\phi c\phi t$, where $\phi\rho$ is intrinsic space dimension (actually a one-dimensional intrinsic space) and $\phi c\phi t$ is intrinsic time dimension, which underlies the flat four-dimensional spacetime (the Minkowski space) of the Special Relativity, usually denoted by (x^0, x^1, x^2, x^3); $x^0 = ct$, but which shall be denoted by (Σ, ct) in this article for convenience, where Σ is the Euclidean 3-space with dimensions x^1, x^2 and x^3.

Every particle or object with a three-dimensional inertial
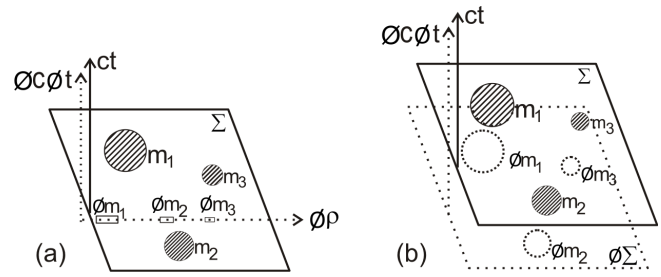
Fig. 6: a) The flat 4-dimensional spacetime and its underlying flat 2-dimensional intrinsic spacetime with the inertial masses of three objects scattered in the Euclidean 3-space and their one-dimensional intrinsic inertial masses aligned along the isotropic one-dimensional intrinsic space with respect to observers in spacetime. b) The flat 2-dimensional intrinsic spacetime with respect to observers in spacetime in a is a flat four-dimensional intrinsic spacetime containing 3-dimensional intrinsic inertial masses of particles and objects in 3-dimensional intrinsic space with respect to intrinsic-mass-observers in intrinsic spacetime.

mass m in the Euclidean 3-space Σ has its one-dimensional intrinsic mass to be denoted by ϕm underlying it in the one-dimensional intrinsic space $\phi\rho$. The one-dimensional intrinsic space $\phi\rho$ underlying the Euclidean 3-space Σ is an isotropic dimension with no unique orientation in Σ. This means that $\phi\rho$ can be considered to be orientated along any direction in Σ. The straight line intrinsic time dimension $\phi c\phi t$ likewise lies parallel to the straight line time dimension ct along the vertical in the graphical presentation of the flat spacetime of SR of Fig. 2 or Fig. 5.

If we temporarily consider the Euclidean 3-space Σ as an hyper-surface, $t = const$, represented by a plane-surface along the horizontal (instead of a line along the horizontal as in the previous diagrams) and the time dimension ct as a vertical normal line to the hyper-surface, then the graphical representation of the flat four-dimensional spacetime (Σ, ct) and its underlying flat two-dimensional intrinsic spacetime $(\phi\rho, \phi c\phi t)$ in the context of SR described in the foregoing paragraph is depicted in Fig. 6a.

Figure 6a is valid with respect to observers in the flat physical four-dimensional spacetime (Σ, ct). The one-dimensional intrinsic masses of all particles and objects are aligned along the singular isotropic one-dimensional intrinsic space $\phi\rho$, whose inertial masses are scattered arbitrarily in the physical Euclidean 3-space Σ with respect to these observers, in (Σ, ct), as illustrated for three such particles and objects in Fig. 6a.

On the other hand, the intrinsic space is actually a flat three-dimensional domain to be denoted by $\phi\Sigma$, with mutually orthogonal dimensions ϕx^1, ϕx^2 and ϕx^3, at leat in the small, with respect to intrinsic-mass-observers in $\phi\Sigma$. The intrinsic masses ϕm of particles and objects are likewise three-dimensional with respect to the intrinsic-mass-observers in $\phi\Sigma$. The intrinsic mass ϕm of a particle or object in the intrinsic space $\phi\Sigma$ lies directly underneath the inertial mass m

of the particle or object in the physical Euclidean 3-space Σ, as illustrated for three such particles or objects in Fig. 6b.

The flat four-dimensional physical spacetime (Σ, ct) containing the three-dimensional inertial masses m of particles and objects in the Euclidean 3-space Σ is the outward manifestation of the flat four-dimensional intrinsic spacetime $(\phi\Sigma, \phi c\phi t)$ containing the three-dimensional intrinsic masses ϕm of the particles and objects in $\phi\Sigma$ in Fig. 6b. It is due to the fact that the flat three-dimensional intrinsic space $\phi\Sigma$ is an isotropic space, that is, all directions in $\phi\Sigma$ are the same, with respect to observers in the physical Euclidean 3-space Σ that the dimensions ϕx^1, ϕx^2 and ϕx^3 of $\phi\Sigma$, which are mutually orthogonal, at least locally, with respect to the intrinsic-mass-observers in $\phi\Sigma$, are effectively directed along the same non-unique direction in $\phi\Sigma$, thereby effectively constituting a singular one-dimensional intrinsic space (or an intrinsic space dimension) $\phi\rho$ with no unique orientation in $\phi\Sigma$ and consequently with no unique orientation in the physical Euclidean 3-space Σ overlying $\phi\Sigma$ with respect to observers on the flat spacetime (Σ, ct), as illustrated in Fig. 6a.

As follows from the foregoing paragraph, Fig. 6a is the correct diagram with respect to observers in spacetime (Σ, ct). It is still valid to say that the flat four-dimensional spacetime (Σ, ct) is the outward (or physical) manifestation of the flat two-dimensional intrinsic spacetime $(\phi\rho, \phi c\phi t)$ and that three-dimensional inertial mass m in Σ is the outward (or physical) manifestation of one-dimensional intrinsic mass ϕm with respect to observers in (Σ, ct) in Fig. 6a. Observers on the flat four-dimensional spacetime (Σ, ct) must formulate intrinsic physics in intrinsic spacetime as two-dimensional intrinsic theories on flat intrinsic spacetime $(\phi\rho, \phi c\phi t)$.

It is for convenience that the three-dimensional Euclidean space Σ shall be represented by a line along the horizontal as done in Figs. 2a and 2b and Fig. 5 and as shall be done in the rest of this article, instead of a plane surface along the horizontal in Figs. 6a and 6b. Thus the flat four-dimensional spacetime and its underlying flat two-dimensional intrinsic spacetime shall be presented graphically in the two-world picture as Fig. 7. The origins O and O* are not actually separated contrary to their separation in Fig. 7.

Figure 7 is Fig. 5 modified by incorporating the flat two-dimensional intrinsic spacetimes underlying the flat four-dimensional spacetimes of the positive and negative universes into Fig. 5. Figure 7 is a fuller diagram than Fig. 5. As mentioned earlier, the intrinsic spacetime and intrinsic parameters in it along with their properties and notations shall be derived elsewhere.

The intrinsic spacetime dimensions $\phi\rho$ and $\phi c\phi t$ and one-dimensional intrinsic masses ϕm of particles and objects in the intrinsic space $\phi\rho$ are hidden (or non-observable) to observers on the flat four-dimensional spacetime (Σ, ct). The symbol ϕ attached to the intrinsic dimensions, intrinsic coordinates and intrinsic masses is used to indicate their intrinsic (or hidden) natures with respect to observers in spacetime.
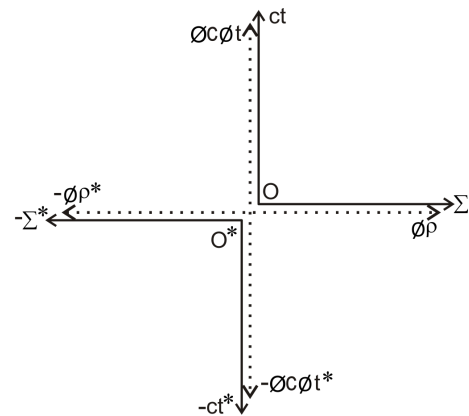
Fig. 7: Combined flat four-dimensional spacetimes and combined underlying flat two-dimensional intrinsic spacetimes of the positive and negative universes.

When the symbol ϕ is removed from the flat two-dimensional intrinsic spacetime $(\phi\rho, \phi c\phi t)$ we obtain the observed flat four-dimensional spacetime (Σ, ct) and when ϕ is removed from the one-dimensional intrinsic mass ϕm in $\phi\rho$ we obtain the observed three-dimensional inertial mass m in the Euclidean 3-space Σ.

As the inertial mass m moves at velocity $\vec{v}$ in the Euclidean 3-space Σ of the flat four-dimensional spacetime (Σ, ct) relative to an observer in (Σ, ct), the intrinsic mass ϕm performs intrinsic motion at intrinsic speed ϕv in the one-dimensional intrinsic space $\phi\rho$ of the flat two-dimensional intrinsic spacetime $(\phi\rho, \phi c\phi t)$ relative to the observer in (Σ, ct), where $|\phi v| = |\vec{v}|$. The inertial mass m of a particle in Σ and its intrinsic mass ϕm in $\phi\rho$ are together always in their respective spaces, irrespective of whether m is in motion or at rest relative to the observer.

Finally in the *ansatz* being presented in this sub-section, the intrinsic motion of the intrinsic rest mass ϕm_0 of a particle at intrinsic speed ϕv in an intrinsic particle's frame $(\phi\tilde{x}', \phi c\phi\tilde{t}')$ relative to the observer's intrinsic frame $(\phi\tilde{x}, \phi c\phi\tilde{t})$ on flat two-dimensional intrinsic spacetime $(\phi\rho, \phi c\phi t)$ pertains to two-dimensional intrinsic Special Theory of Relativity to be denoted by ϕSR, while the corresponding motion of the rest mass m_0 of the particle at velocity $\vec{v}$ in the particle's frame $(\tilde{x}', \tilde{y}', \tilde{z}', c\tilde{t}')$ relative to the observer's frame $(\tilde{x}, \tilde{y}, \tilde{z}, c\tilde{t})$ on the flat four-dimensional spacetime (Σ, ct), pertains to the Special Theory of Relativity (SR) as usual. The SR on flat four-dimensional spacetime (Σ, ct) is mere outward manifestation of ϕSR on the underlying flat two-dimensional intrinsic spacetime $(\phi\rho, \phi c\phi t)$.

The intrinsic motion at intrinsic speed ϕv of the intrinsic rest mass ϕm_0 of a particle in the particle's intrinsic frame $(\phi\tilde{x}', \phi c\phi\tilde{t}')$ relative to the observer's intrinsic frame $(\phi\tilde{x}, \phi c\phi\tilde{t})$, gives rise to rotation of the intrinsic coordinates $\phi\tilde{x}'$ and $\phi c\phi\tilde{t}'$ relative to the intrinsic coordinates $\phi\tilde{x}$ and $\phi c\phi\tilde{t}$ on the vertical intrinsic spacetime plane (which are on the $(\phi\rho, \phi c\phi t)$-plane) in Fig. 7. It must be observed that rotation

of the intrinsic coordinate $\phi\tilde{x}'$ can take place on the vertical intrinsic spacetime plane only in Fig. 6a or Fig. 7.

Two-dimensional intrinsic spacetime diagram and its inverse must be drawn on the vertical $(\phi\rho, \phi c\phi t)$-plane in the two-world picture and intrinsic Lorentz transformation (ϕLT) and its inverse derived from them in the context of ϕSR. The intrinsic Lorentz invariance (ϕLI) on the flat two-dimensional intrinsic spacetime must be validated and every result in the context of the two-dimensional intrinsic Special Theory of Relativity (ϕSR), each of which has its counterpart in SR, must be derived from the ϕLT and its inverse in the manner the results of SR are derived from the LT and its inverse.

Once ϕSR has been formulated as described above, then SR being mere outward (or physical) manifestation on the flat four-dimensional spacetime (Σ, ct) of ϕSR on the flat two-dimensional intrinsic spacetime $(\phi\rho, \phi c\phi t)$, the results of SR namely, the LT and its inverse, the Lorentz invariance (LI) on the flat four-dimensional spacetime and every other results of SR can be written directly from the corresponding results of ϕSR, without having to draw spacetime diagrams involving the rotation of the coordinates $(\tilde{x}', \tilde{y}', \tilde{z}', c\tilde{t}')$ of the primed frame relative to the coordinates $(\tilde{x}, \tilde{y}, \tilde{z}, c\tilde{t})$ of the unprimed frame on the flat four-dimensional spacetime (Σ, ct) in the context of SR. This procedure shall be demonstrated in the next sub-section.

4.4 New spacetime/intrinsic spacetime diagrams for derivation of Lorentz transformation/intrinsic Lorentz transformation in the two-world picture

Consider two frames of reference with extended unprimed straight line affine coordinates $\tilde{x}, \tilde{y}, \tilde{z}, c\tilde{t}$ and extended primed straight line affine coordinates $\tilde{x}', \tilde{y}', \tilde{z}', c\tilde{t}'$ respectively on the flat metric four-dimensional spacetime (Σ, ct). Let a three-dimensional observer (or a 3-observer), Peter, say, be located in 3-space of the unprimed frame and another 3-observer, Paul, say, be located in 3-space of the primed frame.

Corresponding to the 3-dimensional observer Peter in the 3-space of the unprimed frame, there is the one-dimensional observer (or 1-observer) in the time dimension of the unprimed frame to be denoted by $\tilde{P}$eter. Likewise corresponding to the 3-observer Paul in 3-space of the primed frame is the one-dimensional observer (or 1-observer) $\tilde{P}$aul in the time dimension of the primed frame. Thus there is the 4-observer (Peter, $\tilde{P}$eter) in the unprimed frame $(\tilde{x}, \tilde{y}, \tilde{z}, c\tilde{t})$ and the 4-observer (Paul, $\tilde{P}$aul) in the primed frame $(\tilde{x}', \tilde{y}', \tilde{z}', c\tilde{t}')$ in the positive universe. There is the symmetry-partner 4-observer (Peter*, $\tilde{P}$eter*) in the symmetry-partner unprimed frame $(-\tilde{x}^*, -\tilde{y}^*, -\tilde{z}^*, -c\tilde{t}^*)$ and symmetry-partner 4-observer (Paul*, $\tilde{P}$aul*) in the symmetry-partner primed frame $(-\tilde{x}'^*, -\tilde{y}'^*, -\tilde{z}'^*, -c\tilde{t}'^*)$ in the negative universe.

Before proceeding further, let us shine some light on the concepts of metric spacetime and affine spacetime that have been introduced in the preceding two paragraphs. As

well known, the metric spacetime (Σ, ct) is the physical four-dimensional spacetime, which is flat with constant Lorentzian metric tensor in the context of SR (and is postulated to be curved with Riemannian metric tensor in the context of the General Theory of Relativity, GR). The matter (or mass) of particles and objects are contained in the metric 3-space Σ (with Euclidean metric tensor in the context of SR). Thus particles and objects exist and move in the four-dimensional metric spacetime in the theories of relativity. The coordinates or dimensions of the metric spacetime shall be denoted by x, y, z and ct without label (in the Cartesian system of coordinates of 3-space) in this article.

On the other hand, the coordinates of an affine spacetime shall be differentiated from those of a metric spacetime by an over-head tilde label as $\tilde{x}, \tilde{y}, \tilde{z}$ and $c\tilde{t}$. These are mere mathematical entities without physical (or metrical) quality used to identify the positions and to track the motion of material points relative to a specified origin in a metric spacetime. The affine coordinates $\tilde{x}, \tilde{y}, \tilde{z}$ and $c\tilde{t}$ are straight line coordinates that can be of any extensions in the flat metric spacetime of SR. Just as it is said that "the path of a fish in water cannot be known", so is the path (i.e. the locus of the affine coordinates) of a material point through a metric spacetime non-discernible or without metrical quality. An affine spacetime can be described as mere mathematical scaffolding without physical (or metrical) significance for identifying possible positions of material particles in the metric spacetime. The extended three-dimensional affine space constituted by the affine coordinates $\tilde{x}, \tilde{y}$ and $\tilde{z}$ cannot hold matter (or mass of particles and objects).

Now corresponding to the unprimed frame $(\tilde{x}, \tilde{y}, \tilde{z}, c\tilde{t})$ of the 4-observer (Peter, $\tilde{P}$eter) prescribed on the flat four-dimensional metric spacetime (Σ, ct) earlier, is the unprimed intrinsic frame $(\phi\tilde{x}, \phi c\phi\tilde{t})$ of intrinsic 2-observer (ϕPeter, $\phi\tilde{P}$eter) in the two-dimensional metric intrinsic spacetime $(\phi\rho, \phi c\phi t)$ underlying (Σ, ct) in the first quadrant in Fig. 7 and corresponding to the primed frame $(\tilde{x}', \tilde{y}', \tilde{z}', c\tilde{t}')$ of the 4-observer (Paul, $\tilde{P}$aul) prescribed in the metric spacetime (Σ, ct) is the primed intrinsic frame $(\phi\tilde{x}', \phi c\phi\tilde{t}')$ of intrinsic 2-observer (ϕPaul, $\phi\tilde{P}$aul) in the two-dimensional metric intrinsic spacetime $(\phi\rho, \phi c\phi t)$ underlying (Σ, ct) in Fig. 7. The intrinsic coordinates $\phi\tilde{x}$ and $\phi c\phi\tilde{t}$ of the unprimed intrinsic frame in $(\phi\rho, \phi c\phi t)$ are extended straight line affine intrinsic coordinates like the coordinates $\tilde{x}, \tilde{y}, \tilde{x}$ and $c\tilde{t}$ of the unprimed frame in (Σ, ct). The intrinsic coordinates $\phi\tilde{x}'$ and $\phi c\phi\tilde{t}'$ of the primed intrinsic frame in $(\phi\rho, \phi c\phi t)$ are likewise extended straight line affine intrinsic coordinates like the coordinates $\tilde{x}', \tilde{y}', \tilde{x}'$ and $c\tilde{t}'$ of the primed frame in (Σ, ct).

The summary of all of the foregoing is that we have prescribed a pair of frames with extended straight line affine coordinates namely, $(\tilde{x}, \tilde{y}, \tilde{z}, c\tilde{t})$ of 4-observer (Peter, $\tilde{P}$eter) and $(\tilde{x}', \tilde{y}', \tilde{z}', c\tilde{t}')$ of 4-observer (Paul, $\tilde{P}$aul) on the flat four-dimensional metric spacetime (Σ, ct) and underlying pair of intrinsic frames with extended straight line affine intrinsic co-

ordinates namely, $(\phi\tilde{x}, \phi c\phi\tilde{t})$ of intrinsic 2-observer (ϕPeter, $\phi\tilde{P}$eter) and $(\phi\tilde{x}', \phi c\phi\tilde{t}')$ of intrinsic 2-observer (ϕPaul, $\phi\tilde{P}$aul) on the flat two-dimensional metric intrinsic spacetime $(\phi\rho, \phi c\phi t)$ that underlies (Σ, ct) in the first quadrant (or in our universe) in Fig. 7.

The perfect symmetry of state between the positive and negative universes requires that there are identical symmetry-partner pair of frames with extended straight line affine coordinates $(-\tilde{x}^*, -\tilde{y}^*, -\tilde{z}^*, -c\tilde{t}^*)$ of symmetry-partner 4-observer (Peter*, $\tilde{P}$eter*) and $(-\tilde{x}'^*, -\tilde{y}'^*, -\tilde{z}'^*, -c\tilde{t}'^*)$ of symmetry-partner 4-observer (Paul*, $\tilde{P}$aul*) on the flat four-dimensional metric spacetime $(-\Sigma^*, -ct^*)$ and underlying pair of intrinsic frames with extended straight line affine intrinsic coordinates namely, $(-\phi\tilde{x}^*, -\phi c\phi\tilde{t}^*)$ of intrinsic 2-observer (ϕPeter*, $\phi\tilde{P}$eter*) and $(-\phi\tilde{x}'^*, -\phi c\phi\tilde{t}'^*)$ of intrinsic 2-observer (ϕPaul*, $\phi\tilde{P}$aul*) on the flat two-dimensional metric intrinsic spacetime $(-\phi\rho^*, -\phi c\phi t^*)$ that underlies $(-\Sigma^*, -ct^*)$ in the third quadrant (or in negative universe) in Fig. 7.

As done at the beginning of section 2, let us consider the propagation at a constant speed v of the rest mass m_0 of a particle along the coordinate $\tilde{x}'$ of the particle (or primed) frame $(\tilde{x}', \tilde{y}', \tilde{z}', c\tilde{t}')$ relative to the 3-observer Peter in the 3-space $\tilde{\Sigma}(\tilde{x}, \tilde{y}, \tilde{z})$ of the observer's frame $(\tilde{x}, \tilde{y}, \tilde{z}, c\tilde{t})$ in the positive universe (or our universe), where the coordinates $\tilde{x}'$ and $\tilde{x}$ shall be taken to be collinear. Correspondingly, the intrinsic rest mass ϕm_0 of the particle is in intrinsic motion at intrinsic speed ϕv along the intrinsic coordinate $\phi\tilde{x}'$ of the particle's intrinsic frame (or the primed intrinsic frame) $(\phi\tilde{x}', \phi c\phi\tilde{t}')$ relative to the intrinsic observer's frame $(\phi\tilde{x}, \phi c\phi\tilde{t})$ with respect to the intrinsic 1-observer ϕPeter in the one-dimensional intrinsic space $(\phi\tilde{x})$ of the observer's frame and hence with respect to the 3-observer Peter in $\tilde{\Sigma}(\tilde{x}, \tilde{y}, \tilde{z})$ overlying $\phi\tilde{x}$, where the intrinsic coordinates $\phi\tilde{x}'$ and $\phi\tilde{x}$ are necessarily collinear since they are affine intrinsic coordinates in the singular isotropic one-dimensional metric intrinsic space $\phi\rho$.

The intrinsic motion at intrinsic speed ϕv of the intrinsic rest mass ϕm_0 of the particle along the intrinsic coordinate $\phi\tilde{x}'$ of the particle's intrinsic frame $(\phi\tilde{x}', \phi c\phi\tilde{t}')$ relative to the observer's intrinsic frame $(\phi\tilde{x}, \phi c\phi\tilde{t})$ described in the foregoing paragraph, will cause the anti-clockwise rotation of the extended straight line affine intrinsic coordinates $\phi\tilde{x}'$ and $\phi c\phi\tilde{t}'$ of the primed intrinsic frame at equal intrinsic angle $\phi\psi$ relative to the extended straight line affine intrinsic coordinates $\phi\tilde{x}$ and $\phi c\phi\tilde{t}$ respectively of the unprimed intrinsic frame.

The perfect symmetry of state between the positive and negative universes discussed earlier, implies that the rest mass of the symmetry-partner particle (its sign is yet to be determined), is in simultaneous motion at constant speed v along the coordinate $-\tilde{x}'^*$ of the particle's frame $(-\tilde{x}'^*, -\tilde{y}'^*, -\tilde{z}'^*, -c\tilde{t}'^*)$ relative to the symmetry-partner 3-observer* Peter* in the 3-space $-\tilde{\Sigma}^*(-\tilde{x}^*, -\tilde{y}^*, -\tilde{z}^*)$ of the observer's frame $(-\tilde{x}^*, -\tilde{y}^*, -\tilde{z}^*, -c\tilde{t}^*)$ in the negative universe. Correspondingly, the intrinsic rest mass of the symmetry-partner particle is in intrinsic motion at constant intrinsic speed ϕv along

the intrinsic coordinate $-\phi\tilde{x}'^*$ of the particle's intrinsic frame $(-\phi\tilde{x}'^*, -\phi c\phi\tilde{t}'^*)$ relative to the intrinsic observer's frame $(-\phi\tilde{x}^*, -\phi c\phi\tilde{t}^*)$, with respect to the intrinsic 1-observer* ϕPeter* in the intrinsic space $-\phi\tilde{x}^*$ of the intrinsic observer's frame and consequently with respect to the 3-observer* Peter* in the 3-space $-\tilde{\Sigma}^*(-\tilde{x}^*, -\tilde{y}^*, -\tilde{z}^*)$ of the observer's frame overlying $-\phi\tilde{x}^*$ in the negative universe. Consequently the extended affine intrinsic coordinates $-\phi\tilde{x}'^*$ and $-\phi c\phi\tilde{t}'^*$ of the particle's frame will be rotated anti-clockwise at equal intrinsic angle $\phi\psi$ relative to the extended straight line affine intrinsic coordinates $-\phi\tilde{x}^*$ and $-\phi c\phi\tilde{t}^*$ respectively of the observer's intrinsic frame.

Now on the larger spacetime/intrinsic spacetime of combined positive universe and negative universe depicted in Fig. 7, the extended straight line affine intrinsic time coordinate $\phi c\phi\tilde{t}'$ of the primed intrinsic frame in the first quadrant can rotate into the second quadrant with respect to the 3-observer (Peter) in the 3-space $\tilde{\Sigma}(\tilde{x}, \tilde{y}, \tilde{z})$ along the horizontal in the first quadrant in Fig. 7. This is so since the intrinsic angle $\phi\psi$ has values in the negative half-plane in Fig. 1b, which correspond to the second and third quadrants in Fig. 7. Similarly the extended straight line affine intrinsic time coordinate $-\phi c\phi\tilde{t}'^*$ of the primed intrinsic frame in the third quadrant can rotate into the fourth quadrant with respect to 3-observer* (Peter*) in the 3-space $-\tilde{\Sigma}^*$ along the horizontal in the third quadrant, since $\phi\psi$ has value in the positive half-plane in Fig. 1b, which corresponds to the fourth and first quadrants in Fig. 7, with respect to 3-observers* in $-\Sigma^*$ along the horizontal in the third quadrant in Fig.7. Thus the rotation of the intrinsic coordinates $\phi\tilde{x}'$ and $\phi c\phi\tilde{t}'$ relative to $\phi\tilde{x}$ and $\phi c\phi\tilde{t}$ respectively in Fig. 8a is possible (or will ensue) in the two-world picture.

The intrinsic coordinate $\phi\tilde{x}$ is the projection along the horizontal of the inclined $\phi\tilde{x}'$ in Fig. 8a. That is, $\phi\tilde{x} = \phi\tilde{x}' \cos\phi\psi$. Hence we can write,

$$\phi\tilde{x}' = \phi\tilde{x} \sec\phi\psi \,.$$

This transformation of affine intrinsic space coordinates is all that should have been possible with respect to the intrinsic 1-observer ϕPeter in the intrinsic space $\phi\tilde{x}$ of the intrinsic observer's frame along the horizontal and consequently with respect to 3-observer (Peter) in the 3-space $\tilde{\Sigma}(\tilde{x}, \tilde{y}, \tilde{z})$ of the observer's frame from Fig. 8a, but for the fact that the negative intrinsic time coordinate $-\phi c\phi\tilde{t}'^*$ of the negative universe rotated into the fourth quadrant also projects component $-\phi c\phi\tilde{t}' \sin\phi\psi$ along the horizontal, which must be added to the right-hand side of the last displayed equation yielding,

$$\phi\tilde{x}' = \phi\tilde{x} \sec\phi\psi - \phi c\phi\tilde{t}' \sin\phi\psi \,.$$

The dummy star label used to differentiate the coordinates and parameters of the negative universe from those of the positive universe has been removed from the component $-\phi c\phi t'^* \sin\phi\psi$ projected along the horizontal by the coordi-
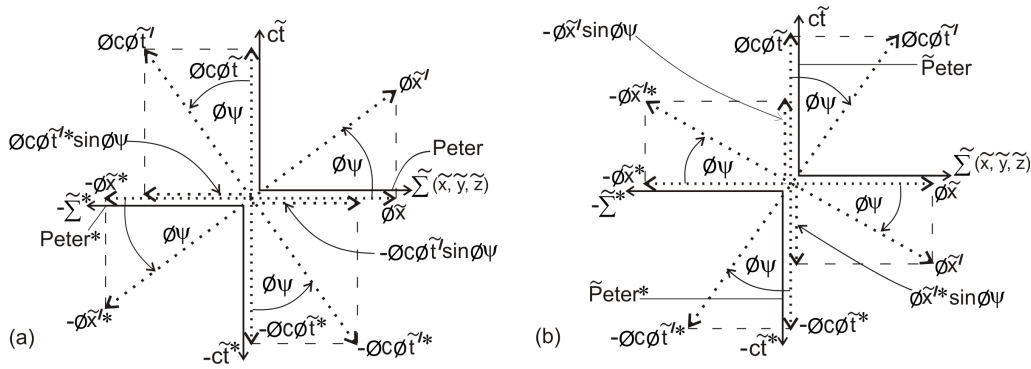
Fig. 8: a) The diagram used to derive partial intrinsic Lorentz transformations / partial Lorentz transformations with respect to 3-observers in the 3-spaces in the positive and negative universes. b) The complementary diagram to a used to derive partial intrinsic Lorentz transformations / partial Lorentz transformations with respect to 1-observers in the time dimensions in the positive and negative universes.

nate $-\phi c \phi \tilde{t}'^{*}$ of the negative universe rotated into the fourth quadrant in Fig. 8a, since the projected component is now an intrinsic coordinate in the positive universe.

But the intrinsic coordinates $\phi c \phi \tilde{t}$ and $\phi c \phi \tilde{t}'$ are also related as, $\phi c \phi \tilde{t} = \phi c \phi \tilde{t}' \cos \phi \psi$ hence $\phi c \phi \tilde{t}' = \phi c \phi \tilde{t} \sec \phi \psi$, along the vertical in the same Fig. 8a. By replacing $\phi c \phi \tilde{t}'$ by $\phi c \phi \tilde{t} \sec \phi \psi$ in the last displayed equation we have

$$\phi \tilde{x}' = \phi \tilde{x} \sec \phi \psi - \phi c \phi \tilde{t} \tan \phi \psi \qquad (11)$$

(w.r.t. 3-observer Peter in $\tilde{\Sigma}$).

Likewise the affine intrinsic time coordinate $\phi c \phi \tilde{t}$ is the projection along the vertical of the inclined affine intrinsic coordinate $\phi c \phi \tilde{t}'$ in Fig. 8b. Hence $\phi c \phi \tilde{t} = \phi c \phi \tilde{t}' \cos \phi \psi$ or

$$\phi c \phi \tilde{t}' = \phi c \phi \tilde{t} \sec \phi \psi .$$

This affine intrinsic time coordinate transformation is all that should have been possible with respect to the 1-observer P̃eter in the time dimension $c \tilde{t}$ of the observer's frame from Fig. 8b, but for the fact that the inclined negative intrinsic space coordinate $-\phi \tilde{x}'^{*}$ of the negative universe rotated into the second quadrant also projects component $-\phi \tilde{x}' \sin \phi \psi$ along the vertical, which must be added to the right-hand side of the last displayed equation yielding,

$$\phi c \phi \tilde{t}' = \phi c \phi \tilde{t} \sec \phi \psi - \phi \tilde{x}' \sin \phi \psi .$$

The dummy star label has again been removed from the component $-\phi \tilde{x}'^{*} \sin \phi \psi$ projected along the vertical in the second quadrant by the inclined intrinsic coordinate $-\phi \tilde{x}'^{*}$ of the negative universe rotated into the second quadrant, since the projected component is now an intrinsic coordinate in the positive universe.

But the intrinsic coordinate $\phi \tilde{x}$ is related to $\phi \tilde{x}'$ along the horizontal in the same Fig. 8b as, $\phi \tilde{x} = \phi \tilde{x}' \cos \phi \psi$ or $\phi \tilde{x}' = \phi \tilde{x} \sec \phi \psi$ along the horizontal in Fig. 8b. Then by replacing $\phi \tilde{x}'$ by $\phi \tilde{x} \sec \phi \psi$ in the last displayed equation we have

$$\phi c \phi \tilde{t}' = \phi c \tilde{t} \sec \phi \psi - \phi \tilde{x} \tan \phi \psi \qquad (12)$$

(w.r.t. 1-observer P̃eter in $c \tilde{t}$).

The concept of 1-observer in the time dimension added to 3-observer in 3-space to have 4-observer in four-dimensional spacetime introduced above is in agreement with the known four-dimensionality of particles and bodies in 4-geometry of relativity. Anti-clockwise (or positive) rotation of the intrinsic space coordinate $\phi \tilde{x}'$ by intrinsic angle $\phi \psi$ towards the intrinsic time coordinate $\phi c \phi \tilde{t}$ along the vertical with respect to the 3-observer (Peter) in the 3-space $\tilde{\Sigma}(\tilde{x}, \tilde{y}, \tilde{z})$ of the observer's frame in Fig. 8a, corresponds to clockwise (or positive) rotation of the intrinsic time coordinate $\phi c \phi \tilde{t}'$ by equal intrinsic angle $\phi \psi$ towards the intrinsic space coordinate $\phi \tilde{x}$ along the horizontal with respect to the 1-observer (P̃eter) in the time dimension $c \tilde{t}$ of the observer's frame in Fig. 8b. The explanation of the fact that anti-clockwise rotation of the primed intrinsic spacetime coordinates relative to unprimed intrinsic spacetime coordinates is positive rotation with respect to 3-observers in 3-spaces in Fig. 8a, while clockwise rotation of primed intrinsic spacetime coordinates relative to unprimed intrinsic spacetime coordinates is positive rotation with respect to 1-observers in the time dimensions in Fig. 8b, requires further development of the two-world picture than in this paper. It shall be presented elsewhere.

The partial intrinsic Lorentz transformation of affine intrinsic space coordinates (11) with respect to the 3-observer Peter in the 3-space $\tilde{\Sigma}(\tilde{x}, \tilde{y}, \tilde{z})$ of the observer's frame and the partial intrinsic Lorentz transformation of affine intrinsic time coordinates (12) with respect to the 1-observer P̃eter in the time dimension $c \tilde{t}$ of the observer's frame must be collected to obtain the intrinsic Lorentz transformation of extended straight line affine intrinsic spacetime coordinates with respect to 4-observers (Peter, P̃eter) in the observer's frame as follows:

$$\left. \begin{array}{c} \phi c \phi \tilde{t}' = \phi c \phi \tilde{t} \sec \phi \psi - \phi \tilde{x} \tan \phi \psi \\ \text{(w.r.t. 1-observer P̃eter in } c\tilde{t}) \\[2mm] \phi \tilde{x}' = \phi \tilde{x} \sec \phi \psi - \phi c \phi \tilde{t} \tan \phi \psi \\ \text{(w.r.t. 3-observer Peter in } \tilde{\Sigma}) \end{array} \right\} , \qquad (13)$$
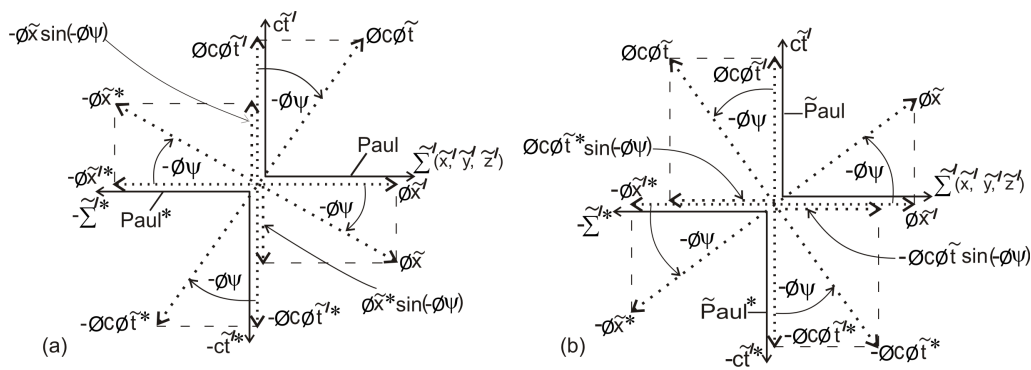
Fig. 9: The inverse diagrams to Figures 8a and 8b respectively, used to derive inverse intrinsic Lorentz transformations / inverse Lorentz transformations in the positive and negative universes.

where $-\frac{\pi}{2} < \phi\psi < \frac{\pi}{2}$ (temporarily).

The range $-\frac{\pi}{2} < \phi\psi < \frac{\pi}{2}$ of the intrinsic angles $\phi\psi$ in system (13) in the positive universe is temporary as indicated. This temporary range shall be modified later in this section. The fact that the intrinsic angle $\phi\psi$ can have values in the range $[0, \frac{\pi}{2})$ in the first quadrant in Figs. 8a and 8b in the two-world picture, instead of the range $[0, \frac{\pi}{4})$ of the angle ϕ in the Minkowski diagrams, (Figs. 3a and 3b in the one-world picture), is due to the non-existence of light-cones in the two-world picture, as shall be established shortly.

In order to obtain the inverses of equations (11) and (12) and hence the inverse to system (13), let us draw the inverses of Figs. 8a and 8b. The inverse to Fig. 8a obtained by rotating all intrinsic coordinates clockwise by negative intrinsic angle $-\phi\psi$ with respect to 3-observer in the 3-spaces $\tilde{\Sigma}$ and $-\tilde{\Sigma}^*$ in Fig. 8a is depicted in Fig. 9a and the the inverse to Fig. 8b obtained by rotating all intrinsic coordinates anti-clockwise by negative intrinsic angle $-\phi\psi$ with respect to 1-observer in the time dimensions $c\tilde{t}$ and $-c\tilde{t}^*$ in Fig. 8b is depicted in Fig. 9b.

The clockwise sense of negative rotation (i.e. by negative intrinsic angle) of intrinsic coordinates in Fig. 9a is valid with respect to the 3-observer (Paul) in the 3-space $\tilde{\Sigma}'$ of the primed (or particle's) frame with respect to whom positive rotation is anti-clockwise. Hence the transformation of intrinsic coordinates derived from Fig. 9a is valid with respect to the 3-observer (Paul) in $\tilde{\Sigma}'$. On the other hand, the anti-clockwise sense of negative rotation of intrinsic coordinates in Fig. 9b is valid relative to the 1-observer (P̃aul) in the time dimension $c\tilde{t}'$, with respect to whom positive rotation is clockwise. Hence the intrinsic coordinate transformation derived from Fig. 9b is valid relative to the 1-observer (Paul) in $c\tilde{t}'$.

Again the affine intrinsic time coordinate $\phi c\phi\tilde{t}'$ is the projection along the vertical of the inclined $\phi c\phi\tilde{t}$ in Fig. 9a. That is, $\phi c\phi\tilde{t}' = \phi c\phi\tilde{t}\cos(-\phi\psi) = \phi c\phi\tilde{t}\cos\phi\psi$. Hence we can write,

$$\phi c\phi\tilde{t} = \phi c\phi\tilde{t}'\sec\phi\psi\,.$$

This transformation of affine intrinsic time coordinates is

all that should have been possible along the vertical in Fig. 9a by the 3-observer (Paul) in $\tilde{\Sigma}'$ of the particle's frame, but for the fact that the unprimed negative intrinsic space coordinate $-\phi\tilde{x}^*$ of the negative universe rotated into the second quadrant projects component, $-\phi\tilde{x}\sin(-\phi\psi) = \phi\tilde{x}\sin\phi\psi$, along the vertical, which must be added to the right-hand side of the last displayed equation to have as follows:

$$\phi c\phi\tilde{t} = \phi c\phi\tilde{t}'\sec\phi\psi + \tilde{x}\sin\phi\psi\,.$$

The dummy star label has again been removed from the component $-\phi\tilde{x}^*\sin(-\phi\psi)$ projected along the vertical in the second quadrant by the negative intrinsic space coordinate $-\phi\tilde{x}^*$ of the negative universe rotated into the second quadrant in Fig. 9a, since the projected component is now an intrinsic coordinate in the positive universe.

But $\phi\tilde{x}$ and $\phi\tilde{x}'$ are related as $\phi\tilde{x}\cos(-\phi\psi) = \phi\tilde{x}'$ hence, $\phi\tilde{x} = \phi\tilde{x}'\sec\phi\psi$, along the horizontal in the same Fig. 9a. By using this in the last displayed equation we have

$$\phi c\phi\tilde{t} = \phi c\phi\tilde{t}'\sec\phi\psi + \phi\tilde{x}'\tan\phi\psi \qquad (14)$$

(w.r.t. 3-observer Paul in $\tilde{\Sigma}'$).

Likewise the affine intrinsic space coordinate $\phi\tilde{x}$ is related to $\phi\tilde{x}'$ and the component $-\phi c\phi\tilde{t}\sin(-\phi\psi)$ projected along the horizontal with respect to the 1-observer P̃aul in the time dimension $c\tilde{t}'$ of the particle's frame in Fig. 9b as

$$\phi\tilde{x} = \tilde{x}'\sec\phi\psi + \phi c\phi\tilde{t}\sin\phi\psi\,.$$

Then by using the relation, $\phi c\phi\tilde{t} = \phi c\phi\tilde{t}'\sec\phi\psi$, which also holds along the vertical in the same Fig. 9b in the last displayed equation, we have

$$\phi\tilde{x} = \phi\tilde{x}'\sec\phi\psi + \phi c\phi\tilde{t}'\tan\phi\psi \qquad (15)$$

(w.r.t. 1-observer P̃aul in $c\tilde{t}'$).

By collecting the partial intrinsic coordinate transformations (14) and (15) we obtain the inverse intrinsic Lorentz transformation to system (13) with respect to 4-observer

(Paul, P̃aul) in the particle's (or primed) frame as follows:

$$
\left.
\begin{aligned}
&\phi c \phi \tilde{t} = \phi c \phi \tilde{t}' \sec \phi \psi + \phi \tilde{x}' \tan \phi \psi \\
&\quad \text{(w.r.t. 3-observer Paul in } \tilde{\Sigma}') \\
&\phi \tilde{x} = \phi \tilde{x}' \sec \phi \psi + \phi c \phi \tilde{t}' \tan \phi \psi \\
&\quad \text{(w.r.t. 1-observer P̃aul in } c\tilde{t}')
\end{aligned}
\right\}, \quad (16)
$$

where $-\frac{\pi}{2} < \phi \psi < \frac{\pi}{2}$ (temporarily).

Again the range $-\frac{\pi}{2} < \phi \psi < \frac{\pi}{2}$ of the intrinsic angles $\phi \psi$ in system (16) in the positive universe is temporary as indicated. It shall be modified shortly in this section.

By considering the origin $\phi \tilde{x}' = 0$ of the intrinsic space coordinate $\phi \tilde{x}'$ of the primed intrinsic frame, system (16) simplifies as follows:

$$
\phi \tilde{x} = \phi c \phi \tilde{t}' \tan \phi \psi \quad \text{and} \quad \phi c \phi \tilde{t} = \phi c \phi \tilde{t}' \sec \phi \psi . \quad (17)
$$

Then by dividing the first into the second equation of system (17) we have

$$
\frac{\phi \tilde{x}}{\phi c \phi \tilde{t}} = \sin \phi \psi .
$$

But, $\phi \tilde{x} / \phi \tilde{t} = \phi v$, is the intrinsic speed of the primed intrinsic frame relative to the unprimed intrinsic frame. Hence,

$$
\sin \phi \psi = \phi v / \phi c = \phi \beta \quad (18)
$$

$$
\sec \phi \psi = \frac{1}{\sqrt{1 - \phi v^2 / \phi c^2}} = \phi \gamma . \quad (19)
$$

By using relations (18) and (19) in systems (13) we have

$$
\phi c \phi \tilde{t}' = \frac{1}{\sqrt{1 - \phi v^2 / \phi c^2}} \left(\phi c \phi \tilde{t} - \frac{\phi v}{\phi c} \phi \tilde{x} \right)
$$

(w.r.t. 1-observer P̃eter in $c\tilde{t}$),

$$
\phi \tilde{x}' = \frac{1}{\sqrt{1 - \phi v^2 / \phi c^2}} \left(\phi \tilde{x} - \frac{\phi v}{\phi c} \phi c \phi \tilde{t} \right)
$$

(w.r.t. 3-observer Peter in $\tilde{\Sigma}$), or

$$
\left.
\begin{aligned}
&\phi \tilde{t}' = \phi \gamma \left(\phi \tilde{t} - \frac{\phi v}{\phi c^2} \phi \tilde{x} \right) \\
&\quad \text{(w.r.t. 1-observer P̃eter in } c\tilde{t}) \\
&\phi \tilde{x}' = \phi \gamma \left(\phi \tilde{x} - \phi v \phi \tilde{t} \right) \\
&\quad \text{(w.r.t. 3-observer Peter in } \tilde{\Sigma})
\end{aligned}
\right\}. \quad (20)
$$

And by using equations (18) and (19) in system (16) we have

$$
\phi c \phi \tilde{t} = \frac{1}{\sqrt{1 - \phi v^2 / \phi c^2}} \left(\phi c \phi \tilde{t}' + \frac{\phi v}{\phi c} \phi \tilde{x}' \right)
$$

(w.r.t. 3-observer Peter in $\tilde{\Sigma}'$),

$$
\phi \tilde{x} = \frac{1}{\sqrt{1 - \phi v^2 / \phi c^2}} \left(\phi \tilde{x}' + \frac{\phi v}{\phi c} \phi c \phi \tilde{t}' \right)
$$

(w.r.t. 1-observer P̃eter in $c\tilde{t}'$), or

$$
\left.
\begin{aligned}
&\phi \tilde{t} = \phi \gamma \left(\phi \tilde{t}' + \frac{\phi v}{\phi c^2} \phi \tilde{x}' \right) \\
&\quad \text{(w.r.t. 3-observer Paul in } \tilde{\Sigma}') \\
&\phi \tilde{x} = \phi \gamma \left(\phi \tilde{x}' + \phi v \phi \tilde{t}' \right) \\
&\quad \text{(w.r.t. 1-observer P̃aul in } c\tilde{t}')
\end{aligned}
\right\}. \quad (21)
$$

Systems (20) and (21) are the explicit forms of the intrinsic Lorentz transformation (ϕLT) of extended affine intrinsic coordinates and its inverse respectively on the flat two-dimensional metric intrinsic spacetime ($\phi \rho, \phi c \phi t$) that underlies the flat four-dimensional metric spacetime (Σ, ct) in the positive universe in Fig. 7.

As can be easily verified, either system (13) or (16) or its explicit form (20) or (21) implies intrinsic Lorentz invariance (ϕLI) on ($\phi \rho, \phi c \phi t$):

$$
\phi c^2 \phi \tilde{t}^2 - \phi \tilde{x}^2 = \phi c^2 \phi \tilde{t}'^2 - \phi \tilde{x}'^2 . \quad (22)
$$

Just as the 4-observer (Peter, P̃eter) in the unprimed frame ($\tilde{x}, \tilde{y}, \tilde{z}, c\tilde{t}$) derives system (13) given explicitly as system (20) from Figs. 8a and 8b and the 4-observer (Paul, P̃aul) in the primed frame derives the system (16) given explicitly as system (21) from Figs. 9a and 9b in the positive universe, the symmetry-partner 4-observer* (Peter*, P̃eter*) in the unprimed frame ($-\tilde{x}^*, -\tilde{y}^*, -\tilde{z}^*, -c\tilde{t}^*$) in the negative universe derives the ϕLT and its inverse from Figs. 8a and 8b and the symmetry-partner observer* (Paul*, P̃aul*) in the primed frame ($-\tilde{x}'^*, -\tilde{y}'^*, -\tilde{z}'^*, -c\tilde{t}'^*$) in the the negative universe derives the inverse ϕLT from Figs. 9a and 9b, and the 4-observers (Peter*, P̃eter*) and (Paul*, P̃aul*) write

$$
\left.
\begin{aligned}
&-\phi c \phi \tilde{t}'^* = -\phi c \phi \tilde{t}^* \sec \phi \psi - (-\phi \tilde{x}^*) \tan \phi \psi \\
&\quad \text{(w.r.t. 1-observer* P̃eter* in } -c\tilde{t}^*) \\
&-\phi \tilde{x}'^* = -\phi \tilde{x}^* \sec \phi \psi - (-\phi c \phi \tilde{t}^*) \tan \phi \psi \\
&\quad \text{(w.r.t. 3-observer* Peter* in } -\tilde{\Sigma}^*)
\end{aligned}
\right\} \quad (23)
$$

and

$$
\left.
\begin{aligned}
&-\phi c \phi \tilde{t}^* = -\phi c \phi \tilde{t}'^* \sec \phi \psi + (-\phi \tilde{x}'^*) \tan \phi \psi \\
&\quad \text{(w.r.t. 3-observer* Paul* in } -\tilde{\Sigma}'^*) \\
&-\phi \tilde{x}^* = -\phi \tilde{x}'^* \sec \phi \psi + (-\phi c \phi \tilde{t}'^*) \tan \phi \psi \\
&\quad \text{(w.r.t. 1-observer* P̃aul* in } -c\tilde{t}'^*)
\end{aligned}
\right\}, \quad (24)
$$

where $-\frac{\pi}{2} < \phi \psi < \frac{\pi}{2}$ (temporarily).

The range $-\frac{\pi}{2} < \phi \psi < \frac{\pi}{2}$ of the intrinsic angles $\phi \psi$ in systems (23) and (24) in the negative universe is temporary as indicated. It shall be modified shortly in this section.

Systems (23) and (24) can also be put in their explicit

forms respectively as follows by virtue of Eqs. (18) and (19):

$$-\phi\tilde{t}'^* = \phi\gamma\left(-\phi\tilde{t}^* - \frac{\phi v}{\phi c^2}\left(-\phi\tilde{x}^*\right)\right)$$
(w.r.t. 1-observer* $\tilde{P}$eter* in $-c\tilde{t}^*$)

$$-\phi\tilde{x}'^* = \phi\gamma\left(-\phi\tilde{x}^* - \phi v(-\phi\tilde{t}^*)\right)$$
(w.r.t. 3-observer* Peter* in $-\tilde{\Sigma}^*$)
$\qquad$ (25)

and

$$-\phi\tilde{t}^* = \phi\gamma\left(-\phi\tilde{t}'^* + \frac{\phi v}{\phi c^2}\left(-\phi\tilde{x}'^*\right)\right)$$
(w.r.t. 3-observer* Paul* in $-\tilde{\Sigma}'^*$)

$$-\phi\tilde{x}^* = \phi\gamma\left(-\phi\tilde{x}'^* + \phi v(-\phi\tilde{t}'^*)\right)$$
(w.r.t. 1-observer* $\tilde{P}$aul* in $-c\tilde{t}'^*$)
$\qquad$ (26)

Again system (23) or (24) or the explicit form (25) or (26) implies intrinsic Lorentz invariance on the flat two-dimensional intrinsic spacetime $(-\phi\rho^*, -\phi c\phi t^*)$ in the negative universe:

$$(-\phi c^2 \phi\tilde{t}^*)^2 - (-\phi\tilde{x}^*)^2 = (-\phi c^2 \phi\tilde{t}'^*)^2 - (-\phi\tilde{x}'^*)^2. \quad (27)$$

The intrinsic LT of system (13) and its inverse of system (16) or their explicit forms of systems (20) and (21) and the intrinsic Lorentz invariance (22) they imply, pertain to two-dimensional intrinsic Special Theory of Relativity (ϕSR) on the flat two-dimensional metric intrinsic spacetime $(\phi\rho, \phi c\phi t)$ that underlies the flat four-dimensional metric spacetime (Σ, ct) in the positive universe in Fig. 7. In symmetry, the intrinsic LT and its inverse of system (23) and (24) or their explicit forms (25) and (26) and the intrinsic Lorentz invariance (27) they imply pertain to the intrinsic Special Theory of Relativity (ϕSR) on flat two-dimensional metric intrinsic spacetime $(-\phi\rho^*, -\phi c\phi t^*)$ that underlies the flat four-dimensional metric spacetime $(-\Sigma^*, -ct^*)$ in the negative universe.

Having derived the intrinsic LT of system (13) on page 40 and its inverse of system (16) on page 42 and their explicit forms of systems (20) and (21) in the context of intrinsic 2-geometry ϕSR in the positive universe, we must now obtain their outward (or physical) manifestations on the flat four-dimensional spacetime in the context of 4-geometry Special Theory of Relativity (SR). We do not have to draw a new set of diagrams in the two-world picture in which extended straight line affine spacetime coordinates $\tilde{x}'$ and $c\tilde{t}'$ of the primed frame are rotated relative to the extended affine coordinates $\tilde{x}$ and $c\tilde{t}$ respectively of the unprimed frame on the vertical (x, ct)-plane, while the affine coordinates $\tilde{y}'$ and $\tilde{z}'$ of the primed frame along which relative motion of SR do not occur are not rotated on the vertical spacetime plane. Indeed such diagram does exist. Figures 8a and 8b and their inverses Figs. 9a and 9b, in which the intrinsic spacetime coordinates are rotated being the only diagrams of Special Relativity/intrinsic Special Relativity (SR/ϕSR) in the two-world picture.

As discussed earlier, the flat four dimensional metric spacetime $(\Sigma, ct) \equiv (x, y, z, ct)$ is the outward (or physical) manifestation of the flat two-dimensional metric intrinsic spacetime $(\phi\rho, \phi c\phi t)$ in Fig. 7. Likewise the extended mutually orthogonal straight line affine coordinates $\tilde{x}, \tilde{y}$ and $\tilde{z}$ constitute a flat affine 3-space, shown as a straight line and denoted by $\tilde{\Sigma}(\tilde{x}, \tilde{y}, \tilde{z})$ along the horizontal in the first quadrant. It is the outward manifestation of the extended straight line affine intrinsic coordinate $\phi\tilde{x}$ underlying it in Figs. 8a and 8b. And the extended straight line affine time coordinate $c\tilde{t}$ is the outward (or physical) manifestation of the extended straight line affine intrinsic time coordinate $\phi c\phi\tilde{t}$ along the vertical in Figs. 8a and 8b. The extended straight line affine spacetime coordinates $\tilde{x}', \tilde{y}', \tilde{z}'$ and $c\tilde{t}'$ are likewise the outward manifestations of the extended affine intrinsic spacetime coordinates $\phi\tilde{x}'$ and $\phi c\phi\tilde{t}'$ in Figs. 9a and 9b.

It follows by virtue of the foregoing paragraph that the LT and its inverse in the context of SR are the outward (or physical) manifestations of the intrinsic Lorentz transformation (ϕLT) of system (13) or (20) and its inverse of system (16) or (21). We must simply remove the symbol ϕ in systems (13) and (16) to have the LT and its inverse in SR respectively as follows:

$$c\tilde{t}' = c\tilde{t}\sec\psi - \tilde{x}\tan\psi$$
(w.r.t. $\tilde{P}$eter in $c\tilde{t}$)

$$\tilde{x}' = \tilde{x}\sec\psi - c\tilde{t}\tan\psi, \quad \tilde{y}' = \tilde{y}, \quad \tilde{z}' = \tilde{z}$$
(w.r.t. Peter in $\tilde{\Sigma}$)
$\qquad$ (28)

and

$$c\tilde{t} = c\tilde{t}'\sec\psi + \tilde{x}'\tan\psi$$
(w.r.t. Paul in $\tilde{\Sigma}'$)

$$\tilde{x} = \tilde{x}'\sec\psi + c\tilde{t}'\tan\psi, \quad \tilde{y} = \tilde{y}', \quad \tilde{z} = \tilde{z}'$$
(w.r.t. $\tilde{P}$aul in $c\tilde{t}'$)
$\qquad$ (29)

where $-\frac{\pi}{2} < \psi < \frac{\pi}{2}$ (temporarily).

The trivial transformations $\tilde{y} = \tilde{y}'$ and $\tilde{z} = \tilde{z}'$ of the coordinates along which relative motion of SR does not occur have been added to the first and second equations of systems (28) obtained by simply removing symbol ϕ from system (13) on page 40 and to the first and second equations of system (29) obtained by simply removing symbol ϕ from system (16) on page 42, thereby making the resulting LT of system (28) and its inverse of system (29) consistent with the 4-geometry of SR. The angle ψ being the outward manifestation in spacetime of the intrinsic angle $\phi\psi$ in intrinsic spacetime, has the same temporary range in systems (28) and (29) as does $\phi\psi$ in systems (13) and (16). This temporary range of ψ shall also be modified shortly in this section.

System (28) indicates that the affine spacetime coordinates $\tilde{x}'$ and $c\tilde{t}'$ are rotated at equal angle ψ relative to the affine spacetime coordinates $\tilde{x}$ and $c\tilde{t}$ respectively, while $\tilde{y}$ is not rotated relative $\tilde{y}'$ and $\tilde{z}'$ is not rotated relative to $\tilde{z}$ by angle ψ in the context of SR and system (29) indicates that $\tilde{x}$

and $c\tilde{t}$ are rotated by equal negative angle $-\psi$ relative to $\tilde{x}'$ and $c\tilde{t}'$ respectively. However the relative rotations of the affine coordinates of the four-dimensional spacetime do not exist in reality, as discussed earlier. The indicated rotations in systems (28) and (29) may be referred to as intrinsic (i.e. non-observable or hypothetical) relative rotations of affine spacetime coordinates only, which is what the actual relative rotations of affine intrinsic spacetime coordinates in Figs. 8a and 8b and Figs. 9a and 9b represent.

By considering the spatial origin $\tilde{x}' = \tilde{y}' = \tilde{z}' = 0$ of the primed frame, system (29) reduces as follows:

$$c\tilde{t} = c\tilde{t}' \sec\psi \quad \text{and} \quad \tilde{x} = \tilde{x}' \tan\psi . \tag{30}$$

And by dividing the second equation into the first equation of system (30) we have

$$\frac{\tilde{x}}{c\tilde{t}} = \sin\psi .$$

But, $\tilde{x}/\tilde{t} = v$, is the speed of the primed frame ($\tilde{x}'$, $\tilde{y}'$, $\tilde{z}'$, $c\tilde{t}'$) frame relative to the unprimed frame ($\tilde{x}$, $\tilde{y}$, $\tilde{z}$, $c\tilde{t}$), for relative motion along the collinear $\tilde{x}$ and $\tilde{x}'$ coordinates of the frames. Hence

$$\sin\psi = v/c = \beta , \tag{31}$$

$$\sec\psi = \frac{1}{\sqrt{1 - v^2/c^2}} = \gamma . \tag{32}$$

Relations (31) and (32) on flat four-dimensional spacetime corresponds to relations (18) and (19) respectively on flat two-dimensional intrinsic spacetime. By using Eqs. (31) and (32) in systems (28) and (29) we obtain the LT and its inverse in their usual explicit forms respectively as follows:

$$\left.\begin{array}{c} \tilde{t}' = \gamma\left(\tilde{t} - \dfrac{v}{c^2}\,\tilde{x}\right) \\ \text{(w.r.t. P̃eter in } c\tilde{t}) \\[6pt] \tilde{x}' = \gamma\left(\tilde{x} - v\tilde{t}\right), \quad \tilde{y}' = \tilde{y}, \quad \tilde{z}' = \tilde{z} \\ \text{(w.r.t. Peter in } \tilde{\Sigma}) \end{array}\right\} \tag{33}$$

and

$$\left.\begin{array}{c} \tilde{t} = \gamma\left(\tilde{t}' + \dfrac{v}{c^2}\,\tilde{x}'\right) \\ \text{(w.r.t. Paul in } \tilde{\Sigma}') \\[6pt] \tilde{x} = \gamma\left(\tilde{x}' + v\tilde{t}'\right), \quad \tilde{y} = \tilde{y}', \quad \tilde{z} = \tilde{z}' \\ \text{(w.r.t. P̃eter in } c\tilde{t}') \end{array}\right\}. \tag{34}$$

Systems (33) and (34) are the outward (or physical) manifestations on flat four-dimensional spacetime (Σ, ct) in the context of SR of systems (20) and (21) respectively on the flat two-dimensional intrinsic spacetime $(\phi\rho, \phi c\phi t)$ in the context of ϕSR in the positive universe.

Systems (28) and (29) or the explicit form (33) or (34) implies Lorentz invariance (LI) in SR in the positive universe:

$$c^2\tilde{t}^2 - \tilde{x}^2 - \tilde{y}^2 - \tilde{z}^2 = c^2\tilde{t}'^2 - \tilde{x}'^2 - \tilde{y}'^2 - \tilde{z}'^2 . \tag{35}$$

This is the outward manifestation on flat four-dimensional spacetime of SR of the intrinsic Lorentz invariance (ϕLI) (22) on page 42 on flat two-dimensional intrinsic spacetime of ϕSR. Just as the intrinsic LT and its inverse of system (13) on page 40 and (16) on page 42 in the context of ϕSR are made manifest in systems (28) and (29) respectively in SR in the positive universe, the intrinsic LT and its inverse of systems (23) and (24) in ϕSR are made manifest in LT and its inverse in SR in the negative universe respectively as follows:

$$\left.\begin{array}{c} -c\tilde{t}'^* = -c\tilde{t}^* \sec\psi - (-\tilde{x}^*) \tan\psi \\ \text{(w.r.t. P̃eter}^* \text{ in } -c\tilde{t}^*) \\[6pt] -\tilde{x}'^* = -\tilde{x}^* \sec\psi - (-c\tilde{t}^*) \tan\psi , \\ -\tilde{y}'^* = -\tilde{y}^*, \quad -\tilde{z}'^* = -\tilde{z}^* \\ \text{(w.r.t. Peter}^* \text{ in } -\tilde{\Sigma}^*) \end{array}\right\} \tag{36}$$

and

$$\left.\begin{array}{c} -c\tilde{t}^* = -c\tilde{t}'^* \sec\psi + (-\tilde{x}'^*) \tan\psi \\ \text{(w.r.t. Paul}^* \text{ in } -\tilde{\Sigma}'^*) \\[6pt] -\tilde{x}^* = -\tilde{x}'^* \sec\psi + (-c\tilde{t}'^*) \tan\psi , \\ -\tilde{y}^* = -\tilde{y}'^*, \quad -\tilde{z}^* = -\tilde{z}'^* \\ \text{(w.r.t. P̃aul}^* \text{ in } -c\tilde{t}'^*) \end{array}\right\}. \tag{37}$$

And by using equations (31) and (32) in systems (36) and (37) we obtain the LT and it inverse in their usual explicit forms in the negative universe as follows:

$$\left.\begin{array}{c} -\tilde{t}'^* = \gamma\left(-\tilde{t}^* - \dfrac{v}{c^2}\,(-\tilde{x}^*)\right) \\ \text{(w.r.t. P̃eter}^* \text{ in } -c\tilde{t}^*) \\[6pt] -\tilde{x}'^* = \gamma\left(-\tilde{x}^* - v(-\tilde{t}^*)\right), \quad -\tilde{y}'^* = -\tilde{y}^*, \quad -\tilde{z}'^* = -\tilde{z}^* \\ \text{(w.r.t. Peter}^* \text{ in } -\tilde{\Sigma}^*) \end{array}\right\} \tag{38}$$

and

$$\left.\begin{array}{c} -\tilde{t}^* = \gamma\left(-\tilde{t}'^* + \dfrac{v}{c^2}\,(-\tilde{x}'^*)\right) \\ \text{(w.r.t. Paul}^* \text{ in } -\tilde{\Sigma}'^*) \\[6pt] -\tilde{x}^* = \gamma\left(-\tilde{x}'^* + v(-\tilde{t}'^*)\right), \quad -\tilde{y}^* = -\tilde{y}'^*, \quad -\tilde{z}^* = -\tilde{z}'^* \\ \text{(w.r.t. P̃aul}^* \text{ in } -c\tilde{t}'^*) \end{array}\right\}. \tag{39}$$

Systems (38) and (39) are the outward manifestations on flat four-dimensional spacetime $(-\Sigma^*, -ct^*)$ of SR of systems (25) and (26) respectively on flat two-dimensional intrinsic spacetime $(-\phi\rho^*, -\phi c\phi t^*)$ of ϕSR in the negative universe. Either the LT (36) or its inverse (37) or the explicit form (38) or (39) implies Lorentz invariance in SR in the negative universe:

$$(-c\tilde{t}^*)^2 - (-\tilde{x}^*)^2 - (-\tilde{y}^*)^2 - (-\tilde{z}^*)^2 = $$
$$= (-c\tilde{t}'^*)^2 - (-\tilde{x}'^*)^2 - (-\tilde{y}'^*)^2 - (-\tilde{z}'^*)^2 . \tag{40}$$

This is the outward manifestation on the flat four-dimensional spacetime of SR of the intrinsic Lorentz invariance (27)
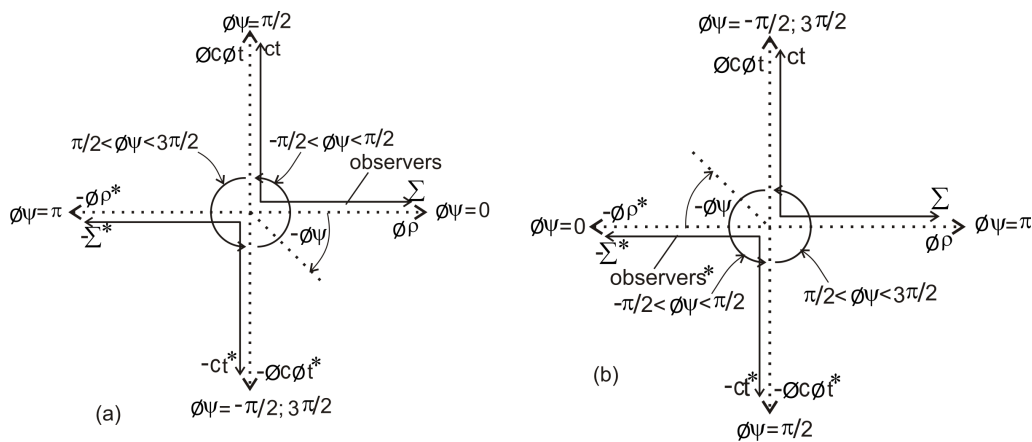
Fig. 10: The concurrent open intervals $(-\frac{\pi}{2}, \frac{\pi}{2})$ and $(\frac{\pi}{2}, \frac{3\pi}{2})$ within which the intrinsic angle $\phi\psi$ could take on values: a) with respect to 3-observers in the positive universe and b) with respect to 3-observers in the negative universe.

on page 43 on flat two-dimensional intrinsic spacetime of ϕSR in the negative universe. The restriction of the values of the intrinsic angle $\phi\psi$ to a half-plane $(-\frac{\pi}{2} < \phi\psi < \frac{\pi}{2})$ with respect to observers in the positive universe in systems (13) and (16) and with respect to observers* in the negative universe in systems (23) and (24) is a temporary measure as indicated in those systems. The intrinsic angle $\phi\psi$ actually takes on values on the entire plane $[-\frac{\pi}{2} \leqslant \phi\psi \leqslant \frac{3\pi}{2}]$ with respect to observers in the positive and negative universes, except that certain values of $\phi\psi$ namely, $-\frac{\pi}{2}$, $\frac{\pi}{2}$ and $\frac{3\pi}{2}$, must be excluded, as shall be discussed more fully shortly. The values of $\phi\psi$ in the first cycle as well as negative senses of rotation (by negative intrinsic angle $-\phi\psi$) with respect to 3-observers in the 3-spaces in the positive and negative universes are shown in Figs. 10a and 10b respectively.

We have thus obtained a (new) set of spacetime/intrinsic spacetime diagrams namely, Figs. 8a and 8b and their inverses Figs. 9a and 9b in the context of Scheme II in Table 1 or in the two-world picture, for deriving intrinsic Lorentz transformation (ϕLT) and its inverse in terms of extended straight line affine intrinsic spacetime coordinates $\phi\tilde{x}'$, $\phi c\phi\tilde{t}'$ and $\phi\tilde{x}$, $\phi c\phi\tilde{t}$ on the flat two-dimensional metric intrinsic spacetime ($\phi\rho$, $\phi c\phi t$) of the two-dimensional intrinsic Special Theory of Relativity (ϕSR) in both the positive and negative universes and for deriving the Lorentz transformation (LT) and its inverse in terms of extended straight line affine spacetime coordinates $\tilde{x}$, $\tilde{y}$, $\tilde{z}$, $c\tilde{t}$ and $\tilde{x}'$, $\tilde{y}'$, $\tilde{z}'$, $c\tilde{t}'$, as outward (or physical) manifestations on the flat four-dimensional spacetime of SR of the intrinsic Lorentz transformation (ϕLT) and its inverse of ϕSR in both the positive and negative universes. Figures 8a and 8b and their inverses Figs. 9a and 9b must replace the Minkowski diagrams of Figs. 3a and 3b in the context of Scheme I in Table 1 or in the one-world picture.

The skewness of the rotated spacetime coordinates in the Minkowski diagrams of Figs. 3a and 3b (and in the Loedel and Brehme diagrams of Figs. 4a and 4b), from which the LT and its inverse have sometimes been derived until now in the existing one-world picture, has been remarked to be undesirable earlier in this paper because the observer at rest with respect to the frame with rotated spacetime coordinates could detect the skewness of the coordinates of his frame as an effect of the uniform motion of his frame. Moreover the skewness of the rotated coordinates of the "moving" frame vis-a-vis the non-skewed coordinates of the "stationary" frame (in the Minkowski diagrams) gives apparent preference to one of two frames in uniform relative motion. On the other hand, neither the skewness of the rotated intrinsic spacetime coordinates of the "moving" frame nor of the "stationary" frame occurs in Figs. 8a, 8b, 9a and 9b. The diagrams of Figs. 8a, 8b, 9a and 9b in the two-world picture do not give apparent preference for any one of the pair of intrinsic frames in relative intrinsic motion and consequently do not give apparent preference for any one of the pair of frames on four-dimensional spacetime in relative motion, since both intrinsic frames have mutually orthogonal intrinsic spacetime coordinates in each of those figures.

Although the negative universe is totally elusive to people in our (or positive) universe, just as our universe is totally elusive to people in the negative universe, from the point of view of direct experience, we have now seen in the above that the intrinsic spacetime coordinates of the two universes unite in prescribing intrinsic Lorentz transformation and intrinsic Lorentz invariance on the flat two-dimensional intrinsic spacetime and consequently in prescribing Lorentz transformation and Lorentz invariance on flat four-dimensional spacetime in each of the two universes. It can thus be said that there is intrinsic (or non-observable) interaction of four-dimensional spacetime coordinates of the two universes in Special Relativity.

The singularities at $\phi\psi = \frac{\pi}{2}$ and $\phi\psi = -\frac{\pi}{2}$ or $\phi\psi = \frac{3\pi}{2}$ in systems (13) and (16), (of Scheme II in Table 1 or in the two-world picture), correspond to the singularities at $\alpha = \infty$ and $\alpha = -\infty$ in the coordinate transformation of systems (4) and (5) in the Minkowski one-world picture. Being smooth

for all values of α, except for the extreme values, $\alpha = \infty$ and $\alpha = -\infty$, at its boundary represented by the vertical line in Fig. 1a, which corresponds to a line along the ct- and $-ct^*$-axes in Fig. 2a, the only (positive) Minkowski space including the time reversal dimension, (to be denoted by $(\Sigma, ct, -ct^*)$), in Fig. 2a in the one-world picture is usually considered to be sufficiently smooth. Similarly being smooth for all values of the intrinsic angle $\phi\psi$ in the first cycle, except for $\phi\psi = -\frac{\pi}{2}, \frac{\pi}{2}$ and $\phi\psi = \frac{3\pi}{2}$ along their interface in Fig. 2b, the positive Minkowski space including the time reversal dimension $(\Sigma, ct, -ct^*)$ and the negative Minkowski space including time reversal dimension $(-\Sigma^*, -ct^*, ct)$ of the two-world picture in Fig. 2b must be considered to be sufficiently smooth individually.

An attempt to compose the positive Minkowski space including the time reversal dimension $(\Sigma, ct, -ct^*)$ and the negative Minkowski space including time reversal dimension $(-\Sigma^*, -ct^*, ct)$ into a single space, over which $\phi\psi$ has values within the range $[-\frac{\pi}{2}, \frac{3\pi}{2}]$ or $[0, 2\pi]$, cannot work since the resultant space possesses interior (and not boundary) discontinuities at $\phi\psi = \frac{\pi}{2}$ in the case of the range $[-\frac{\pi}{2}, \frac{3\pi}{2}]$ and $\phi\psi = -\frac{\pi}{2}$, $\phi\psi = \frac{\pi}{2}$ and $\phi\psi = \frac{3\pi}{2}$ in the case of the range $[0, 2\pi]$, thereby making the single space generated non-smooth. This implies that the larger spacetime domain of combined positive and and negative universes cannot be considered as a continuum of event domain or as constituting a single world or universe. The lines of singularity $\phi\psi = \frac{\pi}{2}$ and $\phi\psi = -\frac{\pi}{2}$ along the vertical ct- and and $-ct^*$-axes respectively represent event horizons, (the special-relativistic event horizons), to observers in 3-spaces Σ and $-\Sigma^*$ in the positive and negative universes respectively. These event horizons at $\phi\psi = \frac{\pi}{2}$ and $-\frac{\pi}{2}$ show up as singularities in the intrinsic Lorentz transformation (ϕLT) and its inverse of systems (13) and (16) and consequently in the LT and its inverse of systems (28) and (29) in the positive universe and in ϕLT and its inverse of systems (23) and (24) and consequently in the LT and its inverse of systems (36) and (37) in the negative universe.

The observers in 3-space on one side of the event horizons along the dimensions ct and $-ct^*$ in Fig. 5 and Fig. 7 cannot observe events taking place on the other side. This makes a two-world interpretation of Scheme II in Table 1 with the spacetime/intrinsic spacetime diagram of Fig. 7 mandatory.

4.5 Reduction of the LT and its inverse to length contraction and time dilation formulae from the point of view of what can be measured with laboratory rod and clock

Nature makes use of all the terms of the LT, system (28) or (33), and its inverse, system (29) or (34) to establish Lorentz invariance. However man could not detect all the terms of the LT and its inverse with his laboratory rod and clock. First of all, it is the last three equations of system (28) or (33) written by or with respect to the 3-observer (Peter) in 3-space in

the unprimed frame with affine coordinates $\tilde{x}, \tilde{y}$ and $\tilde{z}$ and the first equation of system (29) or (34) written by or with respect to the 3-observer Paul in 3-space in the primed frame with affine coordinates $\tilde{x}', \tilde{y}'$ and $\tilde{z}'$ that are relevant for the measurements of distance in space by a rod in 3-space and of time duration by a clock kept in 3-space respectively of a special-relativistic event by 3-observers in 3-space. By collecting those equations we have the following:

$$\tilde{x}' = \tilde{x} \sec\psi - c\tilde{t} \tan\psi, \quad \tilde{y}' = \tilde{y}, \quad \tilde{z}' = \tilde{z} \qquad (41a)$$

(w.r.t. 3-observer Peter in $\tilde{\Sigma}$), and

$$c\tilde{t} = c\tilde{t}' \sec\psi + \tilde{x}' \tan\psi \qquad (41b)$$

(w.r.t. 3-observer Paul in $\tilde{\Sigma}'$).

Now when Peter picks his laboratory rod to measure length, he will be unable to measure the term $-c\tilde{t}\tan\psi$ of the first equation of system (41a) with his laboratory-rod. Likewise when Paul picks his clock to measure time duration, he will be unable to measure the term $\tilde{x}'\tan\psi$ in (41b) with his clock. Thus from the point of view of what can be measured by laboratory rod and clock by observers in 3-space, system (41a) and Eq. (41b) reduce as follows:

$$\tilde{x} = \tilde{x}' \cos\psi, \quad \tilde{y} = \tilde{y}', \quad \tilde{z} = \tilde{z}', \quad \tilde{t} = \tilde{t}' \sec\psi. \qquad (42)$$

System (42) becomes the following explicit form in terms of particle's speed relative to the observer by virtue of Eq. (32) on page 44:

$$\left.\begin{array}{l} \tilde{x} = \tilde{x}' \sqrt{1 - v^2/c^2}, \quad \tilde{y} = \tilde{y}', \quad \tilde{z} = \tilde{z}' \\[2mm] \tilde{t} = \dfrac{\tilde{t}'}{\sqrt{1 - v^2/c^2}} \end{array}\right\}. \qquad (43)$$

These are the well known length contraction and time dilation formulae for two frames in relative motion along their collinear $\tilde{x}$- and $\tilde{x}'$-axes in SR. Showing that they pertain to the measurable sub-space of the space of SR is the essential point being made here.

4.6 The generalized form of intrinsic Lorentz transformation in the two-world picture

Now let us rewrite the intrinsic Lorentz transformation (ϕLT) and its inverse of systems (13) on page 40 and (16) on page 42 in the positive universe in the generalized forms in which they can be applied for all values of $\phi\psi$ in the concurrent open intervals $(-\frac{\pi}{2}, \frac{\pi}{2})$ and $(\frac{\pi}{2}, \frac{3\pi}{2})$ in Fig. 10a by factorizing out $\sec\phi\psi$ to have respectively as follows:

$$\left.\begin{array}{l} \phi c\phi\tilde{t}' = \sec\phi\psi \, (\phi c\phi\tilde{t} - \phi\tilde{x} \sin\phi\psi) \\[2mm] \phi\tilde{x}' = \sec\phi\psi \, (\phi\tilde{x} - \phi c\phi\tilde{t} \sin\phi\psi) \end{array}\right\} \qquad (44)$$

and

$$\left.\begin{array}{l} \phi c\phi\tilde{t} = \sec\phi\psi \, (\phi c\phi\tilde{t}' + \phi\tilde{x}' \sin\phi\psi) \\[2mm] \phi\tilde{x} = \sec\phi\psi \, (\phi\tilde{x}' + \phi c\phi\tilde{t}' \sin\phi\psi) \end{array}\right\}. \qquad (45)$$

The 3-observers in the Euclidean 3-space Σ of the positive universe "observe" intrinsic Special Relativity (ϕSR) and consequently observe Special Relativity (SR) for intrinsic angles $\phi\psi$ in the range $(-\frac{\pi}{2}, \frac{\pi}{2})$. However as Fig. 10a shows, 3-observers in the positive universe could construct ϕSR and hence SR relative to themselves for all intrinsic angles $\phi\psi$ in the concurrent open intervals $(-\frac{\pi}{2}, \frac{\pi}{2})$ and $(\frac{\pi}{2}, \frac{3\pi}{2})$, by using the generalized intrinsic Lorentz transformation (ϕLT) and its inverse of systems (44) and (45) and obtaining the LT and its inverse as outward manifestations on flat four-dimensional spacetime of the ϕLT and its inverse so derived, although they can observe Special Relativity for intrinsic angles $\phi\psi$ in $(-\frac{\pi}{2}, \frac{\pi}{2})$ in Fig. 10a only.

Likewise the ϕLT and its inverse in the negative universe of systems (25) on page 43 and (26) on page 43, shall be written in the generalized forms in which they can be applied for all intrinsic angles $\phi\psi$ in the concurrent open intervals $(-\frac{\pi}{2}, \frac{\pi}{2})$ and $(\frac{\pi}{2}, \frac{3\pi}{2})$ in Fig. 10b respectively as follows:

$$\left.\begin{array}{l} -\phi c\, \phi\tilde{t}'^* = \sec\phi\psi\,(-\phi c\, \phi\tilde{t}^* - (-\phi\tilde{x}^*)\sin\phi\psi) \\ -\phi\tilde{x}'^* = \sec\phi\psi\,(-\phi\tilde{x}^* - (-\phi c\, \phi\tilde{t}^*)\sin\phi\psi) \end{array}\right\} \quad (46)$$

and

$$\left.\begin{array}{l} -\phi c\, \phi\tilde{t}^* = \sec\phi\psi\,(-\phi c\, \phi\tilde{t}'^* + (-\phi\tilde{x}'^*)\sin\phi\psi) \\ -\phi\tilde{x}^* = \sec\phi\psi\,(-\phi\tilde{x}'^* + (-\phi c\, \phi\tilde{t}'^*)\sin\phi\psi) \end{array}\right\}. \quad (47)$$

The 3-observers* in the Euclidean 3-space $-\Sigma^*$ of the negative universe "observe" intrinsic Special Relativity (ϕSR) and hence observe Special Relativity (SR) for intrinsic angles $\phi\psi$ in the open interval $(-\frac{\pi}{2}, \frac{\pi}{2})$ in Fig. 10b. Again as Fig. 10b shows, 3-observers* in the negative universe could construct ϕSR and hence SR relative to themselves for all intrinsic angles $\phi\psi$ in the concurrent open intervals $(-\frac{\pi}{2}, \frac{\pi}{2})$ and $(\frac{\pi}{2}, \frac{3\pi}{2})$, by using the generalized ϕLT and its inverse of ϕSR of systems (46) and (47) and obtaining LT and its inverse of SR as outward manifestations on flat four-dimensional spacetime of the ϕLT and its inverse so constructed, although they can observe SR for intrinsic angles $\phi\psi$ in $(-\frac{\pi}{2}, \frac{\pi}{2})$ in Fig. 10b only.

The fact that the intrinsic Lorentz transformation (ϕLT) and its inverse represent continuous rotation of intrinsic spacetime coordinates $\phi\tilde{x}'$ and $\phi c\, \phi\tilde{t}'$ of the primed frame relative to the intrinsic spacetime coordinates $\phi\tilde{x}$ and $\phi c\, \phi\tilde{t}$ respectively of the unprimed frame through all intrinsic angles $\phi\psi$ in the closed range $[0, 2\pi]$, excluding rotation by $\phi\psi = -\frac{\pi}{2}, \frac{\pi}{2}$ and $\phi\psi = \frac{3\pi}{2}$, is clear from the concurrent open intervals $(-\frac{\pi}{2}, \frac{\pi}{2})$ and $(\frac{\pi}{2}, \frac{3\pi}{2})$ of the intrinsic angle $\phi\psi$ in Figs. 10a and 10b over which the generalized ϕLT and its inverse of systems (44) and (45) in the positive universe and systems (46) and (47) in the negative universe could be applied. We shall not be concerned with the explanation of how the intrinsic coordinates $\phi\tilde{x}'$ and $\phi c\, \phi\tilde{t}'$ of the particle's intrinsic frame can be rotated continuously relative to the intrinsic coordinates $\tilde{x}$ and $\phi c\, \phi\tilde{t}$ of the observer's intrinsic frame through intrinsic angles $\phi\psi$ in the range $[0, 2\pi]$, while avoiding $\phi\psi = \frac{\pi}{2}$ and $\phi\psi = \frac{3\pi}{2}$ in this paper.

4.7 Non-existence of light cones in the two-world picture

The concept of light-cone does not exist in the two-world picture. This follows from the derived relation, $\sin\phi\psi = \phi v/\phi c$, (Eq. (18) on page 42), which makes the intrinsic speed ϕv of relative intrinsic motion of every pair of intrinsic frames lower than the intrinsic light speed ϕc, ($\phi v < \phi c$), for all values of $\phi\psi$ in the concurrent open intervals $(-\frac{\pi}{2}, \frac{\pi}{2})$ and $(\frac{\pi}{2}, \frac{3\pi}{2})$ in Fig. 10a in the context of ϕSR and consequently speed v of relative motion of every pair of frames lower than the speed of light c, ($v < c$), for all intrinsic angles $\phi\psi$ in the concurrent open intervals $(-\frac{\pi}{2}, \frac{\pi}{2})$ and $(\frac{\pi}{2}, \frac{3\pi}{2})$ in Fig. 10a. The intrinsic angle $\phi\psi = \frac{\pi}{2}$ corresponds to intrinsic speed $\phi v = \phi c$ and $\phi\psi = -\frac{\pi}{2}$ or $\phi\psi = \frac{3\pi}{2}$ corresponds to $\phi v = -\phi c$, which are excluded from ϕSR. They correspond to speed $v = c$ and $v = -c$ respectively, which are excluded from SR.

We therefore have a situation where all intrinsic angles $\phi\psi$ in the closed range $[0, 2\pi]$, except $\phi\psi = \frac{\pi}{2}$ and $\phi\psi = \frac{3\pi}{2}$, (in Fig. 10a), are accessible to intrinsic Special Relativity (ϕSR) with intrinsic timelike geodesics and consequently to SR with timelike geodesics with respect to observers in the positive universe. All intrinsic angles $\phi\psi$ in the closed interval $[0, 2\pi]$, except $\phi\psi = \frac{\pi}{2}$ and $\phi\psi = \frac{3\pi}{2}$, (in Fig. 10b), are likewise accessible to ϕSR with intrinsic timelike geodesics and hence to SR with timelike geodesics with respect to observers* in the negative universe.

Intrinsic spacelike geodesics of for which $\phi v > \phi c$ and spacelike geodesics for which $v > c$ do not exist for any value of the intrinsic angle $\phi\psi$ in the four quadrants, that is, for $\phi\psi$ in the closed range $[0, 2\pi]$, on the larger spacetime/intrinsic spacetime domain of combined positive and negative universes in Fig. 7. Since the existence of light cones requires regions of spacelike geodesics outside the cones, the concept of light cones does not exist in the two-world picture.

4.8 Prospect for making the Lorentz group compact in the two-world picture

The impossibility of making the Lorentz group SO(3,1) compact in the context of the Minkowski geometry in the one-world picture has been remarked earlier in this paper. It arises from the fact that the unbounded parameter space $-\infty < \alpha < \infty$ of the Lorentz boost (the matrix L in (6) on page 33), in the one-world picture, is unavoidable. Compactification of the Lorentz group in the two-world picture would be interesting.

Now the new intrinsic matrix ϕL^* that generates the intrinsic Lorentz boost, $\phi\mathbf{x} \to \phi\mathbf{x}' = \phi L^* \phi\mathbf{x}$, on the flat two-dimensional intrinsic spacetime in Eq. (13) on page 40 in the positive universe or (23) on page 42 in the negative universe in the two-world picture is the following:

$$\phi L^* = \begin{pmatrix} \sec\phi\psi & -\tan\phi\psi \\ -\tan\phi\psi & \sec\phi\psi \end{pmatrix}, \quad (48)$$

where $\phi\psi$ takes on values in the concurrent open intervals $(-\frac{\pi}{2}, \frac{\pi}{2})$ and $(\frac{\pi}{2}, \frac{3\pi}{2})$ in the positive and negative universes, as

explained earlier and illustrated in Figs. 10a and 10b.

The corresponding new matrix L^* that generates the Lorentz boost, $\mathbf{x} \rightarrow \mathbf{x}' = L^*\mathbf{x}$, on flat four-dimensional spacetime in Eq. (28) on page 43 in the positive universe or (36) on page 44 in the negative universe in the two-world picture is the following

$$L^* = \begin{pmatrix} \sec\psi & -\tan\psi & 0 & 0 \\ -\tan\psi & \sec\psi & 0 & 0 \\ 0 & 0 & 1 & 0 \\ 0 & 0 & 0 & 1 \end{pmatrix} \qquad (49)$$

where, ψ takes on values in the concurrent open intervals $(-\frac{\pi}{2}, \frac{\pi}{2})$ and $(\frac{\pi}{2}, \frac{3\pi}{2})$ like $\phi\psi$, in the positive and negative universes.

The matrix L^* can be said to be the outward manifestation on flat four-dimensional spacetime of SR of the intrinsic matrix ϕL^* on flat two-dimensional intrinsic spacetime of ϕSR. It must be recalled however that while the intrinsic angle $\phi\psi$ in (48) measures actual rotation of intrinsic coordinates $\phi\tilde{x}'$ and $\phi c\phi\tilde{t}'$ of the primed frame relative to the intrinsic coordinates $\phi\tilde{x}$ and $\phi c\phi\tilde{t}$ of the unprimed frame, (as in Figs. 8a, 8b, 9a and 9b), in the context of ϕSR, the angle ψ in (49) represents intrinsic (i.e. non-observable or hypothetical) rotation of spacetime coordinates $\tilde{x}'$ and $c\tilde{t}'$ of the primed frame relative to $\tilde{x}$ and $c\tilde{t}$ of the unprimed frame.

The concurrent open intervals $(-\frac{\pi}{2}, \frac{\pi}{2})$ and $(\frac{\pi}{2}, 3\pi)$ wherein the intrinsic angle $\phi\psi$ and the angle ψ take on values in the positive and negative universes imply that the intrinsic matrix ϕL^* (the intrinsic Lorentz boost) and the Lorentz boost L^* in the two-world picture are unbounded. It must be recalled that the matrix L that generates the Lorentz boost in the Minkowski one-world picture given by Eq. (6) on page 33 is likewise unbounded because the parameter α in that matrix takes on values in the unbounded interval $(-\infty, \infty)$.

Also by letting $\phi\psi \rightarrow \frac{\pi}{2}$ and $\phi\psi \rightarrow -\frac{\pi}{2}$ or $\frac{3\pi}{2}$ in the intrinsic matrix ϕL^*, we have $\sec\phi\psi = \tan\phi\psi \rightarrow \infty$ and $\sec\phi\psi = \tan\phi\psi \rightarrow -\infty$ respectively, which shows that ϕL^* (or the intrinsic Lorentz boost) and hence the Lorentz boost L^* in the two-world picture are not closed. Whereas $\alpha \rightarrow \infty$, $\cosh\alpha \rightarrow \infty$, $\sinh\alpha \rightarrow \infty$, and $\alpha \rightarrow -\infty$, $\cosh\alpha \rightarrow \infty$, $\sinh\alpha \rightarrow -\infty$ in matrix L, which implies that the Lorentz boost in the Minkowski one-world picture is closed (since no entry of L is outside the range $-\infty < \alpha < \infty$ of the parameter α [6]). Thus L is not bounded but is closed, while ϕL^* and L^* are not bounded and not closed. The matrices L, L^* and the intrinsic matrix ϕL^* are therefore non-compact.

It is required that ϕL^* be both closed and bounded for it to be compact. Likewise the matrix L^*. It follows from this and the foregoing paragraphs that making the the intrinsic Lorentz boost (48) and consequently the Lorentz boost (49) in the two-world picture compact has not been achieved in this paper. As deduced in sub-section 1.1, making the Lorentz boost compact implies making SO(3,1) compact. Thus SO(3,1) has yet not been made compact in the two-world picture since the Lorentz boost has yet not been made compact.

There is good prospect for making SO(3,1) compact in the two-world picture however. This is so since the intrinsic matrix ϕL^* and consequently the matric L^* (the Lorentz boost in the two-world picture) will become compact by justifiably replacing the concurrent open intervals $(-\frac{\pi}{2}, \frac{\pi}{2})$ and $(\frac{\pi}{2}, \frac{3\pi}{2})$, in which the intrinsic angle $\phi\psi$ and the angle ψ take on values in ϕL^* and L^* respectively, by the concurrent closed intervals $[-(\frac{\pi}{2} - \epsilon), \frac{\pi}{2} - \epsilon]$ and $[\frac{\pi}{2} - \epsilon, \frac{3\pi}{2} - \epsilon]$, where ϵ is a small nonzero angle. This will make each of ϕL^* and L^* to be both closed and bounded and hence to be compact. It will certainly require further development of the two-world picture than in this initial paper to make SO(3,1) compact in two-world − if it will be possible.

This paper shall be ended at this point with a final remark that although the possibility of the existence of a two-world picture (or symmetry) in nature has been exposed, there is the need for further theoretical justification than contained in this initial paper and experimental confirmation ultimately, in order for any one to conclude the definite existence of the two-world picture. The next natural step will be to include the light-axis and the distinguished frame of reference of electromagnetic waves in the two-world picture that encompasses no light cones and to investigate the signs of mass and other physical parameters, as well as the possibility of invariance of natural laws in the negative universe.

Acknowledgements

References

1. Bonnor W. B. Negative mass in general relativity. *Gen. Relat. & Grav.*, 1989, v. 21, 1143–1157.

2. Segre E. Nuclei and particles. W. A. Benjamin Inc., Reading, 1977.

3. . Muirhead H. The Special Theory of Relativity. The McMillan Book Company, New York, 1973.

4. Einstein A. On the electrodynamics of moving bodies. In: *The Principle of Relativity*, a collection of memoirs on relativity, with notes by A. Sommerfeld, translated by W. Perrett and G. B. Jeffery, Methuen, 1923 (with reprints by Dover Publications).

5. Minkowski H. Space and time. *Ibid.*

6. Tung W. Group theory in physics. World Scientific Publishing Co. Pte Ltd., Singapore, 1985.

7. Loedel E. Geometric representation of Lorentz transformation. *Am. J. Phys.*, 1957, v. 25, 327.

8. Brehme R. W. A geometric representation of Galilean and Lorentz transformations. *Am. J. Phys.*, 1962, v. 30, 489.

9. Adler R., Bazin M., Schiffer M. Introduction to General Relativity. Second edition, McGraw-Hill Book Company, New York, 1975.

Two-World Background of Special Relativity. Part II

Akindele O. J. Adekugbe

P. O. Box 2575, Akure, Ondo State 340001, Nigeria
E-mail: adekugbe@alum.mit.edu

The two-world background of the Special Theory of Relativity started in part one of this article is continued in this second part. Four-dimensional inversion is shown to be a special Lorentz transformation that transforms the positive spacetime coordinates of a frame of reference in the positive universe into the negative spacetime coordinates of the symmetry-partner frame of reference in the negative universe in the two-world picture, contrary to the conclusion that four-dimensional inversion is impossible as actual transformation of the coordinates of a frame of reference in the existing one-world picture. By starting with the negative spacetime dimensions in the negative universe derived in part one, the signs of mass and other physical parameters and physical constants in the negative universe are derived by application of the symmetry of laws between the positive and negative universes. The invariance of natural laws in the negative universe is demonstrated. The derived negative sign of mass in the negative universe is a conclusion of over a century-old effort towards the development of the concept of negative mass in physics.

1 Introduction

A brief summary of the new geometrical representation of Lorentz transformation and its inverse in the two-world picture and the other associated issues presented in part one of this article [1], is appropriate at the beginning of this second part.

Having deduced from the $\gamma = \sec \psi$ parametrization of the Lorentz boost that a pair of flat four-dimensional spacetimes (or a pair of Minkowski's spaces), which are four-dimensional inversions of each other namely, $(\Sigma, ct) \equiv (x^1, x^2, x^3, ct)$ and $(-\Sigma^*, -ct^*) \equiv (-x^{1*}, -x^{2*}, -x^{3*}, -ct^*)$, co-exist in nature and that this implies the co-existence in nature of a pair of symmetrical worlds (or universes), referred to as our (or positive) universe and negative universe, a pair of two-dimensional intrinsic spacetimes denoted respectively by $(\phi\rho, \phi c\phi t)$ and $(-\phi\rho^*, -\phi c\phi t^*)$, which underlie the flat four-dimensional spacetimes (Σ, ct) of the positive universe and $(-\Sigma^*, -ct^*)$ of the negative universe respectively, were introduced (as *ansatz*) in [1]. The derived graphical representation of the larger spacetime/intrinsic spacetime of the co-existing "anti-parallel" worlds (or universes) was then derived and presented as Fig. 7 of [1].

A new set of intrinsic spacetime diagrams that involve rotations of the primed affine intrinsic spacetime coordinates $\phi\tilde{x}'$ and $\phi c\phi\tilde{t}'$ relative to the unprimed affine intrinsic spacetime coordinates $\phi\tilde{x}$ and $\phi c\phi\tilde{t}$ of a pair of frames in relative motion in the positive universe, which are united with the symmetrical rotations of the primed affine intrinsic spacetime coordinates $-\phi\tilde{x}'^*$ and $-\phi c\phi\tilde{t}'^*$ relative to the unprimed affine intrinsic spacetime coordinates $-\phi\tilde{x}^*$ and $-\phi c\phi\tilde{t}^*$ of the symmetry-partner pair of frames in simultaneous identical relative motion in the negative universe, are then drawn

on the larger spacetime/intrinsic spacetime of combined positive and negative universes, as Figs. 8a, 8b, 9a and 9b of [1]. The intrinsic Lorentz transformations (ϕLT) and its inverse are derived from the set of intrinsic spacetime diagrams and intrinsic Lorentz invariance (ϕLI) validated in the context of the intrinsic Special Theory of Relativity (ϕSR) on each of the flat two-dimensional intrinsic spacetimes ($\phi\rho, \phi c\phi t$) of the positive universe and $(-\phi\rho^*, -\phi c\phi t^*)$ of the negative universe.

The flat four-dimensional spacetimes (Σ, ct) and $(-\Sigma^*, -ct^*)$ being the outward (or physical) manifestations of their underlying flat two-dimensional intrinsic spacetimes $(\phi\rho, \phi c\phi t)$ and $(-\phi\rho^*, -\phi c\phi t^*)$ respectively and the Special Theory of Relativity (SR) on each of the spacetimes (Σ, ct) and $(-\Sigma^*, -ct^*)$ being mere outward manifestations of the intrinsic Special Theory of Relativity (ϕSR) on each of $(\phi\rho, \phi c\phi t)$ and $(-\phi\rho^*, -\phi c\phi t^*)$ respectively, the Lorentz transformation (LT) and its inverse are written directly and Lorentz invariance (LI) validated on each of the flat four-dimensional spacetimes (Σ, ct) and $(-\Sigma^*, -ct^*)$, as outward manifestations of intrinsic Lorentz transformation (ϕLT) and its inverse and intrinsic Lorentz invariance (ϕLI) derived graphically on each of $(\phi\rho, \phi c\phi t)$ and $(-\phi\rho^*, -\phi c\phi t^*)$.

There is consequently no need to draw spacetime diagrams involving relative rotations of the primed affine spacetime coordinates $\tilde{x}'$ and $c\tilde{t}'$ relative to the unprimed affine spacetime coordinates $\tilde{x}$ and $c\tilde{t}$ of a pair of frames in relative motion along their collinear $\tilde{x}'-$ and $\tilde{x}-$ axes in the positive universe, which would be united with the symmetrical rotations of the primed affine spacetime coordinates $-\tilde{x}'^*$ and $-c\tilde{t}'^*$ relative to the unprimed affine spacetime coordinates $-\tilde{x}^*$ and $-c\tilde{t}^*$ of the symmetry-partner pair of frames in simultaneous identical relative motion in the negative universe, on the larger spacetime of combined positive and negative

universes, in deriving LT and its inverse and in validating LI in the positive and negative universes. Indeed such diagrams do not exist and if drawn, they must be understood that they are intrinsic (that is, non-observable) or hypothetical diagrams only, as noted in [1].

The fact that the derived intrinsic Lorentz transformation represents rotation of intrinsic spacetime coordinates $\phi\tilde{x}'$ and $\phi c\phi\tilde{t}'$ of a particle's frame relative to intrinsic spacetime coordinates $\phi\tilde{x}$ and $\phi c\phi\tilde{t}$ respectively of the observer's frame at intrinsic angle $\phi\psi$, where $\phi\psi$ can vary continuously in the entire range $[0, 2\pi]$, except that $\phi\psi = \frac{\pi}{2}$ and $\phi\psi = \frac{3\pi}{2}$ must be avoided, are shown in [1]. The non-existence of the light cone concept and good prospect for making SO(3,1) compact in the two-world picture are also shown in [1].

The next natural step in the theoretical justification of the two-world background of the Special Theory of Relativity started in part one of this article, to which this second part is devoted, is the derivations of the signs of mass and other physical parameters and physical constants and investigation of Lorentz invariance of natural laws in the negative universe. The matter arising from [1] namely, the formal derivation (or isolation) of the flat two-dimensional intrinsic spacetimes $(\phi\rho, \phi c\phi t)$ and $(-\phi\rho^*, -\phi c\phi t^*)$ that underlie the flat four-dimensional spacetimes (Σ, ct) and $(-\Sigma^*, -ct^*)$ respectively, which were introduced (as *ansatz*) in [1], requires further development of the two-world picture than in this second part of this article to resolve.

2 Four-dimensional inversion as special Lorentz transformation of the coordinates of a frame of reference in the two-world picture

The intrinsic Lorentz transformation (ϕLT) and its inverse in the two-world picture have been written in the generalized forms of equations (44) and (45) of part one of this article [1]. They can be applied for all intrinsic angles $\phi\psi$ in the first cycle, while avoiding $\phi\psi = -\frac{\pi}{2}$, $\phi\psi = \frac{\pi}{2}$ and $\phi\psi = \frac{3\pi}{2}$, of relative rotation of the affine intrinsic spacetime coordinates $\phi\tilde{x}'$ and $\phi c\phi\tilde{t}'$ of the intrinsic particle's (or primed) frame $(\phi\tilde{x}', \phi c\phi\tilde{t}')$ relative to the affine intrinsic coordinates $\phi\tilde{x}$ and $\phi c\phi\tilde{t}$ of the intrinsic observer's (or unprimed) frame $(\phi\tilde{x}, \phi c\phi\tilde{t})$ on the larger two-dimensional intrinsic spacetime of combined positive and negative universes. They are reproduced here as follows

$$\left.\begin{array}{l} \phi c\phi\tilde{t}' = \sec\phi\psi(\phi c\phi\tilde{t} - \phi\tilde{x}\sin\phi\psi) \\[2mm] \phi\tilde{x}' = \sec\phi\psi(\phi\tilde{x} - \phi c\phi\tilde{t}\sin\phi\psi) \end{array}\right\} \quad (1)$$

and

$$\left.\begin{array}{l} \phi c\phi\tilde{t} = \sec\phi\psi(\phi c\phi\tilde{t}' + \phi\tilde{x}'\sin\phi\psi) \\[2mm] \phi\tilde{x} = \sec\phi\psi(\phi\tilde{x}' + \phi c\phi\tilde{t}'\sin\phi\psi) \end{array}\right\}, \quad (2)$$

where, as mentioned above, the intrinsic angle $\phi\psi$ can take on values in the range $[0, 2\pi]$, while avoiding $\phi\psi = \frac{\pi}{2}$ and $\phi\psi = \frac{3\pi}{2}$.

Systems (1) and (2) on the flat two-dimensional intrinsic spacetime (or in the intrinsic Minkowski space) $(\phi\rho, \phi c\phi t)$ of intrinsic Special Theory of Relativity (ϕSR) are made manifest outwardly (or physically) on the flat four-dimensional spacetime (the Minkowski space) (Σ, ct) of the Special Theory of Relativity (SR) in the positive universe respectively as follows, as developed in [1]

$$\left.\begin{array}{l} c\tilde{t}' = \sec\psi(c\tilde{t} - \tilde{x}\sin\psi) \\[2mm] \tilde{x}' = \sec\psi(\tilde{x} - c\tilde{t}\sin\psi), \quad \tilde{y}' = \tilde{y}, \quad \tilde{z}' = \tilde{z} \end{array}\right\} \quad (3)$$

and

$$\left.\begin{array}{l} c\tilde{t} = \sec\psi(c\tilde{t}' + \tilde{x}'\sin\psi), \\[2mm] \tilde{x} = \sec\psi(\tilde{x}' + c\tilde{t}'\sin\psi), \quad \tilde{y} = \tilde{y}', \quad \tilde{z} = \tilde{z}' \end{array}\right\}, \quad (4)$$

where, again, the angle ψ can take on values in $[0, 2\pi]$, excluding $\psi = \frac{\pi}{2}$ and $\psi = \frac{3\pi}{2}$.

However, it must be noted, as discussed in [1], that while the intrinsic angle $\phi\psi$ measures actual rotation of the affine intrinsic coordinates $\phi\tilde{x}'$ and $\phi c\phi\tilde{t}'$ of the intrinsic particle's frame $(\phi\tilde{x}', \phi c\phi\tilde{t}')$ relative to the intrinsic coordinates $\phi\tilde{x}$ and $\phi c\phi\tilde{t}$ respectively of the intrinsic observer's frame $(\phi\tilde{x}, \phi c\phi\tilde{t})$ in system (1), the angle ψ refers to intrinsic (i.e. non-observable) or hypothetical rotation of the coordinates $\tilde{x}'$ and $c\tilde{t}'$ of the particle's frame $(\tilde{x}', \tilde{y}', \tilde{z}', c\tilde{t}')$ relative to the coordinates $\tilde{x}$ and $c\tilde{t}$ of the observer's frame $(\tilde{x}, \tilde{y}, \tilde{z}, c\tilde{t})$ respectively in system (3). The affine spacetime coordinates $\tilde{x}', \tilde{y}', \tilde{z}', c\tilde{t}'$ of the particle's frame are not rotated relative to the coordinates $\tilde{x}, \tilde{y}, \tilde{z}, c\tilde{t}$ of the observer's frame and conversely in the present geometrical representation of Lorentz transformation and its inverse in the two-world picture started in [1].

We shall for now assume the possibility of continuous rotation of the intrinsic coordinates $\phi\tilde{x}'$ and $\phi c\phi\tilde{t}'$ of the intrinsic particle's frame by intrinsic angle $\phi\psi = \pi$, while avoiding $\phi\psi = \frac{\pi}{2}$, relative to the intrinsic coordinates $\phi\tilde{x}$ and $\phi c\phi\tilde{t}$ of the intrinsic observer's frame in the two-world picture, as developed in [1]. As also mentioned in [1], the explanation of how rotation through all angles ψ in $[0, \pi]$ while avoiding $\psi = \frac{\pi}{2}$ can be achieved shall not be of concern in this paper.

Then by letting $\phi\psi = \pi$ we have $\sec\phi\psi = -1$, $\sin\phi\psi = 0$ and system (1) simplifies as follows

$$\phi c\phi\tilde{t}' = -\phi c\phi\tilde{t} \quad \text{and} \quad \phi\tilde{x}' = -\phi\tilde{x}. \quad (5)$$

The meaning of system (5) is that upon rotation through intrinsic angle $\phi\psi = \pi$ of the intrinsic coordinates $\phi\tilde{x}'$ and $\phi c\phi\tilde{t}'$ of the intrinsic particle's frame relative to the intrinsic coordinates $\phi\tilde{x}$ and $\phi c\phi\tilde{t}$ respectively of the intrinsic observer's frame in the positive universe, the rotated intrinsic coordinates $\phi\tilde{x}'$ and $\phi c\phi\tilde{t}'$ transform into (or become) intrinsic coordinates of an observer's frame with negative sign $-\phi\tilde{x}$ and $-\phi c\phi\tilde{t}$ respectively.

The outward manifestation on flat four-dimensional spacetime of system (5) is the following

$$c\tilde{t}' = -c\tilde{t}, \quad \tilde{x}' = -\tilde{x}, \quad \tilde{y}' = -\tilde{y}, \quad \tilde{z}' = -\tilde{z}. \quad (6)$$

System (6) is valid because the intrinsic space coordinates $\phi\tilde{x}'$ and $-\phi\tilde{x}$ are made manifest in the coordinates $\tilde{x}'$, $\tilde{y}'$, $\tilde{z}'$ of 3-space $\tilde{\Sigma}'$ and the coordinates $-\tilde{x}$, $-\tilde{y}$, $-\tilde{z}$ of 3-space $-\tilde{\Sigma}$ respectively, as explained in [1].

Although the coordinates $c\tilde{t}'$ and $\tilde{x}'$ of the particle's frame are not rotated relative to the coordinates $c\tilde{t}$ and $\tilde{x}$ of the observer's frame, once the intrinsic coordinates $\phi\tilde{x}'$ and $\phi c\phi\tilde{t}'$ of the intrinsic particle's frame are rotated by intrinsic angle $\phi\psi = \pi$ relative to the intrinsic coordinates $\phi\tilde{x}$ and $\phi c\phi\tilde{t}$ of the intrinsic observer's frame, thereby giving rise to system (5), then system (6) will arise automatically as the outward manifestation of system (5). It may be observed that system (6) cannot be derived by letting $\psi = \pi$ in system (3).

According to system (5), the intrinsic particle's frame whose intrinsic coordinates $\phi\tilde{x}'$ and $\phi c\phi\tilde{t}'$ are inclined at intrinsic angle $\phi\psi = \pi$ relative to the respective intrinsic coordinates $\phi\tilde{x}$ and $\phi c\phi\tilde{t}$ of the intrinsic observer's frame in the positive universe, although is at rest relative to the observer's frame, since $\sin\phi\psi = \phi v/\phi c = 0 \Rightarrow \phi v = 0$ for $\phi\psi = \pi$, it possesses negative intrinsic spacetime coordinates relative to the intrinsic observer's frame in the positive universe. This implies that the intrinsic particle's frame has made transition into the negative universe. As confirmation of this fact, letting $\phi\psi = \pi$ in Fig. 8a of [1] causes the inclined intrinsic coordinate $\phi\tilde{x}'$ to lie along $-\phi\tilde{x}^*$ along the horizontal in the third quadrant and the inclined intrinsic coordinate $\phi c\phi\tilde{t}'$ to lie along $-\phi c\phi\tilde{t}^*$ along the vertical in the third quadrant in that figure.

The negative intrinsic coordinates $-\phi\tilde{x}$ and $-\phi c\phi\tilde{t}$ in system (5) are clearly the intrinsic coordinates of the symmetry-partner intrinsic observer's frame in the negative universe. Then by putting a dummy star label on the unprimed negative intrinsic coordinates in system (5) as our conventional way of denoting the coordinates/intrinsic coordinates and parameters/intrinsic parameters of the negative universe, in order to differentiate them from those of the positive universe we have

$$\phi c\phi\tilde{t}' = -\phi c\phi\tilde{t}^*, \quad \phi\tilde{x}' = -\phi\tilde{x}^*. \tag{7}$$

Likewise, by putting dummy star label on the negative spacetime coordinates in system (6), since they are the coordinates if the symmetry-partner observer's frame in the negative universe we have

$$c\tilde{t}' = -c\tilde{t}^*, \quad \tilde{x}' = -\tilde{x}^*, \quad \tilde{y}' = -\tilde{y}^*, \quad \tilde{z}' = -\tilde{z}^*. \tag{8}$$

System (8) is the outward manifestation on flat four-dimensional spacetime of system (7). System (7) is the form taken by the generalized intrinsic Lorentz transformation (1) for $\phi\psi = \pi$ and system (8) is the form taken by the generalized Lorentz transformation (3) for $\psi = \pi$.

Since the intrinsic particle's frame $(\phi\tilde{x}', \phi c\phi\tilde{t}')$ is at rest relative to the symmetry-partner intrinsic observer's frame $(-\phi\tilde{x}^*, -\phi c\phi\tilde{t}^*)$ in the negative universe in system (7), which is so since $\sin\phi\psi = \phi v/\phi c = 0 \Rightarrow \phi v = 0$, as mentioned ear-

lier, the intrinsic coordinates $-\phi\tilde{x}^*$ and $-\phi c\phi\tilde{t}^*$ of the intrinsic "stationary" observer's frame are identical to the coordinates $-\phi\tilde{x}'^*$ and $-\phi c\phi\tilde{t}'^*$ of the symmetry-partner intrinsic particle's frame in the negative universe. Consequently system (7) is equivalent to the following transformation of the primed intrinsic coordinates of the intrinsic particle's frame in the positive universe into the primed intrinsic coordinates of the symmetry-partner intrinsic particle's frame in the negative universe:

$$\phi c\phi\tilde{t}' = -\phi c\phi\tilde{t}'^*, \quad \phi\tilde{x}' = -\phi\tilde{x}'^*$$

or

$$\phi c\phi\tilde{t}' \to -\phi c\phi\tilde{t}'^*, \quad \phi\tilde{x}' \to -\phi\tilde{x}'^*. \tag{9}$$

This is inversions in the origin (or intrinsic two-dimensional inversions) of the intrinsic coordinates $\phi\tilde{x}'$ and $\phi c\phi\tilde{t}'$ of the intrinsic particle's frame $(\phi\tilde{x}', \phi c\phi\tilde{t}')$ in the positive universe, which arises by virtue of actual rotations of the intrinsic coordinates $\phi\tilde{x}'$ and $\phi c\phi\tilde{t}'$ by intrinsic angle $\phi\psi = \pi$ relative to the intrinsic coordinates $\phi\tilde{x}$ and $\phi c\phi\tilde{t}$ respectively of the intrinsic observer's frame $(\phi\tilde{x}, \phi c\phi\tilde{t})$ in the positive universe. The intrinsic two-dimensional inversion (9) is still the generalized intrinsic Lorentz transformation (1) for $\phi\psi = \pi$.

The outward manifestation on the flat four-dimensional spacetime of system (9), which also follows from system (8), is the following

$$c\tilde{t}' = -c\tilde{t}'^*, \quad \tilde{x}' = -\tilde{x}'^*, \quad \tilde{y}' = -\tilde{y}'^*, \quad \tilde{z}' = -\tilde{z}'^*$$

or

$$c\tilde{t}' \to -c\tilde{t}'^*, \quad \tilde{x}' \to -\tilde{x}'^*, \quad \tilde{y}' \to -\tilde{y}'^*, \quad \tilde{z}' \to -\tilde{z}'^*. \tag{10}$$

This is the corresponding inversions in the origin (or four-dimensional inversions) of the coordinates $\tilde{x}'$, $\tilde{y}'$, $\tilde{z}'$ and $c\tilde{t}'$ of the particle's frame in the positive universe, which arises as outward manifestation of system (9). The four-dimensional inversion (10) is still the generalized Lorentz transformation of system (3) for $\psi = \pi$. It shall be reiterated for emphasis that the coordinates $\tilde{x}'$, $\tilde{y}'$, $\tilde{z}'$ and $c\tilde{t}'$ of the particle's frame in the positive universe are not actually rotated by angle $\psi = \pi$ relative to the coordinates $\tilde{x}$, $\tilde{y}$, $\tilde{z}$ and $c\tilde{t}$ of the observer's frame in the positive universe, but that system (10) arises as a consequence of system (9) that arises from actual rotation of intrinsic coordinates.

Corresponding to system (9) expressing inversions in the origin of intrinsic coordinates of the intrinsic particle's frame, derived from the intrinsic Lorentz transformation (1) for $\phi\psi = \pi$, is the following inversions in the origin of the unprimed intrinsic coordinates of the intrinsic observer's frame, which can be derived from the inverse intrinsic Lorentz transformation (2) for $\phi\psi = \pi$:

$$\phi c\phi\tilde{t} = -\phi c\phi\tilde{t}^*, \quad \phi\tilde{x} = -\phi\tilde{x}^*$$

or

$$\phi c\phi\tilde{t} \to -\phi c\phi\tilde{t}^*, \quad \phi\tilde{x} \to -\phi\tilde{x}^*. \tag{11}$$

And the outward manifestation on flat four-dimensional spacetime of system (11) is the following four-dimensional

inversions of the coordinates of the observer's frame

or

$$c\tilde{t} = -c\tilde{t}^*, \quad \tilde{x} = -\tilde{x}^*, \quad \tilde{y} = -\tilde{y}^*, \quad \tilde{z} = -\tilde{z}^*$$

$$c\tilde{t} \to -c\tilde{t}^*, \quad \tilde{x} \to -\tilde{x}^*, \quad \tilde{y} \to -\tilde{y}^*, \quad \tilde{z} \to -\tilde{z}^*. \quad (12)$$

We have thus shown that intrinsic two-dimensional inversion is the special intrinsic Lorentz transformation (1) or its inverse (2) for $\phi\psi = \pi$. It transforms the intrinsic spacetime coordinates of a frame in the positive universe into the intrinsic spacetime coordinates of the symmetry-partner frame in the negative universe or conversely. Four-dimensional inversion is likewise the special Lorentz transformation (3) or its inverse (4) for $\psi = \pi$, which transforms the spacetime coordinates of a frame in the positive universe into the spacetime coordinates of the symmetry-partner frame in the negative universe or conversely.

On the other hand, it has been concluded in the context of the existing one-world background of the Special Theory of Relativity (or in the one-world picture) that four-dimensional inversion in impossible as actual transformation of the coordinates of a frame of reference. This, as discussed in [2, see p.39], for example, is due to the fact four-dimensional inversion carries the time axis from the future light cone into the past light cone, which is impossible without going through regions of spacelike geodesics that requires the introduction of imaginary spacetime coordinates in the one-world picture.

The light cone concept does not exist in the two-world picture, as deduced in sub-section 4.7 of [1]. Consequently continuous relative rotation of intrinsic spacetime coordinates of two frames through all intrinsic angles $\phi\psi$ in $[0, 2\pi]$, while avoiding $\phi\psi = \frac{\pi}{2}$ and $\phi\psi = \frac{3\pi}{2}$, is possible, (granting that how $\phi\psi = \frac{\pi}{2}$ and $\phi\psi = \frac{3\pi}{2}$ are avoided shall be explained,) without going into regions of spacelike geodesics in the two-world picture. Four-dimensional inversion, (which does not involve actual relative rotation of spacetime coordinates of two frames), being mere outward manifestation of intrinsic two-dimensional inversion that involves actual relative rotation of intrinsic spacetime coordinates of two frames, is therefore possible as transformation of the coordinates of a frame of reference in the two-world picture.

3 Sign of mass in the negative universe derived from generalized mass expression in Special Relativity in the two-world picture

Now the intrinsic particle's frame $(\phi\tilde{x}', \phi c\phi\tilde{t}')$ contains the intrinsic rest mass ϕm_0 of the particle at rest relative to it and the particle's frame $(\tilde{x}', \tilde{y}', \tilde{z}', c\tilde{t}')$ contains the rest mass m_0 of the particle at rest relative to it in the positive universe. The question arises; what are the signs of the intrinsic rest mass and rest mass of the symmetry-partner particle contained in the symmetry-partner intrinsic particle's frame $(-\phi\tilde{x}'^*, -\phi c\phi\tilde{t}'^*)$ and symmetry-partner particle's frame $(-\tilde{x}'^*, -\tilde{y}'^*, -\tilde{z}'^*, -c\tilde{t}'^*)$ respectively in the negative universes? The answer to this question shall be sought from the the

generalized intrinsic mass relation in the context of the intrinsic Special Theory of Relativity (ϕSR) and from the corresponding generalized mass relation in the context of the Special Theory of Relativity (SR) in the two-world picture in this section and by requiring the symmetry of laws between the positive and negative universes in the next section.

The well known mass relation on flat four-dimensional spacetime (Σ, ct) in the context of SR is the following

$$m = \frac{m_0}{\sqrt{1 - v^2/c^2}}. \quad (13)$$

The corresponding intrinsic mass relation on the flat two-dimensional intrinsic spacetime $(\phi\rho, \phi c\phi t)$ in the context of the intrinsic Special Theory of Relativity (ϕSR) is

$$\phi m = \frac{\phi m_0}{\sqrt{1 - \phi v^2/\phi c^2}}. \quad (14)$$

The three-dimensional masses m_0 and m in the three-dimensional Euclidean space are the outward manifestation of the one-dimensional intrinsic masses ϕm_0 and ϕm respectively in the one-dimensional intrinsic space, as illustrated in Fig. 6a of [1].

Then by using the relation, $\sec \phi\psi = (1 - \phi v^2/\phi c^2)^{-\frac{1}{2}}$ and $\sec \psi = (1 - v^2/c^2)^{-\frac{1}{2}}$ derived and presented as Eqs. (19) and (32) respectively in [1], Eqs. (14) and (13) can be written respectively as follows

$$\phi m = \phi m_0 \sec \phi\psi \quad (15)$$

and

$$m = m_0 \sec \psi. \quad (16)$$

Eqs. (15) and (16) are the generalized forms in the two-world picture of the intrinsic mass relation in the context of ϕSR and mass relation in the context of SR respectively. They can be applied for all intrinsic angle $\phi\psi$ and all angles ψ in the range $[0, 2\pi]$, except that $\phi\psi = \frac{\pi}{2}$ and $\phi\psi = \frac{3\pi}{2}$ must be avoided.

By letting $\phi\psi = \pi$ in Eq. (15) and $\psi = \pi$ in Eq. (16) we have

$$\phi m = -\phi m_0 \equiv -\phi m_0^* \quad (17)$$

and

$$m = -m_0 \equiv -m_0^*. \quad (18)$$

However the intrinsic particle's frame is stationary relative to the intrinsic observer's frame for $\phi\psi = \pi$, since then $\sin \phi\psi = \phi v/\phi c = 0 \Rightarrow \phi v = 0$, as noted earlier. Consequently the intrinsic special-relativistic mass $\phi m = \phi m_0 (1 - \phi v^2/\phi c^2)^{-\frac{1}{2}}$ must be replaced by the intrinsic rest mass ϕm_0 in (17) and the special-relativistic mass $m = m_0 (1 - v^2/c^2)^{-\frac{1}{2}}$ must be replaced by the rest mass m_0 in (18) to have respectively as follows

$$\phi m_0 = -\phi m_0^* \text{ or } \phi m_0 \to -\phi m_0^* \quad (19)$$

and

$$m_0 = -m_0^* \text{ or } m_0 \to -m_0^*. \quad (20)$$

Just as the positive intrinsic coordinates $\phi\tilde{x}'$ and $\phi c\phi\tilde{t}'$ of the intrinsic particle's frame in the positive universe

transform into the negative intrinsic coordinates $-\phi\tilde{x}'^*$ and $-\phi c\phi\tilde{t}'^*$ of the symmetry-partner intrinsic particle's frame in the negative universe expressed by system (9), by virtue of the generalized intrinsic Lorentz transformation (1) for $\phi\psi = \pi$, the positive intrinsic rest mass ϕm_0 of the particle contained in the intrinsic particle's frame $(\phi\tilde{x}', \phi c\phi\tilde{t}')$ in the positive universe, transforms into negative intrinsic rest mass $-\phi m_0^*$ contained in the intrinsic particle's frame $(-\phi\tilde{x}'^*, -\phi c\phi\tilde{t}'^*)$ in the negative universe, by virtue of the generalized intrinsic mass relation (15) for $\phi\psi = \pi$. The negative intrinsic rest mass $-\phi m_0^*$ is certainly the intrinsic rest mass of the symmetry-partner particle in the negative universe.

Likewise as the positive coordinates $\tilde{x}'$, $\tilde{y}'$, $\tilde{z}'$ and $c\tilde{t}'$ of a particle's frame in the positive universe transform into negative coordinates $-\tilde{x}'^*$, $-\tilde{y}'^*$, $-\tilde{z}'^*$ and $-c\tilde{t}'^*$ of the symmetry-partner particle's frame in the negative universe, expressed by system (10), by virtue of the generalized Lorentz transformation (3) for $\psi = \pi$, the positive rest mass m_0 of the particle contained in the particle's frame $(\tilde{x}', \tilde{y}', \tilde{z}', c\tilde{t}')$ in the positive universe, transforms into negative rest mass $-m_0^*$ contained in the symmetry-partner particle's frame $(-\tilde{x}'^*, -\tilde{y}'^*, -\tilde{z}'^*, -c\tilde{t}'^*)$ in the negative universe, by virtue of the generalized relativistic mass relation (16) for $\psi = \pi$. Again the negative rest mass $-m_0^*$ is certainly the rest mass of the symmetry-partner particle in the negative universe.

It follows from the foregoing two paragraphs that the intrinsic particle's frame containing positive intrinsic rest mass of the particle in the positive universe, to be denoted by $(\phi\tilde{x}', \phi c\phi\tilde{t}'; \phi m_0)$, corresponds to the symmetry-partner intrinsic particle's frame containing negative intrinsic rest mass $(-\phi\tilde{x}'^*, -\phi c\phi\tilde{t}'^*; -\phi m_0^*)$ in the negative universe. The particle's frame containing the positive rest mass of the particle $(\tilde{x}', \tilde{y}', \tilde{z}', c\tilde{t}'; m_0)$ in the positive universe, likewise corresponds to the symmetry-partner particle's frame containing negative rest mass $(-\tilde{x}', -\tilde{y}'^*, -\tilde{z}'^*, -c\tilde{t}'^*; -m_0^*)$ in the negative universe.

The conclusion that follows from the foregoing is that intrinsic rest masses and rest masses of material particles and objects (that appear in classical, that is, in non-special-relativistic intrinsic physics and physics) are negative quantities in the negative universe. The special-relativistic intrinsic masses $\phi m = \gamma(\phi v)\phi m_0$ and special-relativistic masses $m = \gamma(v)m_0$ of material particles and objects that appear in special-relativistic intrinsic physics and special-relativistic physics respectively are therefore negative quantities in the negative universe.

4 Derivation of the signs of physical parameters and physical constants in the negative universe by application of symmetry of laws between the positive and negative universes

Four-dimensional inversion is the transformation of the positive spacetime coordinates of a frame in the positive universe

into the negative spacetime coordinates of the symmetry-partner frame in the negative universe, as systems (10) and (12) show. Thus the simultaneous negation of spacetime coordinates in the classical or special-relativistic form of a natural law amounts to writing that law in the negative universe.

Now the prescribed perfect symmetry of state between the positive and negative universes discussed in sub-section 4.1 of part one of this article [1], will be impossible unless there is also a perfect symmetry of laws between the two universes. That is, unless natural laws take on identical forms in the two universes. Perfect symmetry of laws between the positive and negative universes is immutable, as shall be demonstrated shortly in this article. It must be recalled that Lorentz invariance in the negative universe, (which is an important component of the invariance of laws in the negative universe), has been validated from the derived LT and its inverse in the negative universe of systems (38) and (39) of [1].

The simultaneous negation of space and time coordinates in a natural law in the positive universe in the process of writing it in the negative universe will change the form of that law in general unless physical quantities and constants, such as mass, electric charge, temperature, flux, etc, which also appear in the law (usually as differential coefficients in the instantaneous differential laws) are given the appropriate signs. By combining the simultaneous negation of space and time dimensions with the invariance of laws, the signs of physical quantities and constants in the negative universe can be derived. The derivations of the signs of the fundamental quantities namely, mass, electric charge and absolute temperature in the negative universe shall be done below. The signs of all derived (or non-fundamental) physical quantities and physical constants can then be inferred from their dimensions, as shall be demonstrated.

Consider a body of constant mass m being accelerated by a force $\vec{F}$ directed along the positive X-axis of the frame attached to it. In the positive universe, Newton's second law of motion for this body is the following

$$\vec{F} = \left(m\frac{d^2x}{dt^2}\right)\hat{\imath}. \qquad (21)$$

Since the dimensions of 3-space of the negative universe is inversion in the origin of the dimensions of 3-space of the positive universe, the dimensions, unit vector and force, $(x, y, z, t; \hat{\imath}; \vec{F})$, in the positive universe correspond to $(-x^*, -y^*, -z^*, -t^*; -\hat{\imath}^*; -\vec{F}^*)$ in the negative universe. Thus in the negative universe, we must let $x \to -x^*$, $t \to -t^*$, $\hat{\imath} \to -\hat{\imath}^*$ and $\vec{F} \to -\vec{F}^*$, while leaving m unchanged meanwhile in (21) to have as follows

$$-\vec{F}^* = \left(m\frac{d^2(-x^*)}{d(-t^*)^2}\right)(-\hat{\imath}^*) = \left(m\frac{d^2x^*}{dt^{*2}}\right)\hat{\imath}^*. \qquad (22)$$

While Eq. (21) states that a body pushed towards the positive x-direction by a force $\vec{F}$, moves along the positive x-direction, (away from the force), in the positive universe,

Eq. (22) states that a body pushed in the $-x^*$-direction in the negative universe by a force $-\vec{F}^*$, moves in the $+x^*$-direction, with unit vector $+\hat{\imath}^*$, (towards the force), in the negative universe. This implies that Newton's second law of motion is different in the negative universe, contrary to the required invariance of natural laws in that universe.

In order for (22) to retain the form of (21), so that Newton's second law of motion remains unchanged in the negative universe, we must let $m \rightarrow -m^*$ in it to have as follows

$$-\vec{F}^* = \left(-m^* \frac{d^2 x^*}{dt^{*2}}\right)(\hat{\imath}^*) = \left(m^* \frac{d^2 x^*}{dt^{*2}}\right)(-\hat{\imath}^*), \qquad (23)$$

which is of the form of (21) upon cancelling the signs. The fact that we must let $m \rightarrow -m^*$ in (22) to arrive at (23) implies that mass is a negative quantity in the negative universe.

Newton's second law has been chosen because it involves spacetime coordinates and mass and no other physical quantity or constant. However the negation of mass in the negative universe does not depend on the natural law adopted, it follows from any chosen law once the signs in the negative universe of other physical quantities and physical constants that appear in that law have been correctly substituted, in addition to the simultaneous negation of space and time coordinates in the law.

The negation of mass also follows from the required invariance of the metric tensor with the reflection of spacetime dimensions. For if we consider the Schwarzschild metric in empty space at the exterior of a spherically symmetric gravitational field source, for example, then the non-trivial components of the metric tensor are, $g_{00} = -g_{11}^{-1} = 1 - 2GM/rc^2$. By letting $r \rightarrow -r^*$, we must also let $M \rightarrow -M^*$ in order to preserve the metric tensor in the negative universe. It can be verified that this is true for all other metric tensors in General Relativity.

Thus negative mass in the negative universe has again been derived from the symmetry of natural laws between the positive and negative universes, which has been derived from the generalized mass relation in the Special Theory of Relativity in the two-world picture in the preceding section.

For electric charge, the electrostatic field $\vec{E}$ emanating from a particle (assumed spherical in shape) with net electric charge q in the positive universe is given at radial distance r from the centre of the particle as follows

$$\vec{E} = \frac{q\vec{r}}{4\pi\epsilon_0 r^3}. \qquad (24)$$

The symmetry-partner electrostatic field emanating from the symmetry-partner particle in the negative universe is inversion in the origin of the electrostatic field in the positive universe. Hence the electrostatic field in the negative universe points in opposite direction in space as its symmetry-partner field $\vec{E}$ of Eq. (24) in the positive universe. This implies that the symmetry-partner electrostatic field in the negative universe is $-\vec{E}^*$. By letting $r \rightarrow -r^*$, $\vec{r} \rightarrow -\vec{r}^*$ and $\vec{E} \rightarrow -\vec{E}^*$ in

(24), while retaining q and ϵ_0 meanwhile we have

$$-\vec{E}^* = \frac{q(-\vec{r}^*)}{4\pi\epsilon_0(-r*)^3} = \frac{q\vec{r}^*}{4\pi\epsilon_0 r^{*3}} \qquad (25)$$

In order for (25) to retain the form of (24), so that Coulomb's law remains unchanged in the negative universe, we must let $q/\epsilon_0 \rightarrow -(q^*/\epsilon_0^*)$ to have

$$-\vec{E}^* = -\frac{q^* \vec{r}^*}{4\pi\epsilon_0^* r^{*3}}, \qquad (26)$$

which is of the form of Eq. (24) upon cancelling the signs. The negative sign of $-(q^*/\epsilon_0^*)$ is associated with the electric charge, while the electric permittivity of free space retains its positive sign in the negative universe. This can be ascertained from the relation for the divergence of electric field namely,

$$\vec{\nabla} \cdot \vec{E} = \frac{\rho}{\epsilon_0}. \qquad (27)$$

In the negative universe, we must let $\vec{\nabla} \rightarrow -\vec{\nabla}^*$, $\vec{E} \rightarrow -\vec{E}^*$, $\rho \rightarrow \rho^*$, (since $\rho = q/V \rightarrow -q^*/(-V^*) = q^*/V^* = \rho^*$), while retaining ϵ_0 meanwhile in (27) to have

$$-\vec{\nabla}^* \cdot (-\vec{E}^*) = \frac{\rho^*}{\epsilon_0}. \qquad (28)$$

In order for (28) to retain the form of (27), we must let $\epsilon_0 \rightarrow \epsilon_0^*$, which confirms the positivity of the electric permittivity of free space in the negative universe. The conclusion then is that the electric charge of a particle in the negative universe has opposite sign as the electric charge of its symmetry-partner in the positive universe.

We are now left to determine the sign in the negative universe of the last fundamental quantity namely, absolute temperature. It has been found impossible to determine the sign of absolute temperature in the negative universe in a unique manner from consideration of the equations of thermodynamics, kinetic theory of gases and transport phenomena. It has been necessary to make recourse to the more fundamental notions of the "arrow of entropy" and "arrow of time" in order to propagate. These notions have been made tangible by the works of Prigogine [3].

We know that entropy always increases or always "flows" along the positive direction of the "entropy axis" S in our (or the positive) universe, even as time always increases or always "flows" into the future direction, that is, along the positive time axis ct in our universe. Thus the arrow of time and the arrow of entropy lie parallel to each other in our universe. Or in the words of Prigogine, "a [positively directed] arrow of time is associated with a [positively directed] arrow of entropy". Thus absolute entropy is a positive quantity in our (or positive) universe, just as time is a positive quantity in our (or positive) universe. The arrow of time and the arrow of entropy likewise lie parallel to each other in the negative universe. We then infer from this that entropy is negatively directed and is hence a negative quantity in the negative uni-

verse, since time is negatively directed and is hence a negative quantity in the negative universe.

Having determined the sign of absolute entropy in the negative universe from the above reasoning, it is now an easy matter to determine the sign of absolute temperature in the negative universe. For let us write the following fundamental relation for absolute entropy in our universe:

$$S = k \ln W, \qquad (29)$$

where k is the Boltzmann constant and W is the number of micro-states in an ensemble in the quantum-mechanical formulation [4]. In the negative universe, we must let $S \rightarrow -S^*$ and $W \rightarrow W^*$ while retaining k meanwhile to have as follows

$$-S^* = k \ln W^*. \qquad (30)$$

In order for (30) to retain the form of (29) we must let $k \rightarrow -k^*$, in (30), to have as follows

$$-S^* = -k^* \ln W^*, \qquad (31)$$

which is of the form of (29) upon cancelling the signs. Thus the Boltzmann constant is a negative quantity in the negative universe.

The average energy ε of a molecule, for one degree-of-freedom motion of a diatomic molecule in a gas maintained at thermal equilibrium at temperature T, is given as follows

$$\varepsilon = \frac{2}{3} k T, \qquad (32)$$

where, again, k is the Boltzmann constant. In the negative universe, we must let $\varepsilon \rightarrow -\varepsilon^*$, (since the kinetic energy $\frac{1}{2}mv^2$ of molecules, like mass m, is a negative quantity in the negative universe), and $k \rightarrow -k^*$, in (32) while retaining T meanwhile to have as follows

$$-\varepsilon^* = \frac{2}{3} (-k^*) T, \qquad (33)$$

which is of the form of (32) upon cancelling the signs. The transformation, $T \rightarrow T^*$, required to convert Eq. (33) into Eq. (32) implies that absolute temperature is a positive quantity in the negative universe.

In summary, the fundamental quantities namely, mass m, electric charge Q and absolute temperature T, transform between the positive and negative universes as, $m \rightarrow -m^*$, $Q \rightarrow -Q^*$ and $T \rightarrow T^*$.

By writing various natural laws in terms of negative spacetime dimensions, negative mass, negative electric charge and positive absolute temperature and requiring the laws to retain their usual forms in the positive universe, the signs of other physical quantities and constants in the negative universe can be derived. However a faster way of deriving the signs in the negative universe of derived physical quantities and constants is to check the signs of their dimensions in the negative universe, as demonstrated for a few quantities and constants below.

Let us consider the Boltzmann constant k and absolute entropy S, whose negative signs in the negative universe have been deduced above. They both have the unit, Joule/Kelvin, or dimension $ML^2/T^2\Theta$ in the positive universe, where M represents mass "dimension", L represents length dimension, T represents time dimension and Θ represents absolute temperature "dimension". In the negative universe, we must let $M \rightarrow -M^*$, $L \rightarrow -L^*$, $T \rightarrow -T^*$ and $\Theta \rightarrow \Theta^*$, to have the dimensions of Boltzmann constant and absolute entropy in the negative universe as $-M^*(-L^*)^2/(-T^*)^2\Theta^* = -M^*L^{*2}/T^{*2}\Theta^*$. The Boltzmann constant and absolute entropy are negative quantities in the negative universe, since their common dimension is negative in the negative universe.

The Planck constant has the unit Joule/second and dimension ML^2/T^3 in the positive universe. In the negative universe, it has dimension of $-M^*(-L^*)^2/(-T^*)^3$, which is positive. Hence the Planck constant is a positive quantity in the negative universe.

The specific heat capacity c_p has the unit Joule/kg×Kelvin and dimension $L^2/T^2\Theta$ in the positive universe. In the negative universe it has dimension $(-L^*)^2/(-T^*)^2\Theta^*$, which is positive. Hence specific heat capacity is a positive quantity in the negative universe.

The electric permittivity of space ϵ has the unit of Joule×metre/Coulomb^2 and dimension ML^3/T^2C^2 in the positive universe, where C is used to represent the charge "dimension". In the negative universe, it has dimension $(-M^*)(-L^*)^3/(-T^*)^2(-C^*)^2 = M^*L^{*3}/T^{*2}C^{*2}$, which is positive. Hence the electric permittivity of space is a positive quantity in the negative universe. This fact has been derived earlier in the process of deriving the sign of electric charge in the negative universe. Likewise magnetic permeability of space μ has dimension ML/C^2 in the positive universe and dimension $-M^*(-L^*)/(-C^*)^2 = M^*L^*/C^{*2}$, in the negative universe. It is hence a positive quantity in both the positive and negative universes.

An angular measure in space in the positive universe has the same sign as the symmetry-partner angular measure in the negative universe. This follows from the fact that an arc length, $s = r\theta$ [metre], in the positive universe corresponds to a negative arc length, $s^* = -(r^*\theta^*)$ [−metre*], in the negative universe. In other words, an arc length in the positive universe and its symmetry-partner in the negative universe transform as, $r\theta \rightarrow -(r^*\theta^*)$. But the radii of the symmetry-partner arcs transform as, $r \rightarrow -r^*$. It follows from these two transformations that an angular measure in space in the positive universe has the same sign as its symmetry-partner in the negative universe, that is, $\pm\theta \rightarrow \pm\theta^*$ and $\pm\varphi \rightarrow \pm\varphi^*$, etc.

Finally, a dimensionless quantity or constant in the positive universe necessarily has the same sign as its symmetry-partner in the negative universe, as follows from the above. Examples of dimensionless constants are the dielectric constants, ϵ_r and μ_r.

Table 1 gives a summary of the signs of some physical

Physical quantity/constant	Symbol	Intrinsic quantity/ constant	Sign	
			positive universe	negative universe
Distance/dimension of space	dx; x	$d\phi x$; ϕx	+	−
Interval/dimension of time	dt; t	$d\phi t$; ϕt	+	−
Mass	m	ϕm	+	−
Electric charge	q	q	+ or −	− or +
Absolute entropy	S	ϕS	+	−
Absolute temperature	T	T	+	+
Energy (total, kinetic)	E	ϕE	+	−
Potential energy	U	ϕU	+ or −	− or +
Radiation energy	$h\nu$	$h\phi\nu$	+	−
Electrostatic potential	Φ_E	$\phi\Phi_E$	+ or −	+ or −
Gravitational potential	Φ_g	$\phi\Phi_g$	−	−
Electric field	$\vec{E}$	ϕE	+ or −	− or +
Magnetic field	$\vec{B}$	ϕB	+ or −	− or +
Planck constant	h	h	+	+
Boltzmann constant	k	ϕk	+	−
Thermal conductivity	k	ϕk	+	−
Specific heat capacity	c_p	ϕc_p	+	+
Speed	v	ϕv	+	+
Electric permittivity	ϵ_0	$\phi\epsilon_0$	+	+
Magnetic permeability	μ_0	$\phi\mu_0$	+	+
Angle	θ, φ	$\phi\theta, \phi\varphi$	+ or −	+ or −
Parity	Π	$\phi\Pi$	+ or −	− or +
$\vdots$	$\vdots$	$\vdots$	$\vdots$	$\vdots$

Table 1: The signs of physical parameters/intrinsic parameters and physical constants/intrinsic constants in the positive and negative universes.

quantities and physical constants in the positive and negative universes. The signs in the positive and negative universes of other physical quantities and constants that are not included in Table 1 can be easily determined from the signs of their dimensions in the negative universe. The appropriateness of the names positive universe and negative universe is made clearer by Table 1.

5 Demonstrating the invariance of the natural laws in the negative universe

It shall be shown in this section that the simultaneous negations of spacetime dimensions and mass, along with simultaneous reversal of the sign of electric charge, retention of the positive sign of absolute temperature and substitution of the signs of other physical quantities and physical constants in the negative universe summarized in column 5 of Table 1 in its complete form, render all natural laws unchanged. However only the invariance of a few laws in the negative universe namely, mechanics (classical and special-relativistic), quantum mechanics, electromagnetism and propagation of light, the theory of gravity, cosmology and fundamental interactions in elementary particle physics shall be demonstrated for examples.

5.1 Further on the invariance of classical mechanics, classical gravitation and Special Relativity in the negative universe

Demonstrating the invariance of classical mechanics in the negative universe consists essentially in showing that Newton's laws of motion for a body under an impressed force and due to interaction of the body with an external force field are invariant under the simultaneous operations of inversion of all coordinates (or dimensions) of 3-space (parity inversion), time reversal and mass negation. The laws are given respectively as follows in the positive universe:

$$\vec{F}_{\text{mech}} = m\,\frac{d^2 r}{dt^2}\,\hat{r} \qquad (34)$$

and

$$\vec{F}_{\text{field}} = m\,(-\nabla\Phi)\,\hat{k}, \qquad (35)$$

where $\hat{r}$ and $\hat{k}$ are unit vectors in the directions of the forces $\vec{F}_{\text{mech}}$ and $\vec{F}_{\text{field}}$ respectively.

In the negative universe, we must let $\vec{F}_{\text{mech}} \to -\vec{F}^*_{\text{mech}}$, $\vec{F}_{\text{field}} \to -\vec{F}^*_{\text{field}}$, $m \to -m^*$, $r \to -r^*$, $t \to -t^*$, $\nabla \to -\nabla^*$, $\Phi \to \Phi^*$ (for gravitational and elastic potentials), $\hat{r} \to -\hat{r}^*$ and $\hat{k} \to -\hat{k}^*$ in (34) and (35) to have as follows

$$-\vec{F}^*_{\text{mech}} = -m^*\,\frac{d^2(-r^*)}{d(-t^*)^2}\,(-\hat{r}^*) = m^*\,\frac{d^2 r^*}{dt^{*2}}\,(-\hat{r}^*) \qquad (36)$$

and

$$-\vec{F}^{\,*}_{\text{field}} = -m^*(-(-\nabla^*)(\Phi^*))(-\hat{k}^*)$$
$$= m^*(-\nabla^*\Phi^*)(-\hat{k}^*) \qquad (37)$$

Equations (36) and (37) are the same as Eqs. (34) and (35) respectively upon cancelling the signs.

The invariance in the negative universe of the classical laws of motion (34) and (35) in the positive universe implies that a body of negative mass $-m^*$ in the negative universe moves along a trajectory, when impressed upon by an external mechanical force $-\vec{F}^{\,*}_{\text{mech}}$, or when it is moving within a force field with potential function Φ^* in the negative universe, which is identical to the trajectory followed by the symmetry-partner body of positive mass m in the positive universe, which is impressed upon by an external symmetry-partner mechanical force $\vec{F}_{\text{mech}}$ or which is moving within a symmetry-partner force field with potential function Φ in the positive universe.

The invariance in the negative universe of trajectories of a body implied by the invariance in the negative universe of the differential classical laws of motion (34) and (35) for the body, established above can be alternatively formulated as the invariance in the negative universe of the variational formula of Maupertuis. In the positive universe, this is given as follows

$$\delta \int_{P_1}^{P_2} \left(\frac{2}{m} (E - U) \right)^{1/2} dt = 0 . \qquad (38)$$

In the negative universe, we must let $m \to -m^*$, $E \to -E^*$, $U \to -U^*$ and $dt \to -dt^*$ in (38) to have as follows

$$\delta \int_{p_1^*}^{p_2^*} \left(\frac{2}{-m^*} (-E^* - (-U^*)) \right)^{1/2} (-dt^*) =$$
$$= \delta \int_{p_1^*}^{p_2^*} \left(\frac{2}{m^*} (E^* - U^*) \right)^{1/2} dt^* = 0 . \qquad (39)$$

The summary of the above is that although inertial mass, kinetic energy, distances in space and periods of time are negative in the negative universe, material particles in the negative universe perform identical motions under impressed forces and external force fields as their symmetry-partners perform under symmetry-partner impressed forces and external force fields in the positive universe. Thus outward external forces lead to outward motions of bodies both in the positive and negative universes. Attractive gravitational field in the positive universe correspond to symmetry-partner repulsive gravitational field in the negative universe, but they both give rise to attractive motions of particles (towards the field sources) in both universes. In brief, the transformation of classical mechanics in the positive universe into the negative universe does not give rise to strange motions and associated strange phenomena.

Demonstrating the invariance of classical gravitation (or classical gravitational interaction) in the negative universe

consists in showing the invariance in the negative universe of the Newtonian law of gravity in differential form and the implied Newtonian law of universal gravity,

$$\vec{\nabla} \cdot \vec{g} = -4\pi G \varrho \qquad (40)$$

or

$$\nabla^2 \Phi = 4\pi G \varrho \qquad (41)$$

and

$$\vec{F} = m\vec{g} = -\frac{GMm\vec{r}}{r^3} , \qquad (42)$$

where

$$\varrho = m/V \ (\text{mass} - \text{density}), \qquad (43)$$
$$\Phi = -GM/r , \qquad (44)$$
$$\vec{g} = -GM\vec{r}/r^3 . \qquad (45)$$

In writing equations (43)–(45) in the negative universe, we must let $m \to -m^*$; $M \to -M^*$; $r \to -r^*$ and $V \to -V^*$ (volume of m) to have

$$\frac{m}{V} \to \frac{-m^*}{-V^*} = \frac{m^*}{V^*} \Rightarrow \varrho \to \varrho^* \qquad (46)$$

$$-\frac{GM}{r} \to -\frac{G(-M^*)}{-r^*} = -\frac{GM^*}{r^*} \Rightarrow \Phi \to \Phi^* \qquad (47)$$

and

$$-\frac{GM\vec{r}}{r^3} \to -\frac{G(-M)(-\vec{r}^*)}{(-r^*)^3} = \frac{GM^*\vec{r}^*}{r^{*3}} \Rightarrow \vec{g} \to -\vec{g}^*. \qquad (48)$$

By using the transformations (46)–(48) along with $\vec{\nabla} \to -\vec{\nabla}^*$ in equations (40)–(42) we have

$$(-\vec{\nabla}^*) \cdot (-\vec{g}^*) = -4\pi G \varrho^*$$

or

$$\vec{\nabla}^* \cdot \vec{g}^* = -4\pi G \varrho^*, \qquad (49)$$

$$(-\nabla^*)^2 \Phi^* = 4\pi G \varrho^*$$

or

$$\nabla^{*2} \Phi^* = 4\pi G \varrho^* \qquad (50)$$

and

$$\vec{F}^* = (-m^*)(-\vec{g}^*) = -\frac{G(-M^*)(-m^*)(-\vec{r}^*)}{(-r^*)^3}$$

or

$$\vec{F}^* = m^*\vec{g}^* = -\frac{GM^*m^*\vec{r}^*}{r^{*3}} . \qquad (51)$$

A comparison of equations (40)–(42) in the positive universe with the corresponding equations (49)–(51) in the negative universe, shows that the Newtonian law of gravity in differential form and the implied Newtonian law of universal gravity are invariant in the negative universe. The invariance of classical gravitation (or classical gravitational interaction) in the negative universe has thus been demonstrated. This is true despite the fact that gravitational potential does not change sign while gravitational field (or gravitational acceleration) changes sign in the negative universe according to equations (47) and (48).

Demonstrating the invariance of Special Relativity in the negative universe consists in showing the invariance of Lorentz transformation, time dilation and length contraction formulae and the special-relativistic expressions for mass and other quantities in that universe. Now in the positive universe, for motion at speed v of a particle of rest mass m_0 along the x-axis of the coordinate system attached to it relative to an observer, the Lorentz transformation of the coordinates $(\tilde{x}', \tilde{y}', \tilde{z}', c\tilde{t}')$ of the primed (or particle's) frame into the coordinates $(\tilde{x}, \tilde{y}, \tilde{z}, c\tilde{t})$ of the unprimed (or observer's) frame has been written as system (3). The special-relativistic mass is given in the positive universe by the usual expression (13), which shall be re-written here as

$$m = \gamma m_0 \,. \tag{52}$$

In the negative universe, we must let $(\tilde{x}', \tilde{y}', \tilde{z}', c\tilde{t}'; m_0) \rightarrow (-\tilde{x}'^*, -\tilde{y}'^*, -\tilde{z}'^*, -c\tilde{t}'^*; -m_0^*)$, and also $(\tilde{x}, \tilde{y}, \tilde{z}, c\tilde{t}; m) \rightarrow (-\tilde{x}^*, -\tilde{y}^*, -\tilde{z}^*, -c\tilde{t}^*; -m^*)$, yielding the Lorentz transformation of the coordinates of the frame of reference attached to the symmetry-partner particle in motion relative to the symmetry-partner observer in the negative universe written as system (38) in [1], which shall be re-written here as follows

$$\left.\begin{array}{l} -\tilde{x}'^* = \gamma\left(-\tilde{x}^* - v(-\tilde{t}^*)\right) \\[2mm] -\tilde{t}^* = \gamma\left(-\tilde{t}^* - \dfrac{v}{c^2}(-\tilde{x}^*)\right) \\[2mm] -\tilde{y}'^* = -\tilde{y}^*, \quad -\tilde{z}'^* = -\tilde{z}^* \end{array}\right\} , \tag{53}$$

while the expression for special-relativistic mass in the negative universe becomes the following

$$-m^* = -\gamma m_0^*. \tag{54}$$

The expressions for time dilation and length contraction in the negative universe are similarly given respectively as follows

$$\Delta(-\tilde{t}^*) = \gamma\,\Delta(-\tilde{t}'^*), \tag{55}$$

$$\Delta(-\tilde{x}^*) = \gamma^{-1}\,\Delta(-\tilde{x}'^*). \tag{56}$$

Although the negative signs must be retained in (53), (54), (55) and (56) in the negative universe, mathematically the signs cancel, thereby making Lorentz transformation and the other equations of Special Relativity to retain their usual forms in the negative universe. Thus Lorentz invariance, (and local Lorentz invariance in gravitational fields), hold in the negative universe.

5.2 Invariance of quantum mechanics in the negative universe

The time-dependent Schrödinger wave equation is the following in the positive universe

$$H(\vec{r}, t, m, q)\,|\Psi(\vec{r}, t, m, q)\rangle = i\hbar\,\frac{\partial}{\partial t}\,|\Psi(\vec{r}, t, m, q)\rangle. \tag{57}$$

By writing (57) in the negative universe, while leaving Ψ

unchanged meanwhile, we have

$$-H^*(-\vec{r}^*, -t^*, -m^*, -q^*)\,|\Psi(\vec{r}, t, m, q)\rangle$$
$$= i\hbar^*\,\frac{\partial}{\partial(-t^*)}\,|\Psi(\vec{r}, t, m, q)\rangle, \tag{58}$$

where the fact that the Boltzmann constant transforms as $\hbar \rightarrow \hbar^*$ between the positive and negative universes in Table 1 has been used.

Now the wave function should transform between the positive and negative universes either as

$$\Psi(\vec{r}, t, m, q) \rightarrow \Psi^*(-\vec{r}^*, -t^*, -m^*, -q^*) =$$
$$= \Psi^*(\vec{r}^*, t^*, m^*, q^*) \tag{59}$$

or as

$$\Psi(\vec{r}, t, m, q) \rightarrow -\Psi^*(-\vec{r}^*, -t^*, -m^*, -q^*) =$$
$$= -\Psi^*(\vec{r}^*, t^*, m^*, q^*). \tag{60}$$

The parity of the wave function is conserved in (59) and inverted in (60).

Let us consider the following wave function in the positive universe,

$$\Psi(\vec{r}, t) = A\sin\left(\vec{k}\cdot\vec{r} - \omega t\right) \tag{61}$$

The symmetry-partner wave function in the negative universe is obtained by letting $\vec{r}\rightarrow -\vec{r}^*$, $\vec{k}\rightarrow -\vec{k}^*$, $\omega\rightarrow -\omega^*$, $t\rightarrow -t^*$ and $A\rightarrow -A^*$ in (61) to have

$$\Psi^*(\vec{r}, t) = -A^*\sin\left(-\vec{k}^*\cdot(-\vec{r}^*) - (-\omega^*)(-t^*)\right)$$
$$= -A^*\sin\left(\vec{k}^*\cdot\vec{r}^* - \omega^* t^*\right). \tag{62}$$

The transformation $A \rightarrow -A^*$ is necessary since inversion in the origin of the coordinates of a Euclidean 3-space inverts the amplitude of a wave in that space. On the other hand, the phase of a wave function, being a dimensionless number, does not change sign in the negative universe. Thus the transformation (60) and not (59) is the correct transformation of the wave function between the positive and negative universes. This is obviously so since (60) is a parity inversion situation, which is in agreement with the natural parity inversion of a wave, $\Pi \rightarrow -\Pi$, between the positive and negative universes included in Table 1. By incorporating the transformation (60) into (58) we obtain the following

$$-H^*(-\vec{r}^*, -t^*, -m^*, -q^*)\,|-\Psi^*(-\vec{r}^*, -t^*, -m^*, -q^*)\rangle =$$
$$= -i\hbar^*\,\frac{\partial}{\partial t^*}\,|-\Psi^*(-\vec{r}^*, -t^*, -m^*, -q^*)\rangle$$

or

$$H^*(\vec{r}^*, t^*, m^*, q^*)\,|\Psi^*(\vec{r}^*, t^*, m^*, q^*)\rangle =$$
$$= i\hbar^*\,\frac{\partial}{\partial t^*}\,|\Psi^*(\vec{r}^*, t^*, m^*, q^*)\rangle. \tag{63}$$

This is of the form of Eq. (57). The invariance of the Schrödinger wave equation in the negative universe has thus been established. It is straight forward to demonstrate the invariance in the negative universe of the Dirac's equation for the electron and of Gordon's equation for bosons.

5.3 Invariance of Maxwell equations in the negative universe

The Maxwell equations in a medium with electric charge density ρ and electric current density $\vec{J}$ are given in the positive universe as follows

$$\left.\begin{array}{ll} \vec{\nabla} \cdot \vec{E} = \dfrac{\rho}{\epsilon}\,, & \vec{\nabla} \cdot \vec{B} = 0 \\[2mm] \vec{\nabla} \times \vec{B} = \mu \vec{J} + \epsilon \mu\, \dfrac{\partial \vec{E}}{\partial t}\,, & \vec{\nabla} \times \vec{E} = -\dfrac{\partial \vec{B}}{\partial t} \end{array}\right\}. \quad (64)$$

Now, $\rho = \frac{charge}{volume}$, is the electric charge density of the medium in the positive universe. The charge density of the symmetry-partner medium in the negative universe is the positive quantity, $\frac{-charge^*}{-volume^*} = \frac{charge^*}{volume^*} = \rho^*$. The magnitude of an electric current is, $I = \frac{charge}{time}$ or $I = \rho v A$, in the positive universe and the magnitude of its symmetry-partner in the negative universe is the positive quantity, $\frac{-charge^*}{-time^*} = \frac{charge^*}{time^*} = I^*$ or $\rho^* v A^* = I^*$, since speed v and area A do not change sign in the negative universe. Similarly the magnitude of an electric current density of a medium in the positive universe is, $J = \frac{current}{area}$, and the magnitude of the current density of the symmetry-partner medium in the negative universe is, $\frac{current^*}{area^*} = J^*$. Thus in obtaining the Maxwell equations in the negative universe, we must let $\vec{E} \to -\vec{E}^*$, $\vec{B} \to -\vec{B}^*$, $\rho \to \rho^*$, $\vec{J} \to \vec{J}^*$, $\vec{\nabla} \to -\vec{\nabla}^*$, $\epsilon \to \epsilon^*$, $\mu \to \mu^*$ and $t \to -t^*$ in system (65) to have as follows

$$\left.\begin{array}{l} -\vec{\nabla}^* \cdot (-\vec{E}^*) = \dfrac{\rho^*}{\epsilon^*}\,, \quad -\vec{\nabla}^* \cdot (-\vec{B}^*) = 0 \\[2mm] -\vec{\nabla}^* \times (-\vec{B}^*) = \mu^* \vec{J}^* + \epsilon^* \mu^*\, \dfrac{\partial(-\vec{E}^*)}{\partial(-t^*)} \\[2mm] -\vec{\nabla}^* \times (-\vec{E}^*) = -\dfrac{\partial(-\vec{B}^*)}{\partial(-t^*)} \end{array}\right\}. \quad (65)$$

System (65) with the negative signs is the form the Maxwell equations are written by physicists[*] in the negative universe. The signs cancel mathematically thereby making system (65) to retain the form of system (64) and thereby establishing the invariance of Maxwell equations in the negative universe.

The law of propagation of electromagnetic waves derived from the Maxwell equations remain invariant in the negative universe as a consequence of the above. The equations are given in the positive universe as follows

$$\nabla^2 \vec{E} = \frac{1}{c^2}\frac{\partial^2 \vec{E}}{\partial t^2}\,, \qquad \nabla^2 \vec{B} = \frac{1}{c^2}\frac{\partial^2 \vec{B}}{\partial t^2}\,, \quad (66)$$

while in the negative universe, the electromagnetic wave equations are given as follows

$$\left.\begin{array}{l} (-\nabla^*)^2(-\vec{E}^*) = \dfrac{1}{c^2}\dfrac{\partial^2(-\vec{E}^*)}{\partial(-t^*)^2} \\[2mm] (-\nabla^*)^2(-\vec{B}^*) = \dfrac{1}{c^2}\dfrac{\partial^2(-\vec{B}^*)}{\partial(-t^*)^2} \end{array}\right\}. \quad (67)$$

Thus as the perpendicular electric field and magnetic field $\vec{E}$ and $\vec{B}$ propagate as electromagnetic wave at the speed of light in the positive universe, the symmetry-partner perpendicular fields $-\vec{E}^*$ and $-\vec{B}^*$ propagate as the identical symmetry-partner electromagnetic wave at the speed of light in the negative universe.

The foregoing shows that although electric charge as well as electric field and magnetic field change signs in the negative universe, the laws of propagation of electric and magnetic fields and electromagnetic waves remain invariant in the negative universe.

5.4 Invariance of General Relativity and cosmology in the negative universe

Since system of coordinates does not enter the covariant tensor formulation of Einstein's field equations, the equations are equally valid for the negative dimensions of the negative universe. The most general form of Einstein's field equations in the positive universe is the following

$$R_\mu^\nu - \frac{1}{2}\,R\,g_\mu^\nu + \Lambda\,g_\mu^\nu = -\frac{8\pi G}{c^2}\,T_\mu^\nu\,, \quad (68)$$

where the energy-momentum tensor T_μ^ν is defined as follows

$$T_\mu^\nu = (p + \rho)\,u^\nu u_\mu - p\,g_\mu^\nu\,, \quad (69)$$

Λ is the cosmological constant, p and ρ are the pressure and density of the universe respectively, while the other quantities in (68) and (69) are as defined in the theory. Λ is usually set to zero in General Relativity when considering local gravitational problems but retained in cosmological problems.

For the static exterior field of a spherical body, we must let $\Lambda = T_\mu^\nu = 0$ in (68) and require the vanishing of the Ricci tensor to have as follows

$$R_{\mu\nu} = 0 \quad (70)$$

Adopting a metric with signature $(+ - - -)$, the Schwarzschild solution to the field equation (70) is the following

$$\begin{aligned} ds^2 = c^2 dt^2 \left(1 - \frac{2GM}{rc^2}\right) &- \frac{dr^2}{\left(1 - \frac{2GM}{rc^2}\right)} - \\ &- r^2\left(d\theta^2 + \sin^2\theta\, d\varphi^2\right). \end{aligned} \quad (71)$$

By letting $t \to -t^*$, $r \to -r^*$, $\theta \to \theta^*$, $\varphi \to \varphi^*$ and $M \to -M^*$ in (71) we find that the Schwarzschild line element or metric tensor remains invariant in the negative universe. Other forms of exterior line elements or metric tensors, such as Kerr's line element, as well as interior metric tensors remain invariant in the negative universe as well. This is so because ds^2 is quadratic in intervals cdt, dr, $rd\theta$ and $r\sin\theta d\varphi$, and the components of the metric tensor are dimensionless. This concludes the invariance of general relativity in the negative universe.

Now the metric of spatially homogeneous universe in co-moving coordinates is the Robertson-Walker metric

$$ds^2 = c^2 dt^2 - R(t)^2 \left(\frac{du^2 + u^2 \left(d\theta^2 + \sin^2 \theta \, d\varphi^2 \right)}{\left(1 + \frac{k}{4} u^2\right)^2} \right), \quad (72)$$

where $u = r/r_0$ and the constant k is -1, 0 or $+1$, corresponding to spherical space, Euclidean space or pseudo-spherical space. Assuming that the universe is filled with perfect fluid, the field equation (68) along with the energy-momentum tensor (69) have been cast in the following forms, from which various models of the universe have been derived in General Relativity, as can be found in the standard texts on General Relativity

$$\frac{8\pi G \rho}{c^2} = -\Lambda + \left[\frac{3k}{R(t)^2} + \frac{3\dot{R}(t)^2}{c^2 R(t)^2} \right], \quad (73)$$

$$\frac{8\pi G}{c^2} \left(\frac{p}{c^2} \right) = \Lambda - \left[\frac{k}{R(t)^2} + \frac{\dot{R}(t)^2}{c^2 R(t)^2} + \frac{2\ddot{R}(t)}{c^2 R(t)} \right], \quad (74)$$

$$R(t) = R_0 \exp(Ht), \quad R_0 = R(t = 0), \quad (75)$$

where $R(t)$ is the "radius" of the universe, H is the Hubble constant given by

$$H = \frac{\dot{R}(t)}{R(t)} = \frac{1}{R(t)} \frac{dR(t)}{dt} \quad (76)$$

and the cosmological constant Λ is related to the Hubble constant H as follows

$$\Lambda = \frac{3H^2}{c^2}. \quad (77)$$

The parameters that appear in cosmological model, that is, in Eqs. (73) through (75), are the global time t, the "radius" of the universe $R(t)$, the mass-density of the universe ρ, the pressure of the universe p, the Hubble constant H, and the cosmological constant Λ. Also the rate of expansion $\dot{R}(t)$, as well as the acceleration $\ddot{R}(t)$, of the expanding universe enter into the equations. In the negative universe, we must let $t \to -t^*$, $R(t) \to -R^*(-t^*)$, $p \to p^*$, $H \to -H^*$, $\Lambda \to \Lambda^*$, $\dot{R}(t) \to \dot{R}^*(-t^*)$ and $\ddot{R}(t) \to -\ddot{R}^*(-t^*)$ in (73) through (75). Doing this, we find that the equations remain unchanged, so that physicists* in the negative universe formulate identical cosmological models as those in the positive universe. Consequently observers* in the negative universe make observation of that universe that are identical to the observation made of the positive universe by observers in the positive universe at all epochs.

It is easy and straight forward to demonstrate the invariance of the kinetic theory of gas, the laws of propagation of heat (conduction, convection and radiation) in continuous media, transport phenomena and other macroscopic laws of physics by following the procedure used to demonstrate the invariance of some macroscopic natural laws above with the aid of the complete form of Table 1.

5.5 Invariance of fundamental interactions in the negative universe

In a formal sense, the invariance in the negative universe of quantum chromodynamics, quantum electrodynamics, the electro-weak theory and quantum gravity must be demonstrated with the aid of the complete form of Table 1 in order to show the invariance in the negative universe of strong, electromagnetic, weak and gravitational interactions among elementary particles, as has been done for the macroscopic natural laws in this section. However we shall not attempt this. Rather we shall make recourse to the CPT theorem to demonstrate the invariance of the strong, electromagnetic and weak interactions in this section.

The CPT theorem, in a simplified form in [5, see p. 712], for instance, states that any hermitian interaction relativistically invariant, commutes with all products of the three operators C (charge conjugation), P (parity inversion), and T (time reversal) in any order. Even if an interaction is not invariant under one or two of the three operations, it must be invariant under CPT. The invariance of strong, weak and electromagnetic interactions under CPT is a well established fact in elementary particle physics [5].

Now the spacetime dimensions $-x^*$, $-y^*$, $-z^*$ and $-ct^*$ (in the Cartesian system of the dimensions of 3-space) of the third quadrant (or of the negative universe) are the products of natural parity inversion operation (P) and time reversal operation (T), (or of natural operation PT), on the spacetime dimensions x, y, z and ct of the first quadrant (or of the positive universe) in Fig. 5 or Fig. 7 of [1]. This implies, for instance, that the parity of a Schrodinger wave in the negative universe is natural inversion of parity of the symmetry-partner Schrodinger wave in the positive universe. The natural parity inversion of classical quantum-mechanical waves between the positive and negative universes equally applies to intrinsic parties of relativistic quantum mechanics and quantum field theories.

As also derived earlier in this paper and included in Table 1, the electric charge Q of a particle in the positive universe corresponds to an electric charge of equal magnitude but of opposite sign $-Q^*$ of the symmetry-partner particle in the negative universe. Thus the electric charge of a particle in the negative universe is the product of natural charge conjugation operation (C) on the electric charge of its symmetry-partner particle in the positive universe.

It follows from the foregoing two paragraphs that strong, weak and electromagnetic interactions among elementary particles in the negative universe are the products of natural operations of parity inversion (P), time reversal (T) and charge conjugation (C), in any order, (or of natural operation CPT), on strong, weak and electromagnetic interactions among elementary particles in the positive universe. The invariance of strong, weak and electromagnetic interactions among elementary particles in the negative universe follow

from this and the CPT theorem.

The invariance of classical gravitation and the General Theory of Relativity (or of gravitational interaction) at the macroscopic level in the negative universe has been demonstrated earlier in this section. The invariance in the negative universe of gravitational interaction among elementary particles follow from this. This section shall be ended with a remark that all natural laws, including the fundamental interactions among elementary particles, take on the same forms in the positive and negative universes and this is perfect symmetry of laws between the positive and negative universes.

6 On the concept of negative mass in physics

The concept of negative mass is not new in physics. The earliest speculations include the elaborate theory of negative mass by Föppl in 1897 and Schuster's contemplation of a universe with negative mass in 1898 [6] . However, as mentioned in [6], the fundamental modern paper on negative mass can be deemed to begin with Bondi [7]. As also stated in [6], Bondi pointed out that the mass in classical mechanics actually consists of three concepts namely, inertial mass, m_i, passive gravitational mass m_p, and active gravitational mass m_a. In Newton's theory of gravity, $m_i = m_p = m_a$. Also in the General Theory of Relativity, the principle of equivalence requires that, $m_i = m_p = m_a$. Although all three mass concepts are usually taken to be positive in physics, the theories do not compel this, as noted in [6].

Several papers on negative mass listed in [6] have appeared after Bondi's paper [7]. As noted in [6], most of those papers investigate the interaction and possible co-existence of particles with masses of both signs. The paper by Bonnor [6] is an important reappraisal of the concept of negative mass in the more recent time. In his analysis, Bonnor starts with the assumption m_i, $m_p > 0$, $m_a < 0$. He arrives at the result that either $m_i < 0$, $m_p < 0$ and $m_a < 0$ for all particles and bodies or $m_i > 0$, $m_p > 0$ and $m_a > 0$ for all particles and bodies. He then chooses to work with the former case, that is, all three mass concepts negative in an hypothetical universe. He substitutes negative mass into mechanics, relativity, gravitation as well as cosmology and finds that observers located in the hypothetical universe would observe strange phenomena, such as pebbles or sand falling on a stretched membrane producing tension and not compression of the membrane, and a push on a trolley causing it to accelerate towards the person who pushed it, etc. It is certain that this our universe is not the hypothetical universe containing negative mass in [6].

The hypothetical universe containing negative mass in [6] is not the negative universe isolated in the two parts of this article either. This is so because only mass is made negative while space and time dimensions, as well as other physical quantities and constants retain their signs (in our universe) in the hypothetical universe of [6]. This proviso leads to the deduced observation of strange phenomena in the hypothet-

ical universe. On the other hand, the negative universe of this article contains negative mass along with the negation of space and time dimensions, as well as the signs of other physical quantities and constants summarized in column 5 of Table 1. As demonstrated in the preceding section, the laws of physics retain their usual forms in the negative universe, and observers located in the negative universe observe phenomena in their universe that are identical to the phenomena observed in our (or positive) universe. There are no strange phenomena in the negative universe of the two parts of this article.

This section is perhaps the conclusion of over a century-old effort towards the development of the concept of negative mass in physics. Schuster's speculation one hundred and ten years ago of a universe containing negative mass must have now been realized. This second part of this article shall be ended at this point, while possible further development of the two-world background of Special Relativity (or the two-world picture) shall be investigated elsewhere.

References

1. Adekugbe A. O. J. Two-world background of Special Relativity. Part I. *Progress in Physics*, 2010, v. 1, 30–48.

2. Berestetskii V. B., Lifshitz E. M. and Pitaevskii L. P. Quantum Electrodynamics. Pergamon Press Ltd, Oxford, 1982.

3. Prigogine I. The arrow of time: an inaugural lecture by Ilya Prigogine at the Second International Centre of Relativistic Astrophysics (ICRA) Network Workshop, February 1–5, 1999, Converso O. and Sigismondi C., Editors, Publication no. 4 of ICRA Network, Pescara, Italy, 1999.

4. Akin-Ojo R. *International Journal of Theoretical Physics*, 1988, v. 27, 1023.

5. Segre E. Nuclei and particles. W. A. Benjamin, Incorporated, Reading, 1977.

6. Bonnor W. B. Negative mass in General Relativity. *Gen. Relat. Grav.*, 1989, v. 21, 1143.

7. Bondi H. Negative mass in General Relativity. *Rev. Mod. Phys.*, 1957, v. 29(3), 423–428.

Fractal Scaling Models of Natural Oscillations in Chain Systems and the Mass Distribution of the Celestial Bodies in the Solar System

Hartmut Müller

Global Scaling Research Institute in memoriam Leonhard Euler, Munich, Germany. E-mail: info@globalscaling.de

The present paper interprets matter as a chain system of quantum harmonic oscillators.
A fractal spectral model of resonant oscillations in chain systems of protons generates
a scaling mass spectrum, that reproduces the mass distribution of the celestial bodies in
the Solar System.

1 Introduction

Fractal scaling models [1] of natural oscillations in chain systems of harmonic oscillators are not based on any statements about the nature of the link or interaction between the elements of the oscillating chain system. Therefore the model statements are quite generally, what opens a wide field of possible applications.

In comparison with empty cosmic space, celestial bodies (stars, planets, moons, asteroids) are compressed matter and the contribution of nucleons to the bodies mass is about 99%. In the framework of the standard particle model, protons and neutrons are baryons, in which the proton connects to a lower quantum energy level and a much more stable state than the neutron. In addition, the proton and neutron have similar rest masses, what permits us to interpret protons and neutrons as similar quantum oscillators with regard to their rest masses.

Based on a fractal scaling model [1] of natural oscillations in this paper we will interpret matter as a chain system of many oscillating protons and find out spectral ranges where the oscillation process stability and energy efficiency are relative high or low.

2 Methods

On the base of continued fraction method [1] we will search the natural frequencies of a chain system of many vibrating protons on the lowest energy level (ground stage) in this form:

$$f = f_p \exp(S), \qquad (1)$$

f is a natural frequency of a chain system of vibrating protons, f_p is the natural oscillation frequency of one proton, S is a finite continued fraction with integer elements:

$$S = n_0 + \cfrac{1}{n_1 + \cfrac{1}{n_2 + \cfrac{\cdot}{\cdot \cdot + \frac{1}{n_k}}}} = [n_0; n_1, n_2, \dots, n_k], \quad (2)$$

where $n_0, n_1, n_2, \dots, n_k \in Z$. The continued fractions (2) are in the canonical form and have a discrete spectrum of eigenvalues. With the help of the Lagrange transformation [2] every continued fraction with integer partial denominators can

be represented as a continued fraction with natural partial denominators, that's always convergent. In this paper we will investigate spectra generated by convergent continued fractions (2). The present paper follows the Terskich [3] definition of a chain system, where the interaction between the elements proceeds only in their movement direction.

Model spectra (2) are not only logarithmic-invariant, but also fractal, because the discrete hyperbolic distribution of natural frequencies repeats itself on each spectral level k. We investigate continued fractions (2) with a finite quantity of layers k, which generate discrete spectra, because in this case all continued fractions S represent rational numbers. Therefore the free link n_0 and the partial denominators n_1 can be interpreted as "quantum numbers".

The partial denominators n_1 run through positive and negative integer values. Maximum spectral density areas (spectral nodes) arise automatically on the distance of one logarithmic unit, where $|n_1| \to \infty$. Fig.1 shows the spectrum on the first layer $k = 1$ for $|n_1| = 2, 3, 4, \dots$ and $|n_0| = 0, 1, 2, \dots$ (logarithmic representation). Integer S-values are labeled.

Fig. 1: The spectrum (2) on the first layer $k = 1$, for $|n_1| = 2, 3, 4, \dots$ and $|n_0| = 0, 1, 2, \dots$ (logarithmic representation). Integer S-values are labeled.

Ranges of relative low spectral density (spectral gaps) and ranges of relative high spectral density (spectral nodes) arise on each spectral layer. In addition to the first spectral layer, Fig. 2 shows the second spectral layer $k = 2$ for $|n_2| = 2, 3, 4, \dots$ and $|n_1| = 2$ (logarithmic representation).
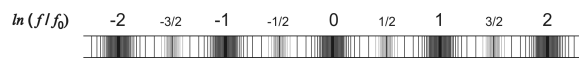
Fig. 2: The spectrum (2) on the first layer $k = 1$, for $|n_0| = 0, 1, 2, \dots$ and $|n_1| = 2, 3, 4, \dots$ and, in addition, the second layer $k = 2$ for $|n_1| = 2$ and $|n_2| = 2, 3, 4, \dots$ (logarithmic representation).

In the spectral node ranges, where the spectral density reachs local maximum, natural frequencies are distributed maximum densely, so that near a spectral node almost each frequency is a natural frequency. The energy efficiency of

Celestial body	Body mass m, kg	$\ln (m/m_p)$	S	d, %
15 Eunomia (A)	3.12×10^{19} [8]	106.54	[106; 2]	0.037
Mimas (S)	$(3.7493 \pm 0.0031) \times 10^{19}$ [7]	106.73	[106; 2]	0.216
Miranda (U)	$(6.59 \pm 0.75) \times 10^{19}$ [8]	107.29	[107; 2]	−0.195
10 Hygiea (A)	$(8.98 \pm 0.01) \times 10^{19}$ [8]	107.60	[107; 2]	0.093
Enceladus (S)	$(1.08022 \pm 0.00101) \times 10^{20}$ [7]	107.78	[108]	−0.204
2 Pallas (A)	$(2.11 \pm 0.26) \times 10^{20}$ [8]	108.50	[108; 2]	0.001
4 Vesta (A)	$(2.67 \pm 0.02) \times 10^{20}$ [8]	108.69	[108; 2]	0.175
Tethys (S)	$(6.17449 \pm 0.00132) \times 10^{20}$ [7]	109.53	[109; 2]	0.028
1 Ceres (P)	$(9.43 \pm 0.07) \times 10^{20}$ [8, 9]	109.95	[110]	−0.045
Dione (S)	$(1.095452 \pm 0.000168) \times 10^{21}$ [7]	110.10	[110]	0.091
Umbriel (U)	$(1.172 \pm 0.135) \times 10^{21}$ [10]	110.10	[110]	0.091
Ariel (U)	$(1.350 \pm 0.120) \times 10^{21}$ [10]	110.23	[110]	0.209
Charon (P)	$(1.52 \pm 0.06) \times 10^{21}$ [11]	110.43	[110; 2]	−0.064
Iapetus (S)	$(1.805635 \pm 0.000375) \times 10^{21}$ [7]	110.60	[110; 2]	0.090
Rhea (S)	$(2.306518 \pm 0.000353) \times 10^{21}$ [7]	110.84	[111]	−0.144
Oberon (U)	$(3.014 \pm 0.075) \times 10^{21}$ [12]	111.12	[111]	0.108
Titania (U)	$(3.53 \pm 0.09) \times 10^{21}$ [12]	111.28	[111; 2]	−0.197
Haumea (P)	$(4.006 \pm 0.040) \times 10^{21}$ [13]	111.40	[111; 2]	−0.090
Pluto (P)	$(1.305 \pm 0.007) \times 10^{22}$ [11]	112.57	[112; 2]	0.018
Eris (P)	$(1.67 \pm 0.02) \times 10^{22}$ [14]	112.83	[113]	−0.150
Triton (N)	2.14 ± 10^{22} [15]	113.07	[113]	0.062
Europa (J)	4.80×10^{22} [16]	113.88	[114]	−0.105
Moon (E)	7.3477×10^{22}	114.30	[114; 2]	−0.175
Io (J)	$(8.9319 \pm 0.0003) \times 10^{22}$ [16]	114.50	[114; 2]	0.001
Callisto (J)	$(1.075938 \pm 0.000137) \times 10^{23}$ [17]	114.69	[114; 2]	0.166
Titan (S)	$(1.3452 \pm 0.0002) \times 10^{23}$ [7]	114.91	[115]	−0.078
Ganymede (J)	$(1.4819 \pm 0.0002) \times 10^{23}$ [16]	115.00	[115]	0.001
Mercury	$(3.3022 \pm 0.0001) \times 10^{23}$	115.81	[116]	−0.164
Mars	$(6.4185 \pm 0.0001) \times 10^{23}$	116.47	[116; 2]	−0.026
Venus	$(4.8685 \pm 0.0001) \times 10^{24}$	118.50	[118; 2]	0.001
Earth	$(5.9722 \pm 0.0006) \times 10^{24}$ [18]	118.69	[118; 2]	0.160
Uranus	$(8.6810 \pm 0.0013) \times 10^{25}$ [12]	121.38	[121; 2]	−0.099
Neptune	$(1.0243 \pm 0.0015) \times 10^{26}$	121.55	[121; 2]	0.041
Saturn	$(5.6846 \pm 0.0001) \times 10^{26}$	123.27	[123; 2]	−0.186
Jupiter	$(1.8986 \pm 0.0001) \times 10^{27}$	124.47	[124; 2]	−0.024
Sun	$(1.9884 \pm 0.0002) \times 10^{30}$ [18]	131.42	[131; 2]	−0.061

Table 1: The masses of celestial bodies — planets, dwarf planets (P), asteroids (A), moons of Jupiter (J), Saturn (S), Uranus (U), Neptune (N) and Earth (E) and the S-values (6) of the nearest spectral nodes. The relative deviation $d = \left(\ln (m/m_p) - S\right)/S$ is indicated in percents.

natural oscillations is very high. Therefore, if a frequency of an oscillation process is located near a node of the fractal spectrum (2), the process energy efficiency (degree of effectiveness) should be relative high. More detailed this topic is described in [1].

Let's assume that the oscillation amplitudes are low, the oscillations are harmonic and the energy level E_f of the vibrating protons depends only on their oscillation frequency (h is the Planck constant):

$$E_f = hf . \tag{3}$$

Atomic nucleuses arise in the result of high energy processes of nucleosynthesis. Einstein's formula defines not only the connection between the rest energy and rest mass of nucleons, but also between binding energy and the mass defect of an atomic nucleus. Therefore we assume that the rest mass m of our model matter corresponds to the energy E_m:

$$E_m = mc^2 . \tag{4}$$

Let's assume that the basis of nucleosynthesis is harmonic oscillations of protons and the energy (4) is identically
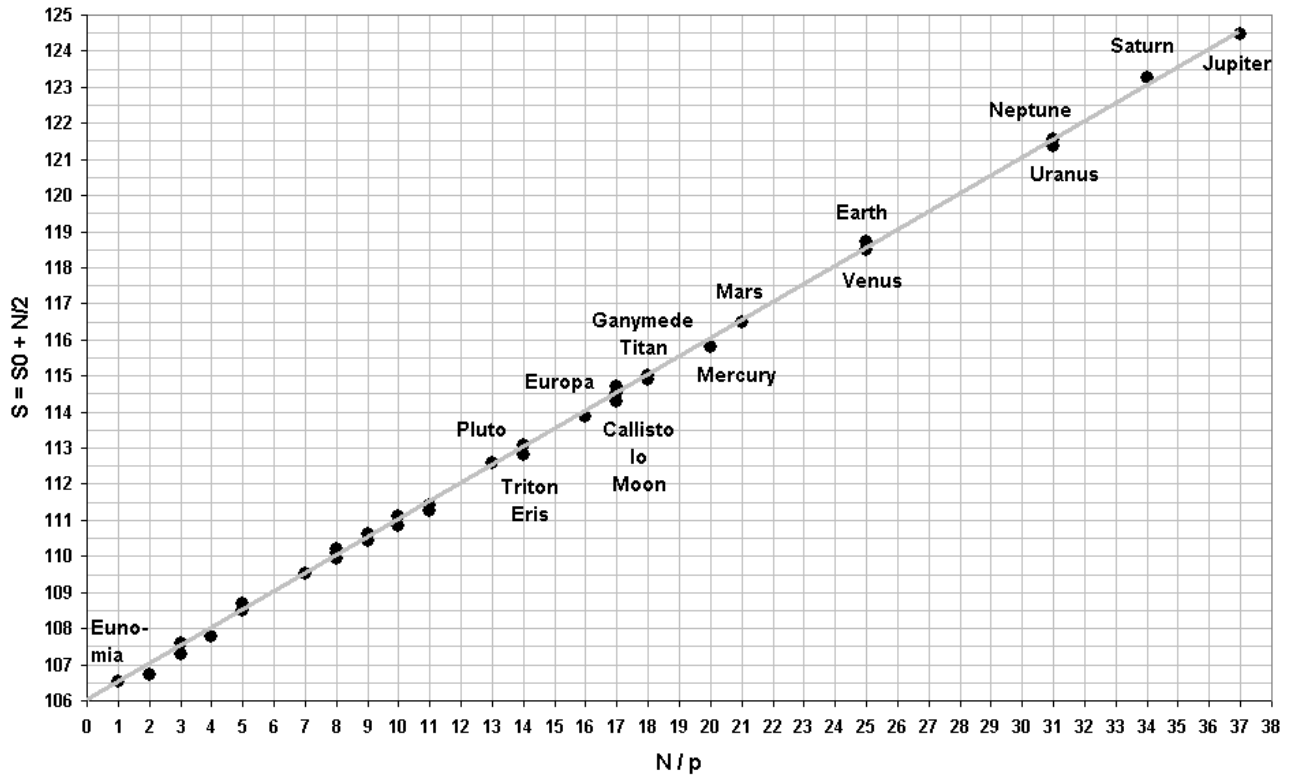
Fig. 3: The S-trajectory for $S_0 = [106]$ and $p = 1$. Logarithmic scaling of Eunomia to Jupiter body mass.

with (3). In this case we can write:

$$ m = f \frac{h}{c^2} \, . \tag{5} $$

In the framework of our oscillation model (1) the equation (5) means not only that mass can be changed into energy, but also that quantum oscillations generate the mass spectrum of our model matter. Under consideration of (1) now we can create a fractal scaling model of the natural mass spectrum of our model matter of vibrating protons. This mass spectrum is described by the same continued fraction (2), for $m_p = f_p \frac{h}{c^2}$:

$$ \ln \frac{m}{m_p} = [n_0; n_1, n_2, \ldots, n_k] \, . \tag{6} $$

Consequently, the frequency spectrum (2) and the mass spectrum (6) are isomorphic, and m_p is the proton rest mass $1.672621637(83) \times 10^{-27}$ kg [4]. As mentioned already, we assume that mass generation processes are based on quantum natural oscillation processes. Celestial bodies are compressed matter, which consist of nucleons over 99%. Therefore we expect that the distribution of the celestial bodies in the proton resonance mass spectrum is not random and near spectral nodes the formation probability of massive bodies is maximum. Like in the Kundt's tube [5], near resonance nodes the matter accumulation reaches maximum intensity. The mass spectrum (6) is fractal and consequently it has a clear hierarchical structure, in which continued fractions (2) of the form $[n_0]$ and $[n_0; 2]$ define main spectral nodes, as Fig. 2 shows.
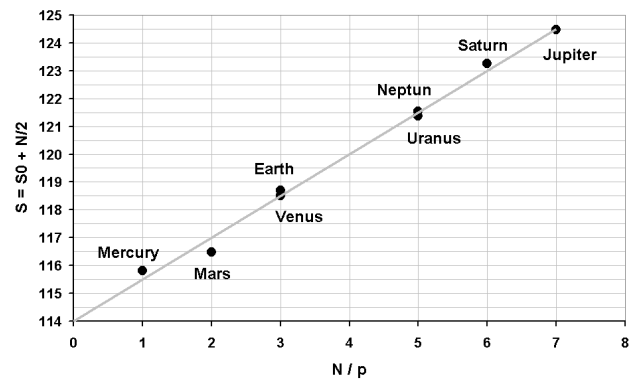
Fig. 4: The S-trajectory for $S_0 = [114]$ and $p = 3$. Possibly, the extrasolar planet Gliese 581d could be a candidate of the node $S = [120]$.

3 Results

In the present paper we will compare the scaling mass spectrum (6) of our model matter in the range of 10^{19} kg to 10^{30} kg with the mass distribution of well-known celestial bodies. These are asteroids, planetoids, moons and planets of the Solar System (including the Sun), which masses were measured precisely enough and which are massive enough to be rounded by their own gravity.

For example, to locate the mass of the planet Venus in the scaling mass spectrum (6) of our model matter, one divides the Venus body mass by the proton rest mass and represents

Particle	Rest mass m, MeV/c^2 [20]	$\ln(m/m_p)$	S	d, %
electron	$0.510998910 \pm 0.000000013$	-7.515	$[-7;-2]$	-0.206
proton	938.27203 ± 0.00008	0.000	$[0]$	0.000
W	80398 ± 25	$4,451$	$[4;2]$	$1,089$
Z	91187.6 ± 2.1	$4,577$	$[4;2]$	$1,711$

Table 2: The rest masses of the electron, proton and the W-Z-bosons and the S-values (6) of the nearest spectral nodes. The relative deviation $d = \left(\ln\left(m/m_p\right) - S\right)/S$ is indicated in percent.

Fig. 5: The electron and W-Z-bosons rest masses lie on the S-trajectory for $S_0 = [0]$ and $p = 3$. It's the same S-trajectory that shows Fig. 4, but prolonged down to negative N.
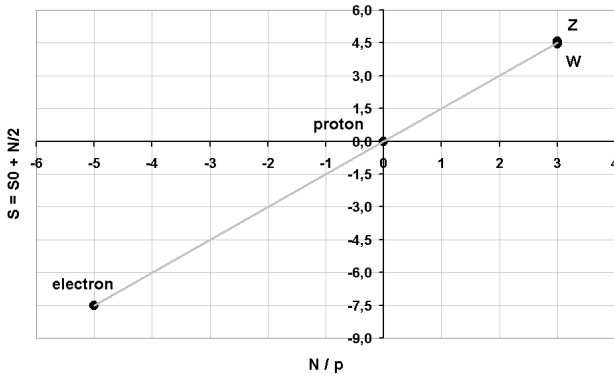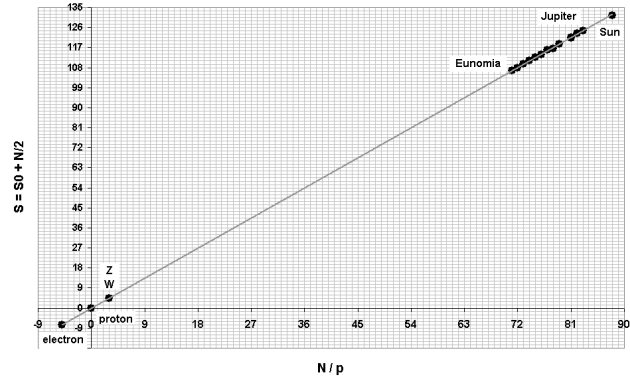

Fig. 6: The S-trajectory for $S_0 = [0]$ and $p = 3$. Logarithmic scaling of the electron rest mass to the body mass of the Sun.

the logarithm as a continued fraction:

$$S_{venus} = \ln\frac{m_{venus}}{m_p} = \ln\left(\frac{4.869 \times 10^{24}\,\text{kg}}{1.67262 \times 10^{-27}\,\text{kg}}\right) \cong$$
$$\cong 118.50 = 118 + \frac{1}{2}. \tag{7}$$

The analysis (6) of the Venus body mass takes the result $n_0 = 118$, $n_1 = 2$. This means, that the Venus body mass corresponds to a spectral node on the first layer $k = 1$ of the spectrum (6). The Sun mass is near the spectral node $[131; 2]$. It's also correct for the Alpha Centauri A and B masses. The Alpha Aquilae (Altair) mass is about 1.7 solar masses, that's near the node $[132]$. Table 1 shows the logarithms (6) calculated from the measured masses m of the celestial bodies and the S-values of the nearest spectral nodes.

Table 1 shows, that spectral nodes are occupied by bodies which have maximum mass in a local group or family. For example, the spectral node $[115]$ is occupied by Ganymede and Titan, the most massive moons of Jupiter and Saturn, the spectral node $[113]$ is occupied by Triton, the most massive moon of Neptune, the body mass of Eris, the largest defined dwarf planet, is also near the spectral node $[113]$, but the spectral node $[110]$ is occupied by Ceres, the most massive body of the asteroid belt. Mercury's mass is near the node $[116]$. Possibly, not Eris, but Mercury is the most massive dwarf planet in the Solar System. Actually, Mercury behaves like a dwarf planet, because it has the highest eccentricity of all the Solar System planets and it has the smallest axial tilt.

For the nodes $[n_0]$ and $[n_0; 2]$ the finite continued fraction (2) is $S = n_0 + 1/n_1$ and the corresponding discrete mass values can be defined by linear S-trajectories, in which $N \in Z$:

$$S = S_0 + \frac{N}{2}. \tag{8}$$

The prime divisibility of $N = pn$, in which p is a prime factor of N, defines sets of S-trajectories which form different sequences of mass-values m of the discrete spectrum (6).

S-trajectories (8) present the discrete scaling mass distribution (6) very clear and can be interpreted as exponential equivalents to linear square-mass trajectories, which are a well-known systematic feature in the hadrons spectrum [6]. Fig. 3 shows the S-trajectory for $S_0 = [106]$ and $p = 1$. Largest bodies are labeled. Possibly, vacant nodes are occupied by extrasolar bodies or bodies still to be discovered in the Solar System.

Possibly, the existence of the discrete spectrum (6) in the range of celestial bodies masses can be interpreted as "macroscopic quantization" [19]. The larger the bodies the more distinctive is this phenomenon. This can be recognized well at the example of the 8 largest planets in the Solar System, as Fig. 4 shows.

For $S_0 = [0]$ and every p is $m_0 = m_p$, so that every S-trajectory can be prolonged down to the proton rest mass. Also the electron and W-Z-bosons rest masses lie on the S-trajectory for $S_0 = [0]$ and $p = 3$, as Fig. 5 shows. Already within the eighties the scaling exponent 3/2 was found in the distribution of particle masses by Valery A. Kolombet [21].

Table 2 shows the logarithms (6) calculated from the measured particle rest masses, and the S-values of the nearest spectral nodes.

The S-trajectory in Fig. 5 is the same as the S-trajectory in Fig. 4, but prolonged down to the electron rest mass for $S = [-7; -2]$. Possibly, there is a fundamental link between particle rest masses and the masses of celestial bodies. Fig. 6 shows the S-trajectory for $S_0 = [0]$ and $p = 3$ in the range of $-9 \leqslant S \leqslant 135$, of the electron rest mass to the body mass of the Sun.

4   Resume

In the framework of the present model discrete scaling distributions arise as result of natural oscillations in chain systems of harmonic oscillators. Particularly, the observable mass distribution of celestial bodies arise as result of natural oscillations in chain systems of protons, that can be understood as contribution to the fundamental link between quantum- and astrophysics. Possibly, the high energy efficiency of natural oscillations is the cause of the fractal scaling distribution of matter in the universe.

Acknowledgements

References

1. Muller H. Fractal scaling models of resonant oscillations in chain systems of harmonic oscillators. *Progress in Physics*, 2009.

2. Khintchine A. Ya. Continued fractions. University of Chicago Press, Chicago, 1964.

3. Terskich V. P. The continued fraction method. Leningrad, 1955 (*in Russian*).

4. Physical constants. Particle Data Group, www.pdg.lbl.gov

5. Kundt A. Uber eine neue Art akustischer Staubfiguren und uber die Anwendung derselben zur Bestimmung der Schallgeschwindigkeit in festen Korpern und Gasen. *Annalen der Physik*, Leipzig, 1866, v. 127 (4), 497–523.

6. Forkel H., Beyer M., Frederico T. Linear square-mass trajectories of radially and orbitally excited hadrons in holographic QCD. arXiv: 0705.1857v2.

7. Jacobson R., Antreasian P., Bordi J. et al. The Gravity Field of the Saturnian System from Satellite Observations and Spacecraft Tracking Data. *Astronomical Journal*, 2006, v. 132, 2520–2526.

8. Baer J., Steven R. Astrometric masses of 21 asteroids, and an integrated asteroid ephemeris. Celestial Mechanics and Dynamical Astronomy. *Springer Science and Business Media*, 2008, v. 100, 27–42.

9. Carry B. et al. Near-Infrared Mapping and Physical Properties of the Dwarf-Planet Ceres. *Astronomy and Astrophysics*, 2007, v. 478, 235-244.

10. Uranus System Nomenclature Table Of Contents. Gazetteer of Planetary Nomenclature. USGS Astrogeology, 2009.

11. Marc W., William M, Eliot F et al. Orbits and photometry of Pluto's satellites: Charon, S/2005 P1, and S/2005 P2. *Astronomical Journal*, 2006, v. 132 (1), 290–298.

12. Jacobson R, Campbell J, Taylor A, Synnott S. The masses of Uranus and its major satellites from Voyager tracking data and Earth based Uranian satellite data. *Astronomical Journal*, 1992, v. 103 (6), 2068–2078.

13. Ragozzine D., Brown M. Orbits and Masses of the Satellites of the Dwarf Planet Haumea = 2003 EL61. *Astronomical Journal*, 2009. arXiv: 0903.4213v1.

14. Brown M, Schaller E. The Mass of Dwarf Planet Eris. *Science*, 2007, v. 316 (5831), 1585.

15. Neptune System Nomenclature Table Of Contents. Gazetteer of Planetary Nomenclature. USGS Astrogeology, 2009.

16. Showman A., Malhotra R. The Galilean Satellites. *Science*, 1999, v. 286, 77–84.

17. Anderson J., Jacobson R. et al. Shape, mean radius, gravity field and interior structure of Callisto. *Icarus*, v. 153, 157–161.

18. Astrophysical Constants and Parameters. Particle Data Group, www.pdg.lbl.gov

19. Shnoll S. et al. Realization of discrete states during fluctuations in macroscopic processes, *Physics Uspekhi*, 1998, v. 41 (10), 1025–1035.

20. Particle listings. Particle Data Group, www.pdg.lbl.gov

21. Kolombet V. Macroscopic fluctuations, masses of particles and discrete space-time, *Biofizika*, 1992, v. 36, 492–499 (in Russian).

Dynamical 3-Space Predicts Hotter Early Universe: Resolves CMB-BBN ^{7}Li and ^{4}He Abundance Anomalies

Reginald T. Cahill

School of Chemistry, Physics and Earth Sciences, Flinders University, Adelaide 5001, Australia
E-mail: Reg.Cahill@flinders.edu.au

The observed abundances of ^{7}Li and ^{4}He are significantly inconsistent with the predictions from Big Bang Nucleosynthesis (BBN) when using the ΛCDM cosmological model together with the value for $\Omega_B h^2 = 0.0224 \pm 0.0009$ from WMAP CMB fluctuations, with the value from BBN required to fit observed abundances being $0.009 < \Omega_B h^2 < 0.013$. The dynamical 3-space theory is shown to predict a 20% hotter universe in the radiation-dominated epoch, which then results in a remarkable parameter-free agreement between the BBN and the WMAP value for $\Omega_B h^2$. The dynamical 3-space also gives a parameter-free fit to the supernova redshift data, and predicts that the flawed ΛCDM model would require $\Omega_\Lambda = 0.73$ and $\Omega_M = 0.27$ to fit the 3-space dynamics Hubble expansion, and independently of the supernova data. These results amount to the discovery of new physics for the early universe that is matched by numerous other successful observational and experimental tests.

1 Introduction

Astrophysical observed abundances of ^{7}Li and ^{4}He are significantly inconsistent with the predictions from Big Bang Nucleosynthesis (BBN) when using the ΛCDM cosmological model, with the value for[*] $\Omega_B h^2 = 0.0224 \pm 0.0009$ from WMAP CMB fluctuations being considerably different from the value from BBN required to fit observed abundances $0.009 < \Omega_B h^2 < 0.013$ (Coc *et al.* [1]).

The most significant long-standing discrepancy is that of ^{7}Li because the pre-Galactic lithium abundance inferred from observations of metal-poor (Population II) stars is at least 2–3 times smaller than predicted by BBN–ΛCDM. The ^{7}Li problem has been most difficult to understand as its primordial abundance should be the most reliable, because of the higher observational statistics and an easier extrapolation to primordial values. Various possible resolutions were discussed in [2], with the conclusion that the lithium problem most likely points to new physics.

It is shown herein that the new physics of a dynamical 3-space [4–6] results in a 20% hotter universe during the radiation dominated epoch, and in a parameter-free analysis the BBN abundances are brought into close agreement with the WMAP value for the baryonic density $\Omega_B h^2 = 0.0224 \pm 0.0009$. The dynamical 3-space also gives a parameter free account of the supernova redshift data, and fitting the ΛCDM to the dynamical 3-space model requires $\Omega_\Lambda = 0.73$ and $\Omega_m = 0.27$, independently of the supernova data. There are numerous other experimental and observational confirmations of the new physics [4, 5], including a recent analysis of the NASA/JPL spacecraft earth-flyby Doppler-shift anomalies [7,8]. The conclusion is that the ΛCDM is flawed, with preci-

sion data from the supernova redshifts [10–12], and WMAP CMB fluctuations [3] in conjunction with BBN computations finally ruling out this model. As briefly noted below that ΛCDM is essentially Newtonian gravity, and various data have indicated the failure of Newtonian gravity.

2 Dynamical 3-space

Newton's inverse square law of gravity [9] has the differential form

$$\nabla \cdot \mathbf{g} = -4\pi G\rho, \qquad \nabla \times \mathbf{g} = 0, \qquad (1)$$

for the matter acceleration field $\mathbf{g}(\mathbf{r}, t)$. Application of this to spiral galaxies and the expanding universe has lead to many problems, including, in part, the need to invent dark energy and dark matter. However (1) has a unique generalisation that resolves these problems. In terms of a velocity field $\mathbf{v}(\mathbf{r}, t)$ (1) has an equivalent form [4, 5]

$$\nabla \cdot \left(\frac{\partial \mathbf{v}}{\partial t} + (\mathbf{v} \cdot \nabla)\,\mathbf{v} \right) = -4\pi G\rho, \qquad \nabla \times \mathbf{v} = 0, \quad (2)$$

where now

$$\mathbf{g} = \frac{\partial \mathbf{v}}{\partial t} + (\mathbf{v} \cdot \nabla)\,\mathbf{v}, \qquad (3)$$

is the Euler acceleration of the substratum that has velocity $\mathbf{v}(\mathbf{r}, t)$. Because of the covariance of v under a change of the spatial coordinates only relative internal velocities have an ontological existence — the coordinates $\mathbf{r}$ then merely define a mathematical embedding space. In the form (2) Newton's law permits a unique generalisation by adding a term of the same order but which can preserve the inverse square law outside of spherical masses,

$$\nabla \cdot \left(\frac{\partial \mathbf{v}}{\partial t} + (\mathbf{v} \cdot \nabla)\,\mathbf{v} \right) + \frac{\alpha}{8}\left((\mathrm{tr}\, D)^2 - \mathrm{tr}\,(D^2) \right) = -4\pi G\rho,$$

---

[*]$H_0 = 100\,h$ km/s/Mpc defines h. Ω_B is baryon density relative to critical density ρ_c.

$$\nabla \times \mathbf{v} = 0, \qquad D_{ij} = \frac{1}{2}\left(\frac{\partial v_i}{\partial x_j} + \frac{\partial v_j}{\partial x_i}\right). \qquad (4)$$

Eqn. (4) has two fundamental constants: G and α. Experimental bore-hole g anomaly data reveals that α is the fine structure constant $\approx 1/137$ to within experimental errors [4, 5]. Eqn (4) has a rich variety of solutions: (i) black holes with a non-inverse square law acceleration field that explains the supermassive black hole mass spectrum and the flat rotation curves of spiral galaxies without the need for dark matter — these black holes may be primordial as well as induced, (ii) the bore-hole g-anomaly, (iii) gravitational light bending, (iv) a parameter free fit to the supernova data [6] without the need for dark energy or dark matter, and other effects. As well the 3-space field $\mathbf{v}(\mathbf{r}, t)$ has been directly detected in numerous laboratory experiments, and now in Doppler shift data from spacecraft earth-flybys [8].

Eqn (4) gives a different account of the Hubble expansion of the universe, and here we outline a new account of the thermal history of the universe. The results are very different from the predictions of the Friedmann equation — the standard equation of cosmology since its inception (FRW-GR). In the Friedmann equations the expansion of the universe is determined solely by the presence of matter or energy, as would be expected since it derives from (1), and it then requires, at the present epoch, some 73% dark energy, 23% dark matter and 4% baryonic matter. Eqn (4), in contrast, requires only the normal matter — this is because (4) has an expanding 3-space solution even in the absence of matter/energy. Fitting the Friedmann Hubble function $H(z)$ to the Hubble function from (4), using the usual distance-redshift modulus as a measure, indeed permits these dark energy and dark matter quantities to be simply predicted, independently of the observed supernova data, for these are the values that best-fit the ΛCDM to the observed uniformly expanding 3-space Hubble solution.

3   Expanding universe from dynamical 3-space

Let us now explore the expanding 3-space from (4). Critically, and unlike the FLRW-GR model, the 3-space expands even when the energy density is zero. Suppose that we have a radially symmetric effective density $\rho(r, t)$, modelling normal matter and EM radiation, and that we look for a radially symmetric time-dependent flow $\mathbf{v}(\mathbf{r}, t) = v(r, t)\,\hat{\mathbf{r}}$ from (4). Then $v(r, t)$ satisfies the equation, with $v' = \frac{\partial v(r,t)}{\partial r}$,

$$\frac{\partial}{\partial t}\left(\frac{2v}{r} + v'\right) + vv'' + 2\frac{vv'}{r} + (v')^2 +$$
$$+ \frac{\alpha}{4}\left(\frac{v^2}{r^2} + \frac{2vv'}{r}\right) = -4\pi G\rho(r, t). \qquad (5)$$

Consider first the zero energy case $\rho = 0$. Then we have a Hubble solution $v(r, t) = H(t)r$, a centreless flow, determined
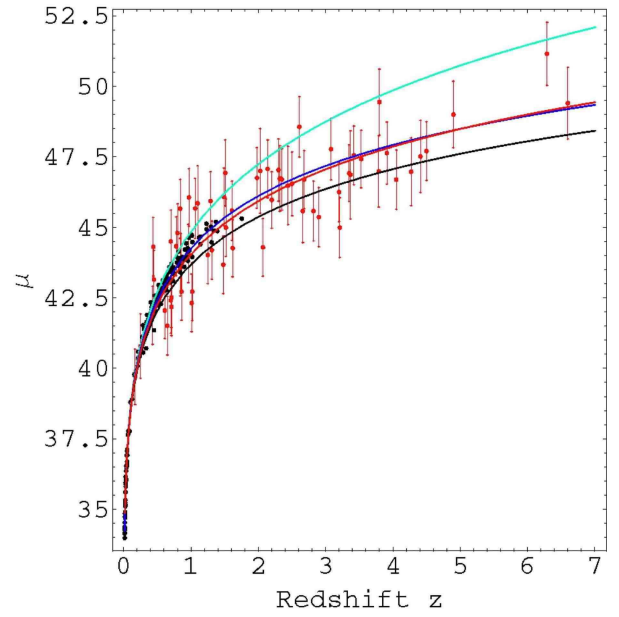

Fig. 1: Hubble diagram showing the supernovae data using several data sets, and the Gamma-Ray-Bursts data (with error bars). Upper curve (green) is ΛCDM "dark energy" only $\Omega_\Lambda = 1$, lower curve (black) is ΛCDM matter only $\Omega_M = 1$. Two middle curves show best-fit of ΛCDM "dark energy"—"dark-matter" (blue) and dynamical 3-space prediction (red), and are essentially indistinguishable. We see that the best-fit ΛCDM "dark energy"—"dark-matter" curve essentially converges on the uniformly-expanding parameter-free dynamical 3-space prediction. The supernova data shows that the universe is undergoing a uniform expansion, although not reported as such in [10–12], wherein a fit to the FRW-GR expansion was forced, requiring "dark energy", "dark matter" and a future "exponentially accelerating expansion".

by

$$\dot{H} + \left(1 + \frac{\alpha}{4}\right)H^2 = 0, \qquad (6)$$

with $\dot{H} = \frac{dH}{dt}$. We also introduce in the usual manner the scale factor $a(t)$ according to $H(t) = \frac{\dot{a}}{a}$. We then obtain the solution

$$H(t) = \frac{1}{(1 + \frac{\alpha}{4})\,t} = H_0\,\frac{t_0}{t}; \qquad a(t) = a_0\left(\frac{t}{t_0}\right)^{4/(4+\alpha)} \qquad (7)$$

where $H_0 = H(t_0)$ and $a_0 = a(t_0) = 1$, with t_0 the present age of the universe. Note that we obtain an expanding 3-space even where the energy density is zero — this is in sharp contrast to the FLRW-GR model for the expanding universe, as shown below. The solution (7) is unique — it has one free parameter — which is essentially the age of the universe $t_0 = t_H = 1/H_0$, and clearly this cannot be predicted by physics, as it is a purely contingent effect — the age of the universe when it is observed by us. Below we include the small effect of ordinary matter and EM radiation.

We can write the Hubble function $H(t)$ in terms of $a(t)$ via the inverse function $t(a)$, i.e. $H(t(a))$ and finally as $H(z)$,

where the redshift observed now, relative to the wavelengths at time t, is $z = a_0/a - 1$. Then we obtain

$$H(z) = H_0(1 + z)^{1+\alpha/4}. \tag{8}$$

To test this expansion we need to predict the relationship between the cosmological observables, namely the apparent photon energy-flux magnitudes and redshifts. This involves taking account of the reduction in photon count caused by the expanding 3-space, as well as the accompanying reduction in photon energy. The result is that the dimensionless "energy-flux" luminosity effective distance is then given by

$$d_L(z) = (1 + z) \int_0^z \frac{H_0 \, dz'}{H(z')} \tag{9}$$

and the distance modulus is defined as usual by

$$\mu(z) = 5 \log_{10}(d_L(z)) + m. \tag{10}$$

Because all the selected supernova have the same absolute magnitude, m is a constant whose value is determined by fitting the low z data.

Using the Hubble expansion (8) in (9) and (10) we obtain the middle curve (red) in Fig. 1, yielding an excellent agreement with the supernovae and GRB data. Note that because $\alpha/4$ is so small it actually has negligible effect on these plots. But that is only the case for the homogeneous expansion — the α dynamics can result in large effects such as black holes and large spiral galaxy rotation effects when the 3-space is inhomogeneous, and particularly precocious galaxy formation. Hence the dynamical 3-space gives an immediate account of the universe expansion data, and does not require the introduction of a cosmological constant or "dark energy" nor "dark matter".

4　Expanding universe — matter and radiation only

When the energy density is not zero we need to take account of the dependence of $\rho(r, t)$ on the scale factor of the universe. In the usual manner we thus write

$$\rho(r, t) = \frac{\rho_m}{a(t)^3} + \frac{\rho_r}{a(t)^4}, \tag{11}$$

for ordinary matter and EM radiation. Then (5) becomes for $a(t)$

$$\frac{\ddot{a}}{a} + \frac{\alpha}{4} \frac{\dot{a}^2}{a^2} = -\frac{4\pi G}{3} \left(\frac{\rho_m}{a^3} + \frac{\rho_r}{a^4} \right), \tag{12}$$

giving

$$\dot{a}^2 = \frac{8\pi G}{3} \left(\frac{\rho_m}{a} + \frac{\rho_r}{2a^2} \right) - \frac{\alpha}{2} \int \frac{\dot{a}^2}{a} \, da + f, \tag{13}$$

where f is the integration constant. In terms of $\dot{a}^2$ this has the solution

$$\dot{a}^2 = \frac{8\pi G}{3} \left(\frac{\rho_m}{(1 - \frac{\alpha}{2}) a} + \frac{\rho_r}{(1 - \frac{\alpha}{4}) 2a^2} + ba^{-\alpha/2} \right), \tag{14}$$
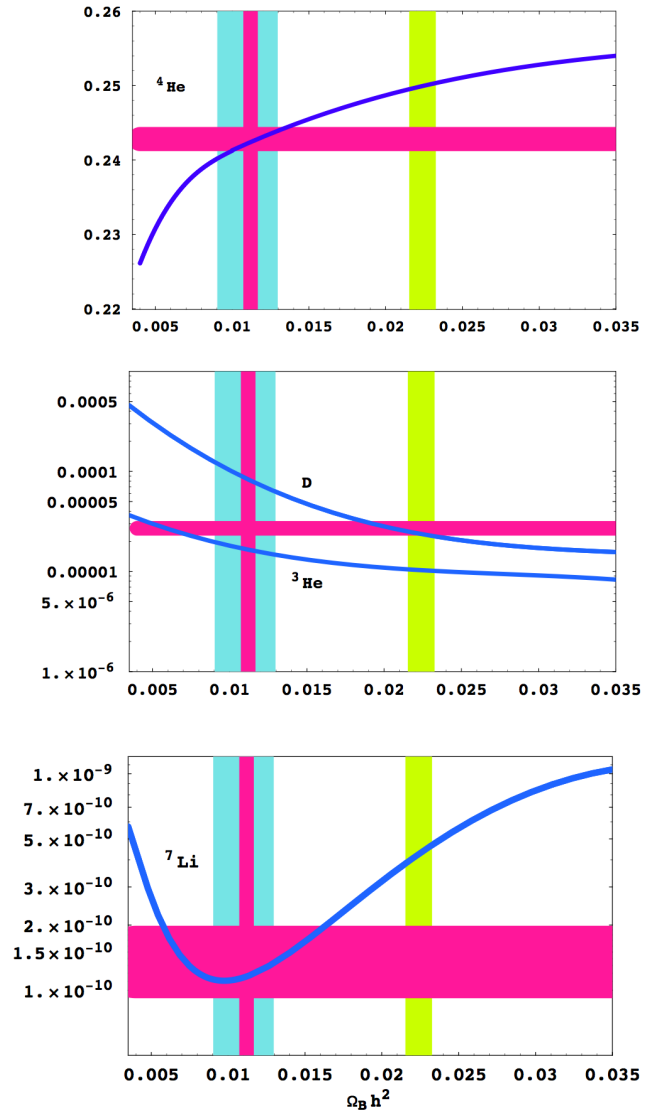
Fig. 2: Shows the Big Bang nucleosynthesis (BBN) number abundances for: the ^{4}He mass fraction (top), D and ^{3}He (middle) and ^{7}Li (bottom) relative to hydrogen vs $\Omega_B h^2$, as blue curves, from Coc et al. [1]. Horizontal (red) bar-graphs show astrophysical abundance observations. The vertical (yellow) bar-graphs show the values $\Omega_B h^2 = 0.0224 \pm 0.0009$ from WMAP CMB fluctuations, while the (blue) bar-graph $0.009 < \Omega_B h^2 < 0.013$ shows the best-fit at 68% CL from the BBN for the observed abundances [1]. We see that the WMAP data is in significant disagreement with the BBN results for $\Omega_B h^2$, giving, in particular, the ^{7}Li abundance anomaly within the ΛCDM model. The dynamical 3-space model has a different and hotter thermal history in the radiation dominated epoch, and the corresponding BBN predictions are easily obtained by a re-scaling of the WMAP value $\Omega_B h^2$ to $\Omega_B h^2/2$. The resultant $\Omega_B h^2 = 0.0112 \pm 0.0005$ values are shown by the vertical (red) bar-graphs that center on the BBN $0.009 < \Omega_B h^2 < 0.013$ range, and which is now in remarkable agreement with BBN computations. So while the BBN — WMAP inconsistency indicates a failure of the Friedmann FRW-GR Big Bang model, it is another success for the new physics entailed in the dynamical 3-space model. Plots adapted from [1].

which is easily checked by substitution into (13), and where b is the integration constant. We have written an overall factor of $8\pi G/3$ even though b, in principle, is independent of G. This gives b convenient units of matter density, but which does not correspond to any actual energy. From now on we shall put $\alpha = 0$. Finally we obtain from (14)

$$t(a) = \int_0^a \frac{da}{\sqrt{\frac{8\pi G}{3}\left(\frac{\rho_m}{a} + \frac{\rho_r}{2a^2} + b\right)}} \,. \qquad (15)$$

When $\rho_m = \rho_r = 0$, (15) reproduces the expansion in (7), and so the density terms in (14) give the modifications to the dominant purely-spatial expansion, which we have noted above already gives an excellent account of the red-shift data. Having $b \neq 0$ simply asserts that the 3-space can expand even when the energy density is zero — an effect missing from FLRW-GR cosmology. From (14) we obtain*

$$\overline{H}(z)^2 = H_0{}^2\left(\overline{\Omega}_m(1+z)^3 + \frac{\overline{\Omega}_r(1+z)^4}{2} + \overline{\Omega}_s(1+z)^2\right), \quad (16)$$

$$\overline{\Omega}_m \equiv \rho_m/\rho_c\,, \quad \overline{\Omega}_r \equiv \rho_r/\rho_c\,, \quad \overline{\Omega}_s \equiv b/\rho_c\,, \qquad (17)$$

$$\overline{\Omega}_m + \frac{\overline{\Omega}_r}{2} + \overline{\Omega}_s = 1\,, \qquad (18)$$

$$H_0 = \left(\frac{8\pi G}{3}\left(\rho_m + \frac{\rho_r}{2} + b\right)\right)^{1/2} \equiv \left(\frac{8\pi G}{3}\rho_c\right)^{1/2}\,, \qquad (19)$$

which defines the usual critical energy density ρ_c, but which here is merely a form for H_0 — it has no interpretation as an actual energy density, unlike in FRW-GR. Note the factor of 2 for $\overline{\Omega}_r$, which is a key effect in this paper, and is not in FRW-GR. In the dynamical 3-space model these $\overline{\Omega}$'s do not correspond to the composition of the universe, rather to the relative dynamical effects of the matter and radiation on the intrinsic 3-space expansion dynamics. $H_0 = 73$ km/s/Mpc with $\overline{\Omega}_m \approx \Omega_B = 0.04$ and $\overline{\Omega}_s = 0.96$ gives an age for the universe of $t_0 = 12.6$ Gyrs, while (22) with $\Omega_M = 0.27$ and $\Omega_\Lambda = 0.73$ gives $t_0 = 13.3$ Gyrs, $\overline{\Omega}_r = \Omega_r = 8.24 \times 10^{-5}$.

5 Friedmann-GR standard ΛCDM cosmology model

We now discuss the strange feature of the standard model dynamics which requires a non-zero energy density for the universe to expand. The well known Friedmann equation is

$$\left(\frac{\dot{a}}{a}\right)^2 = \frac{4\pi G}{3}\left(\frac{\rho_M}{a^3} + \frac{\rho_r}{a^4} + \Lambda\right), \qquad (20)$$

where now $\rho_M = \rho_m + \rho_{DM}$ is the matter composition of the universe, and includes ordinary matter and dark matter, and Λ is the cosmological constant or dark energy, expressed in mass density units. The differences between (13) and (20)

need to be noted: apart from the α term (20) has no integration constant which corresponds to a purely spatial expansion, and in compensation requires the *ad hoc* dark matter and dark energy terms, whose best-fit values are easily predicted; see below. It is worth noting how (20) arises from Newtonian gravity. For radially expanding homogeneous matter (1) gives for the total energy E of a test mass (a galaxy) of mass m

$$\frac{1}{2}mv^2 - \frac{GmM(r)}{r} = E\,, \qquad (21)$$

where $M(r)$ is the time-independent amount of matter within a sphere of radius r. With $E = 0$ and $M(r) = \frac{4}{3}\pi r^3 \rho(t)$ and $\rho(t) \sim 1/r(t)^3$ (21) has the Hubble form $v = H(t)r$. In terms of $a(t)$ this gives (20) after an *ad hoc* and invalid inclusion of the radiation and dark energy terms, as for these terms $M(r)$ is not independent of time, as assumed above. These terms are usually included on the basis of the stress-energy tensor within GR. Eqn. (20) leads to the analogue of (15),

$$t(a) = \int_0^a \frac{da}{\sqrt{\frac{8\pi G}{3}\left(\frac{\rho_M}{a} + \frac{\rho_r}{a^2} + \Lambda a^2\right)}}\,, \qquad (22)$$

$$H(z)^2 = H_0^2\left(\Omega_M(1+z)^3 + \Omega_r(1+z)^4 + \Omega_\Lambda(1+z)^2\right), \quad (23)$$

$$\Omega_M \equiv \rho_M/\rho_c\,, \quad \Omega_r \equiv \rho_r/\rho_c\,, \quad \Omega_\Lambda \equiv \Lambda/\rho_c\,, \qquad (24)$$

$$\Omega_M + \Omega_r + \Omega_\Lambda = 1\,, \qquad (25)$$

$$H_0 = \left(\frac{8\pi G}{3}(\rho_M + \rho_r + \Lambda)\right)^{1/2} \equiv \left(\frac{8\pi G}{3}\rho_c\right)^{1/2}\,. \qquad (26)$$

This has the same value of ρ_c as in (19), but now interpreted as an actual energy density. Note that $\overline{\Omega}_r = \Omega_r$, but that $\overline{\Omega}_m \neq \Omega_M$, as Ω_M includes the spurious "dark matter".

6 Predicting the ΛCDM parameters Ω_Λ and Ω_{DM}

The "dark energy" and "dark matter" arise in the FLRW-GR cosmology because in that model space cannot expand unless there is an energy density present in the space, if that space is flat and the energy density is pressure-less. Then essentially fitting the Friedmann model $\mu(z)$ to the dynamical 3-space cosmology $\mu(z)$ we obtain $\Omega_\Lambda = 0.73$, and so $\Omega_M = 1 - \Omega_\Lambda = 0.27$. These values arise from a best fit for $z \in \{0, 14\}$ [6]. The actual values for Ω_Λ depend on the red-shift range used, as the Hubble functions for the FLRW-GR and dynamical 3-space have different functional dependence on z. These values are of course independent of the actual observed redshift data. Essentially the current standard model of cosmology ΛCDM is excluded from modelling a uniformly expanding dynamical 3-space, but by choice of the parameter Ω_Λ the ΛCDM Hubble function $H(z)$ can be made to best-fit the data. However $H(z)$ has the wrong functional form; when applied to the future expansion of the universe the Friedmann dynamics produces a spurious exponentially expanding universe.

---

*From now-on an "overline" is used to denote the 3-space values. Note that $\overline{H}_0 \equiv H_0$ — the current observable value.

7 Dynamical 3-space and hotter early universe

The 3-space dynamics and the ΛCDM dynamics give different accounts of the expansion of the universe, particularly the thermal history and density during the radiation dominated epoch. ΛCDM gives in that epoch from (22)

$$a(t) = \sqrt{2H_0\,t\,\sqrt{\Omega_r}}\,,$$

while (15) gives

$$a(t) = \sqrt{2H_0\,t\,\sqrt{\Omega_r/2}}\,.$$

Because the CMB is thermal radiation its temperature varies as $T(t) = (2.725 \pm 0.001)/a(t)$ °K, and so the 3-space dynamics predicts an early thermal history that is 20% hotter. This means that a re-analysis of the BBN is required. However this is easily achieved by a scaling analysis. Essentially we can do this by effectively using $H_0/\sqrt{2}$ in place of H_0 in the radiation-dominated epoch, as this takes account of the $\Omega_r/2$ effect. In terms of $\Omega_B h^2$, which determines the BBN, this amounts to the re-scaling $\Omega_B h^2 \rightarrow \Omega_B h^2/2$. This immediately brings the WMAP $\Omega_B h^2 = 0.0224 \pm 0.0009$ down to, effectively, $\Omega_B h^2 = 0.0112 \pm 0.0005$, and into excellent agreement with the BBN value $0.009 < \Omega_B h^2 < 0.013$, as shown in Fig. 2, and discussed in detail in the figure caption.

8 Conclusions

It has been shown that the significant inconsistency between observed abundances of ^{7}Li and ^{4}He with the predictions from Big Bang Nucleosynthesis (BBN) when using the ΛCDM cosmological model together with the value for $\Omega_B h^2 = 0.0224 \pm 0.0009$ from WMAP CMB fluctuations, with the value from BBN required to fit observed abundances being $0.009 < \Omega_B h^2 < 0.013$, are resolved with remarkable precision by using the dynamical 3-space theory. This theory is shown to predict a 20% hotter universe in the radiation-dominated epoch, which then results in a remarkable agreement between the BBN and the WMAP value for $\Omega_B h^2$. The dynamical 3-space also gives a parameter-free fit to the supernova redshift data, and predicts that the flawed ΛCDM model would require $\Omega_\Lambda = 0.73$ and $\Omega_M = 0.27$ to fit the 3-space dynamics Hubble expansion, and independently of the supernova data. These results amount to the discovery of new physics for the early universe. This new physics has also explained (i) the bore-hole g anomaly, (ii) black-hole mass spectrum, (iii) flat rotation curves in spiral galaxies, (iv) enhanced light bending by galaxies, (v) anomalies in laboratory measurements of G, (vi) light speed anisotropy experiments including the explanation of the Doppler shift anomalies in spacecraft earth-flybys, and (vii) the detection of so-called gravitational waves. As well because (4) is non-local it can overcome the horizon problem. The new physics unifies cosmology with laboratory based phenomena, indicating a new era of precision studies of the cosmos.

References

1. Coc A., Vangioni-Flam E., Descouvemont P., Adahchour A. and Angulo C. Updated Big Bang nucleosynthesis compared with WMAP observations and abundance of elements. *ApJ*, 2004, v. 600, 544–552.

2. Cyburt R.H., Fields B.D. and Olive K.A. A bitter pill: the primordial Lithium problem worsens. *JCAP*, 2008, 0811:012.

3. Spergel D.N. *et al. ApJ. Suppl.*, 2003, v. 148, 175.

4. Cahill R.T. Dynamical 3-space: a review. In *Ether Space-time and Cosmology*: *New Insights into a Key Physical Medium*, Duffy M. and Lévy J., eds., *Apeiron*, 2009, 135–200.

5. Cahill R.T. Process physics: from information theory to quantum space and matter. Nova Science Pub., New York, 2005.

6. Cahill R.T. Unravelling the Dark Matter — Dark Energy paradigm. *Apeiron*, 2009, v. 16, no. 3, 323–375.

7. Anderson J.D., Campbell J.K., Ekelund J.E., Ellis J. and Jordan J.F. Anomalous orbital-energy changes observed during spacecraft flybys of Earth. *Phys. Rev. Lett.*, 2008, v. 100, 091102.

8. Cahill R.T. Combining NASA/JPL one-way optical-fiber light-speed data with spacecraft Earth-flyby Doppler-shift data to characterise 3-space flow. *Progress in Physics*, 2009, v. 4, 50–64.

9. Newton I. Philosophiae naturalis principia mathematica. 1687.

10. Riess A.G. *et al. Astron. J.*, 1998, v. 116, 1009.

11. Perlmutter S. *et al. Astrophys. J.*, 1999, v. 517, 565.

12. Perlmutter S. and Schmidt B.P. Measuring cosmology with supernovae. In: *Supernovae and Gamma Ray Bursters*, Weiler K, Ed., Springer, Lecture Notes in Physics, v. 598, 2003, 195–217.

Dynamics of Particles in Non Scaling Fixed Field Alternating Gradient Accelerators

James K. Jones*, Bruno D. Muratori†, Susan L. Smith‡, and Stephan I. Tzenov‖

*STFC Daresbury Laboratory, Daresbury, Warrington, Cheshire, WA4 4AD, United Kingdom. E-mail: james.jones@stfc.ac.uk
†STFC Daresbury Laboratory, Daresbury, Warrington, Cheshire, WA4 4AD, United Kingdom. E-mail: bruno.muratori@stfc.ac.uk
‡STFC Daresbury Laboratory, Daresbury, Warrington, Cheshire, WA4 4AD, United Kingdom. E-mail: susan.smith@stfc.ac.uk
‖STFC Daresbury Laboratory, Daresbury, Warrington, Cheshire, WA4 4AD, United Kingdom. E-mail: stephan.tzenov@stfc.ac.uk

Non scaling Fixed-Field Alternating Gradient (FFAG) accelerators have an unprecedented potential for muon acceleration, as well as for medical purposes based on carbon and proton hadron therapy. They also represent a possible active element for an Accelerator Driven Subcritical Reactor (ADSR). Starting from first principle the Hamiltonian formalism for the description of the dynamics of particles in non-scaling FFAG machines has been developed. The stationary reference (closed) orbit has been found within the Hamiltonian framework. The dependence of the path length on the energy deviation has been described in terms of higher order dispersion functions. The latter have been used subsequently to specify the longitudinal part of the Hamiltonian. It has been shown that higher order phase slip coefficients should be taken into account to adequately describe the acceleration in non-scaling FFAG accelerators. A complete theory of the fast (serpentine) acceleration in non-scaling FFAGs has been developed. An example of the theory is presented for the parameters of the Electron Machine with Many Applications (EMMA), a prototype electron non-scaling FFAG to be hosted at Daresbury Laboratory.

1 Introduction

Fixed-Field Alternating Gradient (FFAG) accelerators were proposed half century ago [1–4], when acceleration of electrons was first demonstrated. These machines, which were intensively studied in the 1950s and 1960s but never progressed beyond the model stage, have in recent years become the focus of renewed attention. Acceleration of protons has been recently achieved at the KEK Proof-of-Principle (PoP) proton FFAG [5].

To avoid the slow crossing of betatron resonances associated with a typical low energy-gain per turn, the first FFAGs designed and constructed so far have been based on the "scaling" principle. The latter implies that the orbit shape and betatron tunes must be kept fixed during the acceleration process. Thus, magnets must be built with constant field index, while in the case of spiral-sector designs the spiral angle must be constant as well. Machines of this type use conventional magnets with the bending and focusing field being kept constant during acceleration. The latter alternate in sign, providing a more compact radial extension and consequently smaller aperture as compared to the AVF cyclotrons. The ring essentially consists of a sequence of short cells with very large periodicity.

Non scaling FFAG machines have until recently been considered as an alternative. The bending and the focusing is provided simultaneously by focusing and defocusing quadrupole magnets repeating in an alternating sequence. There is a number of advantages of the non-scaling FFAG lattice as compared to the scaling one, among which are the relatively small transverse magnet aperture (tending to be much smaller than the one for scaling machines) and the lower field strength. Unfortunately this lattice leads to a large betatron tune variation across the required energy range for acceleration as opposed to the scaling lattice. As a consequence several resonances are crossed during the acceleration cycle, some of them nonlinear created by the magnetic field imperfections, as well as half-integer and integer ones. A possible bypass to this problem is the rapid acceleration (of utmost importance for muons), which allows betatron resonances no time to essentially damage beam quality.

Because non-scaling FFAG accelerators have otherwise very desirable features, it is important to investigate analytically and numerically some of the peculiarities of the beam dynamics, the new type of fast acceleration regime (so-called serpentine acceleration) and the effects of crossing of linear as well as nonlinear resonances. Moreover, it is important to examine the most favorable phase at which the cavities need to be set for the optimal acceleration. Some of these problems will be discussed in the present paper.

An example of the theory developed here is presented for the parameters of the Electron Machine with Many Applications (EMMA) [6], a prototype electron non-scaling FFAG to be hosted at Daresbury Laboratory. The Accelerators and Lasers In Combined Experiments (ALICE) accelerator [7] is used as an injector to the EMMA ring. The energy delivered by this injector can vary from a 10 to 20 MeV single bunch train with a bunch charge of 16 to 32 pC at a rate of 1 to 20

Hz. ALICE is presently designed to deliver bunches which are around 4 ps and 8.35 MeV from the exit of the booster of its injector line. These are then accelerated to 10 or 20 MeV in the main ALICE linac after which they are sent to the EMMA injection line. The EMMA injection line ends with a septum for injection into the EMMA ring itself followed by two kickers so as to direct the beam onto the correct, energy dependent, trajectory. After circulation in the EMMA ring, the electron bunches are extracted using what is almost a mirror image of the injection setup with two kickers followed by an extraction septum. The beam is then transported to a diagnostic line whose purpose it is to analyze in as much detail as possible the effect the non-scaling FFAG has had on the bunch.

The paper is organized as follows. Firstly, we review some generalities and first principles of the Hamiltonian formalism [8–10] suitably modified to cover the case of a non-scaling FFAG lattice. Firstly, a sequence of canonical transformations within the synchrobetatron framework is applied to determine the energy dependent reference orbit. Stability of motion about the stationary reference orbit is described in terms of betatron oscillations with energy dependent Twiss parameters and betatron tunes. Dispersion, measuring the effect of energy variation on the path length along the reference orbit is an essential feature of non-scaling FFAGs. Within the developed synchrobetatron formalism higher order dispersion functions have been introduced and their contribution to the longitudinal dynamics has been further analyzed. Finally, a complete description of the so-called serpentine acceleration in non-scaling lepton FFAGs is given together with conclusions. The calculations of the reference orbit and phase stability are detailed in the appendices.

2 Generalities and first principles

Let the ideal (design) trajectory of a particle in an accelerator be a planar curve with curvature K. The Hamiltonian describing the motion of a particle in a natural coordinate system attached to the orbit thus defined is [8]:

$$H = -(1 + Kx) \times$$

$$\times \sqrt{\frac{(\mathcal{H} - q\varphi)^2}{c^2} - m_{p_0}^2 c^2 - (P_x - qA_x)^2 - (P_z - qA_z)^2} -$$

$$- q(1 + Kx)A_s, \qquad (1)$$

where m_{p_0} is the rest mass of the particle. The guiding magnetic field can be represented as a gradient of a certain function $\psi(x, z; s)$

$$\mathbf{B} = \nabla\psi, \qquad (2)$$

where the latter satisfies the Laplace equation

$$\nabla^2\psi = 0. \qquad (3)$$

Using the median symmetry of the machine, it is straightforward to show that ψ can be written in the form

$$\psi = \left(a_0 + a_1 x + \frac{a_2 x^2}{2!} + \dots\right)z -$$

$$- \left(b_0 + b_1 x + \frac{b_2 x^2}{2!} + \dots\right)\frac{z^3}{3!} + (c_0 + c_1 x + \dots)\frac{z^5}{5!} + \dots . \qquad (4)$$

Inserting the above expression into the Laplace equation (3), one readily finds relations between the coefficients b_k and c_k on one hand and a_k on the other

$$b_0 = a_0'' + Ka_1 + a_2, \qquad (5)$$

$$b_1 = -2Ka_0'' - K'a_0' + a_1'' - K^2a_1 + Ka_2 + a_3, \qquad (6)$$

$$b_2 = 6K^2a_0'' + 6KK'a_0' - 4Ka_1'' - 2K'a_1' +$$
$$+ a_2'' + 2K^3a_1 - 2K^2a_2 + Ka_3 + a_4, \qquad (7)$$

$$c_0 = b_0'' + Kb_1 + b_2. \qquad (8)$$

Prime in the above expressions implies differentiation with respect to the longitudinal coordinate s. The coefficients a_k have a very simple meaning

$$a_0 = (B_z)_{x,z=0}, \qquad a_1 = \left(\frac{\partial B_z}{\partial x}\right)_{x,z=0},$$

$$a_2 = \left(\frac{\partial^2 B_z}{\partial x^2}\right)_{x,z=0}. \qquad (9)$$

In other words, this implies that, provided the vertical component B_z of the magnetic field and its derivatives with respect to the horizontal coordinate x are known in the median plane, one can in principle reconstruct the entire field chart.

The vector potential $\mathbf{A}$ can be represented as

$$A_x = -z\overline{F}(x, z; s), \quad A_z = x\overline{F}(x, z; s), \quad A_s = \overline{G}(x, z; s), \quad (10)$$

where the Poincaré gauge condition

$$xA_x + zA_z = 0, \qquad (11)$$

written in the natural coordinate system has been used. From Maxwell's equation

$$\mathbf{B} = \nabla \times \mathbf{A}, \qquad (12)$$

we obtain

$$2\overline{F} + (x\,\partial_x + z\,\partial_z)\overline{F} = B_s, \qquad (13)$$

$$\frac{Kx}{1 + Kx}\overline{G} + (x\,\partial_x + z\,\partial_z)\overline{G} = zB_x - xB_z. \qquad (14)$$

Applying Euler's theorem for homogeneous functions, we can write

$$\overline{F} = \frac{1}{2}B_s^{(0)} + \frac{1}{3}B_s^{(1)} + \frac{1}{4}B_s^{(2)} + \dots, \qquad (15)$$

$$\overline{G}_u = \left(1 + \frac{Kx}{2}\right) B_u^{(0)} + \left(\frac{1}{2} + \frac{Kx}{3}\right) B_u^{(1)} +$$

$$+ \left(\frac{1}{3} + \frac{Kx}{4}\right) B_u^{(2)} + \dots, \tag{16}$$

$$\overline{G} = \frac{z\,\overline{G}_x - x\,\overline{G}_z}{1 + Kx}. \tag{17}$$

Here $u = (x, z)$ and $B_\alpha^{(k)}$ denotes homogeneous polynomials in x and z of order k, representing the corresponding parts of the components of the magnetic field $\mathbf{B} = (B_x, B_z, B_s)$. Thus, having found the magnetic field represented by equation (4), it is straightforward to calculate the vector potential $\mathbf{A}$.

The accelerating field in AVF cyclotrons and FFAG machines can be represented by a scalar potential φ (the corresponding vector potential $\mathbf{A} = 0$). Due to the median symmetry, we have

$$\varphi = A_0 + A_1 x + \frac{A_2 x^2}{2!} + \dots - \left(B_0 + B_1 x + \frac{B_2 x^2}{2!} + \dots\right) \frac{z^2}{2!} +$$

$$+ (C_0 + C_1 x + \dots) \frac{z^4}{4!} + \dots. \tag{18}$$

Inserting the above expansion into the Laplace equation for φ, we obtain similar relations between B_k and C_k on one hand and A_k on the other, which are analogous to those relating b_k, c_k and a_k.

We consider the canonical transformation, specified by the generating function

$$S_2\left(x, z, \mathcal{T}, \widehat{P}_x, \widehat{P}_z, E; s\right) = x\widehat{P}_x + z\widehat{P}_z + \mathcal{T}E +$$

$$+ q \int d\mathcal{T}\,\varphi(x, z, \mathcal{T}; s), \tag{19}$$

where

$$\mathcal{T} = -t \tag{20}$$

is a canonical variable canonically conjugate to $\mathcal{H}$. The relations between the new and the old variables are

$$\widehat{u} = \frac{\partial S_2}{\partial \widehat{P}_u} = u, \qquad u = (x, z), \qquad \widehat{\mathcal{T}} = \frac{\partial S_2}{\partial E} = \mathcal{T}, \tag{21}$$

$$P_u = \frac{\partial S_2}{\partial u} = \widehat{P}_u - q \int d\mathcal{T}\, E_u(x, z, \mathcal{T}; s) =$$

$$= \widehat{P}_u - q\widetilde{E}_u(x, z, \mathcal{T}; s), \qquad E_u = -\frac{\partial \varphi}{\partial u}, \tag{22}$$

$$\mathcal{H} = \frac{\partial S_2}{\partial \mathcal{T}} = E + q\varphi(x, z, \mathcal{T}; s) =$$

$$= m_{p_0}\gamma c^2 + q\varphi(x, z, \mathcal{T}; s). \tag{23}$$

The new Hamiltonian acquires now the form

$$\widehat{H} = -(1 + Kx) \times$$

$$\times \sqrt{\frac{E^2}{c^2} - m_{p_0}^2 c^2 - \left(\widehat{P}_x - q\widetilde{E}_x - qA_x\right)^2 - \left(\widehat{P}_z - q\widetilde{E}_z - qA_z\right)^2 -}$$

$$- q(1 + Kx)\left(A_s + \widetilde{E}_s\right), \tag{24}$$

where

$$\widetilde{E}_s = \int d\mathcal{T}\, E_s(x, z, \mathcal{T}; s) =$$

$$= -\frac{1}{1 + Kx} \int d\mathcal{T}\, \frac{\partial \varphi(x, z, \mathcal{T}; s)}{\partial s}. \tag{25}$$

We introduce the new scaled variables

$$\widetilde{P}_u = \frac{\widehat{P}_u}{p_0} = \frac{\widehat{P}_u}{m_{p_0} c}, \qquad \Theta = c\mathcal{T}, \qquad \gamma = \frac{E}{E_p} = \frac{E}{m_{p_0} c^2}. \tag{26}$$

The new scaled Hamiltonian can be expressed as

$$\widetilde{H} = \frac{\widehat{H}}{p_0} = -(1 + Kx) \times$$

$$\times \sqrt{\gamma^2 - 1 - \left(\overline{P}_x - \widetilde{q}\widetilde{E}_x - \widetilde{q}A_x\right)^2 - \left(\overline{P}_z - \widetilde{q}\widetilde{E}_z - \widetilde{q}A_z\right)^2 -}$$

$$- \widetilde{q}(1 + Kx)\left(A_s + \widetilde{E}_s\right), \tag{27}$$

where

$$\widetilde{q} = \frac{q}{p_0}. \tag{28}$$

The quantities $\widetilde{E}_x$ and $\widetilde{E}_z$ can be neglected as compared to the components of the vector potential $\mathbf{A}$, so that

$$\widetilde{H} = \beta\gamma(1 + Kx) \times$$

$$\times \left[-\sqrt{1 - \left(\overline{P}_x - \overline{q}A_x\right)^2 - \left(\overline{P}_z - \overline{q}A_z\right)^2} - \overline{q}A_s \right] -$$

$$- \widetilde{q}(1 + Kx)\widetilde{E}_s, \tag{29}$$

where now

$$\overline{q} = \frac{q}{p} = \frac{q}{\beta\gamma p_0}, \qquad \overline{P}_u = \frac{\widehat{P}_u}{p} = \frac{\widehat{P}_u}{\beta\gamma p_0}, \qquad u = (x, z). \tag{30}$$

Since $\overline{P}_u$ and u are small deviations, we can expand the square root in power series in the canonical variables x, $\overline{P}_x$ and z, $\overline{P}_z$. Tedious algebra yields

$$\widetilde{H} = \widetilde{H}_0 + \widetilde{H}_1 + \widetilde{H}_2 + \widetilde{H}_3 + \widetilde{H}_4 + \dots, \tag{31}$$

$$\widetilde{H}_0 = -\beta\gamma - \widetilde{q}(1 + Kx)\widetilde{E}_s, \tag{32}$$

$$\widetilde{H}_1 = \beta\gamma\left(\overline{q}a_0 - K\right)x, \tag{33}$$

$$\widetilde{H}_2 = \frac{\beta\gamma}{2}\left(\overline{P}_x^2 + \overline{P}_z^2\right) + \frac{\widetilde{q}}{2}\left[(Ka_0 + a_1)x^2 - a_1 z^2\right], \tag{34}$$

$$\widetilde{H}_3 = \frac{\beta\gamma}{2} Kx\left(\overline{P}_x^2 + \overline{P}_z^2\right) + \frac{\widetilde{q}a_0' z}{3}\left(z\overline{P}_x - x\overline{P}_z\right) +$$

$$+ \frac{\widetilde{q}}{3}\left[\left(Ka_1 + \frac{a_2}{2}\right)x^3 - \left(Ka_1 + a_2 + \frac{b_0}{2}\right)xz^2\right], \qquad (35)$$

$$\widetilde{H}_4 = \frac{\beta\gamma}{8}\left(\overline{P}_x^2 + \overline{P}_z^2\right)^2 + \frac{\widetilde{q}xz}{12}\left(Ka_0' + 3a_1'\right)\left(z\overline{P}_x - x\overline{P}_z\right) +$$

$$+ \frac{\overline{q}^2\beta\gamma a_0'^2 z^2}{18}\left(x^2 + z^2\right) + + \frac{\widetilde{q}}{4}\left[\left(\frac{Ka_2}{2} + \frac{a_3}{6}\right)x^4 -\right.$$

$$\left. - \left(Ka_2 + \frac{a_3}{3} + \frac{Kb_0}{2} + \frac{b_1}{2}\right)x^2z^2 + \frac{b_1}{6}z^4\right]. \qquad (36)$$

The Hamiltonian decomposition (31) represents the milestone of the synchrobetatron formalism. For instance, $\widetilde{H}_0$ governs the longitudinal motion, $\widetilde{H}_1$ describes linear coupling between longitudinal and transverse degrees of freedom and is the basic source of dispersion. The part $\widetilde{H}_2$ is responsible for linear betatron motion and chromaticity, while the remainder describes higher order contributions.

3 The synchro-betatron formalism and the reference orbit

In the present paper we consider a FFAG lattice with polygonal structure. To define and subsequently calculate the stationary reference orbit, it is convenient to use a global Cartesian coordinate system whose origin is located in the center of the polygon. To describe step by step the fraction of the reference orbit related to a particular side of the polygon, we rotate each time the axes of the coordinate system by the polygon angle $\Theta_p = 2\pi/N_L$, where N_L is the number of sides of the polygon.

Let X_e and P_e denote the reference orbit and the reference momentum, respectively. The vertical component of the magnetic field in the median plane of a perfectly linear machine can be written as

$$B_z(X_e; s) = a_1(s)[X_e - X_c - d(s)],$$
$$a_0(X_e; s) = B_z(X_e; s), \qquad (37)$$

where s is the distance along the polygon side, and X_c is the distance of the side of the polygon from the center of the machine

$$X_c = \frac{L_p}{2\tan(\Theta_p/2)}. \qquad (38)$$

Here L_p is the length of the polygon side which actually represents the periodicity parameter of the lattice. Usually X_c is related to an arbitrary energy in the range from injection to extraction energy. In the case of EMMA it is related to the 15 MeV orbit. The quantity $d(s)$ in equation (37) is the relative offset of the magnetic center in the quadrupoles with respect to the corresponding side of the polygon. In what follows [see equations (47) and (50)] d_F corresponds to the offset in the focusing quadrupoles and d_D corresponds to the one in the defocusing quadrupoles. Similarly, a_F and a_D stand for

the particular value of a_1 in the focusing and the defocusing quadrupoles, respectively.

A design (reference) orbit corresponding to a local curvature $K(X_e; s)$ can be defined according to the relation

$$K(X_e; s) = \frac{q}{p_0\beta_e\gamma_e}B_z(X_e; s), \qquad (39)$$

where γ_e is the energy of the reference particle. In terms of the reference orbit position $X_e(s)$ the equation for the curvature can be written as

$$X_e'' = \frac{q}{p_0\beta_e\gamma_e}\left(1 + X_e'^2\right)^{3/2}B_z(X_e; s), \qquad (40)$$

where the prime implies differentiation with respect to s.

To proceed further, we notice that equation (40) parameterizing the local curvature can be derived from an equivalent Hamiltonian

$$H_e(X_e, P_e; s) = -\sqrt{\beta_e^2\gamma_e^2 - P_e^2} - \widetilde{q}\int dX_e B_z(X_e; s). \qquad (41)$$

Taking into account Hamilton's equations of motion

$$X_e' = \frac{P_e}{\sqrt{\beta_e^2\gamma_e^2 - P_e^2}}, \qquad P_e' = \widetilde{q}B_z(X_e; s), \qquad (42)$$

and using the relation

$$P_e = \frac{\beta_e\gamma_e X_e'}{\sqrt{1 + X_e'^2}}, \qquad (43)$$

we readily obtain equation (40). Note also that the Hamiltonian (41) follows directly from the scaled Hamiltonian (27) with $x = 0$, $\widetilde{P}_x = P_e$, $\widetilde{P}_z = 0$, $A_x = A_z = 0$ and the accelerating cavities being switched off respectively.

Hamilton's equations of motion (42) can be linearized and subsequently solved approximately by assuming that

$$P_e \ll \beta_e\gamma_e. \qquad (44)$$

Thus, assuming electrons $(q = -e)$, we have

$$P_e = \beta_e\gamma_e X_e', \qquad X_e'' = -\frac{ea_1(s)}{p_0\beta_e\gamma_e}(X_e - X_c - d(s)). \qquad (45)$$

The three types of solutions to equations (45) are as follows:

Drift Space

$$X_e = X_0 + \frac{P_0}{\beta_e\gamma_e}(s - s_0), \qquad P_e = P_0, \qquad (46)$$

where X_0 and P_0 are the initial position and reference momentum and s is the distance in longitudinal direction.

Focusing Quadrupole

$$X_e = X_c + d_F + (X_0 - X_c - d_F)\cos\omega_F(s - s_0) +$$

$$+ \frac{P_0}{\beta_e\gamma_e\omega_F}\sin\omega_F(s - s_0), \qquad (47)$$

$$P_e = -\beta_e \gamma_e \omega_F (X_0 - X_c - d_F) \sin \omega_F (s - s_0) +$$
$$+ P_0 \cos \omega_F (s - s_0) , \tag{48}$$

where

$$\omega_F^2 = \frac{e a_F}{p_0 \beta_e \gamma_e} . \tag{49}$$

Defocusing Quadrupole

$$X_e = X_c + d_D + (X_0 - X_c - d_D) \cosh \omega_D (s - s_0) +$$
$$+ \frac{P_0}{\beta_e \gamma_e \omega_D} \sinh \omega_D (s - s_0) , \tag{50}$$

$$P_e = \beta_e \gamma_e \omega_D (X_0 - X_c - d_D) \sinh \omega_D (s - s_0) +$$
$$+ P_0 \cosh \omega_D (s - s_0) , \tag{51}$$

where

$$\omega_D^2 = \frac{e a_D}{p_0 \beta_e \gamma_e} . \tag{52}$$

In addition to the above, the coordinate transformation at the polygon bend when passing to the new rotated coordinate system needs to be specified. The latter can be written as

$$X_e = X_c + \frac{X_0 - X_c}{\cos \Theta_p - P_0 \sin \Theta_p / \beta_e \gamma_e} ,$$

$$P_e = \beta_e \gamma_e \tan \left[\Theta_p + \arctan \left(\frac{P_0}{\beta_e \gamma_e} \right) \right] . \tag{53}$$

Once the reference trajectory has been found the corresponding contributions to the total Hamiltonian (31) can be written as follows

$$\widetilde{H}_0 = -\beta\gamma + \frac{Z}{A E_p} \left(\frac{\mathrm{d}\Delta E}{\mathrm{d}s} \right) \int \mathrm{d}\Theta \sin \phi(\Theta) , \tag{54}$$

$$\widetilde{H}_1 = -(\beta\gamma - \beta_e \gamma_e) K \tilde{x} , \tag{55}$$

$$\widetilde{H}_2 = \frac{1}{2\beta\gamma} \left(\widetilde{P}_x^2 + \widetilde{P}_z^2 \right) + \frac{1}{2} \left[\left(g + \beta_e \gamma_e K^2 \right) \tilde{x}^2 - g \tilde{z}^2 \right] , \tag{56}$$

$$\widetilde{H}_3 = \frac{K\tilde{x}}{2\beta\gamma} \left(\widetilde{P}_x^2 + \widetilde{P}_z^2 \right) + \frac{Kg}{6} \left(2\tilde{x}^3 - 3\tilde{x}\tilde{z}^2 \right) , \tag{57}$$

$$\widetilde{H}_4 = \frac{\left(\widetilde{P}_x^2 + \widetilde{P}_z^2 \right)^2}{8\beta^3 \gamma^3} - \frac{K^2 g}{24} \tilde{z}^4 . \tag{58}$$

Here, we have introduced the following notation

$$g = \frac{q a_1}{p_0} . \tag{59}$$

Moreover, Z is the charge state of the accelerated particle, A is the mass ratio with respect to the proton mass in the case of ions, and $\phi(\Theta)$ is the phase of the RF. For a lepton accelerator like EMMA, $A = Z = 1$. In addition, $(\mathrm{d}\Delta E/\mathrm{d}s)$ is the energy gain per unit longitudinal distance s, which in thin lens approximation scales as $\Delta E/\Delta s$, where Δs is the length

of the cavity. It is convenient to pass to new scaled variables as follows

$$\tilde{p}_u = \frac{\widetilde{P}_u}{\beta_e \gamma_e} , \qquad h = \frac{\gamma}{\beta_e^2 \gamma_e} , \tag{60}$$

$$\tau = \beta_e \Theta , \qquad \Gamma_e = \frac{\beta\gamma}{\beta_e \gamma_e} = \sqrt{\beta_e^2 h^2 - \frac{1}{\beta_e^2 \gamma_e^2}} . \tag{61}$$

Thus, expressions (54)–(58) become

$$\widetilde{H}_0 = -\Gamma_e + \frac{Z}{A \beta_e^2 E_e} \left(\frac{\mathrm{d}\Delta E}{\mathrm{d}s} \right) \int \mathrm{d}\tau \sin \phi(\tau) , \tag{62}$$

$$\widetilde{H}_1 = -(\Gamma_e - 1) K \tilde{x} , \tag{63}$$

$$\widetilde{H}_2 = \frac{1}{2\Gamma_e} \left(\tilde{p}_x^2 + \tilde{p}_z^2 \right) + \frac{1}{2} \left[\left(g_e + K^2 \right) \tilde{x}^2 - g_e \tilde{z}^2 \right] , \tag{64}$$

$$\widetilde{H}_3 = \frac{K\tilde{x}}{2\Gamma_e} \left(\tilde{p}_x^2 + \tilde{p}_z^2 \right) + \frac{K g_e}{6} \left(2\tilde{x}^3 - 3\tilde{x}\tilde{z}^2 \right) , \tag{65}$$

$$\widetilde{H}_4 = \frac{\left(\tilde{p}_x^2 + \tilde{p}_z^2 \right)^2}{8\Gamma_e^3} - \frac{K^2 g_e}{24} \tilde{z}^4 , \tag{66}$$

$$E_p = m_{p_0} c^2 , \qquad g_e = \frac{g}{\beta_e \gamma_e} . \tag{67}$$

The longitudinal part of the reference orbit can be isolated via a canonical transformation

$$F_2 \left(\tilde{x}, \tilde{p}_x, \tilde{z}, \tilde{p}_z, \tau, \eta; s \right) = \tilde{x}\tilde{p}_x + \tilde{z}\tilde{p}_z + (\tau + s) \left(\eta + \frac{1}{\beta_e^2} \right) , \tag{68}$$

$$\sigma = \tau + s , \qquad \eta = h - \frac{1}{\beta_e^2} , \tag{69}$$

where σ is the new longitudinal variable and η is the energy deviation with respect to the energy γ_e of the reference particle.

4 Dispersion and betatron motion

The (linear and higher order) dispersion can be introduced via a canonical transformation aimed at canceling the first order Hamiltonian $\widetilde{H}_1$ in all orders of η. The explicit form of the generating function is

$$G_2(\tilde{x}, \widehat{p_x}, \tilde{z}, \widehat{p_z}, \sigma, \widehat{\eta}; s) = \sigma\widehat{\eta} + \tilde{z}\widehat{p_z} + \tilde{x}\widehat{p_x} +$$
$$+ \sum_{k=1}^{\infty} \widehat{\eta}^k \left[\tilde{x} \mathcal{X}_k(s) - \widehat{p_x} \mathcal{P}_k(s) + \mathcal{S}_k(s) \right] , \tag{70}$$

$$\tilde{x} = \widehat{x} + \sum_{k=1}^{\infty} \widehat{\eta}^k \mathcal{P}_k , \qquad \tilde{p}_x = \widehat{p_x} + \sum_{k=1}^{\infty} \widehat{\eta}^k \mathcal{X}_k , \tag{71}$$

$$\sigma = \widehat{\sigma} + \sum_{k=1}^{\infty} k \widehat{\eta}^{k-1} (\mathcal{P}_k \widehat{p_x} - \mathcal{X}_k \widehat{x}) -$$
$$- \sum_{k=1}^{\infty} k \widehat{\eta}^{k-1} \left(\mathcal{S}_k + \mathcal{X}_k \sum_{m=1}^{\infty} \widehat{\eta}^m \mathcal{P}_m \right) . \tag{72}$$

Equating terms of the form $\widehat{x}\widehat{\eta}^n$ and $\widehat{p}_x\widehat{\eta}^n$ in the new transformed Hamiltonian, we determine order by order the conventional (first order) and higher order dispersions. The first order in $\widehat{\eta}$ (terms proportional to $\widehat{x}\widehat{\eta}$ and $\widehat{p}_x\widehat{\eta}$) yields the well-known result

$$\mathcal{P}_1' = \mathcal{X}_1, \qquad \mathcal{X}_1' + \left(g_e + K^2\right)\mathcal{P}_1 = K. \qquad (73)$$

Since in the case, where betatron motion $(\widehat{x} = 0, \widehat{p}_x = 0)$ can be neglected the new longitudinal coordinate $\widehat{\sigma}$ should not depend on the new longitudinal canonical conjugate variable $\widehat{\eta}$, the second sum in equation (72) must be identically zero. We readily obtain $\mathcal{S}_1 = 0$, and

$$\mathcal{S}_2 = -\frac{\mathcal{X}_1\mathcal{P}_1}{2}. \qquad (74)$$

In second order we have

$$\mathcal{P}_2' = \mathcal{X}_2 - \mathcal{X}_1 + K\mathcal{X}_1\mathcal{P}_1, \qquad (75)$$

$$\mathcal{X}_2' + \left(g_e + K^2\right)\mathcal{P}_2 = -Kg_e\mathcal{P}_1^2 - \frac{K\mathcal{X}_1^2}{2} - \frac{K}{2\gamma_e^2}, \qquad (76)$$

and in addition the function $\mathcal{S}_3(s)$ is expressed as

$$\mathcal{S}_3 = -\frac{1}{3}\left(\mathcal{X}_1\mathcal{P}_2 + 2\mathcal{X}_2\mathcal{P}_1\right). \qquad (77)$$

Close inspection of equations (73), (75) and (76) shows that $\mathcal{P}_1$ is the well-known linear dispersion function, while $\mathcal{P}_2$ stands for a second order dispersion and so on. Up to third order in $\widehat{\eta}$ the new Hamiltonian describing the longitudinal motion and the linear transverse motion acquires the form

$$\widehat{H}_0 = -\frac{\widetilde{\mathcal{K}}_1\widehat{\eta}^2}{2} + \frac{\widetilde{\mathcal{K}}_2\widehat{\eta}^3}{3} + \frac{Z}{A\beta_e^2 E_e}\left(\frac{\mathrm{d}\Delta E}{\mathrm{d}s}\right)\int \mathrm{d}\tau \sin\phi(\tau), \quad (78)$$

$$\widehat{H}_2 = \frac{1}{2}\left(\widehat{p}_x^2 + \widehat{p}_z^2\right) + \frac{1}{2}\left[\left(g_e + K^2\right)\widehat{x}^2 - g_e\widehat{z}^2\right], \qquad (79)$$

where

$$\widetilde{\mathcal{K}}_1 = K\mathcal{P}_1 - \frac{1}{\gamma_e^2}, \quad \widetilde{\mathcal{K}}_2 = \frac{K\mathcal{P}_1}{\gamma_e^2} - K\mathcal{P}_2 - \frac{\mathcal{X}_1^2}{2} - \frac{3}{2\gamma_e^2}. \quad (80)$$

For the sake of generality, let us consider a Hamiltonian of the type

$$\widehat{H}_b = \sum_{u=(x,z)}\left[\frac{\mathcal{F}_u}{2}\widehat{p}_u^2 + \mathcal{R}_u\widehat{u}\widehat{p}_u + \frac{\mathcal{G}_u}{2}\widehat{u}^2\right]. \qquad (81)$$

A generic Hamiltonian of the type (81) can be transformed to the normal form

$$\mathcal{H}_b = \sum_{u=(x,z)}\frac{\chi_u'}{2}\left(\overline{P}_u^2 + \overline{U}^2\right), \qquad (82)$$
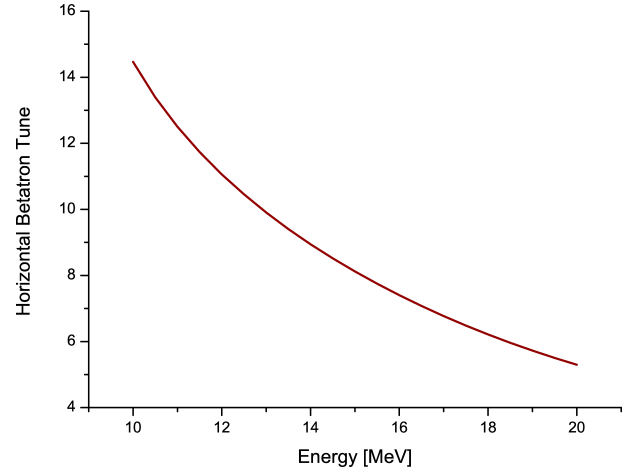

Fig. 1: Horizontal betatron tune for the EMMA ring as a function of energy.

by means of a canonical transformation specified by the generating function

$$\mathcal{F}_2\left(\widehat{x}, \overline{P}_x, \widehat{z}, \overline{P}_z; s\right) = \sum_{u=(x,z)}\left(\frac{\widehat{u}\overline{P}_u}{\sqrt{\beta_u}} - \frac{\alpha_u\widehat{u}^2}{2\beta_u}\right). \qquad (83)$$

Here the prime implies differentiation with respect to the longitudinal variable s. The old and the new canonical variables are related through the expressions

$$\widehat{u} = \overline{U}\sqrt{\beta_u}, \qquad \widehat{p}_u = \frac{1}{\sqrt{\beta_u}}\left(\overline{P}_u - \alpha_u\overline{U}\right). \qquad (84)$$

The phase advance $\chi_u(s)$ and the generalized Twiss parameters $\alpha_u(s)$, $\beta_u(s)$ and $\gamma_u(s)$ are defined as

$$\chi_u' = \frac{\mathrm{d}\chi_u}{\mathrm{d}s} = \frac{\mathcal{F}_u}{\beta_u}, \qquad (85)$$

$$\alpha_u' = \frac{\mathrm{d}\alpha_u}{\mathrm{d}s} = \mathcal{G}_u\beta_u - \mathcal{F}_u\gamma_u, \qquad (86)$$

$$\beta_u' = \frac{\mathrm{d}\beta_u}{\mathrm{d}s} = -2\mathcal{F}_u\alpha_u + 2\mathcal{R}_u\beta_u. \qquad (87)$$

The third Twiss parameter $\gamma_u(s)$ is introduced via the well-known expression

$$\beta_u\gamma_u - \alpha_u^2 = 1. \qquad (88)$$

The corresponding betatron tunes are determined according to the expression

$$\nu_u = \frac{N_p}{2\pi}\int_s^{s+L_p}\frac{\mathrm{d}\theta\,\mathcal{F}_u(\theta)}{\beta_u(\theta)}. \qquad (89)$$

Typical dependence of the horizontal and vertical betatron tunes on energy in the EMMA non-scaling FFAG is shown in Figures 1 and 2.
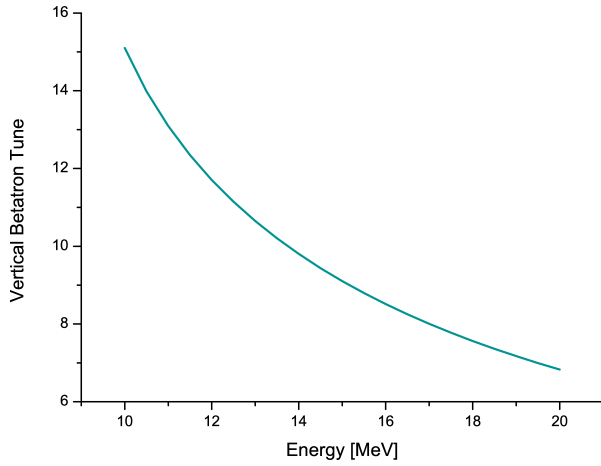
Fig. 2: Vertical betatron tune for the EMMA ring as a function of energy.

Fig. 3: Time of flight as a function of energy for a single 0.394481 meter EMMA cell.

It is worthwhile noting that the canonical transformation specified by the generating function (70) allowed us to cancel terms linear in the transverse canonical coordinates $\widehat{x}$ and $\widehat{p}_x$. In order to take a due account of the dependence of the longitudinal dynamics on the transverse one it is necessary to retain terms in the resulting Hamiltonian that are proportional to higher powers in $\widehat{\eta}$, $\widehat{x}$, $\widehat{p}_x$ and $\widehat{p}_z$. Up to first order in $\widehat{\eta}$, this gives rise to additional terms in the longitudinal Hamiltonian of the form

$$\widehat{H}_{0ad} = -\frac{\widehat{\eta}}{2}\left(\widehat{p}_x^2 + \widehat{p}_z^2\right) - \frac{K\widehat{\eta x}}{2}\left(\widehat{p}_x^2 + \widehat{p}_z^2\right) + \dots . \quad (90)$$

The lengthening of the time of flight for one period of the machine due to betatron oscillations can be expressed as

$$\Delta\Theta = -\frac{1}{2\beta_e}\int_{s}^{s+L_p} d\theta\left[1 + K(\theta)\widehat{x}(\theta)\right]\left[\widehat{p}_x^2(\theta) + \widehat{p}_z^2(\theta)\right]. \quad (91)$$

5 Acceleration in a non-scaling FFAG accelerator

The process of acceleration in a non-scaling FFAG accelerator can be studied by solving Hamilton's equations of motion for the longitudinal degree of freedom. The latter are obtained from the Hamiltonian (41) supplemented by an additional term [similar to that in equation (54)], which takes into account the electric field of the RF cavities. They read as

$$\frac{d\Theta}{ds} = -\frac{\gamma}{\sqrt{\beta^2\gamma^2 - P^2}}, \quad (92)$$

$$\frac{d\gamma}{ds} = -\frac{ZeU_c}{2AE_p}\sum_{k=1}^{N_c}\delta_p(s - s_k)\sin\left(\frac{\omega_c\Theta}{c} - \varphi_k\right). \quad (93)$$

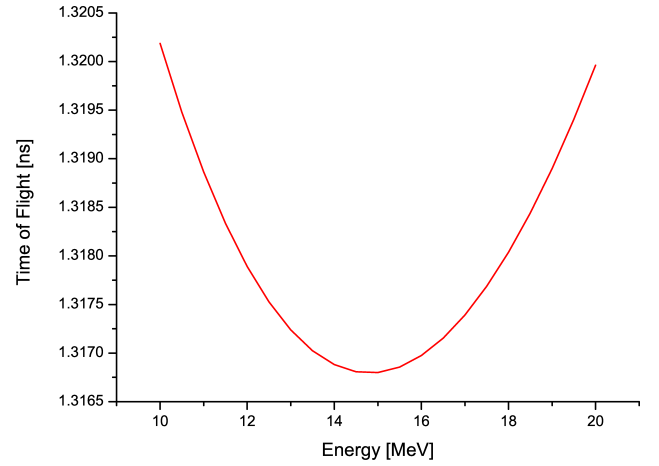Here U_c is the cavity voltage, ω_c is the RF frequency, N_c is the number of cavities and φ_k is the corresponding cavity phase.

One could use the results obtained in the previous section with the additional requirement that the phase slip coefficient $\widetilde{\mathcal{K}}_1$ averaged over one period vanishes. Instead, we shall use an equivalent but more illustrative approach. The path length in a FFAG arc and therefore the time of flight Θ is often well approximated as a quadratic function of energy. The acceleration process is then described by a longitudinal Hamiltonian, which contains terms proportional to the zero-order (conventional phase slip) factor and first-order phase slip factor. It usually suffices to take into account only terms to second order in the energy deviation

$$\Theta = \Theta_0 + 2\mathcal{A}\gamma_m\gamma - \mathcal{A}\gamma^2, \quad (94)$$

as suggested by Figure 3.

Here γ_m corresponds to the reference energy with a minimum time of flight. Provided the time of flight Θ_i at injection energy γ_i and the time of flight Θ_m at reference energy γ_m are known, the constants entering equation (94) can be expressed as

$$\mathcal{A} = \frac{\Theta_m - \Theta_i}{(\gamma_m - \gamma_i)^2}, \qquad \Theta_0 = \Theta_m - \mathcal{A}\gamma_m^2. \quad (95)$$

Next, we pass to a new variable

$$\widehat{\gamma} = \gamma - \gamma_m, \qquad \Theta = \Theta_m - \mathcal{A}\widehat{\gamma}^2, \quad (96)$$

similar to the variable $\widehat{\eta}$ introduced in the previous section. Then, Hamilton's equation of motion (92) can be rewritten in an equivalent form

$$\frac{d\Theta}{ds} = \frac{\Theta_m}{L_p} - \frac{\mathcal{A}\widehat{\gamma}^2}{L_p}. \quad (97)$$

In what follows, it is convenient to introduce a new phase $\widetilde{\varphi}$ and the azimuthal angle θ along the machine circumference as an independent variable according to the relations

$$ds = Rd\theta, \qquad \widetilde{\varphi} = \frac{\omega_c\Theta}{c}, \qquad R = \frac{N_L L_p}{2\pi}. \quad (98)$$

It is straightforward to verify (see the averaging procedure below) that the necessary condition to have acceleration is

$$\frac{\omega_c N_L |\Theta_m|}{2\pi c} = h, \qquad (99)$$

where h is an integer (a harmonic number). Averaging Hamilton's equations of motion

$$\frac{d\widetilde{\varphi}}{d\theta} = -h - ha\widehat{\gamma}^2, \qquad a = \frac{\mathcal{A}}{|\Theta_m|}, \qquad (100)$$

$$\frac{d\widehat{\gamma}}{d\theta} = -\frac{ZeU_c}{2AE_p} \sum_{k=1}^{N_c} \delta_p(\theta - \theta_k) \sin(\widetilde{\varphi} - \varphi_k), \qquad (101)$$

we rewrite them in a simpler form as

$$\frac{d\varphi}{d\theta} = ha\widehat{\gamma}^2, \qquad \frac{d\widehat{\gamma}}{d\theta} = \lambda \sin\varphi, \qquad (102)$$

where

$$\varphi = -\widetilde{\varphi} - h\theta + \psi_0, \qquad \lambda = \frac{ZeU_c \mathcal{D}}{4\pi AE_p}, \qquad (103)$$

$$\mathcal{D} = \sqrt{\mathcal{A}_c^2 + \mathcal{A}_s^2}, \qquad \psi_0 = \arctan\left(\frac{\mathcal{A}_s}{\mathcal{A}_c}\right), \qquad (104)$$

$$\mathcal{A}_c = \sum_{k=1}^{N_c} \cos(h\theta_k + \varphi_k), \qquad \mathcal{A}_s = \sum_{k=1}^{N_c} \sin(h\theta_k + \varphi_k). \qquad (105)$$

The effective longitudinal Hamiltonian, which governs the equations of motion (102) can be written as

$$H_0 = \frac{ha}{3}\widehat{\gamma}^3 + \lambda\cos\varphi. \qquad (106)$$

Since the Hamiltonian (106) is a constant of motion, the second Hamilton equation (102) can be written as

$$\frac{d\widehat{\gamma}}{d\theta} = \pm\lambda \sqrt{1 - \frac{1}{\lambda^2}\left(H_0 - \frac{ha}{3}\widehat{\gamma}^3\right)^2}. \qquad (107)$$

Let us first consider the case of the central trajectory, for which $H_0 = 0$. It is of utmost importance for the so called gutter (or serpentine) acceleration. Equation (107) can be solved in a straightforward manner to give

$$\theta = \frac{J}{b} \, _2F_1\left(\frac{1}{6}, \frac{1}{2}; \frac{7}{6}; J^6\right) - \frac{C}{b}, \qquad (108)$$

where

$$J = \widehat{\gamma} \sqrt[3]{\frac{ha}{3\lambda}}, \qquad b = \lambda \sqrt[3]{\frac{ha}{3\lambda}}, \qquad (109)$$

$$C = \, _2F_1\left(\frac{1}{6}, \frac{1}{2}; \frac{7}{6}; J_i^6\right) J_i. \qquad (110)$$

In the above expressions $_2F_1(\alpha, \beta; \gamma; x)$ denotes the Gauss hypergeometric function of the argument x. This case is illustrated in Figure 4.
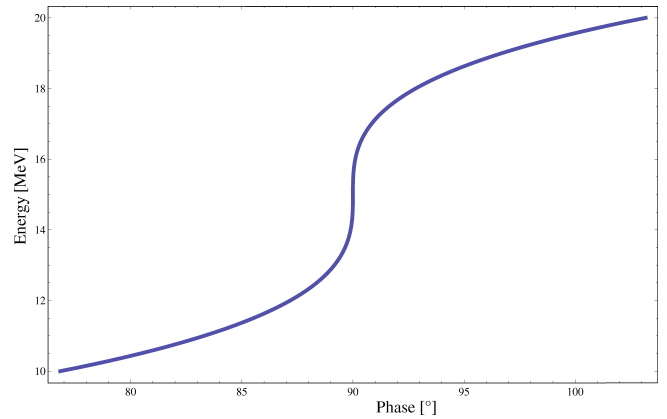

Fig. 4: An example of the so-called serpentine acceleration for the EMMA ring for the central trajectory, where the longitudinal $H_0 = 0$. The harmonic number is assumed to be 11, with the RF wavelength 0.405m. The parameter a from Eq. (100) is taken to be $2.6863 10^{-5}$.

In the general case where $H_0 \neq 0$, we have

$$\theta = \frac{J}{b\sqrt{a_1 c}} F_1\left(\frac{1}{3}; \frac{1}{2}, \frac{1}{2}; \frac{4}{3}; \frac{J^3}{a_1}, -\frac{J^3}{c}\right) - \frac{C_1}{b}, \qquad (111)$$

where

$$a_1 = 1 + \frac{H_0}{\lambda}, \qquad c = 1 - \frac{H_0}{\lambda}, \qquad (112)$$

$$C_1 = \frac{J_i}{\sqrt{a_1 c}} F_1\left(\frac{1}{3}; \frac{1}{2}, \frac{1}{2}; \frac{4}{3}; \frac{J_i^3}{a_1}, -\frac{J_i^3}{c}\right). \qquad (113)$$

Here now, $F_1(\alpha; \beta; \gamma; \delta; x, y)$ denotes the Appell hypergeometric function of the arguments x and y. The phase portrait corresponding to the general case for a variety of values of the longitudinal Hamiltonian H_0 is illustrated in Figure 5. The important question on whether the serpentine acceleration along the separatrix $H_0 = 0$ is stable is addressed in Appendix B.

A qualitative analysis of the fast serpentine acceleration has been presented earlier [11, 12]. However, to the best of our knowledge the results presented here comprise the first attempt to describe the process quantitatively. Although the exact solution is expressed in the form of standard and generalized hypergeometric functions, it can be easily incorporated in modern computational environments like Mathematica.

6 Concluding remarks

Based on the Hamiltonian formalism, the synchro-betatron approach for the description of the dynamics of particles in non-scaling FFAG machines has been developed. Its starting point is the specification of the static reference (closed) orbit for a fixed energy as a solution of the equations of motion in the machine reference frame. The problem of dynamical stability and acceleration is sequentially studied in the natural coordinate system associated with the reference orbit thus determined.
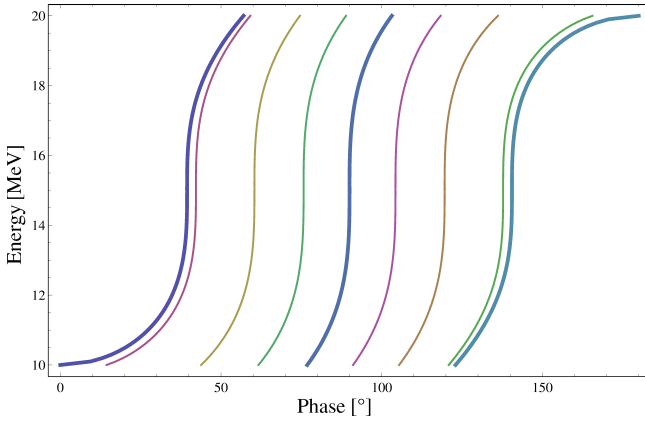
Fig. 5: Examples of serpentine acceleration for the EMMA ring, with varying value of the longitudinal Hamiltonian. The limits of stability are given at values of the longitudinal Hamiltonian of ± 0.31272, corresponding to either a 0 phase at 10MeV, or a π phase at 20MeV.

It has been further shown that the dependence of the path length on the energy deviation can be described in terms of higher order (nonlinear) dispersion functions. The method provides a systematic tool to determine the dispersion functions and their derivatives to every desired order, and represents a natural definition through constitutive equations for the resulting Twiss parameters.

The formulation thus developed has been applied to the electron FFAG machine EMMA. The transverse and longitudinal dynamics have been explored and an initial attempt is made at understanding the limits of longitudinal stability of such a machine.

Unlike the conventional synchronous acceleration, the acceleration process in FFAG accelerators is an asynchronous one in which the reference particle performs nonlinear oscillations around the crest of the RF waveform. To the best of our knowledge, it is the first time that such a fully analytic (quantitative) theory describing the acceleration in non-scaling FFAGs has been developed.

A   Calculation of the reference orbit

The explicit solutions of the linearized equations of motion (45) can be used to calculate approximately the reference orbit. To do so, we introduce a state vector

$$\mathbf{Z}_e = \begin{pmatrix} X_e \\ P_e \end{pmatrix}. \tag{114}$$

The effect of each lattice element can be represented in a simple form as

$$\mathbf{Z}_{out} = \widehat{\mathcal{M}}_{el}\mathbf{Z}_{in} + \mathbf{A}_{el}. \tag{115}$$

Here $\mathbf{Z}_{in}$ is the initial value of the state vector, while $\mathbf{Z}_{out}$ is its final value at the exit of the corresponding element. The transfer matrix $\widehat{\mathcal{M}}_{el}$ and the shift vector $\mathbf{A}_{el}$ for various lattice elements are given as follows:

1. *Polygon Bend.*
   Within the approximation (44) considered here we can linearize the second of equations (53) and write

$$\widehat{\mathcal{M}}_p = \begin{pmatrix} 1/\cos\Theta_p & -X_c \tan\Theta_p/\left(\beta_e\gamma_e\cos\Theta_p\right) \\ 0 & 1/\cos^2\Theta_p \end{pmatrix},$$

$$\mathbf{A}_p = \begin{pmatrix} X_c\left(1 - 1/\cos\Theta_p\right) \\ \beta_e\gamma_e\tan\Theta_p \end{pmatrix}. \tag{116}$$

2. *Drift Space.*

$$\widehat{\mathcal{M}}_O = \begin{pmatrix} 1 & L_O/\beta_e\gamma_e \\ 0 & 1 \end{pmatrix}, \qquad \mathbf{A}_O = 0, \tag{117}$$

where L_O is the length of the drift. Every cell of the EMMA lattice includes a short drift of length L_0 and a long one of length L_1.

3. *Focusing Quadrupole.*
   The transfer matrix can be written in a straightforward manner as

$$\widehat{\mathcal{M}}_F = \begin{pmatrix} \cos(\omega_F L_F) & \sin(\omega_F L_F)/(\beta_e\gamma_e\omega_F) \\ -\beta_e\gamma_e\omega_F\sin(\omega_F L_F) & \cos(\omega_F L_F) \end{pmatrix}, \tag{118}$$

$$\mathbf{A}_F = \begin{pmatrix} (X_c + d_F)[1 - \cos(\omega_F L_F)] \\ \beta_e\gamma_e\omega_F(X_c + d_F)\sin(\omega_F L_F) \end{pmatrix}, \tag{119}$$

where L_F is the length of the focusing quadrupole.

4. *Defocusing Quadrupole.*
   The transfer matrix in this case can be written in analogy to the above one as

$$\widehat{\mathcal{M}}_D = \begin{pmatrix} \cosh(\omega_D L_D) & \sinh(\omega_D L_D)/(\beta_e\gamma_e\omega_D) \\ \beta_e\gamma_e\omega_D\sinh(\omega_D L_D) & \cosh(\omega_D L_D) \end{pmatrix}, \tag{120}$$

$$\mathbf{A}_D = \begin{pmatrix} (X_c + d_D)[1 - \cosh(\omega_D L_D)] \\ -\beta_e\gamma_e\omega_D(X_c + d_D)\sinh(\omega_D L_D) \end{pmatrix}, \tag{121}$$

where L_D is the length of the defocusing quadrupole.

Since the reference orbit must be a periodic function of s with period L_p, it clearly satisfies the condition

$$\mathbf{Z}_{out} = \mathbf{Z}_{in} = \mathbf{Z}_e. \tag{122}$$

Thus, the equation for determining the reference orbit becomes

$$\mathbf{Z}_e = \widehat{\mathcal{M}}\mathbf{Z}_e + \mathbf{A}, \quad \text{or} \quad \mathbf{Z}_e = \left(1 - \widehat{\mathcal{M}}\right)^{-1}\mathbf{A}. \tag{123}$$

Here $\widehat{\mathcal{M}}$ and $\mathbf{A}$ are the transfer matrix and the shift vector for one period, respectively. The inverse of the matrix $1 - \widehat{\mathcal{M}}$

can be expressed as

$$\left(1 - \widehat{\mathcal{M}}\right)^{-1} = \frac{\cos^3 \Theta_p}{1 + \left(1 - \text{Sp}\widehat{\mathcal{M}}\right)\cos^3 \Theta_p} \times$$

$$\times \begin{pmatrix} 1 - \mathcal{M}_{22} & \mathcal{M}_{12} \\ \mathcal{M}_{21} & 1 - \mathcal{M}_{11} \end{pmatrix}. \quad (124)$$

For the EMMA lattice in particular, the components of the one period transfer matrix and shift vector can be written explicitly as

$$\mathcal{M}_{11} = \frac{1}{c_p}\left[c_F c_D + \left(\frac{\omega_D}{\omega_F} - L_0 L_1 \omega_F \omega_D\right) s_F s_D + \right.$$

$$\left. + (L_0 + L_1)\omega_D c_F s_D - L_1 \omega_F s_F c_D\right], \quad (125)$$

$$\mathcal{M}_{12} = \frac{1}{\beta_e \gamma_e c_p}\left\{\left(\frac{L_0 + L_1}{c_p} - X_c t_p\right)c_F c_D + \right.$$

$$+ \left[\left(L_0 L_1 \omega_F \omega_D - \frac{\omega_D}{\omega_F}\right)X_c t_p - \frac{\omega_F L_1}{\omega_D c_p}\right]s_F s_D +$$

$$+ \left[\frac{1}{\omega_D c_p} - (L_0 + L_1)\omega_D X_c t_p\right]c_F s_D +$$

$$\left. + \left(\frac{1}{\omega_F c_p} + L_1 \omega_F X_c t_p - \frac{L_0 L_1 \omega_F}{c_p}\right)s_F c_D\right\}, \quad (126)$$

$$\mathcal{M}_{21} = -\frac{\beta_e \gamma_e}{c_p}(\omega_F s_F c_D + L_0 \omega_F \omega_D s_F s_D - \omega_D c_F s_D), \quad (127)$$

$$\mathcal{M}_{22} = \frac{1}{c_p}\left[\frac{c_F c_D}{c_p} + \left(L_0 \omega_F \omega_D X_c t_p - \frac{\omega_F}{\omega_D c_p}\right)s_F s_D + \right.$$

$$\left. + \omega_F\left(X_c t_p - \frac{L_0}{c_p}\right)s_F c_D - \omega_D X_c t_p c_F s_D\right], \quad (128)$$

$$A_1 = X_c + d_F + (d_D - d_F)(c_F - L_1 \omega_F s_F) + \left(\frac{X_c}{c_p} + d_D\right)\times$$

$$\times\left[L_1 \omega_F s_F c_D - c_F c_D - (L_0 + L_1)\omega_D c_F s_D - \right.$$

$$\left. - \frac{\omega_D s_F s_D}{\omega_F} + L_0 L_1 \omega_F \omega_D s_F s_D\right] +$$

$$+ t_p\left[(L_0 + L_1)c_F c_D + \frac{c_F s_D}{\omega_D} + \right.$$

$$\left. + \frac{s_F c_D}{\omega_F} - \frac{L_1 \omega_F s_F s_D}{\omega_D} - L_0 L_1 \omega_F s_F c_D\right], \quad (129)$$

$$A_2 = -\beta_e \gamma_e \omega_F (d_D - d_F)s_F + \beta_e \gamma_e\left(\frac{X_c}{c_p} + d_D\right)\times$$

$$\times (\omega_F s_F c_D + \omega_F \omega_D L_0 s_F s_D - \omega_D c_F s_D) +$$

$$+ \beta_e \gamma_e t_p\left(c_F c_D - \frac{\omega_F s_F s_D}{\omega_D} - \omega_F L_0 s_F c_D\right). \quad (130)$$
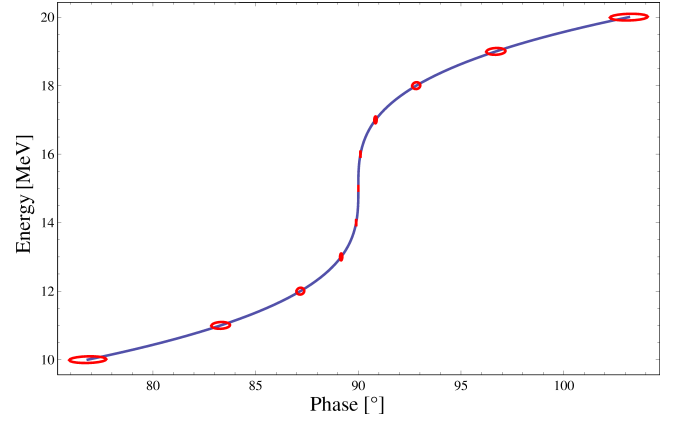

Fig. 6: Phase stability of the standard EMMA ring, for the central trajectory at $H_0 = 0$. The errors are given as 0.1MeV in energy and 1.3° in phase.

For the sake of brevity, the following notations

$$c_p = \cos \Theta_p, \quad c_F = \cos(\omega_F L_F), \quad c_D = \cosh(\omega_D L_D), \quad (131)$$

$$t_p = \tan \Theta_p, \quad s_F = \sin(\omega_F L_F), \quad s_D = \sinh(\omega_D L_D), \quad (132)$$

have been introduced in the final expressions for the components of the one period transfer matrix and shift vector.

B   Phase stability in FFAGs

To study the stability of the serpentine acceleration in FFAG accelerators, we write the longitudinal Hamiltonian (106) in an equivalent form

$$H_0 = \lambda\left(J^3 + \cos\varphi\right). \quad (133)$$

Hamilton's equations of motion can be written as

$$\frac{d\varphi}{d\theta} = 3bJ^2, \qquad \frac{dJ}{d\theta} = b\sin\varphi. \quad (134)$$

Let $\varphi_a(\theta)$ and $J_a(\theta)$ be the exact solution of equations (134) described already in Section V. Let us further denote by φ_1 and J_1 a small deviation about this solution such that $\varphi = \varphi_a + \varphi_1$ and $J = J_a + J_1$. Then, the linearized equations of motion governing the evolution of φ_1 and J_1 are

$$\frac{d\varphi_1}{d\theta} = 6bJ_a J_1, \qquad \frac{dJ_1}{d\theta} = b\varphi_1 \cos\varphi_a. \quad (135)$$

The latter should be solved provided the constraint

$$3J_a^2 J_1 - \varphi_1 \sin\varphi_a = 0, \quad (136)$$

following from the Hamiltonian (133) holds. Differentiating the second of equations (135) with respect to θ and eliminating φ_1, we obtain

$$\frac{d^2 J_1}{d\theta^2} - \frac{6b^2 H_0}{\lambda}J_a J_1 + 15b^2 J_a^4 J_1 = 0. \quad (137)$$

Next, we examine the case of separatrix acceleration with $H_0 = 0$. In Section V we showed that to a good accuracy the energy gain $[J_a(\theta) = b\theta + J_i]$ is linear in the azimuthal variable θ. Therefore, equation (137) can be written as

$$\frac{\mathrm{d}^2 J_1}{\mathrm{d}J_a^2} + 15 J_a^4 J_1 = 0 \,. \qquad (138)$$

The latter possesses a simple solution of the form

$$J_1 = \sqrt{|J_a|}\left[C_1 \mathcal{J}_{1/6}\left(\sqrt{\frac{5}{3}}\, |J_a|^3 \right) + C_2 \mathcal{Y}_{1/6}\left(\sqrt{\frac{5}{3}}\, |J_a|^3 \right) \right], \quad (139)$$

where $\mathcal{J}_\alpha(z)$ and $\mathcal{Y}_\alpha(z)$ stand for the Bessel functions of the first and second kind, respectively. In addition the constants C_1 and C_2 should be determined taking into account the initial conditions

$$\frac{\mathrm{d}J_1(J_i)}{\mathrm{d}J_a} = \varphi_1(J_i)\cos\varphi_i \,, \qquad J_1(J_i) = J_{1i} \,. \qquad (140)$$

References

1. Kolomensky A.A. and Lebedev A.N. Theory of cyclic accelerators. North-Holland Publishing Company, 1966.

2. Kolomensky A.A. et al. Some questions of the theory of cyclic accelerators. Edition AN SSSR, 1956, v.26, no. 2, 7.

3. Symon K.R. et al. *Phys. Rev.*, 1956, v.103, 1837.

4. Kerst D.W. et al. *Review of Science Instruments*, 1960, v.31, 1076.

5. Aiba M. et al. Development of a FFAG proton synchrotron. *Proceedings of EPAC*, 2000, 581.

6. Edgecock R. et al. EMMA — the world's first non-scaling FFAG. *Proceedings of EPAC*, 2008, 3380.

7. Smith S.L. The status of the Daresbury Energy Recovery Linac Prototype (ERLP). *Proceedings of ERL*, 2007, 6.

8. Tzenov S.I. Contemporary accelerator physics. World Scientific, 2004.

9. Symon K.R. Derivation of Hamiltonians for accelerators. ANL/APS/TB-28, 1997.

10. Suzuki T. Equation of motion and Hamiltonian for synchrotron oscillations and synchrotron-betatron coupling. *KEK Report*, 1996, 96–10.

11. Koscielniak S. and Johnstone C. *Nuclear Instrum. and Methods A*, 2004, v. 523, 25.

12. Scott Berg J. *Physical Review Special Topics Accel. Beams*, 2006, v.9, 034001.

————————————————

On Some New Ideas in Hadron Physics

Florentin Smarandache[*] and Vic Christianto[†]

[*]Department of Mathematics, University of New Mexico, Gallup, NM 87301, USA
E-mail: smarand@unm.edu
[†]Sciprint.org — a Free Scientific Electronic Preprint Server, http://www.sciprint.org
E-mail: vxianto@yahoo.com, admin@sciprint.org

We shortly review a series of novel ideas on the physics of hadrons and nuclear matter. Despite being vastly different in scope and content, these models share a common attribute, in that they offer unconventional viewpoints on infrared QCD and nuclear phenomena. In a sense, they are reminiscent of the plethora of formulations that have been developed over the years on classical gravitation: many seemingly disparate approaches can be effectively used to describe and explore the same physics.

1 Introduction

Given the extent and complexity of hadron and nuclear phenomena, any attempt for an exhaustive review of new ideas is outright unpractical. We survey here only a limited number of models and guide the reader to appropriate references for further information. The paper is divided in several sections according to the following plan:

1. The first section discusses the Brightsen model and the Nuclear String hypothesis;

2. Models inspired by Kerr-Newman twistor model and the AdS/CFT conjecture are introduced in the second section;

3. The last section discusses CGLE model of hadron masses and non-equilibrium phase transitions in infrared QCD.

The selection of topics is clearly incomplete and subjective. As such, it may not necessarily reflect the prevalent opinion of theorists working in this field. Our intent is to simply stimulate a constructive exchange of ideas in this active area of research.

2 Brightsen mdodel and the nuclear string hypothesis

In this hadron model, developed by M.Pitkanen [1] based on his TGD theory, it is supposed that ^{4}He nuclei and $A < 4$ nuclei and possibly also nucleons appear as basic building blocks of nuclear strings. This seems like some kind of improvement of the Close Packed Spheron model of L. Pauling in 1960s, which asserts that nuclei is composite form of small numbers of interacting boson-fermion nucleon clusters, i.e. ^{3}He (PNP), triton (NPN) and deuteron (NP). Another extension of Pauling model is known as Brightsen's cluster nuclei model, which has been presented and discussed by F. Smarandache and D. Rabounski [2].

Interestingly, it can be shown that the Close Packed model of nuclei may explain naturally why all the upper quarks have fractional electric charge at the order of $Q = +\frac{2}{\sqrt{3}}$. So far this is one of the most mysterious enigma in the hadron physics. But as described by Thompson [4], in a closed-packed crystal

sheet model, the displacement coefficients would be given by a matrix where the 1-1 component is:

$$c_{11} = \frac{2\rho}{\sqrt{3}} - 1, \qquad (1)$$

where the deformation can be described by the resolved distance between columns, written as ρd. Here d represents diameter of the nuclei entity. Now it seems interesting to point out here that if we supposed that $\rho = 1 + \frac{\sqrt{3}}{2}$, then c from equation (3) yields exactly the same value with the upper quark's electric charge mentioned above. In other words, this seems to suggest plausible deep link between QCD/quark charges and the close-packed nuclei picture [3].

Interestingly, the origin of such fractional quark charge can also be described by a geometric icosahedron model [4]. In this model, the concept of quark generation and electroweak charge values are connected with (and interpreted as) the discrete symmetries of icosahedron geometry at its 12 vertices. Theoretical basis of this analog came from the fact that the gauge model of electroweak interactions is based on SU(2)×U(1) symmetry group of internal space. Meanwhile, it is known that SU(2) group corresponds to the O(3) group of 3D space rotations, hence it appears quite natural to connect particle properties with the discrete symmetries of the icosahedron polygon.

It is worth to mention here that there are some recent articles discussing plausible theoretical links between icosahedron model and close-packed model of nuclei entities, for instance by the virtue of Baxter theory [5]. Furthermore, there are other articles mentioning theoretical link between the close-packed model and Ginzburg-Landau theory. There is also link between Yang-Baxter theory and Ginzburg-Landau theory [6]. In this regards, it is well known that cluster hydrogen or cluster helium exhibit superfluidity [7,8], therefore it suggests deep link between cluster model of Pauling or Brightsen and condensed matter physics (Ginzburg-Landau theory).

The Brightsen model supports a hypothesis that antimatter nucleon clusters are present as a parton (*sensu* Feynman) superposition within the spatial confinement of the proton

(^{1}H$_1$), the neutron, and the deuteron (^{1}H$_2$). If model predictions can be confirmed both mathematically and experimentally, a new physics is suggested. A proposed experiment is connected to orthopositronium annihilation anomalies, which, being related to one of known unmatter entity, orthopositronium (built on electron and positron), opens a way to expand the Standard Model.

Furthermore, the fact that the proposed Nuclear String hypothesis is derived from a theory which consists of many-sheeted spacetime framework called TGD seems to suggest a plausible link between this model and Kerr-Schild twistor model as described below.

3 Multiparticle Kerr-Schild twistor model and AdS/CFT Light-Front Holography model

Kerr's multiparticle solution can be obtained on the basis of the Kerr theorem, which yields a many-sheeted multi-twistorial spacetime over M^4 with some unusual properties. Gravitational and electromagnetic interaction of the particles occurs with a singular twistor line, which is common for twistorial structures of interacting particles [6].

In this regards the Kerr-Newman solution can be represented in the Kerr-Schild form [9]:

$$g_{\mu\nu} = \eta_{\mu\nu} + 2hk_\mu k_\nu, \qquad (2)$$

where $\eta_{\mu\nu}$ is the metric of auxiliary Minkowski spacetime.

Then the Kerr theorem allows one to describe the Kerr geometry in twistor terms. And using the Kerr-Schild formalism, one can obtain exact asymptotically flat multiparticle solutions of the Einstein-Maxwell field equations. But how this model can yield a prediction of hadron masses remain to be seen. Nonetheless the axial stringy system corresponds to the Kerr-Schild null tetrad can be associated with superconducting strings. Interestingly one can find an interpretation of Dirac equation from this picture, and it is known that Dirac equation with an effective QCD potential can describe hadron masses.

What seems interesting from this Kerr-Schild twistor model, is that one can expect to give some visual interpretation of the electromagnetic string right from the solution of Einstein-Maxwell field equations. This would give an interesting clue toward making the string theory a somewhat testable result. Another approach to connect the superstring theory to hadron description will be discussed below, called Light-Front Holography model.

Brodsky et al. [10, 11] were able to prove that there are theoretical links, such that the Superstring theory reduces to AdS/CFT theory, and Ads/CFT theory reduces to the so-called Light Front Holography, which in turn this model can serve as first approximation to the Quantum Chromodynamics theory.

Starting from the equation of motion in QCD, they identify an invariant light front coordinate which allows separation of the dynamics of quark and gluon binding from the kinematics of constituent spin and internal orbital angular momentum. Of most interesting here is that this method gives results in the from of 1-parameter light-front Schrödinger equation for QCD which determines the eigenspectrum and the light-front wavefunctions of hadrons for general spin and orbital angular momentum.

The light-front wave equation can be written as [8]:

$$\left(-\frac{d^2}{d\zeta^2} - \frac{1-4L^2}{4\zeta^2} + U(\zeta)\right)\phi(\zeta) = M^2\phi(\zeta), \qquad (3)$$

which is an effective single-variable light-front Schrödinger equation which is relativistic, covariant, and analytically tractable; here M represents the mass spectra.

Nonetheless, whether this Light-Front Holography picture will yield some quantitative and testable predictions of hadron masses, remains to be seen.

4 Concluding note

We shortly review a series of novel ideas on the physics of hadrons and nuclear matter. Despite being vastly different in scope and content, these models share a common attribute, in that they offer unconventional viewpoints on hadron, nuclear phenomena, and infrared QCD. In a sense, they are reminiscent of the plethora of formulations that have been developed over the years on classical gravitation: many seemingly disparate approaches can be effectively used to describe and explore the same physics.

These very interesting new approaches, therefore, seem to suggest that there is a hitherto hidden theoretical links between different approaches.

In our opinion, these theoretical links worth to discuss further to prove whether they provide a consistent picture, in particular toward explanation of the hadron mass generation mechanism and spontaneous symmetry breaking process.

The present article is a first part of our series of review of hadron physics. Another part is under preparation.

References

1. Pitkanen M. Nuclear string hypothesis. In: F. Smarandache & V. Christianto (eds.) *Hadron Models and Related New Energy Issues*, InfoLearnQuest Publ., USA, 2008.

2. Smarandache F., Rabounski D. Unmatter entities inside nuclei, predicted by the Brightsen Nucleon Cluster Model. *Progress in Physics*, 2005, v. 2.

3. Thompson J.M.T. Instabilities and catastrophes in science and engineering. John Wiley & Sons Ltd, New York, 1982, pp. 96 and 101.

4. Vladimirov Yu.S. Quark icosahedron, charges and Weinberg's angle. *Grav. & Cosmology*, 2004, v. 10, no. 1–2(37–38), 63–70.

5. Esposito G. & Marmo G. arXiv: math-ph/0511063.

6. Gomez C. & Sierra G. arXiv: hep-th/9309007.

7. Mezzacapo F. & Boninsegni M. Structure, superfluidity and quantum melting of hydrogen cluster. arXiv: cond-mat/ 0611775.

8. Serot B.D. & Walecka J.D. arXiv: nucl-th/0010031; nucl-th/9701058.

9. Burinskii A. Axial stringy system of the Kerr spinning particle. *Grav. & Cosmology*, 2004, v. 10, no. 1–2(37–38), 50–60.

10. Brodsky S. Dynamic versus static hadronic structure functions. arXiv: 0901.0781.

11. de Teramond G. F. & Brodsky S. J. Light-front holography: a first approximation to QCD. arXiv: 0809.4899.

LETTERS TO PROGRESS IN PHYSICS

Coordinate Transformations and Metric Extension: a Rebuttal to the Relativistic Claims of Stephen J. Crothers

Jason J. Sharples

School of Physical, Environmental and Mathematical Sciences, University of New South Wales
at the Australian Defence Force Academy, Canberra 2600, Australia
E-mail: j.sharples@adfa.edu.au

The concept of coordinate transformation is fundamental to the theory of differentiable manifolds, which in turn plays a central role in many modern physical theories. The notion of metric extension is also important in these respects. In this short note we provide some simple examples illustrating these concepts, with the intent of alleviating the confusion that often arises in their use. While the examples themselves can be considered unrelated to the theory of general relativity, they have clear implications for the results cited in a number of recent publications dealing with the subject. These implications are discussed.

1 Introduction

Differentiable manifolds play a central role in modern physical theories. Roughly speaking, a differentiable manifold (hereafter manifold) is a topological space whose local equivalence to Euclidean space permits a global calculus. In more precise mathematical terms, a manifold is a topological space M with a collection of coordinate systems that cover all of M. Thus the concept of a coordinate system is fundamental to the notion of manifold.

A coordinate system is defined as a mapping ϕ (with certain properties) from an open set U of a topological space onto an open set $\phi(U)$ of Euclidean space. The open set U is called the coordinate neighborhood of ϕ and the functions $x^1, \ldots, x^n$ on U such that $\phi = \left(x^1, \ldots, x^n \right)$, are the coordinate functions, or more simply the coordinates. A manifold can have an infinite number of equally valid coordinates defined on it.

As an example consider the topological space S^2 (the unit sphere). Further consider the northern and southern hemispheres of the sphere, which are both open subsets of S^2. On each of the hemispheres we can define stereographic coordinates by projecting the respective hemispheres onto two-dimensional Euclidean space. Each of the projections defines a coordinate system, which when taken together cover all of S^2. Thus S^2 is a manifold.

The notion of a metric tensor g on a manifold M is fundamental to the theory of differential geometry (indeed, the metric tensor is alternatively called the first fundamental form). Explicitly, g is a type-(0,2) tensor that defines a scalar product $g(p)$ on the tangent space $T_p(M)$, for each point $p \in M$. On a domain U, corresponding to a particular coordinate system $\{x^1, \ldots, x^n\}$, the components of the metric tensor are $g_{ij} = g(\partial_i, \partial_j)$. It is important to note that the metric components g_{ij} are functions, not tensors. The metric tensor itself is given by $g = g_{ij}\, dx^i \otimes dx^j$, where summation over the indices is implied. It must be stressed that a metric, by virtue of the

fact that it is a tensor, is independent of the coordinate system which is used to express the component functions g_{ij}.

The metric tensor can be represented by its line-element ds^2, which gives the associated quadratic form of $g(p)$. We stress that a line-element is *not* a tensor. A line-element can be expressed in terms of a coordinate system as

$$ds^2 = g_{ij}\, dx^i\, dx^j.$$

Representing the metric in a particular coordinate system by the associated quadratic form is equivalent to expressing it as a square matrix with respect to the coordinate basis. For example, on the unit sphere the metric σ is often written in terms of the line-element with respect to spherical coordinates $\{\theta, \varphi\}$ as

$$ds^2 = d\theta^2 + \sin^2\theta\, d\varphi^2,$$

or equivalently as the matrix

$$[\sigma]_{\{\theta,\varphi\}} = \begin{pmatrix} 1 & 0 \\ 0 & \sin^2\theta \end{pmatrix}.$$

It is important when practicing differential geometry to distinguish between coordinate dependent quantities and coordinate invariant quantities. We have already seen some examples of these: the metric tensor is coordinate invariant (as is any tensor), while the line-element is coordinate dependent. Another example of a coordinate dependent quantity are the Christoffel symbols

$$\Gamma^i_{jk} = g^{im}\left(\partial_k g_{mj} + \partial_j g_{mk} - \partial_m g_{jk}\right)$$

while the scalar curvature (Kretschmann scalar), which is derived from them as

$$f = g^{ab}\left(\partial_c\Gamma^c_{ab} - \partial_b\Gamma^c_{ac} + \Gamma^d_{ab}\Gamma^c_{cd} - \Gamma^d_{ac}\Gamma^c_{bd}\right),$$

is coordinate invariant. Another example of a coordinate invariant quantity is the metric length of a path in a manifold.

Suppose now that we have two different sets of coordinates defined on an open set $U \subset M$. That is to say that we have two mappings ϕ_1 and ϕ_2 that act from U onto two (possibly different) open sets V_1 and V_2 in Euclidean space. It is apparent that we can change from one coordinate system to the other with the maps $\phi_2 \circ \phi_1^{-1}$ or $\phi_1 \circ \phi_2^{-1}$. Such maps define a change of coordinates or *coordinate transformation*. Alternatively if we have a mapping ζ from V_1 into V_2 and a coordinate system (mapping) ϕ from U onto V_1, then the mapping $\zeta \circ \phi$ also defines a coordinate system. In this context ζ is the coordinate transformation. Coordinate invariant quantities, such as the metric, the scalar curvature and lengths, do not change under the action of a coordinate transformation

In what follows we illustrate these concepts by means of some simple examples and discuss some of their implications.

2 Some simple examples

We begin by illustrating the concept of coordinate transformation with a simple example in ordinary Euclidean 3-space (E^3). Suppose that (r, θ, φ) are the usual spherical coordinates on E^3 and consider the spherically symmetric line-element

$$ds^2 = r^2 \, dr^2 + r^2 \, d\Omega^2, \tag{1}$$

where $d\Omega^2 = d\theta^2 + \sin^2\theta \, d\varphi^2$ is the usual shorthand for the line-element on the unit sphere S^2.

Defining a new radial coodinate ρ by $2\rho = r^2$, the line-element can be written in terms of the coordinates (ρ, θ, φ) as

$$ds^2 = d\rho^2 + 2\rho \, d\Omega^2. \tag{2}$$

Note that if ρ is held constant then the line-element reduces to the standard line-element for a sphere of radius $\sqrt{2\rho} = r$.

Note that the coordinate transformation has changed nothing. The metrics corresponding to the line-elements given by (1) and (2) are exactly the same tensor, they have just been expressed in two different sets of coordinates. To illustrate this consider calculating metric length along a radial line. Specifically, consider the path defined in terms of the (r, θ, ϕ) coordinates by

$$\gamma_a = \{(r, \theta, \varphi) : r \in (0, a), \; \theta = \pi/4, \; \varphi = 0\}.$$

Equivalently, we can define the path in terms of the (ρ, θ, φ) coordinates as

$$\gamma_a = \{(\rho, \theta, \varphi) : \rho \in (0, a^2/2), \; \theta = \pi/4, \; \varphi = 0\}.$$

Thus calculating the metric length of the path γ_a with respect to the line-element (1) we find

$$L(\gamma_a) = \int_{r=0}^{r=a} r \, dr = \frac{a^2}{2},$$

while if we calculate it with respect to the line-element (2) we find that

$$L(\gamma_a) = \int_{\rho=0}^{\rho=a^2/2} d\rho = \frac{a^2}{2}.$$

This confirms that the metric length does not depend on the particular coordinate expression (line-element) representing the metric.

This example also illustrates another interesting property of the metric corresponding to (1) or (2). If we set $\rho = b$, where b is a constant, the line-element (2) reduces to the 2D line-element:

$$ds^2 = 2b \, d\Omega^2.$$

This is the line-element of a 2-sphere with a radius of curvature of $\sqrt{2b}$, i.e. the Gaussian curvature is $1/2b$. However, calculating the metric distance d from the origin ($\rho = 0$) to this sperical shell ($\rho = b$), we find that

$$d = \int_0^b d\rho = b.$$

Hence, the metric radius and the radius of curvature are not equal in general. Repeating the calulation with (1) yields the same result.

As another example consider the two-dimensional, non-Euclidean metric

$$ds_1^2 = -x^2 \, dt^2 + dx^2, \tag{3}$$

where it is assumed that $t \in (-\infty, \infty)$ and $x \in (0, \infty)$. In terms of the coordinates $\{t, x\}$ the metric tensor g_1 can therefore be represented as

$$[g_1]_{\{t,x\}} = \begin{pmatrix} -x^2 & 0 \\ 0 & 1 \end{pmatrix}, \tag{4}$$

with a metric determinant of $|g_1| = -x^2$, which suggests that as $x \to 0$ the metric becomes singular.

However, calculating the scalar curvature of the metric we find that $R_{g_1} = 0$, which is independent of x. The metric g_1 therefore defines a flat manifold (N, g_1). The fact that the singularity arises in the coordinate dependent form of the metric, but not in the coordinate invariant scalar curvature, indicates that the apparent singularity may in fact be due solely to a breakdown in the coordinate system $\{t, x\}$ that was chosen to represent the metric, i.e. it may merely be a *coordinate singularity* rather than a true singularity of the manifold described by g_1. A coordinate singularity can be removed by a good choice of coordinates, whereas a true singularity cannot.

Introducing new coordinates $\{T, X\}$, which are defined in terms of the old coordinates $\{t, x\}$ by

$$X = x \cosh t$$
$$T = x \sinh t,$$

the line-element ds_1^2 may be written as

$$ds_1^2 = -dT^2 + dX^2. \tag{5}$$

Note that $t \in (-\infty, \infty)$ and $x \in (0, \infty)$ implies that $T \in (-\infty, \infty)$ and $X \in (0, \infty)$ also.

In terms of the $\{T, X\}$ coordinates, the metric tensor g_1 is represented by

$$[g_1]_{\{T,X\}} = \begin{pmatrix} -1 & 0 \\ 0 & 1 \end{pmatrix}. \qquad (6)$$

and so the metric determinant is $|g_1| = -1$. The apparent singularity has been removed by invoking a good choice of coordinates.

We note further that even though the line-element (5) was only defined for $X \in (0, \infty)$ there is now nothing stopping us from extending the definition to include $X \in (-\infty, \infty)$. We thus make the distinction between the line-element ds_1^2, defined above, and the line-element ds_2^2 defined as

$$ds_1^2 = -d\tau^2 + d\xi^2, \qquad (7)$$

with coordinates $\tau, \xi \in (-\infty, \infty)$. The metric corresponding to the line-element (7), denoted by g_2, defines a manifold (M, g_2) that can be thought of as 2D Minkowski space. By restricting the coordinate ξ to the semi-finite interval $(0, \infty)$ we recover the metric g_1, that is

$$g_2|_{\xi>0} = g_1.$$

It follows that the manifold (N, g_1) is a submanifold of the Minkowski space (M, g_2). Alternatively we say that (M, g_2) is a *coordinate extension* of the manifold (N, g_1). The manifold (N, g_1) is known as the *Rindler wedge* and corresponds to that part of (M, g_2) defined by $|\tau| < \xi$.

3 Implications

In [1] the author notes that the line-element written in terms of coordinates $\{t, r, \theta, \varphi\}$ as

$$ds^2 = A(r)\, dt^2 + B(r)\, dr^2 + C(r)\, d\Omega^2 \qquad (8)$$

corresponds to the most general spacetime metric that is static and spherically symmetric. He then goes on to claim that the line-element written in terms of coordinates $\{t, \rho, \theta, \phi\}$ as

$$ds^2 = A^*(\rho)\, dt^2 + B^*(\rho)\, d\rho^2 + \rho^2\, d\Omega^2 \qquad (9)$$

does *not* correspond to the most general metric that is static and spherically symmetric*. This claim is false, as we will now demonstrate.

Consider the line-element (9) and define the coordinate transformation $\rho = \sqrt{C(r)}$, where C is some function independent of the functions A^* and B^*. Taking the differential we find that

$$d\rho = \frac{C'(r)}{2\sqrt{C(r)}}\, dr$$

and so the line-element (9) can be written in terms of the coordinates $\{t, r, \theta, \varphi\}$ as

$$ds^2 = E(r)\, dt^2 + D(r)\, dr^2 + C(r)\, d\Omega^2, \qquad (10)$$

where

$$E(r) = A^*\left(\sqrt{C(r)}\right) \quad \text{and} \quad D(r) = \frac{B^*\left(\sqrt{C(r)}\right) C'(r)^2}{4C(r)}.$$

Since the functions A^* and B^* are independent of the function C, the functions E and D are also independent of the function C. The line-element (10) is identical to (8) and it follows that the metrics represented by (8) and (9) are the same metric (just expressed in terms of different coordinates), and therefore that both line-elements represent the most general static, sperically symmetric spacetime metric.

Based on the claim of [1], just shown is false, the author goes on to conclude that solutions of the gravitational field equations that are derived from the metric ansatz (9) are particular solutions rather than general solutions. These claims are also false for the same reasons as illustrated above.

The foregoing considerations therefore have bearing on the relativistic arguments contained in [1] and subsequent papers by the author. For example, in [1–8] the author repeatedly makes the following claims:

1. The coordinate ρ, appearing in (9), is not a proper radius;

2. The "Schwarzschild" solution, as espoused by Hilbert and others is different to the Schwarzschild solution obtained originally by Schwarzschild [9];

3. The original Schwarzschild solution is a complete (i.e. inextendible) metric;

4. There are an infinite number of solutions to the static, spherically symmetric solutions to the field equations correponding to a point mass;

5. For line-elements of Schwarzschild form[†], the scalar curvature f remains bounded everywhere, and hence there is no "black hole".

We will now address and dismiss each of these claims.

Claim 1. The claim that ρ is not a proper radius stems from a calculation in [1]. The author defines the proper radius as

$$R_p = \int \sqrt{B(r)}\, dr \qquad (11)$$

where B is the function appearing in (8). Strictly speaking this is not a radius, per se, but a *function* of the coordinate r. In more precise terms, the proper radius should be defined as the metric length of the radial path γ_a defined by[‡]

$$\gamma_a = \{(t, r, \theta, \varphi) : r \in (a_1, a_2),\ t, \theta, \varphi = \text{constant}\}.$$

This then implies that the proper radius is defined as

$$R_p = L_1(\gamma_a) = \int_{a_1}^{a_2} \sqrt{B(r)}\, dr. \qquad (12)$$

---

*Note that in [1] the author has used r again instead of ρ. We use the different symbol ρ to avoid confusion.

[†]Line-elements of "Schwarzschild form" are defined in [2].

[‡]We believe that this is what the definition in [1] was actually aiming at.

The claim in [1] relates to the fact that R_p, as defined by (11), is equal to r only if $B(r) = 1$. This conclusion is based on an imprecise definition of the proper radius and does not take into account the effect of coordinate transformation. If we work in terms of the coordinates appearing in the line-element (9), which we have already shown represents the same metric as (8), then the path γ_a is defined as

$$\gamma_a = \{(t, \rho, \theta, \varphi) : \rho \in (\rho_1, \rho_2),\ t, \theta, \varphi = \text{constant}\},$$

with $\rho_1 = \sqrt{C(a_1)}$ and $\rho_2 = \sqrt{C(a_2)}$. In terms of the line-element (9) the metric length of γ_a is given by

$$L_2(\gamma_a) = \int_{\sqrt{C(a_1)}}^{\sqrt{C(a_2)}} \sqrt{B^*(\rho)}\, d\rho.$$

Noting the effect of the coordinate transformation, that was established earlier, we then find that

$$
\begin{aligned}
R_p = L_1(\gamma_a) &= \int_{a_1}^{a_2} \sqrt{B(r)}\, dr \\
&= \int_{a_1}^{a_2} \left[B^*\!\left(\sqrt{C(r)}\right) \right]^{1/2} \frac{C'(r)}{2\sqrt{C(r)}}\, dr \\
&= \int_{\sqrt{C(a_1)}}^{\sqrt{C(a_2)}} \sqrt{B^*(\rho)}\, d\rho \\
&= L_2(\gamma_a).
\end{aligned}
$$

Hence the proper radius does not depend on the form of the line-element. Proper radius (i.e. a metric length) can be equivalently defined in terms of either of the "radial" coordinates r or ρ.

Claims 2 and 3. The original Schwarzschild solution obtained in [9] is given as the line-element

$$ds^2 = A(R)dt^2 - A(R)^{-1}dR^2 - R^2 d\Omega^2, \qquad (13)$$

where

$$A(R) = 1 - \frac{\alpha}{R} \quad \text{and} \quad R = (r^3 + \alpha^3)^{1/3}.$$

The coordinate $r \in (0, \infty)$ that appears is the standard spherical radial coordinate. The expression $R = (r^3 + \alpha^3)^{1/3}$ defines a transformation of the radial coordinate r into the auxilliary radial coordinate R. The constant α is related to the value of the mass at the origin [9]. Indeed, by imposing the additional boundary condition at infinity, that the solution be consistent with the predictions of Newtonian gravitational theory, it is found that the constant $\alpha = 2m$, where m is the mass at the origin. The line-element (13) can therefore be written as

$$ds^2 = \left(1 - \frac{2m}{R}\right)dt^2 - \left(1 - \frac{2m}{R}\right)^{-1}dR^2 - R^2 d\Omega^2, \qquad (14)$$

with $R \in (2m, \infty)$. Note that if R and t are held constant (say $R = a$ and $t = t_0$) the line-element reduces to that of a 2-sphere with radius $a > 2m$. The line-element therefore defines a manifold that is foliated by 2-spheres with radii greater than $2m$.

The line-element is of precisely the same form as the line-element derived by Hilbert [10], i.e.

$$ds^2 = \left(1 - \frac{2m}{\rho}\right)dt^2 - \left(1 - \frac{2m}{\rho}\right)^{-1}d\rho^2 - \rho^2 d\Omega^2, \qquad (15)$$

where $\rho \in (0, 2m) \cup (2m, \infty)$. The only difference is that (14) is defined over a subset of the domain over which (15) is defined. To obtain the line-element (15) the radial coordinate has been extended to values less than $2m$ in much the same way that the metric corresponding to (5) was extended to the metric corresponding to (7). The only real difference is that in the case at hand there remains a coordinate singularity at $R = 2m$, and so in terms of the coordinates used, the extended manifold must be viewed as a disjoint union of the regions corresponding to $R < 2m$ and $R > 2m$. Both of the disjoint regions satisfy the static, spherically symmetric field equations. In fact it is well-known that there exist coordinates in which the difficulty at $R = 2m$ can be removed, resulting in a single manifold that satisfies the field equations. As a point of historical interest we note that the extended metric is also known as the "Schwarzschild" metric in honour of Schwarzschild's contribution to the field, despite the fact that his original solution is only a subset of the complete solution.

From the above considerations it clear that the manifold corresponding to the line-element (13) is incomplete. Indeed, in deriving this form of the line-element, Schwarzschild imposed a very specific boundary condition, namely that the line-element is continuous everywhere except at $r = 0$, where $r \in (0, \infty)$ is the standard spherical radial coordinate. Imposition of this boundary condition has significant implications for the solution obtained. In particular, as a consequence of the boundary condtion the coordinate R is shifted away from the origin. Indeed, if $r \in (0, \infty)$ then $R \in (\alpha, \infty)$. Hence the manifold represented by (13) is foliated by 2-spheres of radius greater than $\alpha = 2m$ — the spacetime has a hole in its centre!

Claim 4. In [2] the author derives the general solution for the static, spherically symmetric field due to a point mass as

$$ds^2 = \left(\frac{\sqrt{C_n} - \alpha}{\sqrt{C_n}}\right)dt^2 - \left(\frac{\sqrt{C_n}}{\sqrt{C_n} - \alpha}\right)\frac{C_n'^2}{4C_n}dr^2 - C_n d\Omega^2, \quad (16)$$

where r is the standard radial spherical coordinate and

$$C_n(r) = \left[(r - r_0)^n + \alpha^n\right]^{2/n} \qquad (17)$$

with $r_0 \geqslant 0$ and $n > 0$ arbitrary constants. The author also notes that (16) is only defined for $r > r_0$.

Let us now see the effect of transforming coordinates. Firstly, let $\rho = r - r_0$ so that the coordinate ρ is simply a shifted

version of the coordinate r. Taking differentials implies that $d\rho = dr$ and so we may equivalently write the line-element (16) as

$$ds^2 = \left(\frac{\sqrt{C_n} - \alpha}{\sqrt{C_n}}\right)dt^2 - \left(\frac{\sqrt{C_n}}{\sqrt{C_n} - \alpha}\right)\frac{C_n'^2}{4C_n}d\rho^2 - C_n\, d\Omega^2, \quad (18)$$

where now

$$C_n(\rho) = [\rho^n + \alpha^n]^{2/n}$$

and the line-element is defined for $\rho > 0$.

Secondly, define another change of coordinates by $R = \sqrt{C_n(\rho)}$. This is essentially a rescaling of the radial coordinate ρ. Taking differentials we find that

$$dR = \frac{C_n'}{2\sqrt{C_n}}\, d\rho.$$

Thus in terms of the coordinate R the line-element may be written as

$$ds^2 = \left(\frac{R - \alpha}{R}\right)dt^2 - \left(\frac{R}{R - \alpha}\right)dR^2 - R^2\, d\Omega^2, \quad (19)$$

where the coordinate $R > \alpha$.

Hence we have shown that what appeared to be an infinitude of particular solutions are actually just different coordinate expressions of the same solution, which without loss of generality can be expressed in "Schwarzschild coordinates" $\{t, R, \theta, \varphi\}$ by (19). This solution is incomplete, as we have already seen, since the line-element and the corresponding metric are only defined when the coordinate $R > \alpha$. The solution is known as the *exterior* Schwarzschild solution.

Another way of seeing that the metrics corresponding to the line-elements defined by (16) are all the same, is by invoking Birkoff's Theorem [11]. This theorem establishes, with mathematical certainty, that the Schwarzschild solution (exterior, interior or both) is the only solution of the spherically symmetric vacuum field equations*.

Claim 5. In [2] the author notes that the scalar curvature of the metric corresponding to (16) is given by

$$f = \frac{12\alpha^2}{C_n^3} = \frac{12\alpha^2}{[(r - r_0)^n + \alpha^n]^{6/n}}$$

and that as $r \to r_0$ there is no curvature singularity. He then concludes that a "black hole" singularity cannot exist.

In fact, as we have just seen, the line-element (16) only corresponds to the exterior Schwarzschild solution, which is a manifold foliated by 2-spheres with radial coordinate $R > \alpha$. The calculation in [2] therefore only proves that the exterior solution has no curvature singularity. This is a well known fact. Writing (16) in its equivalent form (19) and extending

---

*The assumption of staticity is not actually required, hence all spherically symmetric spacetimes satisfying the vacuum field equations are static.

the coordinate R to obtain the *interior* Schwarzschild solution ($0 < R < \alpha$), the scalar curvature is given by

$$f = \frac{12\alpha^2}{R^3},$$

from which it is clear that

$$\lim_{R \to 0} f = \infty.$$

Hence there is a curvature singularity at $R = 0$. Since the vector ∂_R is timelike for $0 < R < \alpha$, the singularity corresponds to a black hole.

4 Conclusions

We have presented a number of simple examples which hopefully elucidate the concepts of coordinate transformation and metric extension in differential geometry. Implications of the concepts were also discussed, with particular focus on a number of the relativistic claims of [1–8]. It was proven that each of these claims was false. The claims appear to arise from a lack of understanding of the notions of coordinate transformation and metric (coordinate) extension. Any conclusions contained in [1–8] that are based on such claims should therefore be considered as unproven. In particular, the claim that the black hole "is not consistent at all with general relativity" is completely false.

General relativity is a difficult topic, which is grounded in advanced mathematics (indeed, Einstein himself is quoted as saying something along the lines of "Ever since the mathematicians took hold of relativity, I no longer understand it myself!"). A sound understanding of differential geometry is a prerequisite for understanding the theory in its modern form. Thus to paraphrase Lao Tzu [12] — beware of the half-enlightened master.

Postscript

The article by Stephen J. Crothers in the current issue [13] provides a good illustration of the problems discussed above. For example, in his first "counter-example" he considers a metric which is easily seen to be the Schwarzschild metric written in terms of an 'inverted' radial coordinate. Using x to denote the inverted radial coordinate (denoted by r in [13]), and R to denote the usual Schwarzschild radius, the transformation is $R = 2m - x$. In particular, $R = 0$ corresponds to $x = 2m$, and $R = 2m$ corresponds to $x = 0$. It is thus not surprising that the coordinate singualrity is at $x = 0$ and the point singularity is at $x = 2m$. The other counter-examples in [13] can be dismissed through similar arguments.

References

1. Crothers S. J. On the geometry of the general solution for the vacuum field of the point-mass. *Progress in Physics*, 2005, v. 2, 3–14.

2. Crothers S. J. On the general solution to Einstein's vacuum field and its implications for relativistic degeneracy. *Progress in Physics*, 2005, v. 1, 68–73.

3. Crothers S. J. On the ramifications of the Schwarzschild space-time metric. *Progress in Physics*, 2005, v. 1, 77–80.

4. Crothers S. J. On the generalisation of Kepler's 3rd Law for the vacuum field of the point-mass. *Progress in Physics*, 2005, v. 2, 70–75.

5. Crothers S. J. On the vacuum field of a sphere of incompressible fluid. *Progress in Physics*, 2005, v. 2, 76–81.

6. Crothers S. J. On the general solution to Einstein's vacuum field for the point-mass when $\lambda \neq 0$ and its implications for relativistic cosmology. *Progress in Physics*, 2005, v. 3, 8–18.

7. Crothers S. J. Introducing distance and measurement in general relativity: changes for the standard tests and the cosmological large scale. *Progress in Physics*, 2005, v. 3, 41–47.

8. Crothers S. J. A short discussion of relativistic geometry. *Bulletin of Pure and Applied Sciences*, 2005, v. 3(2), 267–273.

9. Schwarzschild K. Über das Gravitationsfeld eines Massenpunktes nach der Einsteinschen Theorie. *Sitzungsberichte der Königlich Preussischen Akademie der Wissenschaften*, 1916, 189–196 (published in English as: Schwarzschild K. On the gravitational field of a point mass according to Einstein's theory. *The Abraham Zelmanov Journal*, 2008, vol. 1, 10–19).

10. Hilbert, D. *Nachr. Ges. Wiss. Gottingen, Math. Phys. Kl.*, 1917, v. 53.

11. Birkoff, G.D. *Relativity and Modern Physics*, Cambridge, MA: Harvard University Press.

12. Lao Tzu. Tao Te Ching. Penguin, 1963.

13. Crothers S.J. The Kruskal-Szekeres "extension": Counter-examples *Progress in Physics*, 2010, v. 1, 3–7.

––––––––––––––––––––

On Crothers' Assessment of the Kruskal-Szekeres "Extension"

Ulrich E. Bruchholz

Wurzen, Germany. E-mail: Ulrich.Bruchholz@t-online.de; http://www.bruchholz-acoustics.de

I agree with Crothers in it that any introduction of Kruskal-Szekeres coordinates is unnecessary. The solution of problems from so-called Schwarzschild solutions appears amazingly simpler than discussed in Crothers' paper.

S. J. Crothers [1] discusses the introduction of Kruskal-Szekeres coordinates, which pursue the target to avoid certain forms of singularity and the change of signature. Crothers argues that this measure is off target. — Let me note following:

1. The Kruskal-Szekeres coordinates as quoted with the equations before Eq. (4) of [1] mingle time and length. That is physically self-defeating. Moreover, any real coordinate transformation does not change the situation with the original coordinates.

2. The solution according to Eq. (1) of [1] is physically difficult for the coordinate singularity. We should take notice of this fact instead of doing inept tries, see item 1.

3. The general central symmetric and time-independent solution of $R_{\mu\nu} = 0$ is the first part of Schwarzschild's actual solution

$$ds^2 = \left(1 - \frac{\alpha}{R}\right)dt^2 - \left(1 - \frac{\alpha}{R}\right)^{-1}dR^2 -$$
$$- R^2(d\theta^2 + \sin^2\theta\, d\varphi^2),$$

in which R is an *arbitrary* function of r within the limit that metrics must be asymptotically Minkowski spacetime, i.e. $R \Rightarrow r$ for great r. α is an integration constant related to the mass,

$$\alpha = \frac{\kappa m}{4\pi}.$$

This solution is based on "virtual" coordinate transformation, which is possible for the degrees of freedom from Bianchi identities.

4. Above solution implies also an isotropic solution without singularity at the event horizon

$$ds^2 = \left(\frac{r - r_g}{r + r_g}\right)^2 dt^2 -$$
$$-\left(1 + \frac{r_g}{r}\right)^4 \left(dr^2 + r^2(d\theta^2 + \sin^2\theta\, d\varphi^2)\right)$$

with

$$r_g = \frac{\alpha}{4} = \frac{\kappa m}{16\pi}.$$

The event horizon (at $r = r_g$) turns up to be a geometric boundary with $g = 0$.

5. Any change of signature is physically irrelevant, because areas with different signature (from normal, according to observer's coordinates) are not locally imaged. Therefore, any singularity in such an area is absolutely irrelevant.

6. It is deduced from the geometric theory of fields [2] that particles do not follow any analytic solution, no matter whether obtained from General Relativity or any quantum theory. One can specify the field only numerically. It has to do with chaos. — It was interesting to see if the discussed analytic solutions are possible at all, or if macroscopic solutions are decided by chaos too.

References

1. Crothers S. J. The Kruskal-Szekeres "extension": counter-examples. *Progress in Physics*, 2010, v. 1, 3–7.

2. Bruchholz U. E. Key notes on a geometric theory of fields. *Progress in Physics*, 2009, v. 2, 107–113.

LETTERS TO PROGRESS IN PHYSICS

An Einstein-Cartan Fine Structure Constant Definition

Robert A. Stone Jr

1313 Connecticut Ave, Bridgeport, CT 06607 (USA). E-mail: robert.a.stone.jr@gmail.com

The fine structure constant definition given in Stone R. A. Jr. *Progress in Physics*, 2010, v.1, 11–13 [1] is compared to an Einstein-Cartan fine structure constant definition. It is shown that the Einstein-Cartan definition produces the correct pure theory value, just not the measure value. To produce the measured value, the pure theory Einstein-Cartan fine structure constant requires only the new variables and spin coupling of the fine structure constant definition in [1].

1 Introduction

Stone in [1] gives Nature's coupling constants, the fine structure constant and the weak angle, and a single mass formula for the W, the proton, the electron and electron generations all as functions of $(4\pi)^n$.

If these 4π coupling constant definitions are correct, then if a literature search found another theoretical definition, one would expect a similar form for the two definitions.

In [1] the fine structure constant (FSC), designated as α_{cs} (α charge to spin), is defined as $\pi\varsigma(4\pi\varrho)^{-2}/(2\sqrt{2})$ with $\varrho = \alpha_{cs}\,\alpha_{sg(1)}\,m_p/(m_e\pi) = 0.959973785$ where $\alpha_{sg(1)} = 2\sqrt{2}/4\pi$ and $\varsigma = (4\pi\varrho)^3\,m_e/m_p = 0.956090324$.

2 An Einstein-Cartan model

Many Einstein-Cartan models are scale independent models where the force magnitude (scale) is related to some internal variable like a length, e.g. l_0. The pure theory scale is l_0 while potential deviation from the pure theory is represented by l. The Einstein-Cartan model of Horie's [2] is such a model.

Equation (4.2) in Horie's paper [2] gives the Einstein-Cartan theoretical definition for the FSC as

$$\alpha_{cs} = \frac{1}{64\pi}\frac{l_0^2}{l^2},\tag{1}$$

where l assumed to be less than and approximately l_0.

When $l = l_0$, (1) gives the FSC value of approximately 4.97×10^{-3}. To match the measured FSC value requires l_0/l to equal about 1.2113 ($l_0^2/l^2 \simeq 1.4672$), a value for l not approximately l_0.

The 4π definition of the fine structure coupling constant is given in [1] as $\alpha_{cs} = \pi\varsigma(4\pi\varrho)^{-2}/(2\sqrt{2})$ and the charged particle weak angle coupling constant as $\alpha_{sg} = 2\sqrt{2}\,(4\pi\varrho)^{-1}$.

Noting that the $\sqrt{2}$ appears with both spin couplings suggests that the origin of the $\sqrt{2}$ is related to the coupling of the other force in the coupling constant to spin.

From the underlying approach, this is true. However the $\sqrt{2}$ is mathematically on the side of the other force because the coupling of spin to charge (and g) is larger than expected by present approaches.

Thus in order to reflect the underlying approach of the 4π definitions, α_{cs} is better written as

$$\alpha_{cs} = \frac{1}{16\pi}\frac{1}{4}\;\;\sqrt{2}\;\;\frac{1}{\varrho^2}\;\;\varsigma.\tag{2}$$

Rewriting Horie's equation (1) in a similar form yields

$$\alpha_{cs} = \frac{1}{16\pi}\frac{1}{4}\;\;1\;\;\frac{1}{(l/l_0)^2}\;\;1.\tag{3}$$

Where as Horie's pure theory Einstein-Cartan model assumes 1 for the coupling, the underlying source coupling value in α_{cs} (and α_{sg}) is larger by $\sqrt{2}$.

Where as Horie's pure theory Einstein-Cartan model can not give a value for l/l_0 for α_{cs}, the definition in [1] gives the value as ϱ. Note that using the correct spin coupling ($\sqrt{2}$) now results in $l \lesseqgtr l_0$ as expected.

Lastly, Horie's pure theory Einstein-Cartan model simply lacks an additional factor ς that appears on the charge side of the coupling constants α_{cs} and α_{cg} [1].

Thus, as a pure theory model, Horie's result is correct. To produce the measured FSC value, Horie's pure theory model only needs the correct spin coupling ($\sqrt{2}$), the correct l/l_0 value (ϱ) and the ς adjustment that come from the approach that produced the 4π definition of Nature's constants.

3 Summary

In [1], several 4π coupling constant definitions were given including the fine structure constant.

It is shown that the 4π fine structure constant definition of [1] is in keeping with Horie's complex connection pure theory Einstein-Cartan fine structure constant definition [2].

Thus not only does the 4π definitions in [1] produce the two weak angle values as experimentally observed, the fine structure constant definition has the three missing constants required by a pure theory Einstein-Cartan fine structure constant definition to produce the measured value.

References

1. Stone R. A. Jr. Is fundamental particle mass 4π quantized? *Progress in Physics*, 2010, v. 1, 11–13.

2. Horie K. Geometric interpretation of electromagnetism in a gravitational theory with space-time torsion. arXiv: hep-th/9409018.

LETTERS TO PROGRESS IN PHYSICS

Valery N. Smirnov (1939–2009) and His Detector

Victor A. Panchelyuga

Research Institute of Hypercomplex Systems in Geometry and Physics, Friazino, Russia
Institute of Theoretical and Experimental Biophysics, Russian Academy of Sscience, Pushchino, Russia
E-mail: panvic333@yahoo.com

Dr. Valery N. Smirnov who passed away recently, was an experimental physicist working on accelerator physics. Despite this fact, the main achievement of his scientific creation was the detector for measurement of perturbations in gravitational fields. This detector, having originally construction suggested by Smirnov, was launched at Moscow Engineer Physical Institute, Russia. Valery N. Smirnov continued his observations with the detector until his last days. We therefore refer to this device as Smirnov's detector.

Dr. Valery N. Smirnov. Pictured in the last decade.

Valery N. Smirnov was born in October 6, 1939, in Magadan, Russia, where his parents worked as reporters. In 1945, his family returned to Moscow, where he lived all his life.

After high school, in 1958, he was employed at the Institute of Radio Engineering. In 1960 he entered to Moscow Engineer Physical Institute, where was gaduated in 1966. Then he returned to the Institute of Radio Engineering. In 1975 he was employed at Kurchatov Institute of Atomic Energy, as an experimental physicist in the field of accelerator physics. Smirnov designed "Fakel" (tourch), the linear accelerator, and also numerous other accelerators for Kurchatov Institute. In 1983, he awarded Kurchatov Prize for the best engineering work done in the field. As one of the stuff of Kurchatov Institute, Smirnov produced some studies at Chernobyl Nuclear

Power Station, in 1987 and 1989, after the catastroph. He was gratituded by the Government for this job.

Some persons work in order only to earn money for live. In contrast, Smirnov spent all his life for scientific studies. He found the main task of his scientific creation when read the papers, published by Prof. Nikolai A. Kozyrev, the famous astronomer and physicist of Pulkovo Observatory, Leningrad. Kozyrev pointed out that, in his regular experiments with gyposcopes, the devices experienced small fluctuations at the moments connected to the dynamics of celestial bodies, e.g. the planets. This effect remained unexplained.

Smirnov supposed that the source of this effect is hidden in the imperfect suspension of Kozyrev's gyroscope. Thus, every period of revolution may be broken due to an external influence. In aim to study his supposition, Smirnov designed a special device, containing a gyroscope which was rotating in a special regime of braking (different braking regimes were ruled by special control electronics). Experiments conducted by him confirmed his initially supposition: the device showed steady sensitivity to the specific moments of celestial bodies dynamics, exact according to Kozyrev.

During the years and until his last days, Smirnov conducted regular observations with the device. He also improved its contruction, making it more sensitive. The experimental results and the technical descriptions were presented by him in the publication [1]. Complete review of the experiments will be submitted to *Progress in Physics* later.

Dr. Valery N. Smirnov passed away in November 4, 2009, being full of new plans for research and creative ideas. In our memory he is still live amongst us, with his device we refer to as Smirnov's detector.

References

1. Smirnov V. N., Egorov N. V., Schedrin I. S. A new detector for perturbations in gravitational field. *Progress in physics*, 2008, v. 2, 129–133.

NEW PARADIGMS IN PHYSICS

A New Paradigm: From Quantum Fields to the Planck Vacuum

William C. Daywitt

National Institute for Standards and Technology (retired), Boulder, Colorado, USA E-mail: wcdaywitt@earthlink.net

The current paradigm in fundamental physics assumes that Newton's gravitational constant G, Planck's (reduced) constant $\hbar$, and the fine structure constant α are primary constants — i.e., these constants are associated with something basic in nature and are thus not reducible to something more fundamental. This assumption leads, for example, to the conclusion [1] that quantum fields are the fundamental building blocks out of which the visible universe is constructed.

The Planck vacuum (PV) theory [2] derives the three constants

$$G = \frac{e_*^2}{m_*^2}, \qquad (1)$$

$$\hbar = \frac{e_*^2}{c}, \qquad (2)$$

$$\alpha = \frac{e^2}{e_*^2}, \qquad (3)$$

where e_* is the bare electronic charge, m_* is the Planck mass, c is the speed of light, and e is the experimentally observed electronic charge. In effect, then, a new paradigm* has emerged where the PV is the source of the visible universe and its properties.

What follows is a brief survey of some equations that demonstrate how the current and new paradigms are related. The details leading to the equations are unimportant here and are left to the references. What is important is how the current primary constants on the left side of (1)–(3) are replaced by the new primary constants e_* and m_* on the right and in the equations to follow.

The Compton relation [3, p.433]

$$\lambda_c = \frac{h}{mc} \qquad \text{or} \qquad r_c mc = \hbar \qquad (4)$$

associates a Compton wavelength λ_c (or a Compton radius $r_c = \lambda_c/2\pi$) with the particle mass m, while the de Broglie relation [3, p.81]

$$p = \frac{\hbar}{r_d} \qquad (5)$$

relates the particle's relativistic momentum ($p = m\gamma v$) to its de Broglie radius $r_d = r_c/\beta\gamma$, where $\beta = v/c$ and $\gamma = 1/\sqrt{1-\beta^2}$. The PV theory explains these relations [2] [4] in terms of the magnitudes, mc^2/r and e_*^2/r^2, of the two distortion forces the particle exerts on the PV, the radius at which

these two forces are equal being the Compton radius r_c. The calculations lead to the string of Compton relations

$$r_* m_* c = r_c mc = e_*^2/c, \qquad (6)$$

where r_c is the Compton radius of any of the elementary particles, m is the particle mass, and r_* and m_* are the Compton radius and mass of the individual Planck particles making up the negative-energy PV state.

The Compton relations (6) yield the free-space permittivities [2]

$$\epsilon = \frac{1}{\mu} = \frac{e_*^2}{r_* m_* c^2} = 1, \qquad (7)$$

while the static electric force between two charges e becomes

$$F_{el} = \frac{e^2}{r^2} = \alpha \frac{e_*^2}{r^2} \qquad (8)$$

showing the fine structure constant α to be closely related to the PV polarizability.

The Heisenberg uncertainty relations

$$\Delta p \cdot \Delta q \geqslant \frac{\hbar}{2} = \frac{e_*^2/c}{2} \qquad (9)$$

where p and q correspond to any two canonically conjugate operators, remain a wave-particle-duality mystery in the current paradigm. The PV theory explains these relations in the following manner: the so-called free particle interacts continually with the invisible PV continuum; as this continuum, like any continuum, can support wavelike disturbances, the reaction of the PV to the particle perturbations produces a wavelike reaction in the particle; then (9), which is currently ascribed to the particle, is actually a straightforward mathematical property of the perturbed continuum [3, p.105].

The gravitational equations of Newton and Einstein transform from the current paradigm to the new paradigm in the following way [5]:

$$F_{gr} = -\frac{mMG}{r^2} = \frac{(-mc^2/r)(-Mc^2/r)}{-m_* c^2/r_*} \qquad (10)$$

and

$$G_{\mu\nu} = \frac{8\pi G}{c^4} T_{\mu\nu} \quad \rightarrow \quad \frac{G_{\mu\nu}/6}{1/r_*^2} = \frac{T_{\mu\nu}}{\rho_* c^2}, \qquad (11)$$

---

*Merriam-Webster Online Dictionary, 2009. Paradigm: a philosophical and theoretical framework of a scientific school or discipline within which theories, laws, and generalizations and the experiments performed in support of them are formulated.

where $c^4/G \, (= m_* c^2 / r_*)$ and $1/r_*^2$ are the ultimate curvature force and Gaussian curvature sustainable by the PV, and ρ_* $(= m_*/(4\pi r_*^3/3))$ is the Planck-particle mass density of the PV.

Finally, the quantum vacuum consists of an electromagnetic (photon) component and a massive-particle ($k_c = 1/r_c$) component [4]. The energy densities of the two transform as

$$\frac{c\hbar}{2\pi^2} \int k^3 \, dk \quad \rightarrow \quad \frac{1}{8} \frac{e_*^2/r_*}{r_*^3} \tag{12}$$

and

$$\frac{c\hbar}{4\pi^2} \int k^2 \left(k_c^2 + k^2\right)^{1/2} dk \quad \rightarrow \quad \frac{1}{16} \frac{e_*^2/r_*}{r_*^3} \tag{13}$$

from the current to the new paradigm respectively.

References

1. Weinberg S. The search for unity: notes for a history of quantum field theory. *Daedalus 106*, 1977, 17.

2. Daywitt W.C. The Planck vacuum. *Progress in Physics*, 2009, v. 1, 20.

3. Leighton R.B. Principles of modern physics. McGraw-Hill Book Co., NY, Toronto, London, 1959.

4. Daywitt W.C. The source of the quantum vacuum. *Progress in Physics*, 2009, v. 1, 27.

5. Daywitt W.C. Limits to the validity of the Einstein field equations and General Relativity from the viewpoint of the negative-energy Planck vacuum state. *Progress in Physics*, 2009, v. 3, 27.

New Ideas for the Extra Dimensions and for Deriving the Basic Laws of Physics

Riadh H. Al Rabeh

College of Engineering, University of Basra, Iraq
Present address: Lydgate Close, Manningtree, Essex, UK. E-mail: alrabeh_rh@yahoo.com

As geometry is constructed from points and their separating distances, physics may be similarly constructed using identical material points and their separating distances with the additional requirement that all points have infinitesimal masses and move all the time at the speed of light. Pairs of such points can get locked together in circles to make doublet particles that can have any speed from zero to that of light, at which point the doublet disintegrates. Using this construct together with the rich mathematical properties of a 3D space, a mechanical definition of time, and simple symmetry rule for displacement, it is possible to derive many of the fundamental laws of physics such as the inverse square laws of gravitation and static electricity, many of the relativistic and quantum mechanical results such as the mass-energy conversion of Einstein and the quantized energy levels of Planck and Bohr. In addition, a better understanding of some illusive terms like inertia and force becomes possible. No arbitrary constants are needed in the process. Extra dimensions (variables that are not a distance) are created as a result of this setup — but they are all found to be discrete. Mass, charge, spin, and time are some notable examples.

1 Introduction

We use common ideas, simple constructs and simple mathematics to shed light on the origin of the grand laws of physics that have hitherto remained untied together. That this is possible was a big astonishment to the author having spent years of search to achieve the same using fields and waves excluding discrete masses. We first postulate the existence of a 3D Euclidian space containing a large number of material points (point masses). The distance between the points is to be a continuous function, which goes well with our intuition, as we never observed material objects jump without passing through all joining points in between. We then realize that this postulate endows the space with an enormously rich structure [1] due to the fact that the distance becomes analytic and infinitely differentiable. The masses must be infinitesimal in order to move continuously at the speed of light without violating Einstein's and other results in this regard. We are tacitly assuming that no space can be defined without material points. As to what is a material point is left undefined.

Material points can acquire other properties like electric charge etc which we will come to meet later. When the separating distance between two material points of suitable attributes is small, they trap each other to make a doublet particle. This combined structure can have any speed — from zero to that of light, in which case it disintegrates into two point particles. Bound states of equal masses do exist in physics as in the case of the exotic particle "positronium" [2]. The normal mass of a material body, composed of a large number of such doublet particles, is simply the total number of doublets and hence it is discrete. We note that an immediate benefit of this setup is a simple mechanism for converting

mass into energy and visa versa if we associate energy flux with point particle flux. In fact it amounts to an ultimate unification of the of mass and energy concepts. We also note that a space with continuously moving material points may be an alternative and fairly convincing way of interpreting Einstein's space time continuum ideas. This becomes even more apparent as we arrive at the same relativistic results using the simple doublet structure.

To reach to the more fundamental laws of physics, we shall put a simple mechanical definition for time and a symmetry rule that governs the displacement of point particles (and doublets as a result) in space. We shall consider such grand ideas with the simplicity they deserve, as Einstein have suggested in more than one occasion — what is needed is simple physical interpretations rather than complicated mathematical descriptions [3]. The transformation between point and doublet particles may be looked at as a process of equilibrium or a continuous forward and backward transformation — an evaporation condensation process if you like, and one that can be observed on larger and larger scales in nature. The trapping and escape of photons in matter(radiation), of electrons out and into the nucleus of different materials, of whole molecules from the surfaces of any liquid and the trapping and escape of large masses in volcano eruptions on planets and stars are few such examples.

Doublet particles are to be taken to represent the simplest form of condensed matter, whereas singlet particles are to represent energy flux. Singlet particles may also combine (along their flight path) in any number and remain as different energy fluxes as long as they do not take the form of circularly bound doublets. Doublets can also come together(condense) and combine to form massive particles. In [4] the doublet

structure is examined further and it is shown that the geometrical rules for the combination(packing) of doublets seem to fit well measured values of different forms of condensed matter.

2 Theory

2.1 Space and Time

Intuitively, it is not possible to define space when it is devoid of matter [6, 7]. Our starting point therefore is to assume the existence of material points with infinitesimal masses that move all the time at the characteristic speed of the space — the speed of light c. The numerical value of $c = 2.99 \times 10^8$ comes from our arbitrary choice for the units of distance and of time. A 3D Euclidean space may(at one instance) be structured out of *all* such material points and the distances that separate them. This space is continuous to go with our intuition — that is to say when material points move, they do not jump, but pass by all the joining points along the path of motion as given earlier.

We then note that time itself can not be defined in a space devoid of motion. Just imagine one is at night in a desert with nothing moving — no moon, no stars and not even a heart beat. In this setup there is no way to see time flowing. So we are led to say that time must be connected with the motion of material points. To get a sense of time we need an observer point and a moving point, since if we move along a straight line without being able to observe anything else moving, we will not be able to see time flowing either. The problem now is that any observation over a distance must rely on light propagation and will introduce the well known complication of a finite value of c.

A simple case however, where this is not a problem is the case of two material points moving on a circle in a doublet formation and the observer point is sitting on the path of this doublet. We can then define time as the *number* of visits of the doublet members. This number has all the characteristics of time since it is an *ever increasing* variable (pointing in one direction- hence the arrow of time expression) and it is *symmetric* in the sense that the zero of count (zero of time) can be placed anywhere. It is, however, *discrete* according to this picture. It is also an independent variable in the sense that it can have any integral value for any value of the other three spatial coordinates. This is well in tune with our intuition of the variable "time", as we always rely in our time measurements on some sort of oscillation and count the number of such oscillations to measure time. If light can be sent to come back in a straight line to a distant point, the distance to that point can be judged from the knowledge of the period taken as given by the number of rotations(visits) of our local doublet members and the assumption that the characteristic speed c is constant all the time. Time can thus be looked at as a measure of the distance travelled by any material object to the distance travelled by a material point as given by the circumference and the number of rotations of our local doublet.

A mathematical fact is that if a particle in an *isolated* system follows one path exactly more than once, it will continue to do so for ever. We can convince ourselves with this if we remembered that the number of points along an even a *differential line segment* of such path is more than enough to fix any number of *constants* in the solution of the differential equation of motion — thus ensuring that the path is fixed and unchanged in subsequent visits. This conclusion is possible only if the line of motion is continuous and analytic (infinitely differentiable) which is the reason for our original assumption. The emergence of such eternal stability can prove useful in explaining the eternal stability of some of the elementary particles like the photon and the electron when in isolation.

We also note that the rich mathematical properties of the path of motion in space lead to new variables or dimensions that are independent of the original three spatial dimensions. Any extra dimension derivable this way appears to be not a distance and only discrete however. We notice also that the creation of such extra variables comes out of a process of a closure or folding in the path of motion and turning it into a multi-valued variable in which every point is described not only by its three space coordinates, but also by other numbers derived from the multiplicity at that space point. We mention angle measurement as one more example of such multiplicity.

Since the velocity of a moving point is a mathematical derivative with respect to time, and as time is represented by a number, we conclude that the process of determining the velocity and acceleration, (or the process of going from static to kinematic and dynamic), is a process of comparison (ratio) of the motion of a larger system with that of a simpler and standard one like a doublet. In other words, the motion of the simple doublet is effectively being used as a yardstick to gauge the velocity and acceleration of more complicated systems. This definition of time breaks down of course for periods that are smaller than one unit of measurement (determined by the smallest possible doublet) whatever that may be. Since time is discrete, velocity, acceleration, force, momentum and any similarly related variable are all discrete. This will later lead to the Heisenberg uncertainty principle.

2.2 Laws of motion — action and reaction

We put here a simple rule for the displacement of material points that goes with the state of natural symmetry possessed by two material points (in isolation) in the form; "*The displacement of any material point must be accompanied by the displacement of another point by the same amount in an opposite direction*". For two isolated points it might be argued that it does not matter if one point made the entire move and the other stays a foot, as the outcome would be the same. This is clearly not the case, since in reality we will have many more points and our rule should apply to every pair of them.

Since mass is composed of many material points of the

same value, and motion is to be discrete, the displacement of ten points one distance can be compensated for by the displacement of one point ten times that distance in the opposite direction, and our equivalent statement of action and reaction becomes; "*The sum of mass times displacement is zero at any point and along any direction*". In other words, the center of mass of an isolated system of points never moves. We can also see that as time is now just a number, differentiation of the displacement with respect to time gives; "*The sum of mass times velocity (linear momentum) is zero at any point and along any direction*", and differentiating again gives; "*The sum of mass times acceleration (force) is zero at any point and along any direction*". Thus we see that it is possible to recover both the second and third Laws of motion of Newton from a simple rule of displacement. We take this to be a strong support of the correctness of this postulate as a rule of displacement.

Our rule of displacement, which we shall call the "*balanced displacement*" (BD) rule, may be considered as the equivalent of Newton's first law of motion since it tells that points can not change their state of motion independently... if a material point moves, another must also move by the same amount and in the opposite direction, and things can then stay like this forever as long as the BD rule is true. The BD rule also provides a neat explanation of the source of inertia of massive bodies. It is simply a balanced displacement requirement. As if the world is sitting on a knife edge and moving anything must be done symmetrically to keep the balance .

Displacement can be resolved into three directions, the first along the separation distance between two moving points plus two components normal to this direction. The two normal components combine to define the spin direction of the doublet. The doublet particle can have left or right hand spin property. Such spin, once initiated, will continue unchanged since the BD rule works correctly all the time– that is until an interaction occurs with another group of points.

The displacement along a radial line separating two moving points can have two directions; to the inward and to the outward directions. This produces the attraction and repulsion type effects. The probability for material points to take any one of six possible motions along three perpendicular directions is presumably equal, this provides a plausible reason for the existence of antiparticles, and the fact that antiparticles can be anti in all their attributes and have the same mass. Thus we have by now two types of coupling constants and two different spins — all new variables and all discrete, since they can only take the values ($+/-$ a constant) representing each of the two opposing directions. Larger values of charge, spin etc must now be in multiples of this constant value.

An interesting conclusion of all this is that the sum of displacements of all material points in the universe is zero at any time and hence the center of mass in the universe never moves. It is also not hard to see that as a result of the BD rule being applicable to every two points separated by a distance,

there is a universal entanglement situation of every single point mass in the universe. If we now imagine doing a back play of all the events of displacements that has occurred since the start of time, we may reach the original point start(the big bang point!). The clear impossibility of such undoing, should tell us that it is impossible to go back in time. We could also say here that time must have started with the first motion and will only stop when everything else stops moving.

As pointed above, the BD rule can give us a neat explanation of inertia which some believed it to be a property of matter and others to be due to the effect of distant masses (the Mach principle). In the present setup we see that it is a result of the symmetry of displacement — i.e. a property of space and matter together with distant and near masses all involved. One interesting example to make the picture clear is the case of the rotation of a thin disc in isolation. Every two diametrically opposed points of the disc follow happily the BD rule and, as such, constitute a self contended system that will, if not disturbed, remain as it is for ever. If we move the disc along the axis of rotation, we must create a movement of other masses equivalent to that of the disc in the opposite direction — as in propelling it with the gases of a rocket for example. The rotational motion of the disc remains unaffected in this case. If we now try to move the disk on a curved path, we need to provide an equivalent opposite motion to the curving and rotating material points of the disc in its new complex motion, and it is this that shows as the gyroscopic effect.

2.3 The inverse square laws

The interaction between two isolated material points can only be a function of the separation distance — because of isolation. Such interaction, as a result, becomes homogenous in the coordinates — that is to say there can be no preference of one coordinate to the other. For such cases we quote few lines from [8] "... the multiplication of a Lagrangian by a constant does not effect the equation of motion. This fact makes it possible, in a number of important cases, some useful inferences concerning the properties of the motion without the necessity of actually integrating the equation of motion. Such cases include those where the potential energy is a homogenous function of the coordinates, i.e. satisfying the condition $U(ar^1, ar^2, \ldots, ar^n) = a^k U(r^1, r^2, \ldots r^n)$, where a is a scaling constant, k is the order of the potential function and n is the number of coordinates". This then lead the reference to the following conclusion "If the potential energy of the system is a homogenous function of degree k in the (Cartesian) coordinates, the equation of motion permits a series of geometrically similar paths and the times of the motion between corresponding points are in the ratio $t'/t = (l'/l)^{1-k/2}$, where l'/l is the ratio of the linear dimensions of the two paths". To follow our notations, put r for l', t' for t to get $r = Kt^{2/(2-k)}$, where $K = l'/(t')^{2/3}$ is a coupling constant and is made up of the values of the radius and the time of one rotation "of a

standard doublet in our case" and r is the separation distance between the two points.

There are only two values for k [8] that result in a bound motion. These are $k = (-1, 2)$. The first gives $r = Kt^{2/3}$ and the second leads to a spring type force or what is known as a "space oscillator". The space oscillator case can be shown to be not a new case and occurs in a field of inverse square when the displacement is small, the region is small with a large number of interacting particles [8]. The first case (the two third power formula) is one form of the famous Kepler third law of motion and if differentiated twice gives the inverse square law $d^2r/dt^2 = (-2/9)K/r^2$ in confirmation of our starting assumption. In [5] this form of the inverse square law (involving time only) was used to predict the motion of many point particles with a notable gain on computing time. The quantity $(-2/9)K$ is the coupling constant of the interaction which takes the value of the universal gravitational constant $K_g = (-2/9)K = G$ for gravity forces or the Coulomb coupling constant $K_e = 1/4\pi\epsilon_0$ for electrostatic forces. The value of G is therefore calculable(in principle) from the dimensions of the doublet used in the dynamic scaling of the problem — when this is known.

The values of the coupling constant for the gravitation and electrostatic forces come from our arbitrary definitions of the units of mass and charge. By now we had four constants; the speed of light c, the Planck's constant h, the gravitational constant G and the permittivity of free space ϵ_0. Our arbitrary physical units from which these are derived are the meter, the second, the kilogram and the Coulomb.

When we have more than two material points, vector superposition of forces, velocities and displacements must be used, with the force (= acceleration since we have equal mass) for each pair calculated separately then added for the lot. For N material points, there are $N - 1$ interacting pairs of points as we exclude the interaction of a point with itself. If N is large, $N - 1$ can be replaced with N. For the case of a large collection of points that are effectively *sitting at the same point*, the center of mass of any such body obeys the same rules of motion given above, since mathematically the two are equivalent. The final interaction force is a resultant of the interaction of all pairs in each collection and will thus be a multiple of the total number of interacting pairs, or equivalently by the product of the masses of any two interacting groups having the same center of mass. This reproduces Newton's law for gravitational interaction and the Coulomb charge interaction and the product of the two masses/charges will appear in the coupling constant.

2.4 The size of a doublet

Take the case of pairs of points with an attractive force locked in doublets to form particles. These doublets will have fixed masses(by assumption) and also fixed spin velocity since the tangential speed of all the material points making a doublet

is fixed at c at all times. It has a fixed radius also since the speed of the constituents are fixed and the coupling constant is also fixed. This creates a particle with fixed and well defined properties. Since the product of the mass of two point masses $2\delta m$, the speed v, and the radius of the doublet r is given by; $2\delta mcr = \delta mcd$, where $d = 2r$; has the units of energy and time (or that of angular momentum) and is the same as that of the Planck's constant, we conclude that a limit must be placed on the smallest allowable doublet, giving $\delta md = \hbar/c$, where $\hbar$ is the reduced Planck constant. This also suggests that (δmd) is a new fundamental physical unit involving mass and distance combined together ($= 3.5177 \times 10^{-43}$ kg m). The numerical value of this constant (or equivalently of the Planck's constant) comes from our arbitrary choice for the unit of mass in addition to that of distance and time used earlier. The quantity $(\delta mcd = \hbar)$ is the angular momentum and also the spin of our doublet particle and it is the unit of measurement of spin. As we have now a lower bound on spin, the orbital momentum of any one or more particles can only be a multiple of this value $\hbar$.

3 Further results

3.1 Heisenberg uncertainty

Since $\delta mvd = \hbar$ can be rewritten as $pd = \hbar$, where $p = \delta mv$ is momentum for one material point, we get (putting Δx for d) the uncertainty principle of Heisenberg usually written as $\Delta p \Delta x = \hbar$. Accordingly, the uncertainty principle refers to the smallest possible angular momentum in nature. As material points always move at c and must have some effective size, it is only natural that there is a minimum radius for the circle of rotation of a doublet. For larger masses, Δx is smaller according to this principle. This need not cause any contradiction. It can be taken in this setup to represent the region inside which the center of mass of all doublets is likely to be located. It becomes smaller as the mass increases, very much like the uncertainty (scatter) in the average of a large number of collected data growing smaller and smaller as the number of data points is larger. Interestingly when this is extended to take the mass of the entire universe, it becomes equivalent to saying that the center of mass of the universe is firmly fixed at a point.

3.2 Einstein mass and energy conversion

As all points making a doublet particle move at the speed of light, the kinetic energy in any doublet must be a function of c^2 and accordingly we can write $E = mc^2$, with m defined as the number of doublets in any larger particle. As we have two point masses in any doublet particle, the more general formula $E = 0.5mv^2$ for kinetic energy is still valid if applied to a single point constituent of a doublet.

3.3 Planck's energy of radiation

For points moving with a speed c around a circle or escaping out of it, we have $c = \omega r$, and $mvr = mc(c/\omega) = h/2\pi$ using the results above. Using $\omega = 2\pi f$, we have $fh = mc^2$ or $E = hf$. This is Planck relation for the energy of radiation of frequency f. Also if we put $p = mc$, we get $E = cp$ for points moving at c. This is the momentum-energy relation for a particle with infinitesimal mass (zero mass in the literature).

3.4 Einstein's relativistic mass

Since points forming a doublet can have two motions — one along a circle with velocity c and one along the center line with velocity v (less than c), the ratio of the kinetic energy of the doublet particle to its total energy must be like $(v/c)^2$, i.e. $E_k/E = (v/c)^2$ since both quantities refer to the same set of masses. Also, as we had $E = mc^2$, we get $E_k^2 = E^2(v^2/c^2) = (E^2/c^2)v^2 = p^2c^2$, which then gives the relation for the total energy as $E^2 = E_0^2 + c^2p^2$. This is the well known relativistic formula for the total energy of a particle in terms of its rest energy and kinetic energy. Here it is derived using the simple doublet structure alone.

3.5 Bohr's energy levels

For a group containing n doublet particles bound together, the single doublet formula given above in the form; $mvd = \hbar$ becomes $m_n vd = n\hbar$ giving the well known Bohr formula for the spin of bound electrons. This formula, despite its success in being very close to experiment, has been criticized as not being based on a model. The doublet model as explained above can be given in support of this very useful, simple and experimentally correct formula. The Bohr formula is normally combined with the centrifugal force expression $F_c = mv^2/r$ and static electric force $F_e = e^2/4\pi\epsilon_0 r^2$ [9] to derive another expression for the energy levels in an atom (and other bound structures) in the form $r_b = (n^2/Z)(4\pi\epsilon_0 h^2/m_e e^2)$, where Z is the total charge of an atom and n is an integer multiple of the spin of the atom. For a single charge atom like hydrogen and lowest spin level corresponding to $n = 1$, we get the Bohr radius $r = r_b = \epsilon_0 h^2/\pi m_e e^2 = 5.2917\times10^{-11}$ m. This formula has been declared wrong, in some of the literature, because it predicts the spin squared as $n^2\hbar^2$ rather $n(n-1)\hbar^2$ as predicted by the wave function theory of quantum mechanics (which has a better agreement with experiment). In the author opinion this is an unfair conclusion, since in any n discrete interactions, a particle does not interact with itself(as given above), leaving only $n(n-1)$ interactions that should replace the n^2 term in the Bohr formula and bring it inline with the corresponding quantum formula.

When a group of doublets form a larger structure, the volume of the new structure will intuitively depend on the number of doublets if these happen to occupy different volumes and not share the same center of rotation. This fits well with the observations about the nucleus of any atom being a func-

tion of the number of the nucleons only. The application of this fact lead to the one third power law for the radius of an atom R in terms of the atomic number A [9] giving $R = r_0 A^{1/3}$; where $r_0 = 1.4\times10^{-15}$ m is an experimental constant. For the nucleus of hydrogen $A = 1$ and r_0 becomes the diameter of a proton. We shall compare this value with that of the electron as calculated in the next section.

3.6 The fine structure constant

When the gravitational and magnetic forces are small, the electrical Coulomb forces $F_e = e^2/4\pi\epsilon_0 r^2$ for electrons are nearly equal to the centrifugal forces $F_c = m_e v^2/r$. In the case $v = c$; $r_e = e^2/4\pi\epsilon_0 m_e c^2 = 2.817\times10^{-15}$, giving the classic radius of the electron. This formula is normally derived in the literature (see [10]) from the potential distribution around the electron due to its charge using energy conservation. The present derivation relies on the doublet model alone. In a doublet however, we have two material points (two masses) contributing to the force which seems to suggest a different value for r_e, giving $r_e = 1.4010\times10^{-15}$ instead. This is probably more plausible as an electron radius, and it is to one's surprise, exactly the same as that for the proton as we found from the hydrogen nucleus in the previous paragraph. If this is correct, it indicates a similarity in the packing in both the electron and the proton despite the large difference in mass. One possible explanation is that this is the result of many doublets occupying the same volume and sharing the same center of rotation — increasing the energy content but not the size. Experimentally, the electron has, so far, behaved as a point charge with no internal details apparent. The proton on the other do have an internal structure.

If in the expressions for the centrifugal and static forces above, the velocity v is less than c, we could calculate v using $mvd = \hbar$ and obtain; $v^2 = e^2/2\epsilon_0 h$, and $v/c = e^2/2\epsilon_0 hc = 1/137.036$. This is the fine structure constant and it now points to the relative velocity of the electron in an orbit to that of light (or that of the material points in a doublet), and can therefore be looked at as a form of a packing factor. If the expression for the doublet radius is divided by the radius of the electron using $mvd_c = \hbar$; we get $d_e/d_c = e^2/4\pi\epsilon_0 \hbar c = 1/137.036$, giving the "fine structure constant" again — now it is a clear packing factor. The quantity d_c is the Compton wavelength of the electron. The ratio of the Compton diameter d_c and the Bohr diameter d_b as found above gives $d_c/d_b = e^2/2\epsilon_0 hc$, that is the fine structure constant again — now representing the next level of particle packing. All these are well known results, but now we have a clearer reasoning for their existence– using expressions derived from the structure of the doublet alone.

3.7 Planck's length scale

The Coulomb force between two point charges is given by $F_e = q^2/4\pi\epsilon_0 r^2$; and the magnetic force between two moving

point charges is given by Ampere's law $F_m = \mu_0 q^2 v^2 / 4\pi r^2$. This can be modified using the identity $c^2 = 1/\epsilon_0 \mu_0$ to give $F_m = (q^2/4\pi\epsilon_0 r^2)(v/c)^2$. Thus if $v = c$ the electric and magnetic forces between two point charges are equal regardless of the value of the separation distance r or charge q, since they cancel out. This is very interesting because it allows the *packing* of doublets without having to overcome the huge electrostatic repulsion forces. This is an *asymptotic freedom* type condition. Such equality is normally broken as the particles go to form a doublet and the electric forces between different doublets become much stronger than the magnetic forces between them, since the speed of the center of a particle doublet is small and the magnetic forces between two doublets, becoming small compared to the electrostatic forces. The situation changes again for a very large collection of moving doublets wherein the magnetic forces become important again because of the shear number of participants (when correctly oriented) rather than the result of very high velocity. We observe this in our daily usage of the magnetic force wherein currents are the result of the orderly movement of a very large number of particles. We note here that Ampere's law is also derivable from the inverse square law when the charges are in motion.

When the electric and the magnetic forces are balanced at the velocity limit c, only gravity and centrifugal forces are left in play. Gravity force is given by $F_g = Gm^2/r^2$ and centrifugal forces by $F_c = mv^2/r$; equating the two and taking into account the Planck formula $mvr = \hbar$ with $v = c$, we obtain $r_p = \sqrt{G\hbar/c^3} = 1.616 \times 10^{-35}$ m. This is the Planck length scale and it gives the smallest possible dimension of any doublet structure. When the separation distance increases beyond this length, the equality changes and the centrifugal force becomes more dominant over gravity as in normal interactions. For large astronomical masses the picture changes again and gravity becomes strong and dominant because of the shear number of participating particles.

3.8   Spin and space quantization

In the presence of more than one doublet contained inside a larger particle, it is not unreasonable to think that space and size limitations allow the compaction of only a limited *integral* number of doublets. This leads to an angle quantization, if doublets shared the same spherical space and to volume quantization if doublets are in separate spheres. Angle quantization leads to the well known quantization of angular momentum and volume quantization gives the nucleus a size that is dependent only on the number of nucleons [9].

4   Final remarks

We have started with identical material points together with the continuous distances separating them and formed a 3D Euclidean space for any point in time. We have assumed that all material points have infinitesimal masses and move all the time at the characteristic speed of space and that of light c. The value of c comes from our arbitrary choice of the ratio of the units of mass and time. We formed doublet particles that have a (center of mass) speed from zero to that of light from every two point particles of suitable attributes. This simple construct produced a simple mechanism for the transformation between mass and energy and when further analyzed, produced the correct relativistic energy and quantum mechanical relations too.

Extra dimensions — all discrete are derived from the properties of the 3D space and the differentiable distances existing between any two material points in it — using the fact that through a single point in space one can have multiple paths of motion. The dimension of time is found to correspond to one such multiplicity– the number of rotations of a standard doublet counted at any one space point.

Velocity, acceleration, force, momentum and any variable dependent on time are found to be discrete as a result of the discreteness of time. This naturally lead to the Heisenberg uncertainty principle and the discrete energy and some other ideas associated with quantum mechanics. The need for discrete description of some of the basic variables of physics can be traced as far back as the Greek philosopher Zeno, who put paradoxes that threatened the rational basis of science till very recently. These were only recently resolved using arguments from calculus in which infinitesimal quantities can integrate to finite quantities in a limiting process. Making time discrete is another neat way to clear Zeno's paradoxes.

The process of timing is found to represent a gauging process of the dynamics of larger systems by those of a simpler system like a doublet. The dimensions of spin etc are created in connection with movements in the directions normal to the line joining any two material points. The inverse square laws are only the result of similarity in the motion of different size systems. The coupling constants in the two opposite directions along the line joining two material points can be ± 1 for repulsion and attraction. To work with individual charges, rather than the resultant outcome, is the square root of this giving; $\sqrt{-1} = \pm i$, to produce the desired effect of repulsion for similar charges and attraction for different charges, and $\sqrt{1} = 1$ to represent attraction only in the case of gravitational forces — since we do not have negative masses in nature as far as we know. Again if we are only concerned with the combined effect of two charges or two masses, then we only need to consider the real quantities ± 1 for the coupling constant for the gravitational and electrostatic forces.

Only four different forces are needed in the present setup. Two of the forces, the magnetic force and the centrifugal force result from the motion of the *sources* of the other two — that is masses and charges. The last two types of forces disappear at zero velocity. As we have identical point masses, the word "force" becomes not essential and can be replaced with just "acceleration". The mathematical ideas of superposition and center of mass are very useful and should be used for all vec-

tor quantities. Four numerical constants appear in the present formulation. At the same time, we have four arbitrary units to fix. Therefore we could assume that the two make two equivalent sets of values or figures.

A transformation from a singlet particle to doublet particle was taken to occur when two material points are locked in a circular motion to form a doublet. In the absence of external factors, this system is self preserving and eternal, since the two rotating points observe the rule of balanced displacement BD all the time and the linear speed is fixed at that of light all time by assumption. Further the coupling constant is fixed and this fixes the radius of the doublet. This made one doublet exactly similar to any other doublet in size, mass, magnitude of spin, but may differ in the other attributes like the sign of spin, sign of charge etc. This allows for creating antiparticles that are identical in mass, but have anti other attributes. The rule of motion in the form of balanced displacement BD is a generator of the three laws of motion of Newton as it leads directly by differentiation to the conservation of momentum and to the usual action reaction for forces. As the measure of time is discrete, all the quantities connected to time are discrete leading naturally to the Heisenberg uncertainty principle and Planck's discrete energy quanta.

The method of using fields rather than particles is not essentially different. Water is composed of particles, but it is describable in terms of a continuous field of pressure. Also a large number of particles with suitable coupling constants can be described using waves, and a group of waves can become concentrated to resemble a particle(the soliton). Particles however, constitute the simples and more natural model for construction of matter. The phenomenon of interference and others have been sighted in the past as arguments against the particle picture. The Newton's corpuscular theory of light, for example, was rejected by simply asking where the corpuscles go at points of zero amplitude in the interference pattern (the dark spots in the interference pattern). These and other objections, have long been shown to be false since interferences happen only at the surfaces of matter and the energy or photons or corpuscles are readily absorbed by matter itself — very much like hitting a body with two bullets from two opposite directions produces no apparent kinetic energy — it is simply transferred to the molecules in each of the two bodies.

Another problem of interest is that when all particles at sight are connected via deterministic laws, as in the present case, one may suspect the disappearance of the *free* will concept. It is a fact that at this moment I can stop writing this article if I wanted to. How a decision like this can be made if the destiny is decided by the fact that all material points in the *world are entangled* together by the balanced displacement rule and the motion of any material point as a result is decided by the fate of every other one. The author believes this problem is closely related to an earlier situation we met above, wherein material points can "decide" whether to have a left handed or right handed spin or some of the other op-

posing attributes. At the point of branching or multiplicity of choices of paths that are equally likely, it takes nearly "zero" energy to change ones mind, and this could be why we feel free to take decisions at a moment where more than one action route is possible. In other words, our free will decisions are mainly done on branching and cross roads situations.

Reference [4], considers further the idea of a doublet particle and the geometry of aggregate of doublets, and show that it is possible to use such building blocks to make more complicated pieces of condensed matter and that there is good evidence that the masses of the elements in the periodic table and those of the elementary particles of physics are well correlated with assumptions given for simple doublets.

The Pauli Exclusion Principle, which is a corner stones of modern physics, has not been considered here. This principle is also derivable from the geometry of space and symmetry.

References

1. Schutz B. Geometrical methods of mathematical physics. Cambridge University Press, 1980.

2. Griffiths D. Introduction to elementary particles. Wiley-VCH Verlag, 2004.

3. Einstein A., Lorentz H.A., Weyl H., Minkowski H. The Principles of Relativity — a collection of papers. Dover, 1952.

4. Al Rabeh R. H. Primes, geometry, and condensed matter. *Progress in Physics*, 2009, v. 3, 54–59.

5. Al Rabeh R. H. Solving multiparticle interactions using the Kepler route. *Progress in Physics*, 2010, v. 1, 19–22.

6. Penrose R. The road to reality. Cape, 2004.

7. Zeh H. D. The physical basis of the direction of time. Springer-Verlag, 2001.

8. Landau L. D., Lifshitz E. M. Mechanics. Pergamon Press, 1960.

9. Alonso M., Finn E. J. University physics, vol. III. Addison-Wesley, 1968.

10. Panofsky W. K. H., Phillips M. Classical electricity and magnetism. Addison-Wesley, 1962.

Major Gravitational Phenomena Explained by the Micro-Quanta Paradigm

Maurizio Michelini

ENEA — Casaccia Research Centre, Rome, Italy. E-mail: m_michelini@alice.it

Some major problems of physics, which remained unsolved within classical and relativistic gravitation theories, are explained adopting the quantum gravity interaction descending from the micro-quanta paradigm. The energy source of the gravitational power P_{gr}, which heats and contracts the Bok's gas globules harbouring the future stars, is identified and defined as well as the gravitational power generated on the solid/fluid planets. Calculations are carried out to make the comparison between P_{gr} predicted for the solar giant planets and the measured infrared radiation power P_{int} coming from the interior. The case of planets with solid crust (Earth, etc.) requires a particular attention due to the threat to stability produced by the thermal dilatation. An analysis is done of the Earth's planetary equilibrium which may be attained eliminating the temperature rise through the migration of hot internal magma across the crust fractured by earthquakes. The temperatures observed up to 420,000 years ago in Antartica through Vostok and Epica ice cores suggest the possibility that the Earth gravitational power P_{gr} may be radiated in space through these temperature cycles (Glacial Eras). In this general frame the Earth's high seismicity and the dynamics of Plate tectonics may find their origin.

1 Introduction

A preceding paper showed that some fundamental forces, i.e. the Gravitational, the relativistic Inertial forces and the Strong force between nucleons and other particles, have the common origin from the interaction of particles with the uniform flux of micro-quanta [1]. The paradigm is characterised by a very high flux of very small quanta (wavelength equal to the Planck's lengh) which collide with particles determining their motion according to the Relativistic Mechanics. Microquanta easily penetrate any large mass, generating the Gravitational and the Strong forces on each particle. Travelling with the speed of light, these quanta explain why all principal interactions travel with this velocity. For these reasons the micro-quanta paradigm represents the underlying reality which supports Special Relativity, a fundameental theory which comes out reinforced by this physical paradigm. The supposed frailty of SR was denounced through several scratching paradoxes, such as the twins paradox, etc. Now the uncertainty on the inertial frames vanishes because the particle kinetic energy depends on the *physical* collisions with the micro-quanta flux. Some new results has been already analised [1], for instance the congruence of the Strong force between nucleons (an explicit expression is given for the first time) with the dynamical structure of the Deuterium nucleus. Here we try to explain some gravitational problems which did not find solution in the frame of the classical and the GR gravitation theories.

2 The quantum gravitational pushing force. Some fundamental concepts

In the last decades some quantum gravitational theories have been proposed, but they found difficulties. All these theories assume, like classical gravitation and General Relativity, that the gravitational mass is the source of the gravitational force, directly or indirectly through the space curvature. The present theory assumes that two masses are not attracted, but are *pushed* towards each other by the gravitational force, because the interaction between two particles is due to collisions with the micro-quanta flux ϕ_0. The cross section $\sigma_i = A_0 m_i$ of any particle is proportional to its inertial mass m_i through the fundamental constant [1] $A_0 \approx 4.7 \times 10^{-11}$ (units SI system). This simple origin of the most general characteristic of particles (i.e. the *mass*) depends on the fact that cross sections are the measure of the particle interaction with the micro-quanta flux filling the Universe. For the sake of simplicity we consider in the following only nucleons since they represent in practice the total mass of any gravitational body. Let's summarise some fundamental concepts. Particles are made of electromagnetic energy supporting a spherical symmetric field which scatters the incident quanta. Due to the very little Compton ratio $K_0 \approx E_0/mc^2 = 3.93 \times 10^{-51}$ between quantum and nucleon rest energy, the colliding quanta follow the optical reflection law. This fact prevents between a pair of particles the beam of quanta directed along the joining line and delimited by the small fractional cross section $\Delta\sigma = K_0 \sigma(\sigma/2\pi r^2)$ centered on each particle. Due to the lack of the quantum beam $\psi(r) = \Delta\sigma\phi_0$, each particle feels a force due to an equal beam $\psi(r)$ colliding on the diametrically opposite $\Delta\sigma$. Since each recoiling quantum leaves the momentum $2E_0/c$, the beam $\psi(r)$ gives rise to the radial pushing force

$$f(r) = \frac{2E_0}{c} \psi(r) = \frac{2E_0}{c} K_0 \sigma \phi_0 \frac{\sigma}{2\pi r^2} , \qquad (1)$$

where $E_0 \cong 5.9 \times 10^{-61}$ is the quantum of energy and $\sigma \cong 7.85 \times 10^{-38}$ is the nucleon cross section. This equation must

be compared with the inertial model of particles [1]

$$mc^2 = \sigma \phi_0 E_0 \tau_0 \qquad (2)$$

where $\tau_0 = 2\lambda_0/c$ is the simultaneous collision time of the micro-quanta, whose wavelength derived from Eq. (2)

$$\lambda_0 = c^3/2A_0\phi_0 E_0 \approx 4 \times 10^{-35} \qquad (3)$$

results very close to the Planck's length. In the time τ_0 a nucleon scatters a high number of quanta

$$\sigma \phi_0 \tau_0 = 1/K_0 \cong 2.54 \times 10^{50} \qquad (4)$$

which press *uniformly* any *free* particle, without changing its state of motion or rest (Principle of Inertia). The force $f(r)$ which pushes the particles towards each other is just the experienced gravitational force. This may be described rearranging Eq. (1) and imposing that the term in brackets equals the gravitational constant G

$$f(r) = \frac{E_0 K_0 \phi_0 A_0^2}{\pi c} \frac{m^2}{r^2} = \frac{Gm^2}{r^2} . \qquad (5)$$

The rihgt side is the newtonian law, but now G cannot in principle be considered constant and uniform throughout the Universe, although within the solar system it is. The newtonian law gives a simple notation of the pushing gravitational force.

It is largely believed that the newtonian gravitation supports the paradigm of the *gravitational* mass. Let's put a question : Who defined this paradigm? In his famous words "Ipotheses non fingo" Newton did not make assumptions on the mechanism of interaction. Many years ago I was impressed by the fact that Newton never declared that masses *generate* the force drawing them. He said that massive bodies show between them an "action at a distance" requiring that the mutual forces are aligned. This feature has been verified by the astronomers of the XIX century.

For some centuries the physicists found natural that the mass of bodies was the source of the gravitational force measured between them, as the experience about the new electrical phenomena taught us. However it has been recognised that the concept of *mass* as a field source is inappropriate, since it does not produce the "action at a distance" condition. Let's notice that this condition is satisfied by the gravitational pushing force.

The history of science taught us that when in the long run physics stagnates, then some old paradigm obstructs the development. In 1939 some difficulties were recognised with the GR theory. For instance it was found that stars of adequate mass undergo an *unlimited* gravitational collapse. The final product of this collapse was named "black hole", but this concept soon appeared *unphysical*. To be short, the enourmous stellar body vanishes but the great gravitational field remains. Contrary to the common conviction, the *unlimited* gravitational collapse is not linked to the GR theory, which is a rigorous logical construction excepting one point: the arbitrary

incorporation in the theory of the (not necessarily *universal*) gravitational constant introducing the empirical gravitational force between the masses.

The unlimited collapse depends in fact on the gravitational mass paradigm, which arbitrarily considers the gravitational force as a *property* of the mass. Recent theoretical studies within the GR mathematical frame [2] esclude the existence of black holes, never really observed. This comes in favour of the new class of observed neutron stars originating from the collapse of large stars with enormous emission of radiation (supernovae).

In the frame of the micro-quanta pushing gravity the mass of particles is not the source of the gravitational force, but is simply a duplicate of the inertial mass. This explains why the Equivalence principle is perfectly verified up to 1 part on 10^{12} by the experiments. As a consequence the large star bodies undergo *limited* collapses, because the increasing gravitational pushing force does not exceed a maximum linked to the micro-quanta flux constants. These collapses originate the neutron stars.

Finally let's recall that in [1] a strong force between nucleons is defined, which is accurate at distances lower than the nuclear diametre. At the usual distances between atomic nuclei, the gravitational force largely exceeds the strong force, giving rise to the concept of *gravitational power*. In the following paragraphs we shall examine the implications of the gravitational power on the evolution of celestial bodies. For instance : i) H_2 galactic gas clouds (Bok globules), ii) dense cold planets, iii) neutron stars. The case of neutron stars will be dealt with subsequently.

3 Gravitational power on the contracting Bok globules

Before considering the solid and liquid aggregation state, let's consider the case of free atoms in gas clouds which interact emitting radiation. The astronomer Bart Bok, observing in 1947 some dark galactic gas globules with low temperature about 8° K and radius around 10^{15} metres, predicted that they might be the forge of the stars. After 43 years J. L. Yun and D. P. Clemens [3] found that practically all Bok globules they observed through CO spectroscopy resulted associated with IR emission, so they could affirm that "almost every Bok globule harbours a young star". They examined a total of 248 globules having an average mass of $11\,M_\odot$ and an average infrared radiation power $P_{rad} \approx 0.5M(L_\odot/M_\odot)$ [4].

At the end of XIX century lord Kelvin and Helmholtz studied a physical mechanism which could explain why the Sun shines from billions years without reducing its luminosity. But they correctly recognised that the gravitational contraction of the outer solar layers cannot explain quantitatively the star luminosity. Only after the advent of Special relativity it was recognised that the solar energy comes from the high temperature fusion of light nuclei through the Einstein's mass-energy equivalence.

To day we don't know which source of energy heats the core of gas globules up to the temperature of star ignition. Of course the gravitational force accelerates the atoms which colliding emit infrared radiation and tend to aggregate towards the cloud centre. The infrared power is generated reducing the atomic kinetic energy, but the average gas temperature, instead of reducing, increases. From which physical source comes the energy which heats the mass and produces radiation? It cannot come from the Einstein's mass-energy equivalence, considering the low gas temperature within the Bok globules.

The problem of correctly defining the source of the gravitational power heating the Bok globules remained unsolved in absence of a theory of the gravitational *interaction* able to specify the rate at which the gravitational waves hit the particles. During the last century the GR theory, which predicts correctly the astronomical observations, didn't solve this problem. The non-existence in GR theory of the standard gravitational waves has been theoretically guessed by several authors and recently shown by A. Loinger [5]. As a matter of fact several groups of physicists are searching for the standard GW's throughout the Universe, but they didn't find a definite result. To define the gravitational power we need to know the collision rate of known waves. It has been shown that each particle of a pair undergoes a pushing force $f(r)$ given by Eq. (1), which recalling Eq. (4) can be written as $f(r) = (2E_0/c\tau_0)(\sigma/2\pi r^2)$, a form expressing clearly the momentum variation in the time τ_0 of the bouncing quantum beam. Assuming that the particle velocity $v \ll c$, which holds up to temperatures of $10^8\,°$K within the star core, this force originates during the time τ_0 of the beam reflection, so the energy released to the particle by the force along the distance of reflection $l_r = c\tau_0$ is $\Delta L \cong f(r) \times l_r = 2E_0(\sigma/2\pi r^2)$. Then the power given up to the particle in the time τ_0 is $p_i = \Delta L/\tau_0 = f(r) \times c$ [1]. Using for the sake of simplicity the newtonian notation (Eq. 5), the gravitational power received by each nucleus of a pair at a distance x_i becomes

$$p_i = Gcm_i^2/x_i^2 \,, \tag{6}$$

where m_i is the mass of nuclei, $x_i = (m_i/\delta)^{1/3}$ is the average distance between nuclei within a body of local density $\delta(r)$ where r is the distance along the body radius. Summing up to all nuclei m_i of a celestial body with radius R, the gravitational power released to the body is defined

$$P_{gr} = \int_0^R p_i(r) \frac{4\pi r^2 \delta(r)}{m_i(r)} \, dr \,. \tag{7}$$

First let's assume the limiting case where the atoms are at rest. From Eq. (6) one gets

$$p_i(r) = Gcm_i^{4/3}\delta^{2/3}(r) \tag{8}$$

which, substituted in Eq. (7) and considering that the molecular mass (mostly Hydrogen) does not vary along r, gives the gravitational power of a gas cloud at absolute zero temperature

$$P_{gr} = Gcm_i^{1/3} \int_0^R 4\pi r^2 \delta^{5/3}(r) \, dr \,. \tag{9}$$

This situation looks like the atoms of very cold gas clouds. However Eq. (9) is inaccurate because does not consider the high temperature reached in the core of galactic gas globules made of free molecules having velocity $v = (2kT/m_i)^{1/2}$. When the distance $x_i(t)$ between two close molecules sometimes reduces to the molecule diametre, there is a collision with probable emission of a visible photon. More in general, putting x_0 the minimun distance, the two atomic nuclei graze with angular velocity

$$\omega \approx \frac{v}{x_0} = \frac{(2kT/m_i)^{1/2}}{x_0} \,. \tag{10}$$

For a very small time, the charged nuclei oscillate with amplitude $x(t) = x_0/\cos(\omega t) = 2x_0 \cos(\omega t)/(1 + \cos(2\omega t))$. Since gas oscillators at temperature T produce radiation with wavelength $\lambda = 2.89 \times 10^{-3}/T$ (Wien's law) the corresponding radiation emitted from a gas cloud is linked to

$$\omega = (2\pi c/\lambda) = 6.52 \times 10^{11}\, T \,. \tag{11}$$

Substituting ω in Eq. (10) one has

$$x_0^2 = 6.49 \times 10^{-47}/Tm_i. \tag{12}$$

Putting in Eq. (6) the distance $x_i = x_0$, the gravitational power of a pair just emitting an infrared photon at a distance r along the radius of the body is

$$p_i(r) = 1.54 \times 10^{46}\, Gcm_i^3(r)\, T(r) \,. \tag{13}$$

Susbstituting in Eq. (7) and integrating to all nuclei of a gas globule made of equal molecules one obtains

$$P_{gr} = 1.54 \times 10^{46}\, Gcm_i^2 \int_0^R 4\pi r^2 \delta(r)\, T(r) \, dr \,. \tag{14}$$

Assuming the H$_2$ molecules of the Bok globules, quick calculations can be made recognising that Eq. (14) contains just the definition of the average temperature T_{av} of a body of mass M. So we have

$$P_{gr} \approx 3.42 \times 10^{-9}\, MT_{av} \,. \tag{15}$$

To calculate the average temperature through the ideal gas equation of state, we need to calculate the average radius R_{av} of the 248 observed globules, which emit infrared radiation corresponding to an external temperature T_0 comprised between 26° and 254° K [3]. This may be obtained putting the radiation power $P_{rad} = 4\pi R_{av}^2 \kappa_s T_0^4$ equal to the observed radiation $P_{rad} \approx 10^{-4}\, M$ which, substituting the average globule mass, gives $P_{rad} \approx 2.2 \times 10^{27}$ Watt. The resulting $R_{av} \approx 2 \times 10^{12}$

gives an average temperature $T_{av} \approx 5 \times 10^4\,^{\circ}$K leading to a gravitational power $P_{gr} \approx 3.8 \times 10^{27}$ Watt.

The observed Bok globules denounced an inner hot core. As appearing in Eq. (14), the inner gravitational power is proportional to the high central temperature, which explains why the inner core temperature increases so rapidly.

Part of the gravitational power escapes as radiation according to the energy balance of the globule

$$C_H M (dT_{av}/dt) = P_{gr} - P_{rad} \qquad (16)$$

where $C_H = 1.44 \times 10^4$ J/kg$\times$K is the specific heat of the molecular Hydrogen. Since it has been found that $P_{gr} \geqslant P_{rad}$, Eq. (16) states that the globule temperature increases.

Had the theory predicted P_{gr} less than the experimental P_{rad}, it should be considered wrong.

Now we have to proof that this inequality holds during the globule lifetime. The micro-quanta paradigm shows that within the gas clouds P_{gr} increments the molecular kinetic energy and produces photons which undergo many Compton scattering with reduction of their energy before escaping from the globule. In fact the photon mean free path results 10^{11}–10^{12} metres in the periphery of a cold large globule ($R = 10^{15}$) whereas takes a figure of 10^2–10^4 metres within the observed Bok globules ($R = 2 \times 10^{12}$). Since the last case shows an optical thickness much greater than the first case, this means that the fraction $Y = P_{rad}/P_{gr}$ of the infrared radiation escaping from the cold large globule is higher than the fraction $Y = 2.2 \times 10^{27}/3.8 \times 10^{27} \approx 0.55$ escaping from the observed Bok globules. The fraction $Y(R)$ is a function of the globule radius and reduces when the globule contracts, increasing the optical thickness. To evaluate the temporal trend of the globule temperature from Eq. (16) we substitute the definition of P_{gr} and put $P_{rad} = Y(R)P_{gr}$

$$C_H M (dT_{av}/dt) = 3.42 \times 10^{-9} M T_{av} (1 - Y(R)). \qquad (17)$$

It appears that T_{av} depends slowly on the mass through the factor $Y(R)$. If one assumes that the observed value $Y \approx 0.55$ does not vary much during the globule lifetime, the solution is

$$T_{av}(t) \approx T_{in} \exp\left(9.96 \times 10^{-14}\, t\right), \qquad (18)$$

where T_{in} is the average temperature of the Bok globule at the initial stage $t = 0$. For instance one may put the initial stage when the radius $R \approx 10^{15}$ corresponds to the cold large globule. In this case the average temperature, calculating the right average gravitational pressure, results $T_{in} \approx 3.2 \times 10^4\,^{\circ}$K, showing that even the cold globule has a hot core. From this initial stage one can calculate the time a Bok globule needs to heat the mass at a temperature T_{av}

$$\Delta t_B \approx 10^{13} \ln \frac{T_{av}}{3.2 \times 10^4}. \qquad (19)$$

The most important event in the life of Bok globules is the ignition of the nuclear reactions which takes place when the inner core attains a temperature of the order of $10^7\,^{\circ}$K. Assuming the corresponding average temperature $T_{av} \approx 8 \times 10^5\,^{\circ}$K, the star ignition occurs after the time

$$\Delta t_F \approx 10^6 \text{ years.} \qquad (20)$$

This result agrees with the computation of the star incubation time given by some classical methods. However Herbig's method predicted that globules producing small stars required an increasing incubation time. For instance a star of $0.2 M_{\odot}$ would require more than 10^9 years before it begins to shine. This implies that these small stars would be only a little fraction in the celestial vault, contrary to the common observation.

Conversely, the gravitational power concept satisfies the experimental evidence because the incubation time depends on the firing temperature of fusion reactions, which is the same for the Hydrogen gas globules. Since the ideal gas equation holds in the case of gas globules (escluding the inner core where the high temperature determines plasma conditions), the thermal energy of the body equals substantially the gravitational energy

$$GM^2/2R \cong C_H M T_{av} \qquad (21)$$

from which the radius R corresponding to a globule of mass M and average temperature T_{av} can be calculated. The high power generated by the nuclear reactions in the inner core (protostar) gives rise to a radiation wind able to sweep away the external globule layers, revealing a young bright star. It may be useful to recall that the fire of nuclear reactions limits, through the radiation wind, the size of the star mass. The different masses of the stars depend probably on the different increasing rate of the inner core temperature at the moment of the nuclear ignition. This very complex phenomenon has been recently observed and described by an equipe of astronomers which observed the formation of a star group within an infrared dark cloud in the G327.3-0.6 region [6].

4 A new dynamical principle in the Universe

Cosmologists have long debated between the expanding universe described by various GR models and the stationary universe described by the Hoyle-Bondi model, where new matter continuosly emerges apparently from the void space.

The micro-quanta flux is the physical reality underlying the Relativistic Mechanics which rules the motion of particles. The gravitational power on the bodies heats cosmic cold gas clouds at different places in the Universe, which become observable at different times when their electromagnetic emissions come within the sensitivity of the astronomical and astrophysical instruments. The energy heating small and large masses in the Universe is drawn from the collisions of particles with the micro-quanta flux filling the space, giving up to each particle a gravitational power produced by the gravitational force due to the mutual screening of masses. Is this the "creation of matter" mentioned by Hoyle? Strictly

speaking, the gravitational power concept implies only the drawing of energy from the underlying reality. Being the energy equivalent to mass, the answer might be yes.

The new dynamical principle describes, more likely, the model of the Universe depicted by the astronomer H. Arp [7]: the Universe has no origin and is in continuous transformation, drawing locally from its interior the possibility of evolution. Any large gas cloud at temperature near the absolute zero may give rise to crowded star clusters or to new galaxies thanks to the gravitational power, which acts also in many other astrophysical situations. For instance influencing even the behaviour of modest astrophysical bodies, such as the planets.

5 Gravitational power on the planets

In the so-called "inert" celestial bodies, such as the planets, atoms are bound to each other by the forces of the Lennard-Jones potential, which determine the equilibrium distance between them. A planet forms when the density of a contracting small cloud takes values corresponding to the solid or liquid state. Obviously this fact stops the contraction and makes largely inaccurate the ideal gas equation, so the equivalence between the gravitational and thermal energy vanishes. Around their rest-place the atomic nuclei oscillate with amplitude and frequency depending on the temperature. Any nucleus of mass m_i and average velocity v shows an absolute temperature given by

$$kT = \frac{1}{2} m_i v^2. \tag{22}$$

The instanteneous velocity $v(t)$ is bound to the oscillation amplitude $x(t) = a \sin(\omega t + \alpha)$ through the relationship

$$v^2(t) = (dx/dt)^2 = a^2 \omega^2 \cos^2(\omega t + \alpha) \tag{23}$$

whose average value is $v^2 = \frac{1}{2} a^2 \omega^2$. Then the oscillation amplitude is given by

$$a = \frac{(4kT/m_i)^{1/2}}{\omega} \tag{24}$$

which is a little different from Eq. (10). The frequency of the emitted photon is linked to the temperature of the gas through the Wien's law which leads to ω given by Eq. (11). Substituting ω and $m_i = A m_0$ into Eq. (24) and putting the numerical values, one gets the radial behaviour of the amplitude depending on $T(r)$ and $A(r)$

$$a(r) = \frac{2.79 \times 10^{-10}}{[T(r) A(r)]^{1/2}}. \tag{25}$$

The electrical forces rule the motion of the oscillating atoms in thermal equilibrium. But the kinetic energy of the atoms came from the same source that heated the ancient Bok globule which produced our Sun and planets. The primeval planets were hot bodies with outer temperature around 950° K, which lose their energy early by radiating in space,

thus allowing life on the Earth during nearly 4 billion years. Abstracting from the heating of solar radiation, all planet surfaces should be presently near the absolute zero. But the astronomers found a sensible infrared radiation which comes from the interior of the giant solar planets [see Table 1]. As explained for the gas globules, also the atoms in the planets receive new kinetic energy from the micro-quanta flux. Each atom receives the major fraction of the gravitational power from the nearest nuclei. The work done on each oscillating atom by the resultant gravitational force always increments its kinetic energy. Let's consider the resultant gravitational force on a nucleus of mass m_i oscillating with amplitude $x(t)$ along the straight line joining some nuclei placed on both sides at equal distance x_i. Pairs of adjacent nuclei are alternatively approaching and removing of a displacement $2x(t)$ due to the thermal motion. Thus the nearest two nuclei gives the greatest contribute, whereas the nuclei at distance $2x_i$ do not contribute and the nuclei at distance $3x_i$ contribute for a few percent, as shown by Eq. (26). Multiplying the resultant force by the velocity c of the colliding quanta gives us (considering that $x \ll x_i$) the released power

$$p_i(t) = Gcm_i^2 \left[\frac{1}{(x_i - 2x)^2} - \frac{1}{(x_i + 2x)^2} + \right.$$
$$\left. + \frac{1}{(3x_i - 2x)^2} - \frac{1}{(3x_i + 2x)^2} \right] \cong 8.3 \, Gcm_i x \delta. \tag{26}$$

To obtain the time averaged power when the amplitude varies from 0 to a we have to multiply by $\frac{2}{\pi}$, so one gets the radial power distribution $p_i(r) \cong \frac{16.6}{\pi} Gcm_i a(r) \delta(r)$ to be substituted in Eq. (7). As a consequence the gravitational power released to a planet results

$$P_{gr} \cong \frac{16.6}{\pi} Gc \int_0^R 4\pi r^2 \delta^2(r) \, a(r) \, dr \tag{27}$$

which, substituting the amplitude $a(r)$ from Eq. (25), gives

$$P_{gr} \cong 2.95 \times 10^{-9} Gc \int_0^R \frac{4\pi r^2 \delta^2(r)}{[T(r) A(r)]^{1/2}} \, dr. \tag{28}$$

If the internal parameters were known, Eq. (28) might be simply computed by numerical integration. But the trends of the internal density, nuclear mass and temperature are in general not known (excepting perhaps the Earth) with an accuracy better than 20%. To the aim of doing some quick calculations we observed that the ratio $B = \delta(r)/T(r) A(r)$ results to be, referring to the Earth's internal parameters recently calculated by D. Alphe et al. [8], independent from the radial coordinate and about equal to $B \approx 4 \times 10^{-2}$ (SI system). Let's recall that Earth is the unique planet whose internal structure is known with an accuracy better than 10%. Substituting B in Eq. (28) one may obtain the approximate formula

$$P_{gr} \approx 2.9 \times 10^{-11} M \, (\delta_{av} B)^{1/2}. \tag{29}$$

Planet	Predicted gravitational power P_{gr} (W)	Measured infrared flux ϕ_{ir} (W/m²)	Internal infrared flux $\Delta\phi_{ir}$ (W/m²)	Measured internal power P_{int} (W)
Jupiter	4.3×10^{17}	13.89	5.57	3.5×10^{17}
Saturn	9.1×10^{16}	4.40	1.93	8.6×10^{16}
Uranus	9.8×10^{15}	0.69	0.04	3.2×10^{14}
Neptune	1.7×10^{16}	0.72	0.45	3.5×10^{15}
Earth	2.6×10^{15}	?	?	?

Table 1: Predicted gravitational power P_{gr} compared with the measured internal power P_{int} observed for the solar giant planets, according to [10].

5.1 Calculation of the gravitational power on Earth and the giant solar planets

When applied to the Earth, Eq. (29) gives a gravitational power $P_{gr} \approx 2.6 \times 10^{15}$ Watt. This approximate formula shows an accuracy comparable to that we would obtain introducing the Earth internal parameters directly in the exact Eq. (28). The predicted P_{gr} is 60 times higher than the classical heat flow (4.4×10^{13} Watt) calculated by laborious evaluation of the geothermal gradient measured throughout the continents and adopting an average thermal conductivity κ measured in laboratory for the principal rocks [9]. Of course the value of the geothermal gradient and of κ for the remaining 70% of the planet surface (under the oceans) had to be inferred, due to the difficulties of making measurements. Because the classical heat flow is likely not affected by a computational error higher than 30%, the discrepancy with P_{gr} has to be attributed to the lack of other forms of heat flow across the crust. The contribution of the radioactive isotopes in the rocks to the total power generated inside the planet becomes negligible when compared to P_{gr}. Useful verifications of the computational formula for P_{gr} (Eq. 29) may be done searching for the constant B_i of the giant planets of the solar system for which the infrared radiation coming from the interior has been measured. A recent book by P. G. Irwin [10] analyses the data collected from various interplanetary spacecrafts launched in the last decades towards Jupiter, Saturn, Uranus and Neptune. A draft of the internal structure of these planets is given from which only rough values of B_i may be obtained. However for Jupiter and Saturn the values of B_i are not much different from the Earth's value, whereas lower values were obtained for Uranus and Neptune, whose structure is dominated by H_2O ice instead of molecular Hydrogen.

In Table 1 the gravitational power P_{gr} computed for the giant planets is compared with the internal infrared power $P_{int} = 4\pi R^2 (\phi_{ir} - \phi_{Sun})$ derived from the measured infrared flux ϕ_{ir} minus the infrared contribution ϕ_{Sun} due to the solar absorbed/emitted radiation. The difference $\Delta\phi_{ir}$ appears to be numerically accurate for Jupiter, Saturn and Neptune because it amounts to a large fraction of the observed flux ϕ_{ir}. Only for Uranus $\Delta\phi_{ir}$ is a small fraction (5.8%) of the

observed flux, so some inaccuracy on the related P_{int} is unavoidable. The agreement between P_{gr} and P_{int} for Jupiter and Saturn confirm that the experimental P_{int} appears to be the gravitational power theoretically predicted. The discrepancy found for Neptune may be likely due to the uncertain factor B. However the high discrepancy between P_{gr} and P_{int} of Uranus has to be attributed to some profound reason. For instance, the fact that the internally generated P_{gr} does not entirely reach the external surface due to the particular peripheral structure of the planet. Let's recall that specific studies suggest that Uranus presents a discontinuity of the internal structure, probably near the surface [11]. As we know, a similar discontinuity (Mohorovich's one) is present also on the Earth. Observing Table 1 one wonders if an experimental method may be adopted (as for the giant planets) to measure the IR flux radiating from the Earth interior. This would give an independent check of the gravitational power generated on the planets.

5.2 The emergent problem of the Earth dilatation

We have seen that the gravitational power discharged on the Earth largely exceeds the classical heat flow by conduction through the crust. The classical method does not consider the heat flow through other ways, for instance the cooling of magma escaping from the Mid Ocean Ridges, from the seismic fractures linked to the Plate tectonics [12] and from volcanic activities on the ocean seafloor. Let's recall that the U.S. Geological Service data show a frequency of about 8 earthquakes per day, Richter magnitude $\geqslant 4$, mostly under the ocean seafloor.

The gravitational power is the physical agent heating and contracting the galactic gas globules. In the case of planets — where the atoms are tightly packaged — P_{gr} can no longer induce a contraction. On the contrary it may induce a thermal expansion which increases the Earth radius. Let's consider the energy balance of the *core + mantle* mass

$$C_{av}M(dT_{av}/dt) = 0.966 P_{gr} - P_{ex}(t), \qquad (30)$$

where $C_{av} = 708$ J/kg×K is the average specific heat. It is taken into account that about 3.4% of P_{gr} is generated into the lithosphere. $P_{ex}(t)$ is the power exiting from the mantle towards the lithosphere. To a first approximation, it equals the classical heat flow by conduction across the solid crust 4.4×10^{13} W plus the heat flow of hot magma which cools penetrating the seismic fractures produced through the crust

$$P_{ex}(t) = Q_0(dV/dt) + 4.4 \times 10^{13}, \qquad (31)$$

where Q_0 is the heat released by 1 m³ of hot magma which enters the crust at a temperature around 1800° K and (dV/dt) is the volume rate of hot magma entering the crust (Eq. 33). Correspondingly the power entering the crust and accumulating before to be radiated into space, obey the energy balance

$$C_{cr}M_{cr}(dT_{cr}/dt) = 0.034 P_{gr} + P_{ex}(t) - P_{int}(t), \qquad (32)$$

where $C_{cr} \approx 1200$ J/kg×K is the average specific heat of the rocks and P_{int} is the infrared radiation power coming from the interior.

Eqs. (30, 31, 32) contain the unknown temperature derivatives of the Earth interior and of the crust. $P_{ex}(t)$ and $P_{int}(t)$ are physical quantities to be found. To a first approximation the exiting power P_{ex} may be evaluated assuming that the expansion rate of the *core + mantle* exceeds the expansion rate allowed by the solid crust, which consequently undergoes seismic fractures incorporating the increased volume of hot magma. The volume rate of magma entering the crust (and partially escaping from the ocean seafloor and volcanic activity) is given by

$$\frac{dV}{dt} \approx 4\pi R^2 \left(\frac{dR_m}{dt} - \frac{dR_{cr}}{dt} \right). \qquad (33)$$

The temperature derivative dT_{av}/dt produces a dilatation of the *mantle* radius

$$dR_m/dt = R_i \alpha_{av} (dT_{av}/dt) \qquad (34)$$

where it has been considered an average *core + mantle* linear expansion coefficient $\alpha_{av} = 1.12 \times 10^{-5}$ °K^{-1} based on the usual data at normal temperature. It is not clear how much α might change at temperature $\geqslant 2000°$ K (mantle) and $\geqslant 5000°$ K (FeNi-core). The *core + mantle* expansion originates a radial compression on the solid crust (spherical shell) whose inner radius R_{cr} shows an annual dilatation

$$dR_{cr}/dt = R_i \alpha_{cr} (dT_{cr}/dt), \qquad (35)$$

where the assumed expansion coefficient of the rocks is $\alpha_{cr} \approx 1.3 \times 10^{-5}$ °K^{-1}.

Let's recall that the 1 m^3 of hot magma at a temperature around 1800° K releases to the crust the heat which is $Q_0 = \delta(c\Delta T + H_f) \approx 6.9 \times 10^9$ J/m^3, where $H_{fus} \approx 3.7 \times 10^5$ J/kg is the average heat of fusion/solification of the rocks. Multiplying by Q_0 the magma flow of Eq. (33), one obtains the heat flow due to the cooling of magma entering the crust fractures, to which is added the classical heat flow by conduction. Part of the magma flow escapes from the Mid ocean Ridges, thus removing the tectonic plates [12] which undergo subduction. Rough estimates of the plate dynamics show an amount of new formed crust of the order of 1.3×10^{10} m^3/y, that is probably a little fraction of the total.

This scheme gives values of $P_{ex}(t)$ depending on the two unknown temperature derivatives.

The infrared radiation $P_{int}(t)$ coming from the interior remains up to now unspecified. A simple equation comes out summing Eq. (30) and Eq. (32)

$$C_{av}M(dT_{av}/dt) + C_{cr}M_{cr}(dT_{cr}/dt) = P_{gr} - P_{int}(t) \qquad (36)$$

which does no longer need to know $P_{ex}(t)$. When the infrared radiation power $P_{int}(t)$ is less than the gravitational power, this equation states that the Earth temperature increases sen-

sibly along some million years, thus producing the dilatation threat.

5.3 Comparison between the effects on Earth and the giant solar planets

Some points of the present analysis about the Earth thermal dilatation require further specification. The lithosphere began to form upon the fluid planet about 4 billion years ago, to account for the evolution of primeval life on the Earth. If the magma estimated by Eq. (33) escaped during 4 billion years, the volume of the lithosphere would be about 16 times the present value. This requires an explanation. One may wonder which fraction of time the tectonic process was operating. A recent hypothesis [13] suggests that plate dynamics was intermittent along the geological periods. As a matter of fact the process of the magma escaping through seismic fractures has just the characteristics of discontinuity. However this does not match with the continuous feeding of heat to the Earth by the gravitational power.

To this aim it is necessary to make reference to the fluid planets, such as the giant solar planets (namely Jupiter and Saturn) where the mass expands freely and the gravitational power generated in the interior flows up to the outer surface where it is radiated in space. For these planets the energy balance

$$C_{av}M(dT_{av}/dt) = P_{gr} - P_{int}(t) \qquad (37)$$

indicates that, when $P_{gr} = P_{int}$, the internal temperature of the planet is constant. No thermal expansion stresses arise because the solid crust is lacking. Let's now return to the Earth. The major problems are:

1. If in Eq. (30) we neglect P_{ex}, the increase of the average temperature $dT_{av}/dt \approx (P_{gr}/C_{av}M)$ would be of the order of 10^{-5} °K/y). Lasting for 10 million years this would increase the internal temperaure of about 100° C. Conversely the *surface* temperature would experience a little increment because an increase of 1° C is sufficient to radiate in space an infrared power equal to the whole P_{gr}. This can be proved recalling that the Earth effective temperature $T_0 = 255°$ K, calculated by P. G. Irwin [10] considering the bond albedo, radiates an infrared power equal to the absorbed solar light. If the planet surface were radiating in addition the predicted power P_{gr}, the surface effective temperature would increase from 255° K to 256° K only;

2. If the duration of the Earth increasing temperature is assumed to be 1 billion years, the resulting temperature would have evaporised the planet. Because this din't happen, there was some mechanism which braked the increasing temperature;

3. At the boundary between astenosphere and lithosphere a modest increase of temperature (for instance 100° C) makes fluid some solid rocks, so reducing the mass of

the solid crust. This explains why the volume of the present solid crust is many times smaller than the volume of the total magma escaped during 4 billion years. Let's assume that the escaping magma that annually solidifies within the crust is counterbalanced by an equal volume of liquefied rocks at the boundary with the astenosphere. This requires that the Earth should give up to the crust some heat flow which can be easily furnished by the gravitational power;

4. The risk still remains of the increasing Earth temperature. Up to now we have assumed that the transfer of the internally generated power towards the outer surface depends on the fact that the expanding volume (dilatation) of the hot interior produces many fractures (deep earthquakes) on the solid crust, which are rapidly filled by hot fluid magma. In this frame the Earth appears to be an intrinsically seismic planet.

In a recent work, the pressure exerted by the expanded *core + mantle* on the elastic solid crust has been assumed to produce a continuous passage of some hot fluid minerals through a complex physical-chemical process conveying some thermal power. A plain description of such a process by P. B. Kelemen may be found in *Scientific American* [13], whereas the fundamental concepts may be found in a previous paper [14]. However the potentiality of the process in transferring internal power towards the outer surface does not appear to have been evaluated.

5.4 The ice core data recording the Glacial Eras

The cycles of the temperature (Fig.1) observed from ice cores in Antartica by two independent teams, Vostok [15] and Epica [16], show an impressive result: the most recent four cycles may be nearly placed one upon other. The cycle durations are between 85–122 ky. Each peak is preceded by a temperature strong rise with slope around 1.8° C/ky and is followed by a partial descent with about the same slope. This fact is worth receiving an explanation. The descent continues with a series of small alternated rises and descents characteristics of each cycle. The Antarctica temperature behaviour has been observed together with the concentrations of CO_2 and CH_4 greenhouse gases and of the local insolation.

Deciphering this lot of data is the main trouble of many scientists. Since the peaks of the greenhouse gases are considerably less than their present concentration, the temperature rising in Antarctica could not be due to the greenhous gas effect. In any case the slope of the present climate effect by greenhouse gases (more than 10° C/ky) is not comparable with the antartic cycling phenomena. Most likely, since there is simultaneity between the temperature peaks and the greenhouse gas peaks, the antartic CO_2 and CH_4 concentrations could be due to the increase of temperature in the equatorial and temperate regions, where the decomposition of organic matter in CO_2 and CH_4 was enhanced, so the greenhouse

gases migrate rapidly through winds towards the poles.

The cycling temperature amplitude $\Delta T(t)$ in Antartica is notable (each cycle shows an amplitude comprised between 10° C and 13° C). Here it is considered as the increase, over the undisturbed average antartic temperature T_A, due to some thermal power $P_{int}(t)$ coming from the planet interior and radiated to space. Since the average temperature measured at the Vostok site is −64° C, it follows that the minimum temperature of the ice core record (see Fig.1) results $T_A \approx 200°$ K. Let's consider 1 m^2 of surface in Antarctica where, in absence of the internal power, the radiation balance is

$$\kappa \epsilon (T_A)^4 \approx 110 \varepsilon \ (\text{W/m}^2) = p_{sun} + p_{atm} \qquad (38)$$

where κ is the Stephan-Boltzmann constant, ε is the snow emissivity, p_{sun} is the specific power from sunlight and p_{atm} is the power released on 1 m^2 by the atmospheric precipitations transported by winds from the oceans. By consequence, in the energy balance the internal power $p_{int}(t) = P_{int}(t)/4\pi R^2$ radiates in space through the temperature increment $\Delta T(t)$

$$p_{int}(t) = \kappa \varepsilon \left[(T_A + \Delta T(t))^4 - T_A^4 \right] \cong 4\kappa \varepsilon T_A^3 \Delta T(t). \qquad (39)$$

Substituting $T_A \approx 200°$ K in this equation one gets

$$p_{int}(t) \approx 1.81 \varepsilon \Delta T(t) \qquad (40)$$

which shows an internal power rising from 0 up to the maximum $p_{int} \approx 19\varepsilon$ W/m^2 and subsequently descending to 0 with a particular series of descents and risings.

We assume that the Earth gravitational power P_{gr} goes beyond the solid crust *via* the hot magma entering the seismic fractures in the crust. The longest duration of magma flow produces the strongest $\Delta T(t)$ rise up to the interglacial peak, which occurs due to the stop of the magma flow consequent to the stop of earthquakes. The seismicity depends on the crust ruptures consequent to the dilatation of the Earth interior (Eq. 33). Resuming, each rising of the $\Delta T(t)$ cycle occurs in presence of the seismic activity. Conversely, when $\Delta T(t)$ descends (due to the radiative emission cooling) the seismic activity should vanish. In this frame each temperature cycle is made of seismic periods alternated with quiet periods.

Some considerations on the nearly equal slopes (excepting the sign) of $\Delta T(t)$ before and after the peak. The constant slope of the strong ascent is due to the increasing magma flow entering the superficial crust. The slope of the descent is linked to the radiative cooling of the superficial mass.

In any case the ice core data imply that the temperatures of the crust $T_{cr}(t)$ and of the Earth interior $T_{av}(t)$ undergo cycles. Assuming in Eq. (36) these temperature cycles, we observe that integrating of the left side along the cycle period gives zero. By consequence the integration of the right side gives

$$P_{gr} \approx (p_{int})_{av} \, 4\pi R^2, \qquad (41)$$

where $(p_{int})_{av}$ is uniform on the Earth surface since the gravitational power flows outside isotropically.
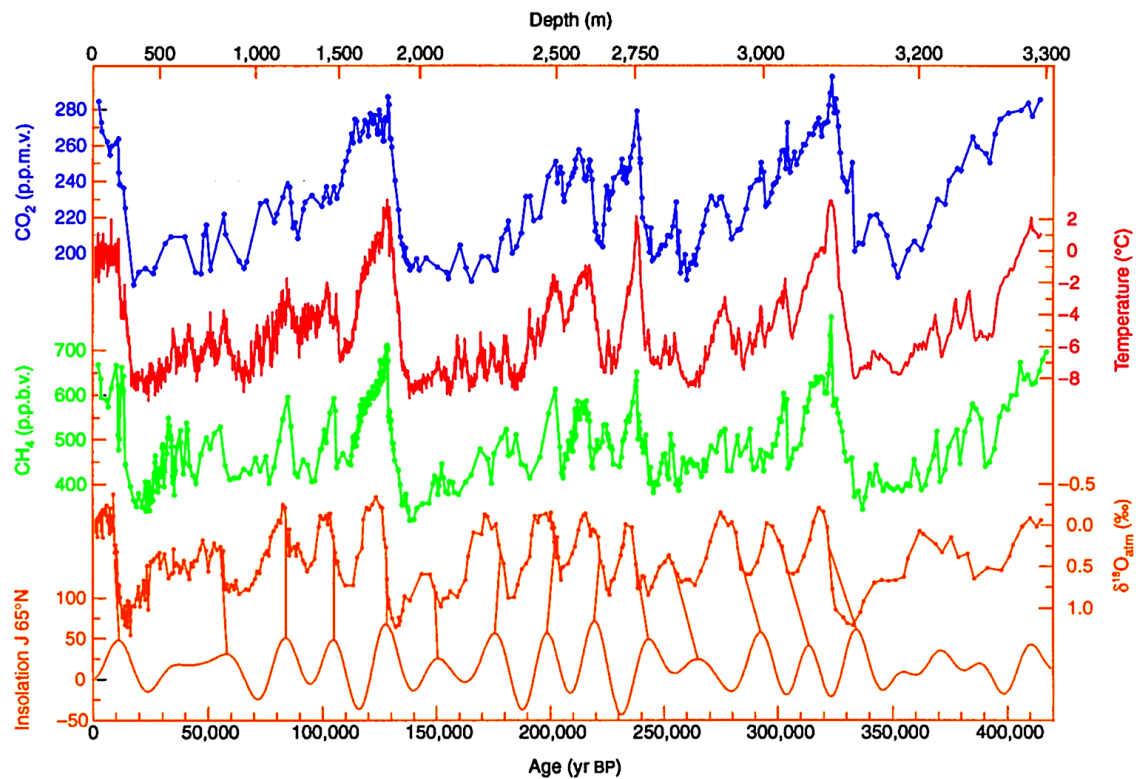
Fig. 1: 420,000 years of ice core data recorded from Vostok, Antartica research station. From bottom to top: Solar variation at $65°N$ due to Milankovitch cycles; ^{18}O isotope of oxygen; levels of methane CH_4; relative temperature respect to local annual temperature; levels of carbon dioxide CO_2.

In particular $(p_{int})_{av}$ may be calculated in Antartica making in Eq. (40) the graphic integration of $\Delta T(t)$, which gives the average $(\Delta T)_{av} \approx 3.9°$ C.

Substituting $(p_{int})_{av}$ in Eq. (41) one gets

$$P_{gr} \approx 1.81\,\varepsilon\,(\Delta T)_{av}\,4\pi R^2 \qquad (42)$$

which, considering the snow emissivity $\varepsilon = 0.82$, gives an independent value of the Earth gravitational power through the ice core data from Antartica

$$P_{gr} \approx 2.9{\times}10^{15} \text{ Watt.} \qquad (43)$$

This empirical value of P_{gr} is higher than the approximate value $2.6{\times}10^{15}$ derived from the theoretical Eq. (28), where the numerical uncertainties on the Earth internal structure, currently discussed in the literature, are present.

6 Some final considerations

After the conceptual default of classical physics about the energetic mechanism of the contracting gas globules leading to the star birth, the introduction of the *gravitational power concept* permits us to explain the genesis of several celestial bodies from the primeval Hydrogen cold clouds. The new dynamical principle describes an Universe (somewhat similar to the Hoyle-Bondi stationary model) putting light on new phenomena such as the discordant redshifts of quasars studied by the astronomer H. Arp. The fluid giant planets do not feel heavy troubles from the gravitational power they receive. Conversely the gravitational power produces on the Earth and any planet or satellite with solid crust, dangerous physical effects through heating and dilatation. Firstly, the internal dilatation stresses the solid crust producing the planetary seismicity originating fractures rapidly filled by the mantle fluid magma. The process presents periods of emphasis followed by stasis, as confirmed by the periodic changes of the temperature slope derived from the ice core data, which show that Glacial and Interglacial Eras depend on the variable rate of the internally generated heat flowing up to the planet surface.

The present contribution to the unsatisfying knowledge of geodynamics is aimed at finding the common origin of different phenomena: the high planet seismicity, the surface thermal cycles around 100.000 years (Glacial Eras) and the Tectonic dynamics (around some ten million years). Much work needs to be done.

References

1. Michelini M. The common physical origin of the Gravitational, Strong and Weak forces. *Apeiron Journal*, 2008, v. 15, 440.

2. Loinger A. GW's towards fundamental principles of GR. arXiv: phys/0709.0490.

3. Yun J. L., Clemens D. P. Star formation in small globules: Bart Bok was correct! *Astroph. J.*, 1990, v. 365, L73.

4. Clemens D. P., Yun J. L., Heyer M. H. Bok globules and small molecular clouds: Deep IRAS Photometry and CO Spectroscopy. *Astroph. J. Suppl.*, 1991, v. 75, 877.

5. Loinger A. Gravitational collapses to bodies of finite volume. arXiv: phys/0612160.

6. Minier V., André Ph., et al. Evidence of triggered star formation in G327.3-0.6. *Astron. and Astrophys.*, v. 501, L1.

7. Arp H. Catalog of discordant redshift associations. Apeiron Publishers, Montreal, 2003.

8. Alphe D., Gillan M.G., et al., The "ab initio" simulation of the Earth core. *Phil. Trans. Roy. Soc. London*, 2002, v. 360, 1227.

9. Stein C. Global Earth Phyisics. Amer. Geophys. Union, 1995.

10. Irwin P. G. Giant planets of our solar system. Springer Praxis, 2003.

11. Podolak M., Podolak J., Marley M. S. *Amer. Astron. Soc. Bulletin*, 1997, v. 29, 994.

12. Turcotte D. L., Schubert G. The plate tectonics geodynamics. 2nd Edition, Cambridge Univ. Press, 2002.

13. Silver P. G., Behn M. D. Intermittent plate tectonics? *Science*, 2008, v. 319, 85.

14. Kelemen P. B. The origin of the Land under the Sea. *Sci. Am.*, 2008, v. 300, no.2, 52.

15. Spiegelman M., Kelemen P. B., Aharonov E. Causes and consequences of flow organization during melt transport: the reaction infiltration instability in compactible media. *J. Geophys. Res.*, 2001, v. 106, 2061.

16. Petit J. R., et al. Climate and atmospheric history of the past 420,000 years from the Vostok ice core in Antartica. *Nature*, 1999, v. 399, 429–436.

17. Laurent A., Barbante C., et al. Eight glacial cycles from the Antartic ice core. *Nature*, 2004, v. 429, 623–628.

———————————

ISSN 1555-5534

9 771555 553907 >